

***Identification of specific genetic changes associated with  
Conjunctival Melanoma***



*A thesis submitted to the Medical School, University of Sheffield in partial  
fulfilment of the requirements for the degree of Doctor of Philosophy*

by

Shamsa E Ihmed Elkasah

Registration No:130200884

Supervisors: Dr. Karen Sisley  
Dr. David Hammond

The University of Sheffield Faculty of Medicine Dentistry & Health

Department of Oncology and Human Metabolism

May 2018

## Acknowledgments

In the Name of Allah, most gracious, most Merciful. This thesis has become a reality with the kind support and help of many individuals. I would like to extend my sincere thanks to all of them.

Foremost, I would like to express my special gratitude to my supervisors, Dr. Karen Sisley and Dr. David Hammond, for being excellent role models, for their patient guidance and motivation, for welcoming me into the scientific community, for patiently showing me the ropes and for many hours of long discussion and continuous support during my PhD study. Their guidance helped me throughout the research and writing of this thesis. I could not have imagined having a better advisor and mentor for my study.

I am highly indebted and thoroughly grateful to all members of the Rare Tumour Research Group who gave me access to research facilities and were supportive and helpful in more ways than they can imagine. It would not have been possible to conduct this research without their precious support of the technical team.

I am indebted to my family. Mum and Dad, thank you for your never-ending love and support. My lovely husband, Ali, for his superhuman patience and my lovely boys for being patient with me; I cannot express my eternal gratitude for without their love and endless support I would not have managed to completed this study successfully.

My sincere thanks also go to my siblings, for believing in me and helping me to overcome many difficulties, also to all my colleagues who made Sheffield feel like home and for their endless emotional and spiritually support throughout the writing of this thesis.

Finally, I dedicate this work to Allah the Creator who made everything possible.

## Abstract

Conjunctival melanoma (ConM) are rare ocular tumours but the incidence, like that of cutaneous melanoma (CM), is increasing and sunlight exposure is considered to be a factor in their development. Little is known about the genetic changes that are associated with this malignancy. Previous studies have reported that ConMs have mutations of the *BRAF* and *NRAS* genes and recently, the *TERT* promoter has also been shown to be commonly mutated in the ConM form. The genetic classification of ocular melanomas, however, has shown itself to be highly reliable in determining the prognosis of patients with UM compared to their counterpart ConM.

The aim of the study was to identify specific genetic changes that can identify ConM patients with a poor prognosis, and to improve the understanding of the genetic alterations that may predispose people to this condition. Array-CGH was carried out using DNA extracted from 21 frozen and archival ConM samples, with another four CM cell lines used as a positive control. The data were analysed by using two different software: Agilent (ADM2 algorithm), and Nexus (FASST2 algorithm) to investigate the global genetic alterations associated with ConM and to detect any recurrent focal somatic copy number alterations (SCNA) that might have been missed in previous reports. In a small trial study, possible genes drivers were investigated using IHC. All these samples were also sequenced to identify any mutations in these genes (*BRAF*, *GNA11*, *GNAQ*, *NRAS* and *TERT*). The present study reported complex genomic profiles that had various abnormalities affecting different chromosomes. All these CNAs distributed across the genome in a pattern reminiscent of CM but differing markedly from UM. The most common oncogene mutation found in conjunctival tumours were *BRAF* mutations 24% (5/21), *NRAS* 10% (2/21), and *TERT* mutations, 47% (8 of 17). The most statistically significant driver genes detected by Nexus software among ConM tumours were *CDKN2A* and *TERT* genes. Although the IHC findings were compatible with common aberration analysis by Nexus software, where the most statistically significant candidate gene were detected, further investigation is needed to detect the role of these genes in ConM prognosis and metastasis.

## Table of Contents

Acknowledgments.....	2
Abstract.....	3
List of figures.....	9
List of tables.....	12
List of abbreviations.....	14
<b>Chapter One</b> .....	<b>17</b>
1. Introduction.....	18
1.1 Cancer as a genetic disease.....	18
1.1.1 Historical aspect and hallmarks of cancer.....	18
1.1.2 Aetiology of cancer development.....	19
1.1.3 Analytical technique used in cancer.....	20
1.2 Overview of eye cancer.....	21
1.3 Conjunctival melanoma.....	25
1.3.1 Epidemiology and incidence.....	25
1.3.2 Histopathological features.....	25
1.3.3 Aetiology.....	27
1.3.3.1 Primary acquired melanosis.....	27
1.3.3.2 Naevus.....	29
1.3.3.3 <i>De Novo</i> lesions.....	30
1.3.4 Clinical/ pathological prognostic factors.....	30
1.3.4.1 Tumour location.....	31
1.3.4.2 Tumour depth and size.....	31
1.3.4.3 Origin if ConM.....	31
1.3.5 Metastasis and survival.....	32
1.3.6 Treatment.....	32
1.3.6.1 Surgical treatment.....	33
1.3.6.2 Exenteration.....	33
1.3.6.3 Radiotherapy.....	33
1.3.6.4 Cryotherapy.....	34
1.3.6.5 Topical chemotherapy.....	34

1.3.7	The genetics basics of conjunctival melanoma	34
1.3.7.1	Oncogenic mutations in ConM	35
1.3.7.1.1	<i>BRAF</i> and <i>NRAS</i>	35
1.3.7.1.2	<i>GNAQ</i> and <i>GNA11</i>	38
1.3.7.1.3	Recent driver mutations	39
1.3.7.2	Chromosomal aberrations in ConM	40
1.4	Hypothesis and aim of the study	44
	<b>Chapter Two</b>	45
2.1	Patients and tumour samples	46
2.1.1	Ethics statement	46
2.1.2	Sample selection	46
2.2	Materials	47
2.2.1	Tissue culture reagents and chemicals	48
2.2.2	Material and equipment for karyotyping	49
2.2.3	Material and equipment for DNA extraction	50
2.2.4	Material for Whole Genomic Amplification (WGA)	50
2.2.5	Material for Array Comparative Genomic Hybridization	51
2.2.6	Material for Genomic DNA sequencing	52
2.2.7	Primer design	53
2.2.8	Material for Fluorescence In situ Hybridisation (FISH)	55
2.2.9	Material for immunohistochemistry (IHC)	55
2.3	Methods	56
2.3.1	Routine tissue culture (Split/Subculture)	56
2.3.2	Cytogenetic analysis (Karyotyping)	57
2.3.2.1	Chromosome harvesting	57
2.3.2.2	Preparation of chromosome spreads	58
2.3.2.3	Giemsa staining/banding	58
2.3.3	DNA extraction	59
2.3.3.1	Isolation and purification DNA from cell lines	59
2.3.3.1.1	Cell lines and fresh frozen tissue samples	59
2.3.3.1.2	Formalin-Fixed Paraffin-Embedding samples	60
2.3.3.2	Genomic DNA quantification and purity Assessment	60
2.3.4	Genomicplex whole Genome Amplification (WGA)	61
2.3.4.1	Fragmentation	62

2.3.4.2 Library Preparation .....	62
2.3.4.3 Amplification .....	62
2.3.5 Array-based Comparative Genomic Hybridization .....	63
2.3.5.1 Fresh frozen tissue and short term culture .....	64
2.3.5.1.1 DNA digestions .....	64
2.3.5.1.2 DNA labelling and cleaning .....	64
2.3.5.1.3 Microarray hybridization and assembly .....	65
2.3.5.2 FFPE Labelling using the Universal Linkage System .....	66
2.3.5.2.1 Heat Fragmentation .....	66
2.3.5.2.2 ULS Labelling Reaction .....	67
2.3.5.2.3 ULS Clean-up .....	67
2.3.5.2.4 Hybridization .....	68
2.3.4.2.5 Microarray washing and scanning .....	68
2.3.5.2.6 Microarray analysis .....	69
2.3.6 Aberration Detection Analysis .....	70
2.3.6.1 Agilent genomic software analysis .....	70
2.3.6.2 Nexus software .....	71
2.3.7 Genomic DNA sequencing .....	71
2.3.7.1 Standard PCR .....	71
2.3.7.2 Agarose gel electrophoresis .....	75
2.3.7.3 DNA purification and sequencing .....	76
2.3.7.4 Sequence analysis .....	76
2.3.8 Fluorescence in situ Hybridisation (FISH) .....	76
2.3.8.1 Cell harvesting and slides preparation .....	76
2.3.8.2 RNase A and pepsin treatment .....	76
2.3.8.3 Fixative and dehydration of slides .....	77
2.3.8.4 Hybridization of the DNA probes to target DNA .....	77
2.3.8.5 Post-hybridization washes .....	77
2.3.8.6 Image detection by fluorescence microscopy .....	78
2.3.9 Immunohistochemistry .....	78
2.3.9.1 Antibody optimization .....	78
2.3.9.2 Tissue Preparation and Antigen Retrieval for IHC .....	78
2.3.9.3 Blocking and Primary Antibody Incubation .....	79
2.3.9.4 Secondary Antibody Incubation and Immunoreactivity .....	79

2.3.9.5 Counterstaining and Mounting.....	80
<b>Chapter Three</b> .....	<b>81</b>
3.1 Introduction.....	82
3.2 Results.....	84
3.2.1 Characterisation of Cells in Culture.....	84
3.2.2 Genetic Characterisations.....	88
3.2.2.1 Karyotyping.....	88
3.2.2.2 Array Comparative Genomic Hybridisation.....	90
3.2.2.3 Mutational analysis for <i>BRAF</i> , <i>NRAS</i> , <i>GNAQ</i> , <i>GNA11</i> and <i>TERT</i> genes.....	92
3.2.2.4 Fluorescence in situ Hybridisation.....	94
3.3 Discussion.....	95
3.3.1 Primary tissue culture characteristics.....	95
3.3.2 Genetic characteristics.....	96
3.3.3 Origin of ConM cell lines Mel 621 and Mel 635.....	98
<b>Chapter Four</b> .....	<b>100</b>
4.1 Introduction.....	101
4.2 Result.....	103
4.2.1 Tumour sample.....	103
4.2.2 Technical issue with DNA purity and quality.....	103
4.2.3 Screening of known oncogenes.....	104
4.2.3.1 <i>BRAF</i> and <i>NRAS</i> screening.....	104
4.2.3.2 <i>GNAQ</i> and <i>GNA11</i> exon 5 screening.....	108
4.2.3.3 <i>TERT</i> promoter screening.....	110
4.2.4 Copy Number Aberrations (CNAs) in ConM tumours.....	113
4.2.5 Common aberrations in different melanoma subtypes.....	120
4.2.6 Copy number aberrations among <i>BRAF</i> and <i>NRAS</i> mutations.....	123
4.2.7 Copy number aberrations among cases with <i>TERT</i> mutation and without mutations.....	125
4.2.8 Common aberrations among primary and metastatic ConM.....	126
4.3 Discussion.....	129
4.3.1 Known oncogene mutations in conjunctival melanoma.....	129
4.3.2 Genetic alterations of conjunctival melanoma.....	132
4.3.3 Do <i>KIT</i> , <i>CCND1</i> , <i>CDK4</i> , <i>RREB1</i> and <i>MYB</i> correlate to the genetic	

alterations in ConM? .....	134
4.3.4 Genetic alterations among primary and metastatic ConM .....	136
<b>Chapter Five</b> .....	138
5.1 introduction .....	139
5.2 Results .....	142
5.2.1 Identifications of common focal SCNA .....	142
5.2.2 Significance Testing of Common recurrent CNAs regions .....	144
5.2.2.1 Common Aberration Analyses .....	144
5.2.2.1.1 Genomic Identification of Significant Targets in Cancer .....	144
5.2.2.1.2 Significance Testing for Aberrant Copy Number (STAC) .....	144
5.2.3 The most statistically significant focal SCNAs .....	148
5.2.3.1 <i>CDKN2A</i> gene .....	148
5.2.3.2 <i>TERT</i> gene .....	150
5.2.3.3 Other significant candidate genes .....	152
5.2.4 Assessment of protein expression by IHC .....	155
5.2.4.1 Evaluation of staining .....	155
5.2.4.2 <i>CDKN2A</i> protein expression .....	156
5.2.4.3 <i>TERT</i> protein expression .....	159
5.3 Discussion .....	163
5.3.1 Most statistically significant candidate genes .....	163
5.3.2 Assessment of protein expression by IHC .....	165
<b>Chapter Six</b> .....	169
6.1 General discussion .....	171
6.1.1 Objective of this PhD study .....	171
6.1.2 Are there any early changes in Conjunctival melanoma? .....	171
6.1.3 Does the data from the array-CGH coexist with the finding of mutations and how does that related to IHC and clinical data? .....	172
6.1.4 Technical issue during this study .....	173
6.1.5 Future Work .....	174
References .....	175
Appendices .....	195

## List of Figure

Figure 1.1: Diagram of the structure of the eye illustrating the tissue origins of ocular Melanoma .....	22
Figure 1.2: Hematoxylin and eosin stained section of the conjunctiva Histologically, the conjunctiva can be divided into three parts .....	26
Figure 1.3: Illustrating types of melanocytic cells that are found in conjunctival melanoma .....	29
Figure 1.4: A typical conjunctival naevus. a) Slit-lamp appearance. b) A light micrograph stained with haematoxylin and eosin .....	30
Figure 1.5: The Mitogen-Activating protein (MAP) Kinase and Phosphatidylinositol 3 Kinase (PI3k) Pathway .....	37
Figure 1.6: Diagram illustrated the promoter region of <i>TERT</i> with nucleotide numbering of the molecular location on chromosome 5 .....	40
Figure 1.7: Diagram showing a new cell line of recurrent conjunctival melanoma .....	42
Figure 1.8: individual chromosome penetrance plot of conjunctival melanoma ..	43
Figure 2.1: Schematic diagram of the array-based comparative genomic hybridization .....	63
Figure 3.1: Illustrating a sample of UM (Mel 585) cells in culture at passage 18 .....	84
Figure 3.2: An example of early culture of primary tumour showing proliferating spindle-shaped cells growing radially outwards from an adherent piece of tissue .....	85
Figure 3.3: Showing growth of Mel 621 cells in culture at passage 11 .....	86
Figure 3.4: Illustrating growth of Mel 635 cells lines at passage 8 .....	87
Figure 3.5: An example of Metaphase Chromosome Spread from highly abnormal sarcoma STS 06/11 cells at passage 65, kindly supplied by Dr. A. Salawu .....	88
Figure 3.6: A and B showing an example of Metaphase Chromosome Spread and karyotype from Mel 621 .....	89
Figure 3.7: Array-CGH ideograms of chromosomal aberrations in primary fresh frozen UM tissue (Mel 562) .....	90

Figure 3.8: Array-CGH ideograms of primary short-term cultures of ConM (Mel 621).....	91
Figure 3.9: Array-CGH ideograms of primary short-term cultures cell of ConM (Mel 635).....	91
Figure 3.10: Array-CGH ideograms of a primary uncultured tumour of ConM (Mel 568).....	92
Figure 3.11: Chromatogram sequencing traces for short-term culture samples showing the wildtype for <i>BRAF</i> , <i>NRAS</i> , <i>GNAQ</i> , <i>GNA11</i> .....	93
Figure 3.12: FISH Image illustrating a lack of genetic imbalance (GI) for chromosomes 3 and 8 as found in primary short-term cultures of both ConM 621 and 635.....	94
Figure 4.1: Wild-type and mutant sequence chromatograms of <i>BRAF</i> exon 15.....	105
Figure 4.2: Wildtype sequence chromatograms of <i>BRAF</i> exon 11.....	106
Figure 4.3: Wildtype and mutant sequence chromatograms of <i>NRAS</i> gene.....	107
Figure 4.4: Wildtype and mutant sequence chromatograms of <i>GNAQ</i> gene.....	108
Figure 4.5: Wildtype and mutant sequence chromatograms of <i>GNA11</i> gen.....	109
Figure 4.6: Wildtype and mutant sequence chromatograms of <i>TERT</i> gene.....	111
Figure 4.7: Individual Array-CGH ideograms of chromosomal aberrations in primary conjunctival melanoma frozen tissue (ConM 15).....	114
Figure 4.8: Individual chromosome penetrance plots of 21 conjunctival melanoma tumours.....	115
Figure 4.9: Frequency Plot of Common Genomic Copy Number Aberrations among 21 conjunctival melanoma tumours using Nexus software.....	116
Figure 4.10: A high-resolution image of chromosomes illustrating focal amplifications of oncogenes and homozygous deletions of tumour suppressor genes revealed by Array-CGH.....	118
Figure 4.11: DNA copy number profiles of different melanoma subtypes.....	121
Figure 4.12: Individual Array-based CGH ideograms for different melanoma subtypes.....	122
Figure 4.13: Frequency plot of the genomic view comparing <i>BRAF</i> mutations with wildtype and <i>NRAS</i> with wildtype.....	124
Figure 4.14: Penetrance plots of DNA copy number profiles among conjunctival melanomas comparing the samples that have <i>TERT</i> mutations and wild type	

Figure 4.15: Penetrance plots of DNA copy number profiles of 21 cases of conjunctival melanomas according to the original clinical data.....	128
Figure 5.1: Summary of work-flow chart for Array-CGH data analysis and short list of candidate gene identification.....	141
Figure 5.2: Frequency Plot and Stacked SCNA from Individual ConM Cases.....	143
Figure 5.3: Statistically significant common genomic CNAs among ConM cases detected by using the GISTIC algorithm.....	147
Figure 5.4: Frequency plot of SCNA affecting the <i>CDKN2A</i> gene locus.....	149
Figure 5.5: Frequency plot of SCNA affecting the <i>TERT</i> gene locus.....	151
Figure 5.6: Evaluation of <i>CDKN2A</i> protein expression in ConM samples using IHC.....	158
Figure 5.7: Evaluation of <i>TERT</i> protein expression in ConM samples using IHC.....	161
Figure 6.1: Outline of the approach used in this PhD study and the major finding in each section.....	170
Figure 1A: Array-CGH ideograms of frozen tissue of ConM (ConM 16) which have GNAQ mutation .....	200

## List of Tables

Table 1.1: Comparison between cutaneous and ocular melanomas (Uveal and Conjunctival melanoma) adapted from Jovanovic et al. (2013)	24
Table 1.2. Summary of some studies investigating genetic alterations in conjunctival melanomas	36
Table 2.1: General laboratory chemicals and reagents	47
Table 2.2: The plastic ware used in this study	48
Table 2.3: Tissue culture medium with supplements	49
Table 2.4: Primer sequences for <i>BRAF</i> , <i>GNAQ</i> , <i>GNA11</i> , <i>NRAS</i> and <i>TERT</i> and the product size expected	54
Table 2.5: Summaries of all the primary antibodies and their conditions that used in this study	56
Table 2.6: Digestion Master mix components	64
Table 2.7: Labelling Master Mix components	65
Table 2.8: Hybridization master mix components	66
Table 2.9: ULS Labelling Master Mix Components	67
Table 2.10: Hybridization master mix components	68
Table 2.11: QC metric thresholds for Array-CGH experiments	70
Table 2.12: A master mix PCR components for each of the genes tested	72
Table 2.13: Thermocycler PCR conditions based on each gene tested	73
Table 4.1 Summary of all the samples sequenced with <i>BRAF</i> exon 11 & 15, <i>NRAS</i> exon 1 and 2, <i>GNAQ/GNA11</i> Q209 exon 5 and <i>TERT</i> promoter	112
Table 4.2: Summary of all the most frequent focal CNAs among the conjunctival melanoma tumours in this study as derived from Agilent software	119
Table 4.3: Summary of the most frequent CNAs among Primary and Metastatic Conjunctival melanomas tumors in this study	127
Table 5.1: Illustrates comparison between STAC and GISTIC logarithms kindly supplied by Dr. A. Salawu	145
Table 5.2: List of significant candidate genes found in 6p25	153
Table 5.3: List of significant candidate genes on chromosome 1q22	154
Table 5.4: Allred scoring system for <i>CDKN2A</i> and <i>TERT</i> antibodies	162
Table 1A: Summary of most copy number variations among conjunctival melanoma tumours used in this study	196

Table 2A: Summary of clinical information among FFPE conjunctival melanoma samples used in this study.....	197
Table 3A: Summary of clinical information among Frozen tissue conjunctival melanoma samples used in this study.....	198
Table 4A Relevance of <i>TERT</i> deletion, mutation and protein expression to conjunctival melanoma.....	199

## List of abbreviations

ATL	Tissue lysis buffer
AL	Lysis buffer
AW1	Wash buffer 1
AW2	Wash buffer 2
AE	Elution buffer
Alu I	Restriction enzymes
Array-CGH	Array Comparative Genomic Hybridisation
Acetylated BSA	Acetylated from bovine serum Albumin
ATS	Allred total score
Bp	Base pair
BAP1	BRCA1-Associated Protein 1
BRAF	B-Raf Proto-Oncogene, Serine/Threonine Kinase
CNVs	Copy number variations
CDKN2A	p16/cyclin-dependent kinase inhibitor 2 A
CCND1	Cyclin D1
ConM	Conjunctival Melanoma
Cy5™	Cyanine 5 fluorophore
Cy3™	Cyanine 3 fluorophore
Cyanine 3-dUTP	Cyanine 3-deoxyuridine triphosphate
Cyanine 5-dUTP	Cyanine 5-deoxyuridine triphosphate
CM	Cutaneous Melanoma
DNA	Deoxyribonucleic acid
DMSO	Dimethyl sulfoxide
DABI	4',6-Diamidine-2'-phenylindole dihydrochloride
Exo-klenow	Exonuclease activity of DNA polymerase I
FASST2	Fast Adaptive States Segmentation Technique 2
FFPE	Formalin Fixed Paraffin Embedded
FISH	Fluorescence in situ hybridization
FBS	Fetal bovine serum
FE	Feature extraction
GISTIC	Genomic Identification of Significant Targets in Cancer
GI	Genetic instability

GNAQ	Guanine nucleotide alpha-subunit Gq
GNA11	Guanine nucleotide binding protein, alpha 11(Gq class)
gDNA	Genomic DNA
HMM	Hidden Markov Model
HPV	Human Papilloma Virus
H <sub>2</sub> O <sub>2</sub>	Hydrogen peroxide
HCL <sub>2</sub>	Hydrochloric acid
IS	Intensity score
IHC	Immunohistochemistry
Kb	Kilobase
KIT	Receptor tyrosine kinase
MYB	Myelo-blastosis
MAPK	Mitogen-activated protein kinase
MCR	Minimal common region
MLPA	Multiplex ligation-dependent probe
MI	Millilitre
ml	microlitre
ng/μl	nanogram/microliter
nm	nanometer
NRAS	Neuroblastoma RAS viral oncogene homolog
NC	Negative control
OaCGH	Oligonucleotide CGH arrays
PBS	Phosphate Buffered Saline
PFA	Paraformaldehyde
PS	Proportion score
PAM	Primary acquired melanosis
pmol	Picomole
PCR	Polymerase Chain Reaction
PTEN	Phosphate and tensin homolog
QC	quality control
RPM	Rotation per minute
RNase	Ribonuclease
RREB1	Ras-responsive element-binding protein 1

Ras I	Restriction enzymes
RPMI-1640	Rosewell Park Memorial Institute
SCNAs	Somatic copy number aberrations
SEER	The Surveillance, Epidemiology, and End Results
SSC	Saline Sodium Citrate
SNR	Signal to Noise Ratio
STAC	Significance Testing for Aberrant Copy Number
SD	Standard deviation
TERT	Telomerase reverse transcriptase
TAE	Tris-Acetate-EDTA
UM	Uveal melanoma
UV	Ultra violet radiation
US	United states
WT	Wild type

# CHAPTER ONE

## Introduction

## 1. Introduction

### 1.1 Cancer as a genetic disease

#### 1.1.1 Historical aspect and hallmarks of cancer

Cancer is the common term given to disease caused by a failure to control growth of cells whose normal processes start to be abnormal. This occurs as a result of mutations in the genes that control cell proliferation and apoptosis. In developed countries, cancer is still the second most common worldwide killer after cardiovascular disease (Jemal et al., 2008, McGuire, 2016). The World Health Organisation defined cancer as the most common human genetic disease that affects many people through North America and Europe and is responsible for around 12% of mortality across the world (Stewart and Kleihues, 2003, Cancer Research UK, 2014). Several theories have been suggested to explain the role of genetics in the development and progression of cancer. Cancer was first documented as a complex genetic disease by Theodor Boveri in 1902, who suggested that alterations in chromosomes could produce unlimited cell growth (Boveri, 1902). Then, Tyzzer (1916) was the first to use the term “somatic mutation” to define the events of cancer progression (Tyzzer, 1916), as reviewed by (Wunderlich, 2007). Some mutations may target genes that serve to suppress cancer development, or tumour suppressor genes as they are known (Stratton et al., 2009). Other genes known as oncogenes, (cancer causing genes) can also be the subject of mutations, and some genes may be abundantly over expressed and act as oncogenes even if they have not mutated (Haber and Stewart, 1985, Zhou et al., 2007). Another theory however, has hypothesised that the accumulation of mutated genes is the main reason for cancer (Nordling, 1953). The first consistent chromosomal abnormality associated with a malignancy was discovered by Nowell and Hungerford (1960) who reported the translocation between chromosomes 9 and 22, and later called the Philadelphia translocation, which occurs in chronic myeloid leukaemia, as reviewed by Nowell (1976) and Nowell (2007). Evidence has supported the theory that the cancers begin after the accumulation of different mutations in genes responsible for cell growth and differentiation (Olopade and Pichert, 2001a). The most important features that a

cell must require for it to become malignant, and for the development and progression of tumours to proceed, have been proposed by Hanahan and Weinberg (2000) as the “six hallmarks of cancer; self-sufficiency of growth signals, insensitivity to antigrowth signals, evasion of apoptosis, sustained angiogenesis and tissue evasion, limitless replicative potential and metastasis” (Hanahan and Weinberg, 2000). A decade later, they expanded these hallmarks to involve another four including: “genome instability and mutation, avoiding immune surveillance, tumour-promoting inflammation and deregulation of cellular energetics”. These hallmarks provide researchers a greater understanding of cancer development and its essential mechanisms (Hanahan and Weinberg, 2011).

### **1.1.2 Aetiology of cancer development**

As discussed above, it has been hypothesised that cancer occurs after the accumulation of multiple mutations in genes responsible for the control of cell growth. These mutations may occur as a result of unrepaired DNA damage or errors in the cell cycle replication process (Jackson and Loeb, 1998, Olopade and Pichert, 2001b). Some studies suggest that a very few cancer cases, only around 0.1-10% depending on type, can be hereditary such as breast cancer and ovarian cancer run together in families with hereditary breast and ovarian cancer syndrome. Colon and endometrial cancers tend to go together in Lynch syndrome (Loeb and Loeb, 2000, Hahn and Weinberg, 2002). Of the remaining cancers, some might arise *de novo* and progress by the accumulation of genetic changes (Houlston and Peto, 1996), whereas others might occur due to acquired factors such as interactions with the environment and unhealthy lifestyles (Anand et al., 2008). For instance, chemical carcinogens such as tobacco smoke are responsible for the tumorigenesis of many cancers, including oral, pharynx and lung cancer, and can affect the behaviour of the respiratory epithelial cells (Fiala et al., 2005, Steiling et al., 2008). In addition, there are also physical carcinogens, including ultraviolet light (UV), that can cause damage to the DNA (Hall and Angele, 1999, Multani et al., 2000). One of the best examples is skin cancer; it has been estimated that about 90% of all skin cancers are caused by exposure to sunlight and the effect of UV radiation (Ramos et al., 2004, Boniol

et al., 2012). Other risk factors include infectious agents, such as viruses and bacteria, which have been identified as causing around 15% of cancers (IRAC, 1994). For example, *Helicobacter pylori* bacteria causes gastric cancer (Ding et al., 2007), Human Papilloma Virus (HPV) can cause prostate or cervical cancer (Adami et al., 2003) and Hepatitis B & C viruses have a strong correlation with liver cancer (Hussain et al., 2007). In addition, the ageing process might be associated with the possibility of developing cancer since the cells in elderly people sometimes show a deterioration in their ability to repair DNA damage that occurs during cell division, especially in response to other environmental factors (Chung et al., 2011, Meng and Lu, 2012). The reason behind this, still unclear, however; whether the link between cancer and age occurs due to an accumulation of genetic and epigenetic mutations or due to a higher susceptibility to oncogenic mutations among ageing people (Lopez-Otin et al., 2013).

### **1.1.3. Analytical techniques used in cancer research**

Chromosomal instability is usually reflected in abnormal karyotypes, with both structural and numerical chromosomal abnormalities. The detection of these abnormalities plays an essential role to identified different type of cancers and serve as diagnostic and prognostic biomarkers (Michor et al., 2005). Several types of cytogenetic and genetic mutations might lead to the onset of cancer. Most of these changes occur at the chromosomal structure, such as aneuploidy, the loss or gain of a number of chromosomes, or polyploidy, an increase in the number of chromosomes by an exact multiple of the haploid number (Mitelman et al., 1997, Kirsch-Volders et al., 2002). Nowadays, there is a better understanding of basic genetic and molecular abnormalities through the using of analytical techniques such as karyotyping, fluorescence in situ hybridisation (FISH) and spectral karyotyping (SKY), which help to build up clear images of clonal and non-clonal alterations at the single cell level. Molecular cytogenetic techniques, are used in the majority of cancer types to identify an abnormal number of chromosomes, with genomic structural rearrangements (Hanahan and Weinberg, 2011). Moreover, FISH techniques go beyond conventional cytogenetics in that they open up the possibility of achieving cytogenetic results from interphase nuclei and metaphase chromosomes (Wang, 2002). In addition, array comparative

genomic hybridisation (array-CGH) has the ability to detect any genomic amplification and deletions (gains and losses), single nucleotide polymorphisms (SNP), to provide information about copy number alterations that might be linked to specific types of cancer (Albertson et al., 2003, Jemal et al., 2008, Siegel et al., 2013). Recently, the use of powerful molecular techniques such as next generation sequencing has helped to achieve the sensitive detection of low frequency mutations, which are driven by molecular alterations (Meyerson et al., 2010). Certainly, the analysis of the genomic sequence has played a significant role in cancer biology, and provides valuable information for cancer diagnosis and therapy. Nonetheless, although there is some information available for some of the most common cancers, there have not been many genetic studies on rare forms of cancer, particularly cancers of the eye.

## 1.2 Overview of eye cancer

Both benign and malignant primary tumours can affect all parts of the eye, and in addition to primary tumours that start within the eye, metastatic tumours spread from other organs including those in the breast, lung and gastrointestinal tract (Spencer, 1985, Damato and Coupland, 2012). There are two types of primary tumours that affect the eye and other related structures: extraocular or intraocular. An extraocular tumour occurs in the surrounding tissue of the eye. One such tumour is Rhabdomyosarcoma of the orbital muscle. This is a type of sarcoma of the head and neck that originates in the soft tissue (muscle), connective tissue (tendon) or bone and is most common in childhood. It comprises 4% of all pediatric tumours, with 10% of all cases occurring in the orbit (Arndt and Crist, 1999, Shields and Shields, 2003, Jurdy et al., 2013). Intraocular tumours however, occur inside the eye and include some very rare primary tumours such as Retinoblastoma and Uveal melanoma (UM), which are the most common primary intraocular tumours in children and adults respectively (McLaughlin et al., 2005, MacCarthy et al., 2009, Sisley et al., 2009, Villegas et al., 2013, Kaliki et al., 2015).

Ocular melanoma is a primary intraocular tumour and includes UM and conjunctival melanoma (ConM). It is a cancer that develops from neural crest derived melanocyte cells, which are responsible for the production of melanin pigment. These cells are normally found in various locations in the body, such as the skin, hair and the uveal tract of the eye (Slominski et al., 2004, Wong et al., 2005, Damato and Coupland, 2012, Jovanovic et al., 2013). Ocular melanoma is considered to be the second most common location for primary malignant melanoma after cutaneous melanoma (CM) (Egan et al., 1988, McLaughlin et al., 2005, Ferlay et al., 2010, Iannaccone et al., 2015). The most common type arises from UM, which includes the choroid, ciliary body and iris and constitutes 82.5% of all ocular melanoma cases, whereas ConM occurs in the thin lining layer that covers the white part of the eye (the conjunctiva) and is far less frequent (McLaughlin et al., 2005), (Figure 1.1).

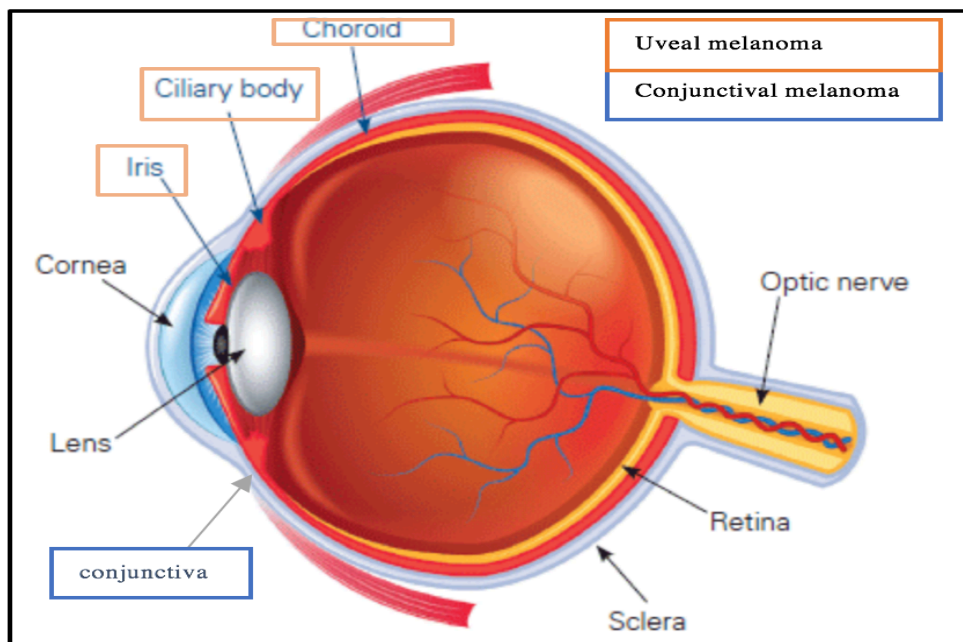


**Figure 1.1: Diagram of the structure of the eye illustrating the tissue origins of Ocular Melanoma.** ConM arises in the mucous membrane of the conjunctiva while UM affects the iris, ciliary body or choroid. Figure adapted from [www.cancernetwork.com](http://www.cancernetwork.com). Accessed on 10/1/2014.

Although, ocular melanoma is the second most common type of melanoma, it is still rare, representing about 3.7% of all melanoma patients (McLaughlin et al., 2005, Damato and Coupland, 2012, Kalirai et al., 2017). The incidence of ocular

melanoma in the United States (US) is estimated to be around six per million people, compared to about 153.5 cases per million for CM (Jovanovic et al., 2013). The incidence of UM and ConM in the US however, are about 4.9 and 0.4 per million respectively, with incidence of UM being higher in males than in females in both the US and Australia (Vajdic et al., 2003b, McLaughlin et al., 2005). Furthermore, the rates of ocular melanoma are about 8-10 times higher amongst white patients, however for CM the increased risk is 16 times more for the white population (Damato and Coupland, 2012), while ConM is only 2.6 times more frequent amongst white patients compared to black patients, which is similar to the frequency of mucosal melanomas (Hu et al., 2008, Jovanovic et al., 2013).

There are many differences between ConM, CM and UM, and these are detailed in (table 1.1). Differences in known genes involvement in these subtypes of melanoma will be discussed in more detail later in the following chapters. Although rare, ocular melanoma is a life-threatening disease, and therefore a good understanding of the basis of genetic and molecular changes may provide the opportunity for the development of targeted therapy to improve the prognosis of patients with metastatic disease (Triozi et al., 2008, Patel et al., 2011, Larsen et al., 2015).

Table 1.1: Comparison between cutaneous and ocular melanomas (Uveal and Conjunctival melanoma) adapted from Jovanovic et al. (2013).

	<i>Cutaneous melanoma</i>	<i>Uveal melanoma</i>	<i>Conjunctival melanoma</i>
<b>Origin</b>	Melanocyte situated in	Melanocyte located	Melanocyte situated
	the basal layer of the epidermis of the skin.	in the Uveal layer of the eye	in the basal layer, of the conjunctiva.
<b>Role of UV as a risk factor</b>	Well supported	Still uncertain	Still uncertain
<b>Male vs Female rate</b>	193.7:125.2 per/million	5.7:4.4 per/million	0.4 per/million both genders
<b>Route of spread</b>	Lymphatogenous	Haematogenous	Lymphatogenous
	Haematogenous		Haematogenous
<b>Most common site of metastases</b>	Skin 38%	Liver 93%	Lymph node
	Lymph node	Lung, Bone	Lung, Liver, Skin, Brain
	Lung, liver, bone		
<b>Five-year survival</b>	80.80%	81.60%	86.30%
<b>Treatment</b>	91.5% Surgery only	28.3% Surgery	Surgery combine
		62.5% Radiotherapy	with adjuvant therapy

### **1.3 Conjunctival melanoma**

ConM occur from melanocytes located in the basal layer of the epithelium of the conjunctival membrane. Unlike other mucous membranes, there is only a small part of the conjunctiva, the bulbar, which is directly exposed to solar UV radiation (Isager et al., 2006, Jovanovic et al., 2013, Kalirai et al., 2017). ConM are rare ocular tumours but their incidence, like that of CM, is increasing (Inskip et al., 2003, Triay et al., 2009). They comprise about 5% of all ocular melanomas and about 1.6% of all non-cutaneous melanomas (Scotto et al., 1976, Seregard, 1998a, Seregard, 1998b, Shields, 2002) compared to their counterpart, UM, which accounts for roughly 80% of all non-cutaneous melanomas (Scotto et al., 1976, Damato and Coupland, 2012). The rarity of this melanoma means that few controlled trials have been conducted to outline the best treatment to improve mortality rates (Shields et al., 2011, Larsen et al., 2015).

#### **1.3.1 Epidemiology and incidence**

The incidence of ConM increases with age, with more than half of patients being over age 60 years, but it is rarely seen before the age of 20, although a few cases of ConM in children have been reported (Strempele and Kroll, 1999, Shields et al., 2000, Brownstein et al., 2006, Jovanovic et al., 2013). It most commonly occurs in the white population, with an incidence of 0.1 to 0.08 per million compared to an incidence of 1% in African-American patients (Shields et al., 2004a, Shields et al., 2011, Shields et al., 2017). In addition, the incidence is nearly equal in both sexes (Seregard and Kock, 1992, Wolff-Rouendaal, 2009, Zembowicz et al., 2010).

#### **1.3.2 Histopathological features**

Histologically, the conjunctiva is divided into three regions; the bulbar conjunctiva covers the eyeball, extending from the limbus (corneo-scleral junction) over the anterior sclera; the tarsal or palpebral conjunctiva lines the posterior surface of the eyelids; and the fornix conjunctiva is a smooth, flexible, protective sac formed between the bulbar and palpebral conjunctiva, which cover the anterior portion of

the eye (Peri-corneal surface), (Figure 1.2). ConM usually develops within the bulbar conjunctiva, rather than the forniceal or palpebral conjunctiva (Shields et al., 2011).

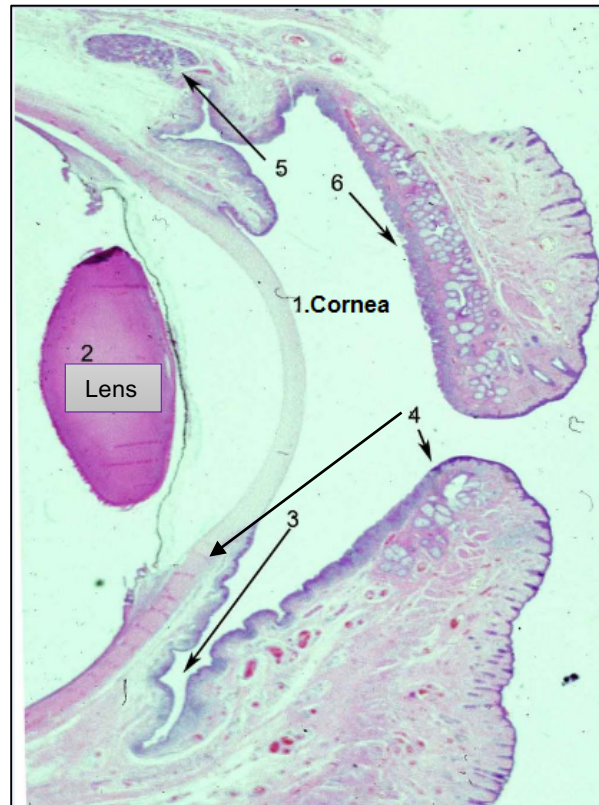


**Figure 1.2: Haematoxylin and eosin stained section of the conjunctiva. Histologically, the conjunctiva can be divided into three parts: 1) cornea. 2) Lens. The inferior fornix conjunctiva (arrow 3) and the bulbar-conjunctiva (arrow 4); the palpebral portion of the lacrimal gland is also shown (arrow 5), the tarsal or palpebral conjunctiva (arrow 6) line the posterior surface of the eyelid. Figure adapted from [www.images.missionforvisionusa.org](http://www.images.missionforvisionusa.org).**

ConM often present as elevated pigmented lesions usually covered with an area rich in blood vessels. Patients usually describe it as a pigmented spot or lump, while irritation and pain are rare (Shields et al., 2000). This lesion can occur on any part of the conjunctiva but the most invasive part is the bulbar conjunctiva. Other less common sites of origin are the palpebral and forniceal conjunctiva, plica semilunaris and the caruncula (Anastassiou et al., 2002, Nasser and Esmaeli, 2011, Harooni et al., 2011).

ConM usually develop from intra-epithelial melanocytes; that are normally sited in the basal layer of the epithelium of the conjunctival membrane, and which have long dendritic processes supplying melanin pigment into the adjacent epithelium to protect the eye from UV light (Shields et al., 2008b). During malignancy, these melanocytes will lose their dendrites and show uncommon structures such as an epithelial morphology with a large nucleus and prominent nucleoli. They also tend to increase in number and invade the more superficial layers of the epithelium, forming nests and increasing in density until most of the epithelium is replaced by atypical melanocytes (Shields et al., 2008a, Damato and Coupland, 2009, Damato and Coupland, 2012).

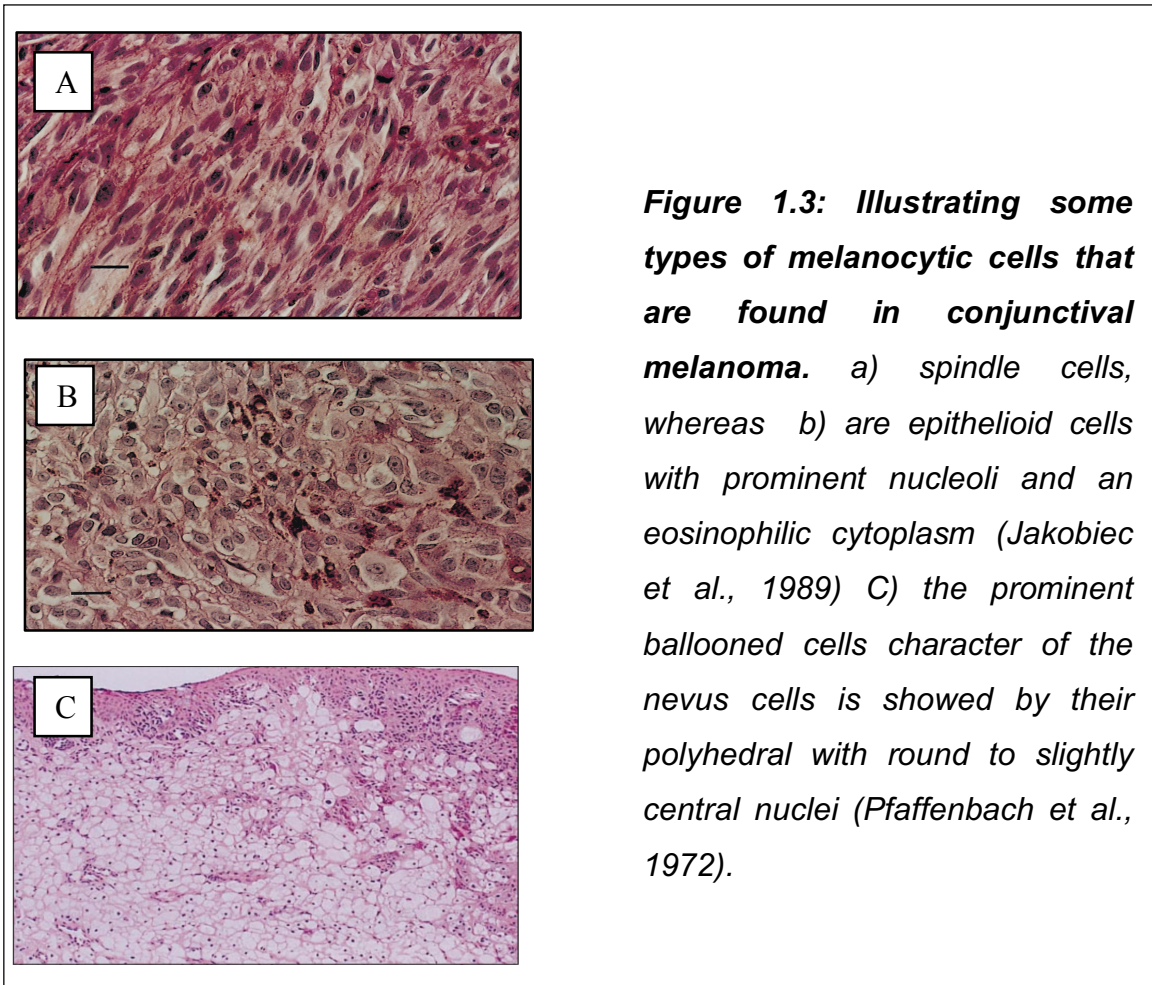
### 1.3.3 Aetiology

The aetiology behind this condition is unclear although some studies have proposed that it is a result of increased exposure of the conjunctiva to UV light (Tucker et al., 1985, Tuomaala et al., 2002, Lake et al., 2011a). Such risk factors that may be associated with this condition include fair skin, a tendency to sunburn and a significant number of cutaneous naevi (Seregard, 1998a, Vora et al., 2017). There is also evidence reported that ConM can arise from primary acquired melanosis (PAM), pre-existing naevi or as *de novo* lesions (discussed in the next section) (Damato and Coupland, 2008). It may be difficult to determine the precursor lesion in many cases but approximately 60% of cases of ConM arise from PAM (Tuomaala et al., 2002, Missotten et al., 2005b, Hu et al., 2008). Data from different studies suggested that 10-74% of ConM cases are associated with PAM and about 1-26% are associated with conjunctival naevi (Shields et al., 2011, Jovanovic et al., 2013).

#### 1.3.3.1 Primary acquired melanosis

Most studies have emphasised that PAM is a serious melanocytic lesion that has potential for malignant transformation (Shields et al., 2000, Shields et al., 2007). It is referred to by other names that reflect this potential, such as precancerous melanosis and benign acquired melanosis; and has also been known as intraepithelial melanocytic hyperplasia, which defines the disease process

(Harooni et al., 2011). However, the name PAM was adopted by the World Health Organization to describe a flat brown patchy lesion of conjunctival pigmentation (Folberg 1996, Shields et al., 2008a). PAM can slowly progress over many years, extending into larger areas of the conjunctiva and skin, and it is usually unilateral and found in middle-aged Caucasians (Kirkwood and Kirkwood, 2010). PAM can arise in any area of the conjunctiva such as the fornix and palpebral conjunctiva, however, if the palpebral conjunctiva is involved the pigmentation may spread into the eyelid margin to include the epidermis (Lin and Ferrucci, 2006). It is mostly found at the limbus and in the interpalpebral area and it may extend to the corneal epithelium, a feature that is usually associated with a worse prognosis (Lin and Ferrucci, 2006). PAM can be classified into two groups based on the presence or absence of atypia. Almost 13% of lesions with atypia eventually progress to invasive melanoma and carry a greater risk for malignant transformation PAM with mild atypia or without atypia is unlikely to show progression to melanoma (Shields et al., 2007)(Irvine et al., 2012). Four different types of atypical melanocytes have been described in ConM including small polyhedral cells, balloon cells, epithelioid cells, and spindle cells (Jakobiec et al., 1989, Jovanovic et al., 2013) (Figure 1.3).



### 1.3.3.2 Naevus

Conjunctival naevi are benign lesions of melanocytic naevus cells usually located at the nasal or temporal limbus and rarely in the fornix, tarsus or cornea, as shown in figure 1.4 (Shields et al., 2004b). Most cases present during the first decade, but they can be found in patients of all ages, including young adults or the elderly (Thiagalingam et al., 2008). They are most common in Caucasians without specific distinction according to the sex of the patient. They can be classified based on histopathology into junctional, compound, subepithelial, and other less common subtypes such as blue and combined naevi (Shields et al., 2004b). Some reported evidence has shown that approximately 20-25% of patients with ConM have a benign conjunctival naevus although conjunctival naevi rarely progress to melanoma, but if this does occur, there is a significant mortality rate of about 13% (Albreiki et al., 2012).

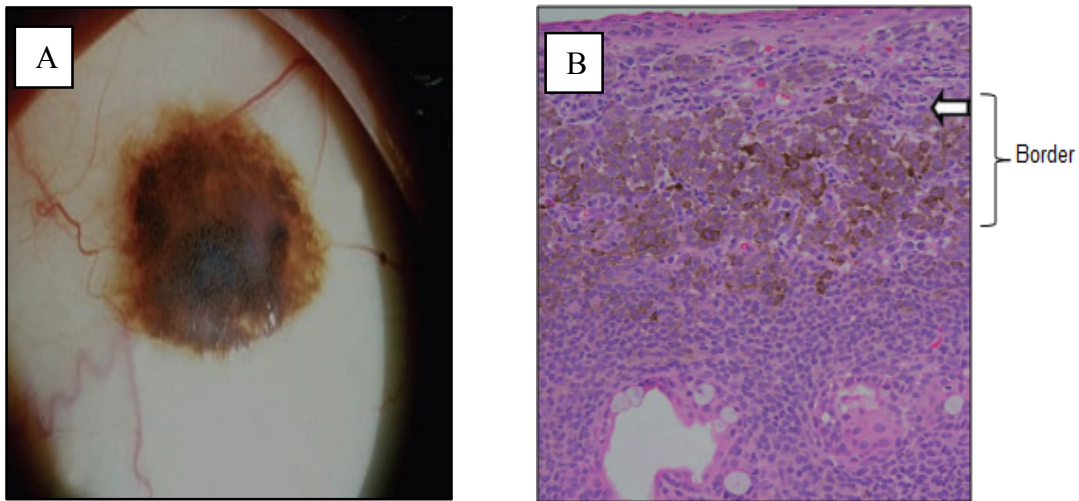


**Figure 1.4: A typical conjunctival naevus. a) Slit-lamp appearance. b) A light micrograph stained with haematoxylin and eosin; the arrow shows the border between the intraepithelial and sub-epithelial naevus. Cysts present in the lower part of the figure and these are typical of conjunctival naevi (Damato and Coupland, 2008).**

#### 1.3.3.3 *De novo* lesions

Melanomas arising from *de novo* lesions are probably far less common than melanomas deriving from PAM or naevi (Seregard and Kock, 1992). Roughly 20% of ConM cases arise from *de novo* lesions (de Wolff-Rouendaal and Oosterhuis, 1983, De Potter et al., 1993, Wolff-Rouendaal, 2009). In addition, it is possible that in some of these cases the precursor lesion may no longer be recognised and *de novo* presentation may in fact be even rarer (Seregard, 1998a). The most common *de novo* site can be found at the limbus, where the lesion typically has a short horizontal growth followed by a rapid vertical growth (Jakobiec et al., 1989).

#### 1.3.4 Clinical /pathological prognostic factors

Various studies have demonstrated that the prognosis of ConM is associated with several clinical and histopathological features (Seregard, 1998a, Shields et al., 2000, Anastassiou et al., 2002, Jovanovic et al., 2013). The most important clinical features associated with prognosis are discussed in the following sections.

#### 1.3.4.1 Tumour location

Tumour locations involving the palpebral conjunctiva, plica, carunculae, fornices and eyelid borders lead to a higher mortality rate (Paridaens et al., 1994, Shields et al., 2000, Anastassiou et al., 2002, Shields et al., 2011, Jovanovic et al., 2013). In addition, other studies reported that tumours found in non-epibulbar locations were also associated with increased mortality compared to epibulbar locations, which show a lower rate of local recurrence and distant metastases (Tuomaala et al., 2002, Missotten et al., 2005a, Jovanovic et al., 2013).

#### 1.3.4.2 Tumour depth and size

Increasing tumour thickness and diameter are also indications of poorer prognosis as well as predictive of lymphatic spread, distant metastases and melanoma-related mortality (Heindl et al., 2011, Damato and Coupland, 2012, Kalirai et al., 2017). Based on histopathologic findings, most authors agree on the depth of the tumour as a prognostic value, but there is controversy about the relevance of tumour thickness. Some authors maintain that a minimal 1.5 mm depth is critical whereas others claim that prognosis is worse in tumour thicknesses of more than 0.8 mm (Folberg et al., 1985, Fuchs et al., 1989), 1.0 mm, or 2.0 mm (Lommatzsch et al., 1990b, Seregard and Kock, 1992).

#### 1.3.4.3 Origin of ConM

Evidence suggests that ConM melanomas arising from *de novo* have a worse prognosis compared to those arising from nevus or from PAM (Reese, 1938, Jay, 1965, Liesegang and Campbell, 1980, Shields et al., 2011). 10 years metastatic diseases usually occurred in 49% of *de novo* compared to 25-26% arising from nevus or PAM (Shields et al., 2011, Jovanovic et al., 2013). These early studies however, did not take account of other potential prognostic factors such as anatomical location, histological thickness and multifocality of the melanoma (Jay, 1965, Liesegang and Campbell, 1980). Finally, Crawford (1980) and Folberg et al. (1985) reported that all these prognostic factors and the recurrences of ConM should be taken into consideration to predict any metastasis (Crawford, 1980, Folberg et al., 1985).

### 1.3.5 Metastases and survival

Metastases in ConM can spread via two ways: lymphatic and haematogenous spreading (Savar et al., 2009, Savar et al., 2011, Jovanovic et al., 2013). The most common regions affected by metastases spread via the lymphatic system to are the parotid, preauricular, submandibular and cervical lymph nodes (Esmaeli et al., 2001, Missotten et al., 2005b). For instance, metastases from a lateral lesion usually spread to the preauricular lymph nodes whereas the medial lesion spreads most commonly to the submandibular lymph nodes (Cook et al., 2002, Lim et al., 2006). In addition, recurrent locations of distant metastases can spread haematogenously to the liver, brain, skin and lungs (Shields et al., 2000, Tuomaala and Kivela, 2004). In rare cases, ConM metastases can extend directly towards the globe or into the orbit, sinuses and cranial cavity (Missotten et al., 2010). In a nationwide study of ConM, Paridaens and colleagues consistently found five and ten-year survival rates at 82.9% and 69.3% (Paridaens et al., 1994). Similarly, Missotten and colleagues reported a five-year survival rate of 86.3% and ten-year survival rate of 71.2% (Missotten et al., 2005a). Berta et al. (2015), meanwhile, found that the 10-year ConM mortality can be up to 30 %, and the recurrence rates after treatment up to 50 %, while the overall incidence of metastasis is 26% (Berta-Antalics et al., 2015). The high rate of recurrent disease remains one of the major problems in the clinical management of ConM.

### 1.3.6 Treatment

The treatment options for ConM involve surgical excision and excision in combination with adjuvant therapies such as cryotherapy, radiotherapy and topical chemotherapy (Mytomicin C) (Lommatzsch et al., 1990a, Finger et al., 1998, Aronow and Singh, 2013, Salazar Mendez et al., 2014, Wong et al., 2014). Newer treatments, such as targeted therapy and immunotherapy for metastases are under investigation, although no established treatment for distant metastasis is available yet (Wong et al., 2014, Brouwer et al., 2017).

#### 1.3.6.1 *Surgical treatment*

The preferred treatment for ConM is usually surgical excision (Folberg, 1996, Shields et al., 1997, Shields et al., 1998, Salazar Mendez et al., 2014). It is currently recommended for a ConM to be removed with a 3-5 mm free conjunctival margin, after which supplemental cryotherapy is performed to the surgical margin (Seregard, 1998b). Missotten et al. (2005) discovered that the chance of recurrence was less when the treatment of primary tumour was excision with brachytherapy compared with other treatments such as excision with cryotherapy or excision alone. Nevertheless, there is still no significant difference in survival between the different treatment approaches (Missotten et al., 2005a).

#### 1.3.6.2 *Exenteration*

The surgical procedures to treat ConM may be classified into local excision or enucleation of the globe with the removal of some of the bulbar conjunctiva, and exenteration of the orbital contents (Seregard, 1998b). To date, both patients and surgeons have preferred to avoid orbital exenteration, both due to the loss of visual function and the resulting poor cosmetic appearance. In some serious cases, however, like deeply invasive and multifocal tumours, exenteration of the orbital contents may be the best option (Paridaens et al., 1994).

#### 1.3.6.3 *Radiotherapy*

In some cases, beta irradiation is immediately used on the surgical margin after tumour excision for better local control and for cosmetic appearance (Paridaens et al., 1994). Many surgeons therefore, recommend using irradiation as an alternative therapy to exenteration (Stannard et al., 2000). Recently, electron beam radiotherapy and proton beam irradiation have been used as other treatments for ConM, but there is limited literature regarding their use (Wong et al., 2014, Heindl et al., 2015).

#### 1.3.6.4 Cryotherapy

Works by freezing the cells, producing ischemia to prevent disruption of the microvasculature (Layton and Glasson, 2002). This helps the epithelial sloughing, involving atypical melanocytes, and the substantia propria, which aids to decrease scar formation. This type of therapy is applied especially in cases with extensive and multifocal tumours. It has the ability to decrease the risk of local recurrence (Jakobiec et al., 1982, Jakobiec et al., 1988, Damato and Coupland, 2009, Lim et al., 2013).

#### 1.3.6.5 Topical chemotherapy

Mitomycin C is a non-specific antibiotic, which isolated from *Streptomyces*, that acts as an alkylating agent to stop DNA synthesis and help breakage of single-stranded DNA (Abraham et al., 2006, Ditta et al., 2011). This topical treatment is not recommended to treat primary tumours with nodular melanomas because of the high rate of local recurrence, but should be considered as an alternative primary treatment for PAM with atypia, and an adjuvant therapy for nodular disease (Finger, 2006, Salazar Mendez et al., 2014).

### 1.3.7 The genetics basis of conjunctival melanoma

There is little known about the genetic alterations involved in ConM, and investigations into the genetic pathogenesis of ConM have thus far been limited mainly to *BRAF* mutational analysis and small cytogenetic studies, as illustrated in (Table 1.2).

### 1.3.7.1 Oncogenic Mutations in ConM

#### 1.3.7.1.1 *BRAF* and *NRAS*

Melanoma that occurs from malignant transformation of melanocytes that includes several genetic changes usually affected many signalling pathways involved mitogen-activated protein kinase (MAPK) or Phosphoinositide 3-kinase (P13K) (Figure 1.5). The MAPK pathway is a significant regulator of cellular proliferation and survival that has been implicated in many different cancers (Luca et al., 2012). All previous studies have shown that ConM share some common genetic alterations with CM but seem to be distinct from UM (Vajdic et al., 2003a, Van Raamsdonk et al., 2010, Westekemper et al., 2011, Zoroquiain et al., 2012, Griewank et al., 2013b). In CM, the most common oncogene mutations are of *BRAF*, *NRAS* and *KIT* while other mutations that have been detected in up to 70% of melanoma patients affect the *RAF* and *RAS* genes (Greene et al., 2009, Dumaz, 2011, Luke and Hodi, 2012). The genetic understanding of ConM is very limited however, with most studies having centered only on the possible role of *BRAF* and its mutation in ConM (Lake et al., 2011b). The *BRAF* gene is a serine/threonine kinase that result in noticeably increased kinase activity of the BRAF protein and leads to constitutive activation of downstream components of the RAS-RAF-MEK-ERK pathway (Wan et al., 2004, Wong et al., 2005). In ConM, *BRAF* mutations match those of CM and have been found predominantly in two small regions of the kinase domain of the *BRAF* molecule (Gear et al., 2004a), most frequently in exon 15, with a single T-A substitution, whilst other mutations have also been found in a region of exon 11 (Brose et al., 2002).

Table 1.2: Summary of some studies investigating genetic alterations in conjunctival melanomas.

Reference	Tissue	Methodology	Finding	No. of cases
<b>Before this PhD study started</b>				
Aubert et al. (1993)	Short-term culture	Tissue culture	Growing cells	IPC292 short-term culture
Dahlenfors et al. (1993)	Short-term culture	karyotyping	4q gain	1 short-term culture
McNamara et al. (1997)	FF	FISH	Trisomy3, 11p gain	1 FFPE
Vajdic et al. (2003)	FFPE	CGH	Loss of 6p,6q,10p,10q(100%), 16q(100%), 17q gain of 8p,11p,13q, and 22q gain	2 FFPE
Spendlove et al. (2004)	FFPE	Direct sequencing	BRAF mutation (14%)	3 of 21 FFPE
Gear et al. (2004)	FFPE	Direct sequencing	BRAF mutation (22%)	5 of 22 FFPE
Nareyeck et al. (2005)	Short-term culture	IHC	Positive (HMB45,S100,MCSP )	2/CRMM1,CRMM2 short-term culture
Goldenberg-Cohen et al. (2005)	FFPE	Direct sequencing	BRAF mutation (40%)	2 of 5 FFPE
Keijser et al. (2007)	Short-term culture	karyotyping	very complex karyogram with gain, loss and rearrangement of almost all chromosome	CM2005.1 short-term culture
Beadling et al. (2008)	FFPE	Direct sequencing	BRAF mutation (26%)	4 of 15 FFPE
			NRAS mutation (0%)	0 of 11 FFPE
			KIT mutation (7.7%)	1 of 13 FFPE
Busam et al. (2010)	FFPE	FISH	RREB1 (6p25) gain 100%	6 of 6 FFPE
			MYB (6q23) loss 100%	6 of 6 FFPE
			CCND1 (11q13) gain 66%	4 of 6 FFPE
Lake and Jmor et al. (2011)	FFPE	Multiplex Ligation-dependant probe amplification (MLPA)	BRAF (7q34) mutation 50%	8 of 16 primary and 4 of 6 metastasis
			CDKN1A (6p21.2) gain	11 of 21 primary ConM/ 3 of 4 metastasis
			RUNX2 (6P21.2) gain	16 of 21 primary ConM/ 4 of 4 metastasis
			MLH1 (3p22.1),	3 of 4 metastais melanoma
			TIMP2(17q25.3) gain	5 of 6 metastais melanoma
			MGMT (20q26.3), ECHS1 (10q26.3) loss	5 and 4 out of 6 respectively metastais
			BDH (3q) gain (85%)	6 of 7melanoma
			FLJ20265 (4P) gain (85%)	6 of 7metastais melanoma
			OPRL1 (20q) gain (71%)	5 of 7metastais melanoma
PAO (10q) gain (100%)	7 of 7 metastasis melanoma			
Mudhar et al. (2013)	FFPE	FISH	RREB1 (6p25) gain 100%	7 of 7 FFPE melanoma
			MYB (6q23) loss 100%	7 of 7 FFPE melanoma
			CCND1 (11q13) gain 85%	6 of 7 FFPE melanoma
<b>After this PhD study started</b>				
Griewank et al. (2013)	FFPE	Direct sequencing	BRAF mutation (29%)	23 of 78 FFPE
			NRAS mutation (18%)	14 of 78 FFPE
		ACGH	losses of 1p,3q,6q,8p,9p,10,11q12q,13,15p and 16q gain of 1q,3p,6p,7,8q,11q,12p,14p, and 17q	30 FFPE melanoma
Griewank et al. (2013)	FFPE	Direct sequencing	BRAF mutation (26%)	10 of 38 FFPE melanoma
			NRAS mutation (13%)	5 of 38 FFPE melanoma
			TERT promotor (32%)	12 of 38 FFPE melanoma
Koopmans et al. (2014)	FFPE	Direct sequencing	TERT promotor (41%)	16 of 39 FFPE melanoma
Larsen et al. (2015)	FFPE	Direct sequencing	BRAF mutation (40%)	19 of 47 FFPE melanoma
Sheng et al. (2015)	FFPE	Direct sequencing	BRAF mutation (8%)	4 of 53 FFPE melanoma
			KIT mutation (11%)	6 of 53 FFPE melanoma
Larsen et al. (2016)	FFPE	Direct sequencing	BRAF mutation (35%)	39 of 111 FFPE melanoma

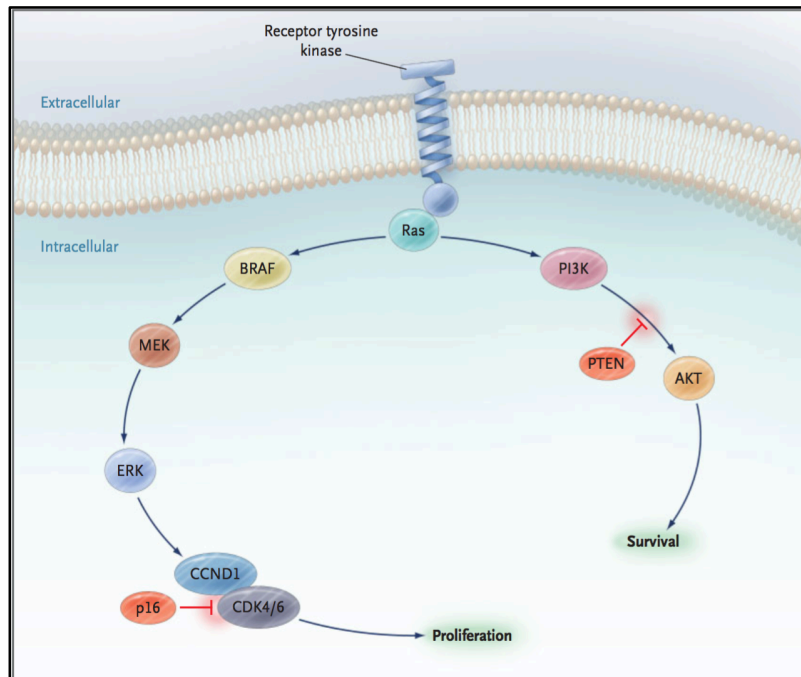


**Figure 1.5: The Mitogen-Activating protein (MAP) Kinase and Phosphatidylinositol 3 Kinase (P13k) Pathway.** Signals from tyrosine can promote proliferation through the MAP kinase pathway (left branch) and survival through the P13 kinase pathway (right branch) (Curtin et al., 2005).

One study reported a G1402A point mutation of exon 11 which encodes a G468R substitution and found it to be associated with *NRAS* mutation (Gorden et al., 2003). However, it is likely that the *BRAF* exon 11 mutation does not provide sufficient stimulus to the MAPK pathway and that the addition of RAS activity is required for adequate activation (Gorden et al., 2003). Previous studies have also shown that *BRAF* V600E mutations are found in 14% to 50% of ConM (Lake et al., 2011a, Griewank et al., 2013b, Larsen et al., 2015). The *BRAF* gene has missense mutations in about 66-80% of primary melanoma tumours, whereas around 59% are found in melanoma cell lines and 80% in melanoma short-term cultures (Brose et al., 2002, Davies et al., 2002). The V600E mutation of *BRAF*, as it is known, is not however found in UM (Seregard, 1998a, Spendlove et al., 2004, Gear et al., 2004b), but to provide more credence for its importance to ConM, *BRAF* mutations have also been detected in approximately 50% of conjunctival naevi (Goldenberg-Cohen et al., 2005).

*NRAS* is one of the family members of the RAS gene. *NRAS* mutations occur in 15% to 20% of melanomas (Omholt et al., 2003, Jakob et al., 2012). Mutations in the other two RAS family members, *HRAS* and *KRAS*, are extremely rare in melanomas (1%–2%). Similar to *BRAF* mutations, *NRAS* mutations have not been detected in UM but have been found in cutaneous nevi (Bauer et al., 2007, Yeh and Bastian, 2009). The majority of *NRAS* mutations affect the nucleotides encoding the G12, G13, and Q61 residues of the protein (Jakob et al., 2012). In melanomas, 80% of *NRAS* mutations affect Q61, while *KRAS* mutations generally affect G12-13 (Riely et al., 2008, Jakob et al., 2012). These mutations lead to GTPase inactivation, resulting in constitutive GTP binding and activation of the protein. RAS activation leads to multiple downstream signalling events. The most well-recognised oncogenic downstream signalling events are phosphorylation and activation of PI3K (phosphatidylinositol 3OH-kinase) and the PI3K/AKT pathway, as well as RAF, leading to mitogen-activated protein (MAP) kinase signalling through the RAS/RAF/MEK/ERK signalling cascade. Clinically, the presence of *NRAS* mutations is associated with primary tumours of greater thickness and poorer prognosis in metastatic disease (Jakob et al., 2012).

#### 1.3.7.1.2 *GNAQ and GNA11*

The most frequent mutation in UM is a somatic mutation in the guanine nucleotide binding protein (G protein), q polypeptide (*GNAQ*) which is detected at chromosome 9q21, as well as guanine nucleotide binding protein (G protein), alpha 11 (Gq class) (*GNA11*) at chromosome 19p13.3 (Raamsdonk et al., 2004). Activating mutations in *GNAQ* and *GNA11* were found in 80% to 90% of uveal melanomas (Van Raamsdonk et al., 2009, Van Raamsdonk et al., 2010). These mutations are also frequent in blue nevi and central nervous system melanocytes (Kusters-Vandeveldt et al., 2010, Wiesner et al., 2012), but are very rare in CM and ConM (Van Raamsdonk et al., 2010, Dratviman-Storobinsky et al., 2010). The vast majority of both mutations (90%) occurs at codon Q209 of exon 5, in a region of the catalytic domain (GTPase), while the minority (5%) of these mutations are found in exon 4 affecting codon R183. Mutation at codon 209 usually occurs as a result of change glutamine substitution to leucine (Q209L) in both *GNA11/GNAQ*, or glutamine substitute to proline (Q209P) in *GNAQ*; furthermore, the mutation in codon 183 is caused by arginine (R) substitution to a

cysteine (C) (Kalinec et al., 1992, Landis et al., 1989). All mutations lead to inhibition of GTPase function and a constitutively GTP-bound activated protein (Kleuss et al., 1994).

#### 1.3.7.1.3 *Recent driver mutations*

A recent driver mutation found in melanoma is the promoter region of *TERT*. This gene is located at chromosome 5p15 and encodes the catalytic reverse transcriptase subunit of telomerase, which is part of the ribonucleoprotein complex of telomeric DNA responsible for maintaining the telomere length at the chromosome ends (Dwyer et al., 2007). This mutation creates a new binding motif for E-twenty-six (ETS) transcription factors (Horn et al., 2013). Although the role of telomerase in tumorigenesis is well established, details regarding its dysregulation in cancer cells remain incompletely understood, particularly in melanoma (Huang et al., 2013b).

A recent study established that the mutation in the *TERT* promoter has been shown in different human cancers, including bladder cancer, hepatocellular carcinoma and different types of gliomas (Killela et al., 2013a). Another two studies have revealed recurrent mutations of the *TERT* promoter in both sporadic and familiar malignant melanomas (Horn et al., 2013, Huang et al., 2013b). They reported that up to 71% of CM harboured novel mutations in the promoter region of *TERT*. These mutations were shown to lead to increased *TERT* expression, most likely by creating ETS transcription-factor-binding sites. Mutations of the *TERT* promoter are quite frequent (32%-41%) in ConM (Griewank et al., 2013a, Koopmans et al., 2014) but have not been detected in UM (Dono et al., 2014). The mutations identified in ConM are identical to those described in CM (Horn et al., 2013, Huang et al., 2013b). The identified hotspot mutations, which cause a cytidine-to-thymidine (C>T) dipyrimidine transition at chromosome 5 base position 1,295,228 (C228T) or at base position 1,295,250 (C250T) (Griewank et al., 2013a, Vinagre et al., 2013, Huang et al., 2013a, Koelsche et al., 2014) (Figure 1.6).

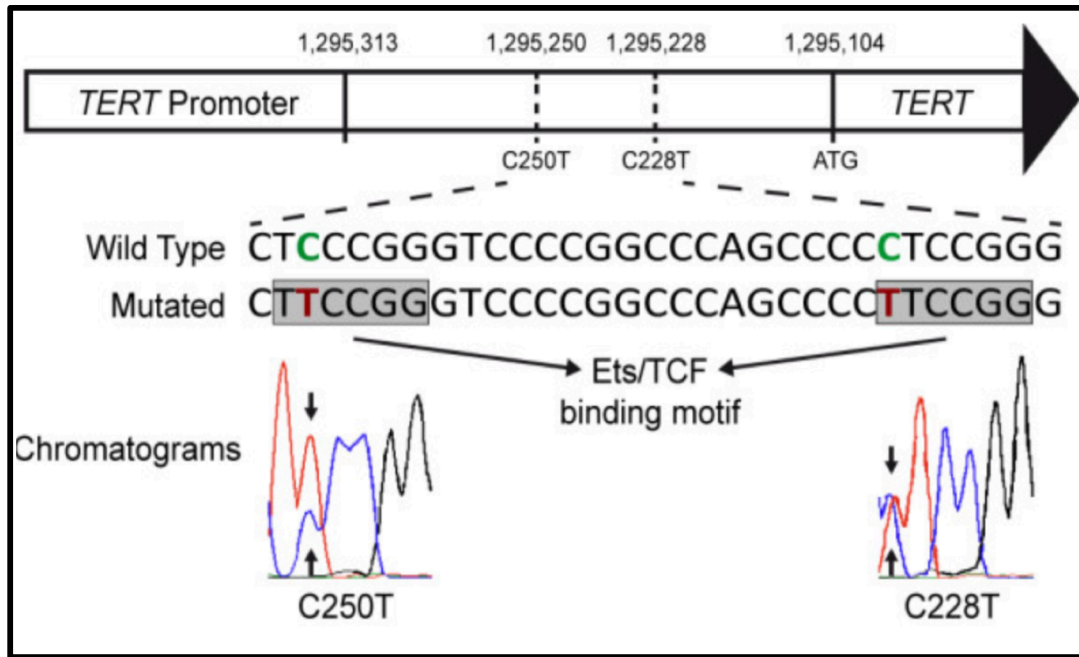


**Figure 1.6:** Diagram illustrated the promoter region of *TERT* with the nucleotide numbering of the molecular location on chromosome 5. DNA sequence of the mutational hotspot region with a wild type and a mutated strand, which displays the nucleotide exchange from cytosine to thymine (represented in red). Chromatogram sequencing represents the heterozygous C228T and C250T mutations (indicated by black arrows). Every mutation formed a new binding motif for E-twenty-six/ternary complex factors (*Ets/TCF*) transcription factors (highlighted by greyish rectangles) (Koelsche et al., 2014).

### 1.3.7.2 Chromosomal aberrations in ConM

Several different procedures have been used to study chromosomal changes in ConM. Fluorescence in situ hybridisation (FISH) is a molecular cytogenetic technique first used in biomedical research in the early 1980s to identify the presence or absence of specific DNA sequences on chromosomes (Langer-Safer et al., 1982) and has been of great value in many studies for clarifying the distinction between melanocytic naevi and CM. Some studies have shown that FISH probes targeting 6p25 (*RREB1*), 6q23 (*MYB*), 11q13 (*CCND1*) and centromere 6 (CEP6) can help in the distinction of conjunctival melanocytic naevi from melanoma (Morey et al., 2009, Gerami et al., 2009, Busam et al., 2010, Mudhar et al., 2013). Busam and colleagues reported gains in *RREB1* (6p25) in

all six of the tumours they studied, and of cyclin D1 (11q13) in four of the six; both of these alterations are frequently found in CM (Busam et al., 2010). In addition, McNamara and colleagues reported in their study that the aberrations seen by using FISH are distinct from those of UM, suggesting different genetic mechanisms for the two ocular tumours (McNamara et al., 1997).

The genetics of ConM have also been investigated by using Multiplex Ligation-Dependent Probe Amplification (MLPA) (Lake et al., 2011a). They reported that eight of 16 of primary tumour samples and four of six of metastatic samples presented *BRAF* V600E gene mutations. Gains of *CDKN1A* and *RUNX2* (both 6p21.2) were detected in 11 and 16 of 21 primary ConM, respectively. Conversely, the most frequent gains in metastatic ConM were *MLH1* (3p22.1) and *TIMP2* (17q25.3), and the most frequent deletions were *MGMT* (20q26.3) and *ECHS1* (10q26.3). Lake's study demonstrated that there were no statistically significant associations between *BRAF* mutation or *CDKN1A* or *RUNX2* amplification and histologic cell type, sex, age, or patient survival (Lake et al., 2011a). Conclusively, all chromosomal changes that have been found so far in ConM indicate a close relationship with CM, in contrast to UM where the most common chromosomal abnormality is monosomy of chromosome 3 (M3) or loss of one copy of chromosome 3, losses of 1p, 8p and gain of 6p and 8q (Griffin et al., 1988, Sisley et al., 1990, Prescher et al., 1990, Aalto et al., 2001). Furthermore, Vajdic et al. (2003a) used chromosomal CGH and found two cases of ConM showing chromosomal changes including 10q and 16q loss, which is similar to what has been found in CM (Vajdic et al., 2003a). Keijser et al. (2007) reported a very complex karyotype in their cytogenetic study, with gains, deletions and changes in nearly all chromosomes being detected in the majority of cultured cells (Figure 1.7) (Keijser et al., 2007). Recently, Griewank et al. (2013) analysed conjunctival melanoma tumours by using Array comparative genomic hybridisation (array-CGH) (Figure 1.8), and reported that their findings were comparable to cutaneous and mucosal melanomas, with gains of 1q, 3p, 7, 17q and losses of 9p, 10, 11, and 12q, but different from UM (Griewank et al., 2013b). This biological information is essential, not only for understanding the pathophysiology of the disease progression, but also for its implications for therapy and for the enrolment of patients in clinical trials of new treatments.

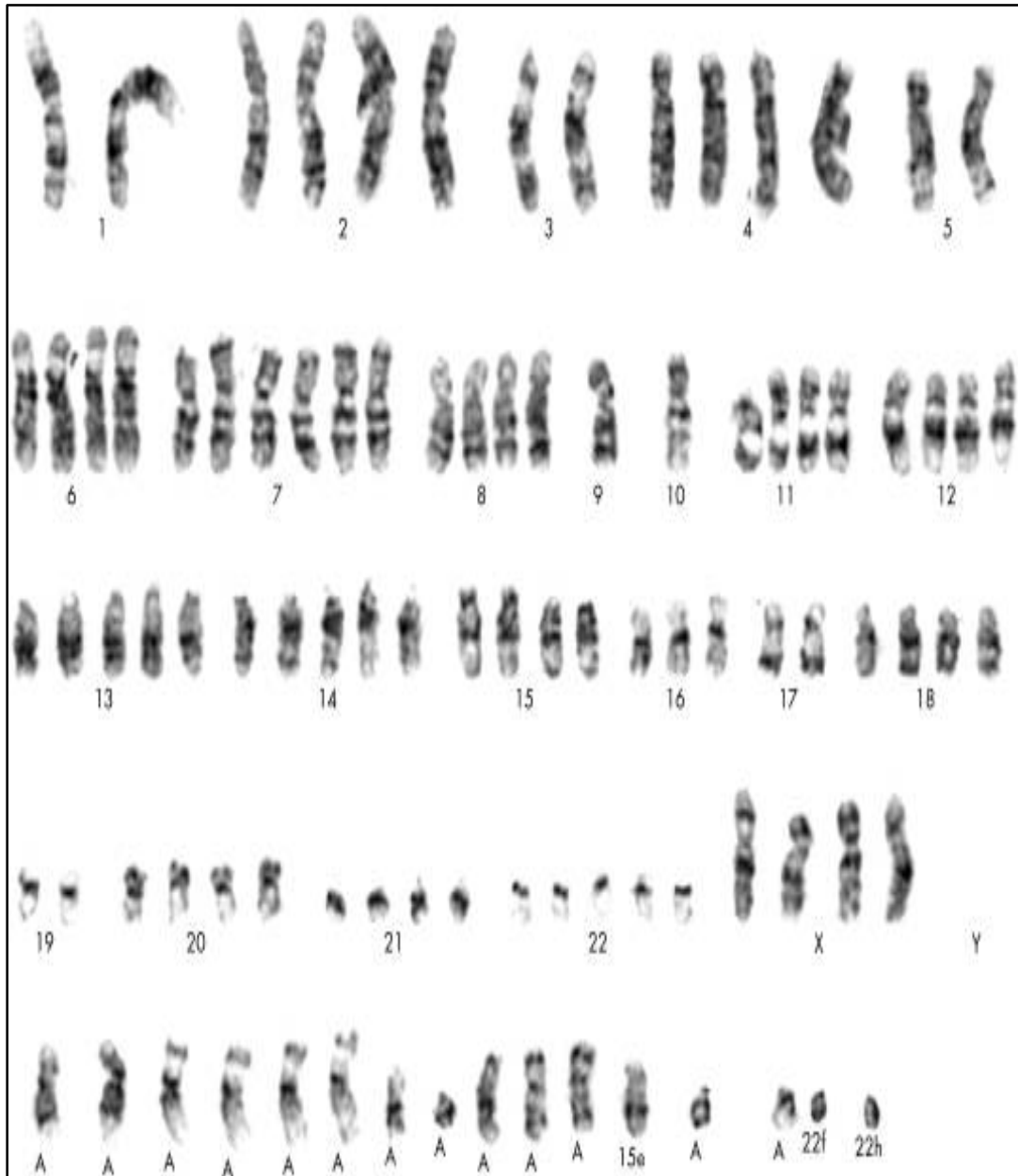


**Figure 1.7: Diagram showing a new cell line of recurrent conjunctival melanoma. A very complex karyogram with gains, deletions and changes in almost all chromosomes being observed in the majority of cultured cells (Keijser et al., 2007).**

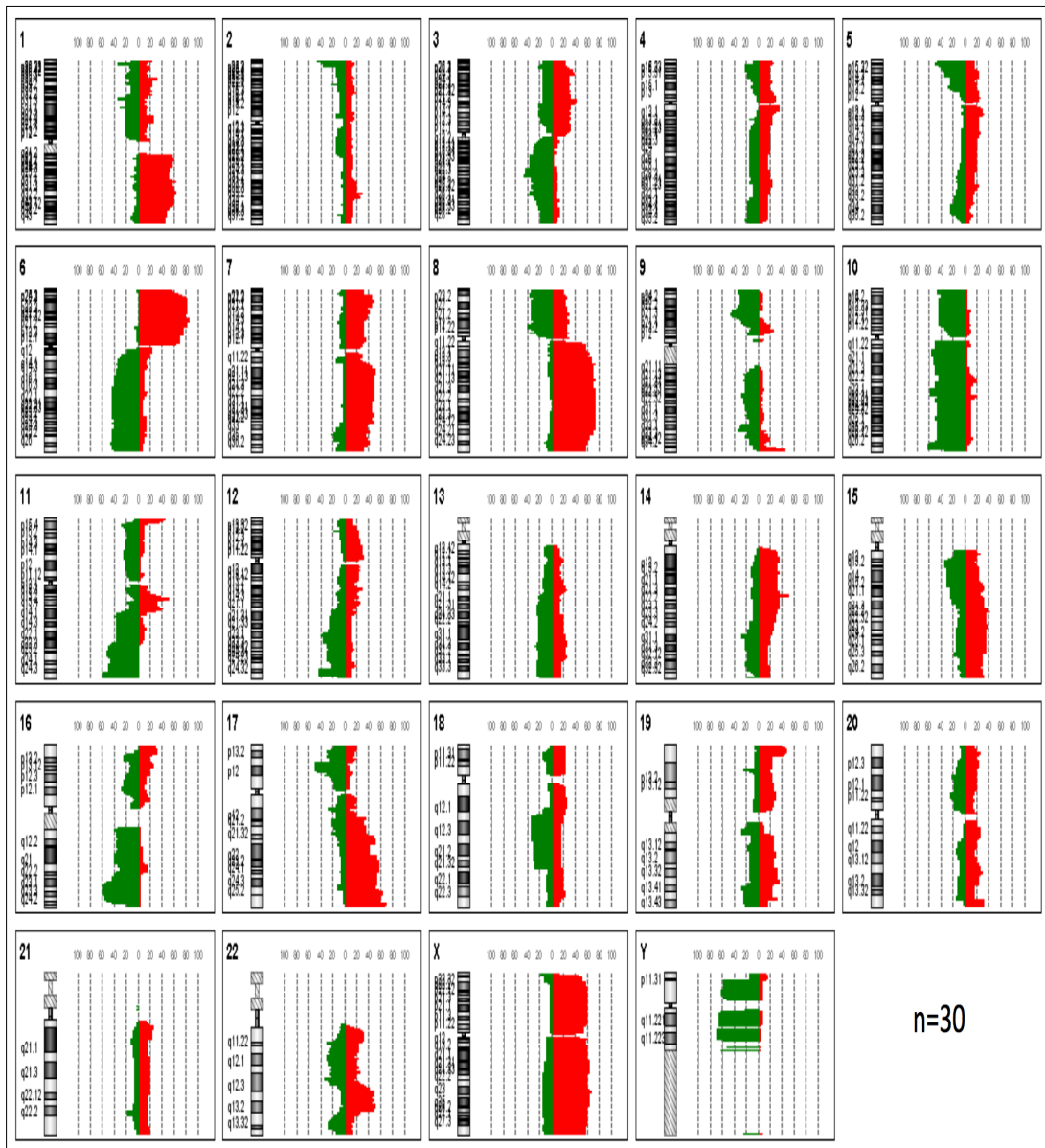


**Figure 1.8: individual chromosome penetrance plot of conjunctival melanoma.** Red bars to the right of the chromosome represent the frequency of amplifications and green bars to the left of the chromosome represent deletions. Dotted lines on the right and left side of each chromosome ideogram indicate the frequency (0% to 100%) of the identified aberrations, the heights of the bars correspond to the relative frequency of aberrations among the cases (Griewank et al., 2013b).

#### 1.4 Hypothesis and aim of the study

ConM are rare ocular tumours, but their incidence, like that of CM, is increasing, with exposure to sunlight being considered to be a factor in their development (Vajdic et al., 2003a, Van Raamsdonk et al., 2010, Westekemper et al., 2011, Zoroquiain et al., 2012, Griewank et al., 2013b). Little is known about the genetic changes that are associated with this malignancy but some ConM seem to be associated with mutations of the *BRAF* gene (Gear et al., 2004a), which is also commonly mutated in the cutaneous form (Akslen et al., 2005). Genetic classification of ocular melanomas has shown itself to be highly reliable in determining the prognosis of patients with UM, but there is insufficient information available to make similar comparisons for ConM. Therefore, techniques such as array-CGH will help to determine these alterations in frozen/archival samples and also screen these sample by direct sequencing for known oncogene such as *GNAQ*, *GNA11*, *BRAF*, *NRAS* and *TERT* genes that have previously been shown to be prognostic markers in other ocular melanomas will give clear information about the genetic instability that might associated with this malignancy especially when correlate the finding with other approach such as IHC. Therefore, the aims of the study were to:

- Identify chromosomal changes that leading to amplifications and deletions among a series of ConM tumours and compared the finding with the other melanoma subtype such UM and CM.
- Identify candidate genes within the target regions of amplification and deletion.
- Correlate genetic abnormalities with clinical and pathological parameters

# CHAPTER TWO

## Materials and Methods

## **2.1 Patients and tumour samples**

### *2.1.1 Ethics statement*

All the tumour samples used in the study were obtained from patients undertaking enucleation at the Royal Hallamshire Hospital, Sheffield, UK. Ethical approval (15/NW/0239) was obtained from the National Research Ethics Committee for the collection and use of fresh and archival tissue samples. All data from archival tissue were analysed namelessly. Tumour samples were collected and stored according to the principles of the Declaration of Helsinki and the use of tissue following the Human Tissue Act, 2004.

### *2.1.2 Sample selection*

Fresh tumour samples were obtained from patients diagnosed with primary ConM at Royal Hallamshire Hospital, Sheffield UK and 17 archival Formalin Fixed Paraffin Embedded (FFPE) blocks from ConM cases were collected from the Histopathology Department of the Royal Hallamshire Hospital, Sheffield, UK and supplied through collaboration by Dr. Hardeep.

## 2.2 MATERIALS

The general laboratory chemicals, reagents and plastic wear used in this study are listed in table 2.1 and 2.2.

Table 2.1: General laboratory chemicals and reagents.

Reagent	Supplier
Ethidium bromide	Fischer®Scientific, UK
Bromophenol blue	Sigma-Aldrich®,UK
DePex	vWR®International, UK
DAKO	Agilent, Stockport, UK
Magnesium sulphate	Fischer®Scientific, UK
Deionised water	
Nail varnish	Boots Chemist, UK
Sterile phosphate buffered saline (PBS)	vWR®International, UK
Gill's haematoxylin	Fischer®Scientific, UK
Agarose	Fischer®Scientific, UK
EDTA	Fischer®Scientific, UK
Hydrogen peroxide	BDH, Pool, UK
Ethanol	Fischer®Scientific, UK
Methanol	Fischer®Scientific, UK
Tween 20	Sigma-Aldrich®, UK
Xylen	Fischer®Scientific, UK
Hydrochloric acid	Fischer®Scientific, UK

Table 2.2: The plastic ware used in this study.

<b>Disposable laboratory equipment</b>	<b>Supplier</b>
Vented tissue culture flasks (T25, T75cm <sup>2</sup> )	Nunc™, Fisher Scientific UK
15, 25 and 50ml tubes	Sarstedt, Leicester, UK
Sterile stripettes (5,10ml)	Corning Incorporated, Costar®
10, 20, 200 and 1000µl pipette tips	Sarstedt, Leicester, UK
10, 20, 200 and 1000µl filter pipette tips	Starlab, Milton Keynes, UK
Blotting papers	Hollingsworth and Vose Ltd., UK
Coverslips (22×22/32/50mm)	VWR International Ltd. Poole, UK
Greiner plastic (3ml) Pasteur pipette	Scientific Laboratory Supplies, UK
Latex examination gloves	Kimberly-Clark, Kent, UK
Plastipak syringes (1ml)	Scientific Laboratory Supplies, UK
Plastic disposable pipettes	SLS, Nottingham, UK
Sterile Scalpels	Swann Morton, Sheffield, UK

### **2.2.1 Tissue culture reagents and chemicals**

*Culture media:* Rosewell Park Memorial Institute medium (RPMI-1640, Lonza, BioWhittaker®) was supplemented as shown in table 2.3 below and then stored at 4°C and warmed to 37°C prior to use.

*Trypsin-EDTA:* 0.4% Trypsin-EDTA solution stored in 50ml aliquots at -20°C (Lonza, BioWhittaker®).

Table 2.3: Tissue culture medium with supplements.

Supplement	Dilution in 500ml of RPMI %	Supplier
Foetal calf serum	20%	Lonza, BioWhittaker®
L-glutamine (200mM in 0.85% NaCl)	1%	Lonza, BioWhittaker®
Penicillin/Streptomycin Antibiotic (10kU/ml)	1%	Lonza, BioWhittaker®
D+ glucose (45% solution)	0.5%	Sigma-Aldrich, UK
Amphotericin antifungals	1%	Lonza, BioWhittaker®

### 2.2.2 Material and equipment for karyotyping

Colcemid: 10µg/ml Karyomax® Colcemid (GIBCO), was stored at 4°C.

Hypotonic solution: 0.075M potassium chloride (KCl) (sigma-Aldrich, UK) was prepared by adding 2.235g KCl in 400ml dH<sub>2</sub>O; it was autoclaved and then stored at 4°C, and warmed to 37°C prior to use.

Fixative solution: 3:1 mixture of methanol and glacial acetic acid was freshly prepared prior to each use.

Microscopy slides: Superfrost slides (Vector) were manually cleaned with Decon 90 detergent (BDH) and then stored in dH<sub>2</sub>O at 4°C for up to one week.

Gurr's buffer: One Gurr's buffer tablet at pH 6.8 (BDH) in 1000ml dH<sub>2</sub>O, stored at room temperature.

Leishman's stain (Giemsa stain): 1:4 mixture of 2.0% Leishman's Stain (BDH) and Gurr's buffer, used within 15 minutes of preparation.

Sorenson's Buffer: 9.47g of disodium hydrogen orthophosphate (Na<sub>2</sub>HPO<sub>4</sub>) (Sigma-Aldrich, UK) and 9.08g potassium dihydrogen orthophosphate (KH<sub>2</sub>PO<sub>4</sub>) (Sigma-Aldrich, UK) made up to 1000ml with ddH<sub>2</sub>O and stored at room temperature for up to one month.

Banding Trypsin: 0.6g of Trypsin was prepared by adding 1:250 powders in 250ml of Sorensen's buffer and then stored in 10ml aliquots at -20°C.

Microscopy: an Olympus® BH-2 light microscope attached to a Cohu high-performance Charge-Coupled Device camera and Powergene software on an

Apple Macintosh PC were used to capture and analyse images of metaphase chromosomes.

### **2.2.3 Material and equipment for DNA extraction**

*DNeasy® Blood and Tissue Kit and FFPE kit containing:*

- ❖ Proteinase K
- ❖ Lysis Buffer (Buffer AL)
- ❖ Tissue Lysis Buffer (Buffer ATL)
- ❖ Elution Buffer (Buffer AE)
- ❖ Wash Buffers (Buffers AW1 and AW2) with addition of the appropriate volume of 100% ethanol to the concentrate
- ❖ DNeasy® mini spin columns and collection tubes
- ❖ NanoDrop® ND-1000 (Thermo Fisher Scientific, Wilmington, USA).

### **2.2.4 Material for Whole Genomic Amplification (WGA)**

GenomePlex ® Complete Whole Genome Amplification Kit were stored at -20C° containing:

- ❖ 10×Fragmentation buffer
- ❖ 1× Library preparation buffer
- ❖ Library preparation solution
- ❖ Library preparation enzyme
- ❖ 10×Amplification Master Mix
- ❖ WGA DNA Polymerase
- ❖ Water Molecular biology reagent
- ❖ Control Human Genomic DNA

GenElute PCR clean-up kit stored at room temperature(20-25°c) containing:

- ❖ GenElute plasmid mini spin column (Sigma-Aldrich)
- ❖ 2 ml collection tube
- ❖ Wash solution concentrated
- ❖ Binding solution
- ❖ Column preparation solution
- ❖ Elution solution

### 2.2.5 Material and equipment for Array Comparative Genomic Hybridisation (Array-CGH)

Restriction Digestion Enzymes: (Promega™) were stored at -20 °C containing:

- ❖ 10X Buffer C
- ❖ *Rsa* 1 (10 U/μl)
- ❖ *Alu* 1 (10 U/μl)
- ❖ Acetylated Bovine Serum Albumin (10μg/ml)

Genomic DNA Enzymatic Labelling Kit: (Agilent) stored at -20°C containing:

- ❖ Random Primers
- ❖ 10X dNTP
- ❖ 5X Buffer
- ❖ Cyanine 3-dUTP (1.0mM)
- ❖ Cyanine 5-dUTP (1.0mM)
- ❖ Exo-Klenow Fragment

Oligo array-CGH Hybridisation Kit: (Agilent) containing:

- ❖ Agilent 10X Blocking Agent. Blocking Agent can be prepared in advance and stored at -20°C CGH block
- ❖ Agilent 2X Oligo array-CGH Hybridisation solution stored at room temperature

Universal Linkage System (ULS) Labelling Kit: (Agilent) stored at 4°C containing:

- ❖ ULS-Cy 3 reagent
- ❖ ULS-Cy 5 reagent
- ❖ 10X Labelling solution
- ❖ KREA *pure*® purification columns with collection tubes

Cot-1 DNA: 1mg/ml stored at -20 °C

Blocking Solution: (Agilent): CGH block® stored at -20C°

Microarray Hybridisation Assembly: (Agilent, Stockport, UK) containing:

- ❖ Hybridisation Gasket Slide (Off the shelf slide)
- ❖ SurePrint® G3 Human CGH Microarray Slide 4×180K
- ❖ Hybridisation Chamber Kit-SureHyb® enabled, Stainless Steel

Microarray Hybridisation Oven: (Agilent) fitted out with removable rotator rack

Wash Buffer Kit: Oligo array-CGH/ChIP-on chip Wash Buffer Kit containing:

- ❖ Oligo array-CGH Wash Buffer 1
- ❖ Oligo array-CGH Wash Buffer 2

Sure, Scan High-Resolution Microarray Scanner (Agilent)

## **2.2.6 Material for Genomic DNA sequencing**

Immolase DNA polymerase kit: (Bioline, London, UK), stored at -20°C and containing:

- ❖ 10× Immunobuffer
- ❖ 50 mM MgCl<sub>2</sub> solution
- ❖ Immolase DNA Polymerase

GC-rich PCR Kit: (Sigma-Aldrich), stored at -20°C and containing:

- ❖ GC-rich Enzyme 1x50ul (100U)
- ❖ GC-rich PCR reaction buffer 5x concentration include 7.5mM MgCl<sub>2</sub> (final concentration 1.5mM) and DMSO
- ❖ GC-rich resolution buffer 5M

dNTPs kit: (Bioline, London, UK) containing dATP, dCTP, dGTP and dTTP (100mM), was made by adding 25µl aliquots from each solution into one tube, then 100µl of dH<sub>2</sub>O added to the mix to make up 10mM of dNTPs.

Thermocycler: A SensoQuest thermal gradient cycler was used with a 96-electroformed gold-plated silver thermos-block (Geneflow, UK).

Agarose: Agarose powder (Fisher) was stored at room temperature.

Running Buffer: 50X stock solution TAE (Tris-Acetate-EDTA) was diluted to 1X prior to use by dissolved 242g tris bases, 57.1 ml glacial acetic acid and 18.6g EDTA into 1000ml of dH<sub>2</sub>O and stored at room temperature.

Electrophoresis Unit: Multi sub choice electrophoresis unit (Geneflow, UK) containing:

- ❖ Gel casting tray (15 × 7cm)
- ❖ Sample comb (for 20 samples)
- ❖ Electrophoresis tank

Ethidium bromide: 10mg/ml ethidium bromide prepared by dissolving 1g ethidium bromide in 100ml dH<sub>2</sub>O and stored at room temperature.

DNA Ladder: 1kb DNA ladder (Promega™) stored at 4°C.

Loading Buffer: 6X Loading buffer (-0.25% (w/v) bromophenol blue and 30% (v/v) glycerol) was prepared by adding 25mg bromophenol blue to 3ml glycerol and made up to 10ml with dH<sub>2</sub>O and then stored at 4°C.

Power source: A Power-Pac 3000 basic power supply for electrophoresis (BioRad).

### **2.2.7 Primer design**

Primer mapping (forward and reverse) primers for *BRAF*, *GNAQ*, *GNA11*, *NRAS* and *TERT* was used to double check gene targets using the sequences available on the NCBI database before we ordered them. These primers (Table 2.4) came lyophilised from (Eurofins Genomics, Ebensburg, Germany) and were reconstituted with nuclease-free H<sub>2</sub>O to obtain a concentration of 10 pmol/μl before being stored at -20 °C. (Houben et al., 2004, Goldenberg-Cohen et al., 2005, Van Raamsdonk et al., 2010, Xu et al., 2014).

Table 2.4: Primer sequences for *BRAF*, *GNAQ*, *GNA11*, *NRAS* and *TERT* and the product size expected.

<i>Gene name</i>	<i>Exon</i>	<i>Primer Direction</i>	<i>Primer sequences (5'@3')</i>	<i>Product size (bp)</i>
<i>BRAF V600E</i>	15	<i>Forward</i>	TCATAATGCTTGCTCTGATAGGA	242
		<i>Reverse</i>	GGCCAAAAATTTAATCAGTGGA	
<i>BRAF 11</i>	<i>First primer</i>	<i>Forward</i>	GTCCCGACTGCTGTGAA	295
		<i>Reverse</i>	GTTTGGCTTGACTTGACTTTT	
	<i>Second primer</i>	<i>Forward</i>	GTCCCGACTGCTGAAC	
		<i>Reverse</i>	ACGGGACTCGAGTGATGATT	
<i>GNAQ</i>	5 Q209	<i>Forward</i>	GACTTGGATGATCATCGTCATT	317
		<i>Reverse</i>	AAGAAAGCAAAGTAAGTTCAC	
<i>GNA11</i>	5 Q209	<i>Forward</i>	CGCTGTGTCCTTCAGGATG	147
		<i>Reverse</i>	CCACCTCGTTGTCCGACT	
<i>NRAS Q12-13</i>	1	<i>Forward</i>	TTGAGGGACAAACCAGATAGGC	262
		<i>Reverse</i>	CCTTCGCCTGTCCTCATGTATT	
<i>NRAS Q 61</i>	2	<i>Forward</i>	GGGTGTTTTTGC GTTCTCTAGTC	318
		<i>Reverse</i>	TCCGACAAGTGAGAGACAGGAGGAT	
<i>TERT<sub>p</sub></i>		<i>Forward</i>	GTCCTGCCCTTCACCTT	187
		<i>Reverse</i>	GCTTCCCACGTGCGCA	

### **2.2.8 Material for Fluorescence *In-situ* Hybridisation (FISH)**

Commercial Probes: Commercial FISH probes (Vysis) were stored at -20°C in the dark. The commercial probes used in this study are CEP 3 *Chr 3 Centromere* 3p11.1-q11.1 SpectrumOrange®1.0µl and CEP 8 *Chr 8 Centromere* 8p11.1-q11.1 Spectrum Green® 1.0µl.

Pepsin: Pepsin (Sigma) stored at -20°C in 25µl aliquots at 100mg/ml stock concentration and diluted 1:2000 in 0.01 NHCl for working concentration.

RNase A: RNase A (Thermos-Fisher) stock stored at -20 °C in 25µl aliquots.

PBS with MgCl<sub>2</sub>: PBS + 50mM MgCl<sub>2</sub> (50ml 1M MgCl<sub>2</sub> + 950ml PBS) stored at room temperature for up to one month.

Fixative Solution: 37% Formaldehyde (Sigma) stored at room temperature in the dark and diluted to 1% in PBS/MgCl<sub>2</sub>.

SSC Buffer: 20X Saline Sodium Citrate (SSC), (Fischer®Scientific, UK) stock prepared as from components outlined below in 1L dH<sub>2</sub>O, adjusted to pH 7.0 and stored at room temperature, 3M NaCl or 300mM NaHCO<sub>3</sub>.

SSCT1: 0.4xSSC/0.3% Tween 20 (200ml 2XSSC + 1.5ml Tween 20 made up to 500ml with deionised water).

SSCT2: 2XSSC/0.1% Tween 20 (500ml 2XSSC + 0.5ml Tween 20).

### **2.2.9 Material for Immunohistochemistry (IHC)**

Bleaching: Made fresh on the day of use by adding 15ml of hydrogen peroxide H<sub>2</sub>O<sub>2</sub> (Sigma-Aldrich, UK) to 285ml of PBS.

Peroxidase quenching solution: 0.3% (methanol/ H<sub>2</sub>O<sub>2</sub>), freshly prepared by adding 270ml methanol to 30 ml of Hydrogen peroxide (H<sub>2</sub>O<sub>2</sub>).

Target retrieval Solution (10x): 1:10, freshly prepared by adding 10ml DAKO (Agilent Stockport, UK) to 90ml deionized water adjusted to pH 6.0.

Normal Blocking Serum: 10% (goat serum/PBS/Casein) normal goat serum (Vector Laboratories, UK) was stored at 4°C diluted in PBS with Casein to give a 10% working concentration.

Primary Antibodies: All primary antibody was provided by (Abcam, Cambridge, UK), and was stored at 4°C and diluted in 2% normal goat serum (table 2.5).

Table 2.5: Summaries of all the primary antibodies and their conditions that used in this study.

<b>Antibodies</b>	<b>Type</b>	<b>Source</b>	<b>Class</b>	<b>Control tissue</b>	<b>Dilution and conditions</b>
<b>Anti-CDKN2A</b>	Monoclonal	Mouse	IgG	Human colon tissue	1:800 overnight at 4C°
<b>Anti-TERT</b>	Polyclonal	Rabbit	IgG	Human tonsil tissue	1:100 overnight at 4C°

Secondary Antibodies: Secondary antibodies (goat anti-Rabbit and goat anti-Mouse, Biotinylated IgG from Vector) were stored at 4°C and diluted in 2% blocking serum (diluted in PBS).

Biotin/Avidin Peroxidase Kit: VECTASTAIN<sup>®</sup> Elite ABC kit (Vector, UK) was stored at 4°C and used according to manufacturers' instructions

DAB substrate Kit: (Sigma-Aldrich, UK) was stored at 4°C. DAB solution was prepared by adding (2 drops of buffer + 4 drops of DAB + 2 drops of peroxide).

DePex: DEPX mountan (Sigma-Aldrich, UK) preserves the stain stored at room temperature and used in a fume hood.

## 2.3 METHODS

All laboratory work was done according to health and safety regulations. All chemicals were used based on the Control of Substances Hazardous to Health (COSHH) guidelines.

### 2.3.1 Routine tissue culture (Split/Subculture)

All ConM cell lines were grown in T75 tissue culture flasks with RPMI-1640 supplemented as described in table 2.1 and incubated at 37°C in a humidified atmosphere of 5% CO<sub>2</sub>. Flasks was checked regularly to keep cells growing and to prevent any contamination. All procedures for tissue culture were done in a laminar flow cabinet. When cells reached 70-80% confluence, they were passaged in order to maintain the culture.

Briefly, the old media in the flasks was discarded and then the cells were washed twice with 5ml of PBS. Cells were then incubated with 3ml of trypsin-EDTA solution at 37°C in a 5% CO<sub>2</sub> incubator for 2 minutes to detach them from the surface of the flask. The flask was knocked gently and the detached cells were observed under the light microscope. Once detached, to inactivate the action of trypsin-EDTA 5ml, of fresh RPMI-1640 medium was added to the flasks and the flask surface was washed several times pipetting up and down to re-suspend the cells. The suspension was then transferred into a 15ml falcon tube and centrifuged at 1000rpm for 5 minutes. The supernatant was discarded and the cell pellet was re-suspended in 10ml of fresh RPMI-1640 medium with good mixing by pipetting. At that time 1ml of the re-suspended cells was seeded in to new T75 tissue culture flasks containing 9ml of the RPMI-1640 medium and then incubated at 37°C in 5% CO<sub>2</sub> to continue growth.

### **2.3.2 Cytogenetic analysis (Karyotyping)**

#### *2.3.2.1 Chromosome harvesting*

When cells reached 60-80% confluence, the media were changed with 10ml of fresh RPMI-1640 medium one day before harvesting. Prior to harvesting, 10 drops of colcemid were added to actively dividing cells for 4 hours at 37°C to arrest the cells at metaphase. The media was then transferred from the flask to a 15ml centrifuge tube to collect any cells attached in the media. Cells were then incubated with 5ml pre-warmed trypsin at 37°C for 2 minutes to detach them from the flask surface. Then 5ml of media was added to stop trypsinisation and the flask surface was washed to suspend the cells. Re-suspended cells were then transferred into a harvesting tube and centrifuged at 1000 rpm for 5 minutes to form a pellet. The supernatant was aspirated off carefully leaving 0.5ml containing the pellet before re-suspending the pellet by flicking the tube with fingertips. Then 5ml of a pre-warmed hypotonic solution (0.075 KCL) was added slowly into the harvesting tube drop by drop whilst the tube was being agitated. The cells were incubated with KCL at 37°C for 30-40 minutes and then centrifuged at 1000 rpm for 10 minutes. The supernatant was aspirated off carefully leaving 0.5ml of it to re-suspend the pellet. 2ml of freshly prepared fixative (methanol: acetic acid, 3:1)

was added slowly to the cells whilst the cells were being agitated. The cells were then centrifuged at 1000 rpm for 10 minutes and the pellet re-suspended again in 2ml of fixative and finally the harvesting tube was stored at -20°C.

#### 2.3.2.2 *Preparation of chromosome spreads*

Slides were placed in Decon 90 detergent overnight. The following day the slides were washed separately under running hot and cold water, and the cleaned slides stored up to one week in distilled water in the fridge until use. Cell preparations were centrifuged at 1000 rpm for 10 minutes to form a pellet. The supernatant was aspirated off by a 150mm glass Pasteur pipette leaving 1 ml. The cells were then re-suspended through gently and 2 drops were added to each slide. Freshly prepared fixative (3:1 methanol: acetic acid) was dropped onto the slides (3-4 drops) and the slides were labelled and left to dry. The slides were then examined for metaphase chromosomes under the inverted light microscope (X10 objective) and stored at room temperature. A few drops of the fresh fixative were added to the remaining cells in the harvesting tube and the tube was re-stored at -20°C for future use.

#### 2.3.2.3 *Giemsa staining/banding*

The slides were arranged along a slide bar over the sink, incubated with trypsin for 35, 40 and 45 seconds (depending on metaphase spread quality) and then washed with Sorensen's buffer. Each slide was covered with Leishman's stain for 1.5 minutes, and then washed with Gurr's buffer over the slide. At that point, the slides were placed flat on a paper towel and blotted dry gently with blotting paper. The slides were then analysed under an Olympus® BH-2 light microscope attached to a software-controlled Cohu® high-performance Charge-Coupled Device camera (Applied Imaging®). The time for trypsin treatment and Giemsa staining varied according to the metaphase spread quality and experiments typically involved multiple attempts using increasing durations until staining was improved and clear banding patterns seen. Images were captured and the total number of chromosomes per metaphase was recorded from a minimum of 30 metaphase spreads. Chromosomal G-banding pattern analysis was carried out by an experienced Cytogeneticist, Dr Karen Sisley.

### 2.3.3 DNA extraction

#### 2.3.3.1 *Isolation and purification DNA*

##### 2.3.3.1.1 Cell lines and fresh frozen tissue samples

Cultured cells were dissociated with trypsin and centrifuged as described in section (2.2.1). Cells were then re-suspended in 200-300µl of PBS according to the size of the pellet and then transferred to a 1.5ml microfuge tube. 20µl of proteinase K and 200µl of Buffer AL were added, then mixed by vortexing and incubated at 56°C for 30 minutes until the mixture was completely lysed. After that, 200µl of (96-100%) ethanol was added to each sample tube and mixed by vortexing. The mixture was transferred to the DNeasy mini spin column, placed in a 2ml collection tube and centrifuged at 8000 rpm for 1 minute, then the contents of the collection tube were discarded and the spin column was placed in a fresh collection tube. For fresh frozen tissue 10-20mg was transferred to a 1.5ml microfuge tube, Proteinase K (20µl) and Tissue Lysis Buffer ATL (180µl) were added to the tissue and mixed carefully by vortex. The tube was then incubated on a heat block at 56°C for up to 24 hours and fresh Proteinase K was added every 6-8 hours until the tissue was completely dissolved. A mixture of Buffer AL (200µl) and absolute ethanol 200µl was then added to each sample tube, and the sample transferred to a labelled DNeasy<sup>®</sup> mini spin column.

After these initial steps, two washing steps were carried out on all samples by adding 500µl of AW1 buffer followed by AW2 buffers respectively. Following the second wash step, spin columns were placed in a fresh, labelled 1.5ml microfuge tube and 200µl of elution buffer AE has added directly to the spin column and centrifuged at 8000 rpm for 1 minute to elute the DNA.

#### 2.3.3.1.2 Formalin-Fixed Paraffin-Embedding (FFPE) samples

10µm thick sections were cut from formalin- fixed, paraffin-embedded tumour tissues. The sections were then de-paraffinized based on standard procedures. Briefly, the sections were placed in 1.5ml microfuge tubes and 1 ml of xylene was added. The supernatant was removed after full speed centrifugation for 1 minute and 1ml absolute ethanol (96-100%) was then added followed again by full centrifugation. The ethanol was removed and the tubes left open and incubated up to 37°C for 10 minute to allowed the ethanol to evaporate completely. Buffer ATL (180µl) and Proteinase K (20µl) were then added to the samples and incubated immediately on a heat block at 56°C for at least 1 hour, with a series of vortexing until the samples were completely lysed. Finally, samples were incubated at 90°C on a heat block to de-paraffinize the tissue.

Samples were then allowed to cool to room temperature and RNase A (2µl) was added, briefly vortexed, then incubated at room temperature for 2 minutes. Buffer AL 200µl was then added to tube with quick vortexing then (200µl) absolute ethanol was added and its contents transferred to labelled DNeasy<sup>®</sup> mini spin columns and centrifuged at 6,000 × g for 1 minute. Subsequent most steps were followed as previously described in section 2.3.3.1.1. To elute the DNA 50µl pre-warmed 1×TE was added directly onto column and then incubated for 15-20 minutes at room temperature followed by centrifugation at 21,000 × g for 1 minute. Samples were added to the same spin column and then incubated 15 minutes again, and finally centrifuged at maximum speed for 1 minute. This double elution step generally increased the yield of DNA from these samples.

#### *2.3.3.2 Genomic DNA quantification and purity assessment*

All DNA samples were measured to assess the concentration of DNA. This was done by using the NanoDrop<sup>®</sup> ND-1000 (Thermo Fisher Scientific, Wilmington, USA). The concentration of the DNA was quantified in ng/µl, the absorbance measurements used to measure different molecules at specific wavelengths and the nucleic acids were found to have absorbance at 260nm. The purity of the DNA

was evaluated by the ratio of absorbance at 260/280 which indicates the absence of protein contamination whereas the ratio of A260/230 was used to measure DNA purity to measure the contamination with other organic compounds such as EDTA, carbohydrates and phenol that are usually absorbed at 230nm.

The surface of the optical lens of the NanoDrop® instrument was wiped with lint-free wipes and 1.5µl of nuclease-free water was loaded on to the instrument for initialization. The same volume of elution buffer (AE) was loaded as blank for short-term culture and fresh frozen tissue samples whereas FFPE samples were blanked with 1×TE. 1.5µl of each DNA samples were then loaded and measured with good cleaning of the optical surface between samples. DNA purity was measured from the value of A260/280 and A260/230 and was suitable for analysis within the acceptable ratio (at least greater than 1.8 and 2, respectively).

#### **2.3.4 GenomePlex Whole Genome Amplification (WGA)**

The WGA process is divided into three steps: fragmentation, OmniPlex library generation, and PCR amplification. The first two steps, fragmentation and library generation, were carried out sequentially, as the ends of the library DNA can degrade thus affecting subsequent steps. OmniPlex library DNA, was generated in the stepped isothermal reactions, which can be stored up to three days at -20 °C without detectable differences in the process. The final WGA DNA was then stored at -20 °C. The starting amount of DNA is critical. One ng of human genomic DNA affords product with gene representation that varies 2-10-fold from the original material, while product yield is only ~50% lower. Less complex genomes such as bacterial DNA can give good representation with as little as 1 ng of input DNA. GenomePlex can be used on archival fixed tissue DNA or degraded samples provided that the extracted DNA is 200bp or greater in size.

#### *2.3.4.1 Fragmentation*

1 µl of 10x Fragmentation Buffer was added to 10 µl of DNA (1 ng/µl) sample in a PCR tube. After that, the tube was placed in a thermal block or cycler at 95°C for 4 minutes. The sample immediately cool down on ice, and then centrifuge briefly to consolidate the contents.

#### *2.3.4.2 Library Preparation*

2 µl of 1x Library Preparation Buffer was added to each sample and 1 µl of Library Stabilization Solution was also added to the PCR tube. The contents were vortex thoroughly by centrifugation, and placed in thermal cycler at 95 °C for 2 minutes. After that, the samples cool on ice and 1 µl of Library Preparation Enzyme was added then the sample was placed in a thermal cycler and incubate as follows:16, 24 and 37 °C for 20 minutes respectively and 75 °C for 5 minutes.

#### *2.3.4.3 Amplification*

The master mix was prepared by adding the following reagents to the 15 µl reaction 7.5 µl of 10x Amplification Master Mix 47.5 µl of Water and 5 µl of WGA DNA Polymerase. The contents were centrifuge briefly and then placed in a thermocycler for nearly 1 hour and half. After cycling is complete, the reactions were maintained at 4 °C or store at –20 °C until ready for analysis or purification. The stability of WGA DNA is equivalent to genomic DNA stored under the same conditions. Finally, GenomePlex WGA amplified DNA was then purified with PCR Cleanup Kit or standard purification methods that isolate single and double stranded DNAs. Once purified, the DNA can be quantified by measuring absorbance, assuming that one A260 unit is equivalent to 50 ng/µl DNA.

### 2.3.5 Array-based Comparative Genomic Hybridisation (Array-CGH)

#### **Array CGH concept**

This recent molecular technique is used to study whole genomic DNA (gDNA) to detect copy number variation. The gDNA isolated from tumour samples and commercial DNA were labelled with two different fluorescent dyes, Cyanine 5 and Cyanine 3, and hybridised to a microarray slide with specific genomic probes used to target regions of interest, including known oncogenes. The array was then washed and scanned. The differential intensity of the fluorescent dyes at each probe serves as a surrogate for the ratio of copy numbers of the probe sequence in the tumour compared to the reference genome. The red spots specify a duplicate region in the genome of the patient's DNA whereas the green spots specify the missing DNA in the patient's genome compared to the reference genome (Commercial DNA) consequently, chromosomal aberration is shown as amplification and deletion. Figure 2.1 shows schematically the main steps of this method.

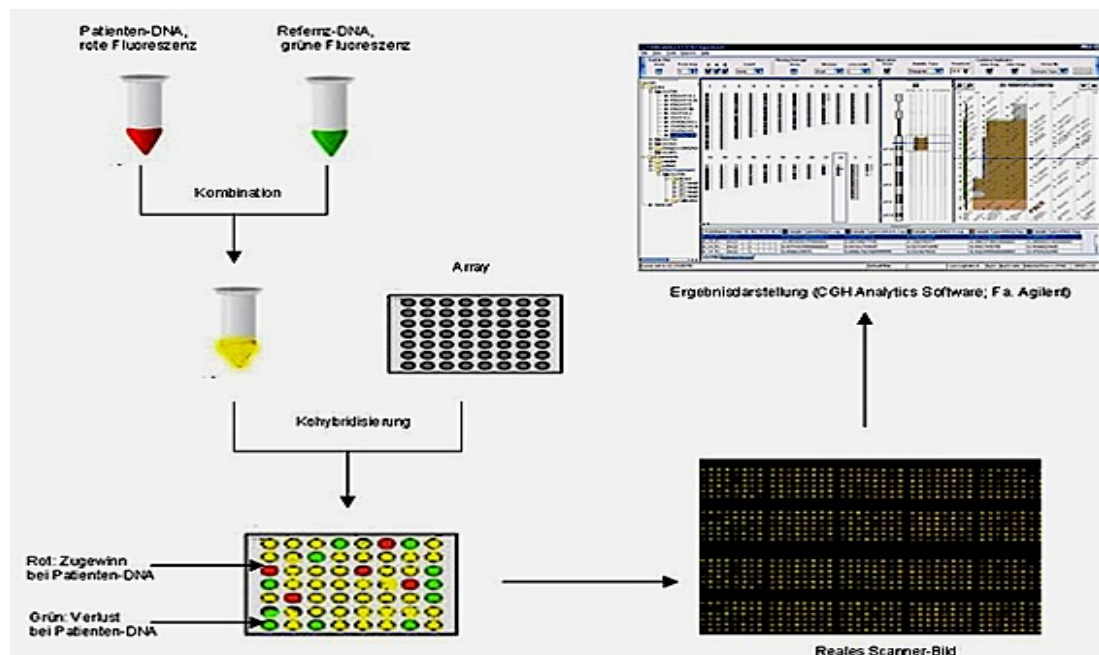


**Figure 2.1: Schematic diagram of the array-based comparative genomic hybridization. Adapted from [www.diagenos.com/analysen/acgh](http://www.diagenos.com/analysen/acgh) Accessed on 11/3/2015.**

### 2.3.5.1 Fresh Frozen Tissue and Short Term-culture

#### 2.3.4.1.1 DNA digestions

Before starting, a gDNA input of 0.5-1µg per sample was required and the DNA digestion for both the test sample and the control was carried out by adding two restriction enzymes, Alu-I and Ras-I, to digest the DNA into smaller strands of random size. A digestion master mix was prepared as shown in table 2.6. 5.8µl of which was added to each tube containing 20.2µl of gDNA to make a total volume of 26µl.

Table 2.6: Digestion Master mix components.

<i>Components</i>	<i>Per tube (µl)</i>	<i>For 8 tubes (µl)</i>
<i>Nuclease-free Water</i>	2.0	18
<i>10X buffer</i>	2.6	23.4
<i>Acetylated BSA (10µg/µl)</i>	0.2	1.8
<i>Alu-1 (10µg/µl)</i>	0.5	4.5
<i>Rsa-1 (10µg/µl)</i>	0.5	4.5
<i>Total</i>	5.8	52.2

Tubes were then transferred to a thermocycler with the heated lid programmed for incubation at 37°C for two hours, followed by incubation at 65°C for 20 minutes and the samples held at 4°C. The digested DNA was then kept overnight at -20°C.

#### 2.3.5.1.2 DNA labelling and cleaning

The digested gDNA was labelled with Cy5 and Cy3 by using Agilent's labelling kit. Firstly, 5µl of random primers were added to each reaction tube, the DNA was denatured and the primers were annealed at 95°C for 3 minutes. A total of 19µl of labelling master mix was made of the components illustrated in table 2.7 with 3µl of Cy3-dUTP (1.0mM) being added to each control sample and a similar labelling master mix with 3µl of Cy5-dUTP (1.0mM) being added to each tumour sample; reaction tubes were then transferred to the thermal cycler and incubated for 2 hours at 37°C, then at 65°C for 10 minutes, and samples held at 4°C.

Table 2.7: Labelling Master Mix components.

<i>Components</i>	<i>Per tube (μl)</i>	<i>For 4 tubes (μl)</i>
<i>5X buffer 10.0 50</i>	10.0	50
<i>10X dNTP 5.0 25</i>	5.0	25
<i>Cy3-dUTP or Cy5-dUTP</i>	3.0	15
<i>Exo-klenow fragment</i>	1.0	5
<i>Total</i>	19.0	95

The labelled gDNA was purified by two washing steps using Amicon 30kDA filters and washed by adding 1X TE buffer and centrifuged at 14,000 x g for 10 minutes at room temperature. The total mixture volume of each sample was measured after purification, and the clean labelled gDNA was quantified with the Cy3 and Cy5 concentration using the NanoDrop® with TE buffer as a blank. The values were then used to determine the yield of gDNA and the specific activity of the labelled DNA. The calculation methods for these parameters are shown below. Samples were stored at -20°C in the dark, until further processing.

$$\mathbf{Dye\ Specific\ Activity\ (pmol/\mu g)} = 340 \times \frac{\mathbf{Dye\ concentration\ (pmol/\mu L)}}{\mathbf{DNA\ concentration\ (\mu g/\mu L)}}$$

$$\mathbf{DNA\ Yield} = \mathbf{DNA\ concentration\ (\mu g/\mu l)} \times \mathbf{volume\ (\mu l)}$$

#### 2.3.5.1.3 Microarray hybridization and assembly

The labelled gDNA (19.5μl) of each test sample and reference were mixed together in a microfuge tube. The component of the hybridization master mix as illustrated below in table 2.8 were then added to each sample.

Table 2.8: Hybridization master mix components.

<i>Components</i>	<i>Per tube (μl)</i>	<i>For 4 tubes (μl)</i>
<i>Human COT-1 DNA</i>	5	25
<i>10X Blocking Agent</i>	11	55
<i>2X Hybridisation Buffer</i>	55	275
<i>Total</i>	71	355

The reaction tubes were transferred to the thermocycler for 3 minutes at 95°C followed by 30 minutes at 37°C. After that, 100μl of the mixture was added to a gasket slide and sandwiched with the active side of the Agilent microarray slide in a clamped hybridisation chamber. The assembled slide chamber was then placed into the rotator rack in a hybridisation oven set to 65°C at 18 rpm, and samples hybridized for 24 hours.

#### 2.3.5.2 FFPE Labelling using the Universal Linkage System (ULS)

The Universal Linkage System (ULS) is a chemical reaction that directly incorporates platinum-conjugated fluorescent dyes into DNA molecules. Optimized for use in FFPE DNA, it was used here to label FFPE tumour samples and matched normal DNA for array CGH. The initial amounts of tumour DNA ranged between 0.5 and 1μg (usually 0.8μg), depending on the amount of DNA available and this was matched with equivalent amounts of normal DNA. If gDNA concentration was less than the amount required, the sample was concentrated by using Speed Vac concentrator (Eppendorf®, UK).

##### *2.3.5.2.1 Heat Fragmentation*

Heat fragmentation was required especially for large DNA fragments such as the commercial reference DNA prior to labelling. The volume of 8μl commercial DNA sample was placed in a 0.2ml PCR tube and then incubated at 95°C in a thermocycler with a heated lid, for 10 minutes' dependent on the average of gDNA molecular weight approximately >10.0 Kb. The reaction tubes were transferred to ice for 3 minutes, centrifuged for 30 second at 6,000× g and subsequently returned to ice until ready for labelling.

### 2.3.5.2.2 ULS Labelling Reaction

ULS-Cy3 and ULS-Cy5 dye master mixes were prepared by mixing the components listed in table 2.9 below in dim conditions because the dyes are light sensitive. The volume of dye used per reaction is dependent on the amount of DNA in the reaction. For most experiments, 1 $\mu$ l dye and 0.8 $\mu$ g of DNA, corresponding to a ratio of 1.25 $\mu$ l/ $\mu$ g was used.

Table 2.9: ULS Labelling Master Mix Components.

<i>Components</i>	<i>Per tube (<math>\mu</math>l)</i>	<i>For 4 tubes (<math>\mu</math>l)</i>
<b>10X Labelling solution</b>	1.0	4.0
<b>ULS-Cy3 or ULS-Cy5</b>	1.0	4.0
<i>Total</i>	2.0	8.0

Dye master mix (2 $\mu$ l) was added to each tube to make the reaction volume up to 10 $\mu$ l and mixed gently by pipetting up and down. The tubes were then transferred to a thermocycler with a heated lid and incubated at 85°C for 30 minutes and held at 4°C or on ice for 3 minutes followed by centrifugation for 1 minute at 6,000 $\times$  g. 10 $\mu$ l of nuclease-free water was added to reaction tube to make the volume up to 20 $\mu$ l for each sample.

### 2.3.5.2.3 ULS Clean-up

Non-reacted ULS-Cy3/ULS-Cy5 can lead to increase background noise therefore KREA pure columns were used to remove unreacted dye. One Agilent KREA pure filter per reaction was re-suspend briefly by vortex, then placed in a collection tube and centrifuged at maximum speed for 1 minute at room temperature. The cap and the flow-through was discarded then 300 $\mu$ l of nuclease-free water was added to each filter and centrifuged again for 1 minute at full speed. The collection tubes with the flow-through were discarded again. The column was then transferred to clean, labelled 1.5ml microfuge tube. The total volume 20 $\mu$ l reaction was then transferred to a KREA pure filter and centrifuged at 16, 000  $\times$  g for 1 minute at room temperature. The purified labelled gDNA collected in the microfuge tube was

stored at 4 °C in the dark until required.

The clean ULS labelled gDNA was then quantified with the Cy3 and Cy5 concentration by using the NanoDrop® as previously described. 1× labelling solution (diluted 1:10) was used as the blank. If the labelling of the ULS-Cy5 and ULS-Cy3 samples were good, 18.5µl for each ULS labelling were combined to make a volume of 37µl. This volume was then reduced to 22µl by speed vacuum centrifugation and stored in the dark until ready for hybridization.

#### 2.3.5.2.4 Hybridization

Combined matched samples were transferred to labelled 0.2ml PCR tubes and 61µl of a hybridization master mix prepared as shown in table 2.10 below was added to each sample making the total volume up to 83µl.

Table 2.10: Hybridization master mix components

<i>Components</i>	<i>Per tube (µl)</i>	<i>For 5 tubes (µl)</i>
<i>Human COT-1 DNA Agilent</i>	<i>5</i>	<i>25</i>
<i>100X Blocking Agent</i>	<i>1.0</i>	<i>5</i>
<i>Agilent 2X Hi-RPM Buffer</i>	<i>55</i>	<i>275</i>
<i>Total</i>	<i>61</i>	<i>305</i>

The sample was mixed by pipetting up and down and briefly centrifuged to drive the contents to the bottom of the tube. Samples were then placed in a thermocycler for incubation at 95°C for 3 minutes, followed by 37°C for 30 minutes. 27µl of Agilent CGH-block was then added to bring the total reaction volume up to 110µl and mixed well by pipetting up and down.

#### 2.3.5.2.5 Microarray washing and scanning

Oligo array-CGH wash buffer 2 was pre-warmed to 37°C overnight for optimal performance. In Oligo array-CGH wash buffer 1, the array-gasket sandwich was detached to obtain the array slide after being removed from the hybridization oven. The array slide was placed in the slide wash buffer 1 for 5 minutes at room temperature with gentle agitation. It was then placed in wash buffer 2 at 37°C for

1 minute, and then removed slowly to reduce droplets on the slide. The microarray slide was then scanned directly using an Agilent DNA Microarray scanner with sure-scan high-resolution technology and Agilent scanner control software (version 8.5.1), at 3 $\mu$ m resolution. To prepare the data for analysis the data were extracted from raw microarray image files using Agilent's Feature Extraction software (version 11.0.1.1). Data analysis started with image processing quality control and measuring the background intensity level of the array. The quality of the array was determined by the distance of the neighbouring probe variance measure and the FE software measured the DLRS (Derivative Log<sub>2</sub> Ratio spread). This is the standard deviation of the log ratio difference between consecutive probes, from which the measure of noise was estimated. The data were then normalised by setting the fluorescent mean log ratio to zero, and the copy number variation was then calculated.

#### *2.3.5.2.6 Microarray analysis*

Agilent Genomic Workbench (version 7.0.4.0) software was obtained from <http://www.genomics.agilent.com> and used to examine, visualise and identify any chromosomal changes from the microarray profiles. This software used a design file matched to the feature extraction files consequently, Agilent GEML-based (\*.xml) array design files were inserted prior to use any FE data. Agilent Feature Extraction (\*.Txt) data files in each experiment were then inserted to the software and a new experiment generated for the FE files. After that, the centralization algorithm was used to center the log ratio and the Quality Control of metric threshold in the original data were evaluated (Table 2.11). The data were examined by using the Aberration Detection Method (ADM-2) algorithm with the threshold adjusted to 6 and then the genomic, genes and chromosomes viewer were used to assess this data along with chromosome ideograms.

Table 2.11: Quality Control of metric thresholds for Array-CGH experiments.

Derivative Log <sub>2</sub> Ratio Standard Deviation (DLRSD)	This metric calculates the standard deviation of the log ratio differences between consecutive probes, to smooth the data and estimate the measure of the noise of an array.	Excellent: <0.2 Good: 0.2–0.3 Evaluate: >0.3
Signal to Noise Ratio	This metric calculates the ratio signal to noise by dividing the signal intensity by background noise. To distinguish the real signal from the signals obtained due to the experimental variation.	Excellent: >100 Good: 30–100 Evaluate: <30
Background Noise	This metric is calculated as the standard deviation of the signals on the negative control probes after rejecting the outlier's features.	Excellent: <5 Good: 5–10 Evaluate: >10

### 2.3.6 Aberration Detection Analysis

#### 2.3.6.1 *Agilent genomic software analysis*

Once the array-CGH technique had been carried out, the data was analysed using Agilent genomic software. Based on the normalised log<sub>2</sub> ratios, a quantitative study of the CNAs was derivative for each tumour samples. Specifically, the aberration detection module (ADM-2) algorithm 2.0 was used, with a threshold adjusted to 6.0. The feature extraction software helped to calculate the log<sub>2</sub> ratio, which detects the copy number differences between the reference and the test sample. Then the deletions and amplifications in the genomic region were measured as a ratio that is plotted against the genomic location. A normalisation algorithm is then used to compare and normalise the data processing. The fluorescence ratio for each array is standardized around zero by identifying a steady value to add to, or subtract from, all values on the array; the algorithm then adjusts the ratio values (log<sub>2</sub>). After that, the result was authorized as follows; log<sub>2</sub> ratio >0.6 was measured to represent amplification and is displayed in red, a log<sub>2</sub> ration ≤−1.0 is measured to represent deletion and is displayed in green whereas the black dots signify the normalised value everywhere around the zero which is between 0.6 and -1.0.

### 2.3.6.2 Nexus software

In this study, we also used the Fast-Adaptive States Segmentation Technique 2 (FASST2) algorithm as applied in Nexus Copy Number Software v8.0 (Biodiscovery), to detect genomic copy number aberrations for each individual array, and thus confirm the results of the aberrations that were determined through the Agilent software. This algorithm uses a Hidden Markov Model (HMM), which instead of assessing the copy number state at each probe, uses many states to cover extra options, such as mosaic events (these involve cancer data, which can often enclose significant mosaicism and normal cell contamination). Then the state values used to make calls depend on a special  $\log_2$  ratio threshold.  $\log_2$  ratio threshold values of +0.20 and -0.23 were used to detect a single copy number gain and loss, individually, while the two or more copies of gains and losses were identified by using a  $\log_2$  ratio threshold between +1.14 and -1.1, respectively. The p-value threshold for significance was set at  $5.0 \times 10^{-6}$  and requiring three contiguous probes for aberration calls. All threshold values were based on software manufacturer's recommendations. Aberrations were then presented as ideograms and can be observed at the whole genome level, or at chromosomal and single gene levels, to best visual analysis.

## 2.3.7 Genomic DNA sequencing

### 2.3.7.1 Standard PCR

PCR is a technique used to amplify a DNA fragment based on three steps: a denaturation step, where the double stranded DNA is separated by a high temperature over 90°C; an annealing step, where specific primers bind to the target DNA; and a primer extension step, where the *Taq* polymerase enzyme produces new double stranded DNA. This process is repeated over several cycles until a sufficient quantity of DNA is reached, master mix for standard PCR for each gene tested as shown in table 2.12 were prepared at different room, using filter tips (Eppendorf® Pipette Tips) with clean pipettes. The Master mix of PCR reaction was then mad up in a clean PCR hood. The PCR reactions tubes were then transferred to the thermocycler adopted based on PCR condition for each gene as elucidated in table 2.13.

Table 2.12: A master mix PCR components for each of the genes tested.,

<b>BRAF exon 11</b>					
<b>BRAF 11 first set</b>			<b>BRAF 11 second set</b>		
Component		per/sample	Component		per/sample
Immunobuffer	10X	3µl	Immunobuffer	10X	5.5µl
MgCl2	50 mM	1.5µl	MgCl2	50 mM	2.75µl
dNTPs	100 mM	0.6µl	dNTPs	100 mM	1.1µl
Forward Primer	10 pmmol/ul	1.2µl	Forward Primer	10 pmmol/ul	2.2µl
Reverse Primer	10 pmmol/ul	1.2µl	Reverse Primer	10 pmmol/ul	2.2µl
Immolase	250 U	0.6µl	Immolase	250 U	1.1µl
H2O		19.0µl	H2O		38.15µl
Amount of DNA	50ng	2µl	Amount of DNA	50ng	2µl
<b>BRAF V600E</b>			<b>TERT promoter</b>		
<b>BRAF V600E</b>			<b>TERTp</b>		
Component		per/sample	Component		per/sample
Immunobuffer	10X	2.5µl	Reaction buffer	5X	10µl
MgCl2	50 mM	0.75µl	Resolution buffer	5mM	5µl
dNTPs	100 mM	0.5µl	dNTPs	100 mM	1µl
Forward Primer	10 pmmol/ul	1µl	Forward Primer	10pmmol/ul	3µl
Reverse Primer	10 pmmol/ul	1µl	Reverse Primer	10 pmmol/ul	3µl
Immolase	250 U	0.5µl	Immolase enzyme	100 U	1µl
H2O		16.75µl	H2O		26µl
Amount of DNA	50ng	2µl	Amount of DNA	100ng	1µl
<b>GNAQ 209</b>			<b>GNA11 Q209</b>		
<b>GNAQ Q209</b>			<b>GNA11 Q209</b>		
Component		per/sample	Component		per/sample
Immunobuffer	10X	2.5µl	Immunobuffer	10X	2.5µl
MgCl2	50 mM	0.75µl	MgCl2	50 mM	0.25µl
dNTPs	100 mM	0.5µl	dNTPs	100 mM	0.5µl
Forward Primer	10 pmmol/ul	1µl	Forward Primer	10 pmmol/ul	1µl
Reverse Primer	10 pmmol/ul	1µl	Reverse Primer	10 pmmol/ul	1µl
Immolase	250 U	0.5µl	Immolase	250 U	0.5µl
H2O		16.75µl	H2O		17.25µl
Amount of DNA	50ng	2µl	Amount of DNA	50ng	2µl
<b>NRAS 61</b>			<b>NRAS 12-13</b>		
<b>NRAS 61</b>			<b>NRAS 12-13</b>		
Component		per/sample	Component		per/sample
Immunobuffer	10X	2.5µl	Immunobuffer	10X	2.5µl
MgCl2	50 mM	0.75µl	MgCl2	50 mM	0.375µl
dNTPs	100 mM	0.5µl	dNTPs	100 mM	0.5µl
Forward Primer	10 pmmol/ul	1µl	Forward Primer	10 pmmol/ul	1µl
Reverse Primer	10 pmmol/ul	1µl	Reverse Primer	10 pmmol/ul	1µl
Immolase	250 U	0.5µl	Immolase	250 U	0.5µl
H2O		16.75µl	H2O		17.125µl
Amount of DNA	50ng	2µl	Amount of DNA	50ng	2µl

Table 2.13: Thermocycler PCR conditions based on each gene tested.

A. Standard PCR for

<b><i>BRAF 11 first run</i></b>	<b><i>Cycle</i></b>	<b><i>Time</i></b>	<b><i>Temperature</i></b>
Initial Denaturation	1	02 min	95 C°
Denaturation	22	30 sec	95 C°
Annealing		30 sec	58C°
Elongation		30 sec	72 C°
Final elongation		05 min	72 C°
Hold on 4			

<b><i>BRAF 11 second run</i></b>	<b><i>Cycle</i></b>	<b><i>Time</i></b>	<b><i>Temperature</i></b>
Initial Denaturation	1	02 min	95 C°
Denaturation	35	30 sec	95 C°
Annealing		30 sec	58 C°
Elongation		30 sec	72 C°
Final elongation		05 min	72 C°
Hold on 4			

<b><i>GNAQ 209</i></b>	<b><i>Cycle</i></b>	<b><i>Time</i></b>	<b><i>Temperature</i></b>
Initial Denaturation	1	10 min	95 C°
Denaturation	30	30 sec	95 C°
Annealing		30 sec	60 C°
Elongation		90 sec	72 C°
Hold on 4			

<b><i>NRAS -12</i></b>	<b><i>Cycle</i></b>	<b><i>Time</i></b>	<b><i>Temperature</i></b>
Initial Denaturation	1	10 min	95 C°
Denaturation	35	30 sec	95 C°
Annealing		60 sec	53 C°
Elongation		60 sec	72 C°
Hold on 4			

B. Touchdown PCR for

<b><i>BRAF V600E</i></b>	<b><i>Cycle</i></b>	<b><i>Time</i></b>	<b><i>Temperature</i></b>
Initial Denaturation	1	10 min	95 C°
Denaturation	3	30 sec	95 C°
Annealing		30 sec	60 C°
Elongation		60 sec	72 C°
Denaturation	3	30 sec	95 C°
Annealing		30 sec	58 C°
Elongation		60 sec	72 C°
Denaturation	3	30 sec	95 C°
Annealing		30 sec	56 C°
Elongation		60 sec	72 C°
Denaturation	30	30 sec	95 C°
Annealing		60 sec	54 C°
Elongation		60 sec	72 C°
Hold on 4			

<b><i>GNA11 209</i></b>	<b><i>Cycle</i></b>	<b><i>Time</i></b>	<b><i>Temperature</i></b>
Initial Denaturation	1	10 min	95 C°
Denaturation	3	30 sec	95 C°
Annealing		30 sec	62 C°
Elongation		60 sec	72 C°
Denaturation	3	30 sec	95 C°
Annealing		30 sec	59 C°
Elongation		60 sec	72 C°
Denaturation	3	30 sec	95 C°
Annealing		30 sec	56 C°
Elongation		60 sec	72 C°
Denaturation	30	30 sec	95 C°
Annealing		30 sec	53 C°
Elongation		60 sec	72 C°
Hold on 4			

<b>NRAS-61</b>	<b>Cycle</b>	<b>Time</b>	<b>Temperature</b>
Initial Denaturation	1	10 min	95 C°
Denaturation	3	30 sec	95 C°
Annealing		30 sec	62 C°
Elongation		60 sec	72 C°
Denaturation	3	30 sec	95 C°
Annealing		30 sec	60 C°
Elongation		60 sec	72 C°
Denaturation	3	30 sec	95 C°
Annealing		30 sec	58 C°
Elongation		60 sec	72 C°
Denaturation	18	30 sec	95 C°
Annealing		30 sec	53 C°
Elongation		60 sec	72 C°
Hold on 4			

<b>TERTp</b>	<b>Cycle</b>	<b>Time</b>	<b>Temperature</b>
Initial Denaturation	1	10 min	95 C°
Denaturation	10	30 sec	95 C°
Annealing		30 sec	61 C°
Elongation		90 sec	72 C°
Denaturation	30	30 sec	95 C°
Annealing		30 sec	56 C°
Elongation		90 sec	72 C°
Final elongation		05 min	72 C°
Hold on 4			

### 2.3.7.2 Agarose gel electrophoresis

A 1.8% agarose gel was prepared by dissolving 2.7g of agarose powder in 150 ml of 1x TAE buffer in a conical flask. The mixture was then heated for 3 minutes in a microwave at high power until the agarose had completely dissolved. The solution was cooled to hand heat and 12µl of ethidium bromide was added. The gel was poured into the gel tray with the comb and left to solidify. Tape from around the edges was removed and the gel tray was placed in the tank containing 1XTAE buffer. 5µl of the sample mixed with 1µl of 6X loading dye were pipetted into the wells. Also, 5µl of 1Kb DNA ladder standard size marker was loaded into the well

to determine the actual size of the PCR product. A power of 100 volts was applied for 45 minutes then the PCR amplified products were visualised using a UV trans-illuminator and photographed.

#### *2.3.7.3 DNA purification and sequencing*

The DNA sequencing of purified samples was achieved to identify any sequence variation by sending 10µl of each template with 1:100 dilute primers mentioned earlier to the core sequencing facility used at University of Sheffield, Medical School UK which carried out the DNA purification and sequencing for all samples.

#### *2.3.7.4 Sequence analysis*

The Finch TV sequence analysis software (Geospiza) was used to visualize the generated sequencing data. The sequences were screened for any point of mutation or mismatch compared with reference sequences for those genes *BRAF*, *GNAQ*, *GNA11*, *NRAS* and *TERTp*.

### **2.3.8 Fluorescence *in situ* Hybridization (FISH)**

FISH is a cytogenetic technique used to localize the presence or absence of specific DNA sequences on chromosomes (metaphase chromosomes or interphase nuclei).

#### *2.3.8.1 Cell harvesting and slide preparation.*

ConM Mel 621 and 635 cells lines were harvested as described in section 2.3.2.1 and stored at -20°C. After that, slides with metaphase spreads were prepared as described in section 2.3.2.2 and stored at -20°C until required.

#### *2.3.8.2 RNase A and pepsin treatment*

RNase A solution was prepared by adding 25µl of RNase A to 5ml of 2XSSC; 125µl of the mixture was then added onto 20x50mm coverslips. The coverslips were fixed on prepared slides with metaphase spreads and then incubated in a moist chamber for 1 hour at 37°C. During incubation, a Coplin jar with 50ml of 0.01M

HCL was warmed in a 37°C waterbath. After that, the coverslips were removed and the slides were washed in 2XSSC on the shaker for 5 minute three times. During the last 2XSSC wash, 25µl of pepsin was added to the warmed 0.01 MHCL. The slides were then incubated in pepsin solution at 37°C for 10 minutes; then the slides were washed twice in PBS on the shaker for 5 minutes. The slides were further washed for 5 minutes in 50ml 1M MgCl<sub>2</sub> +950ml PBS.

#### 2.3.8.3 *Fixative and dehydration of slides*

The slides were fixed in freshly prepared fixative (1.35ml 37% Formaldehyde in 50ml 1xPBS +50mM MgCl<sub>2</sub>) for 10 minutes. After that, the slides were washed in PBS on the shaker for 5 minutes and then the slides were dehydrated in a series of ethanol dilutions 70%, 95% and 100% for 3 minutes each, and the slides left to air dry.

#### 2.3.8.4 *Hybridization of the DNA probes to target DNA*

A DNA probe mastermix was prepared for 5 slides by adding 12µl of ddH<sub>2</sub>O + 35 µl of hybridisation mix + 1.5 µl of 3 α satellite direct labelled orange + 1.5 µl of 8 α satellite direct labelled green. Probes were applied onto 22x22mm coverslips (10µl/coverslip) and applied to the slides. The coverslips were then sealed with rubber solution and allowed to dry. Target DNA and DNA probes were simultaneously denaturated by placing slides on a hot block at 80°C for 1 minute. The DNA probes were then hybridized with the target DNA by placing the slides in a humidified chamber and incubated at 37°C for up to 18 hours.

#### 2.3.8.5 *Post-hybridization washes*

The slides were washed first in SSCT1 (see materials for details) warmed up to 73°C in the water bath for 2 minutes, and then washed in another Coplin jar containing SSCT2 on the shaker for 1 minute at room temperature. After that, the slides were dehydrated through a series of ethanol dilutions (70%, 95% and 100%) for 3 minutes each and left to air dry in a covered box. DAPI was applied in 2 drops onto 22x50mm N° 1 coverslips and applied to the slides. The edges were sealed

with clear nail varnish and left to air dry. Finally, the slides were dated and stored in the dark at 4°C for at least 2 hours until viewing.

#### *2.3.8.6 Image detection by fluorescence microscopy*

The slides were analysed and images captured with an Olympus BX 50 microscope (X100 magnification) using Applied Imaging® software. Chromosome 8 centromere and chromosome 3 centromeres were detected as green and orange signals respectively in each cell. The number of signals per cell was visually scored in 300 non-overlapping cells.

### **2.3.9 Immunohistochemistry (IHC)**

5µm sections were collected onto slides and left it to dry overnight in an oven at 37C°, IHC was achieved using a modified Avidin- Biotin-Peroxidase Complex (ABC) Kit (Vector Laboratories, Peterborough, UK) and as designated by Hsu et al. (1981), at the histopathology with the help of Mrs. Maggie Glover.

#### *2.3.9.1 Antibody optimisation*

The antibodies used in this study were optimized according to manufacturer's instructions with a range of antibody concentration. Dr. Hardeep, Dr. Karen Sisley, Mrs. Maggie Glover and Shamsa Ihmed were independent observers to assess the specific antibody staining and recognized the optimal antibody conditions to carry out this IHC.

#### *2.3.9.2 Tissue Preparation and Antigen Retrieval for IHC*

Tissue sections were dewaxed in 2 x Xylene for 10 minutes each, the tissues were then dehydrated through an ethanol series: 100%, 95% and 70% for 5 minutes each. The sections were then placed in 3% of H<sub>2</sub>O<sub>2</sub>/methanol for 30 min at room temperature to quench any endogenous peroxidase activity and subsequently washed under running tap water for 5 minutes. The sections were then, placed in

bleach (PBS/H<sub>2</sub>O<sub>2</sub>) at room temperature overnight. Antigen retrieval treatment was an important stage for the preparation of FFPE section for staining, and it was done by dipping the tissue section in Target Retrieval Solution (1:10), to isolate the protein cross- link clusters formed from formalin particles on the tissue's antigen binding sites and then incubate the tissue section in a pressure cooker for 2 hours. The solutions were allowed to cool down and the section was rinsed in ddH<sub>2</sub>O twice for 3 minutes, followed by two subsequent PBS washing for 3 minutes.

#### *2.3.9.3 Blocking and Primary Antibody Incubation*

The relevant area of tissue sections on the slide was outlined, by using a wax pen and afterward appropriate 10% blocking serum (goat serum/casein) was applied and incubated at room temperature for 30 minutes, to block the non-specific background staining. The blocking serum was then tapped off and the primary antibody (diluted in 2% blocking serum) was added to the test and positive control slides. To the negative control slide 2% blocking serum (without antibody) was applied. Slides were then incubated overnight at 4°C.

#### *2.3.9.4 Secondary Antibody Incubation and Immunoreactivity*

Slides were rinsed and washed twice in PBS for 5 minutes each and suitable secondary antibodies (diluted in 2% blocking serum) were applied on all slides and incubated for 1 hour at room temperature. ABC reagent was prepared during the secondary antibody incubation. Subsequently, the slides were washed in two baths of PBST for 5 minutes each and ABC reagent applied, and incubated for 30 minutes. After that, the slides were washed with PBST twice for 5 minutes each and then peroxidase substrate solution (DAB) was freshly prepared and applied to the slide. After incubation at room temperature for 5 minutes until the desired brown stain intensity developed (up to 10 minutes), the sections were washed with ddH<sub>2</sub>O to stop the reaction.

#### *2.3.9.5 Counterstaining and Mounting*

The slides were washed under running tap water for 5 minutes and counterstained for 1 minute in Gill's haematoxylin, and then washed with running tap water for a further 5 minutes until the water ran clear. The sections were then dehydrated through a series of ethanol for 3 minutes each (70%, 90, 95%, 100%) and then in a fume hood the slides were given two following incubations in xylene for 5 minutes each. Whereas still wet with xylene, the sections were then mounted with DPX, covered with 22 × 32mm coverslips and permitted to dry overnight. The slides were then scanned by a panoramic digital slide scanner (3D HISTECH, Ltd, UK), and Images were captured from a Qupath viewer at the appropriate magnification (X200-X400).

# CHAPTER THREE

## Characterisation of Conjunctival Melanoma Short-term Cultures

### 3.1 Introduction

Ocular melanomas generally arise from two types, uveal or conjunctival melanoma, which both have different genetic and molecular backgrounds. The function and alterations in the growth of uveal melanocytes have been widely studied and new treatment pathways discovered due to establishment of cell lines (Amaro et al., 2013, Angi et al., 2015, Shoushtari and Carvajal, 2016). In contrast, there is little or no information about conjunctival melanoma cells *in vitro*, because the tumour is rare and hard to culture, and therefore there has been very little success in profiling a cell line. Tumour cell lines based on tissue type or gene mutation are important to create strong platforms for researchers to understand cancer. The establishment of uncontaminated cell lines of conjunctival melanocytes would be highly beneficial to study the cell biology of conjunctival melanocytes and the pathogenesis of ConM. The first ConM cell line, IP 292 was described by Aubert et al. (1993) and later Nareyeck et al. (2005) developed another two ConM cell lines (CRMM1 and CRMM2), the morphology of which both displayed spindle cells, with the IHC showing a high expression of tumour marker HMB-45 (Nareyeck et al., 2005). Both cell lines were also shown to have either *BRAF* (CRMM1, CRMM2) or *NRAS* (CRMM2) mutations (Nareyeck et al., 2005). Karyotyping was the first method used to study the structural and numerical aberrations of chromosomes in tumour cell lines (Royslance, 2002). It detects uses chromosome specific banding patterns, such as C and G, along the length of each chromosome (Langer et al., 2004) to detect changes to chromosome structure including chromosomal deletions and translocations, whilst numerical changes detect aneuploidy, a change in the number of chromosomes (gain or loss) during cell division, or polyploidy, an increase in the number of chromosome by an exact multiple of the haploid number (Kirsch-Volders et al., 2002). This serves to give greater information on any genetic aberrations in the cell lines. Keijser et al. (2007) analysed a ConM cell line, CM2005 and found a very complex karyogram with gains, deletions and rearrangements of almost all chromosomes (Keijser et al., 2007). A literature search, at the start of this study revealed no array-CGH data for conjunctival melanoma cells lines. The aim of this study was therefore to perform tests on two short-term cultures Mel 621 and Mel 635 to characterize them

morphologically and to study their molecular and genetic profiles to help confirm that the conjunctival melanoma cells have a correlating morphology with the previous established ConM.

## 3.2 Results

A small number of ConM samples had been collected prospectively either stored as frozen samples or in the cases of Mel 621 and 635 were grown as short-term cultures for study. These samples were maintained in cell cultures and, once they reached 80-90% confluence, a number of methods were used to detect their genetic and phenotypic characteristics. The findings were compared to other types of melanoma such as UM and CM. Cultures were grown for as long as possible and frozen down at intervals at early passages. This chapter presents the results of the attempts to achieve ConM culture cell lines.

### 3.2.1 Characterisation of Cells in Culture

Both Mel 621 and Mel 635 were initially established in culture by members of the Rare tumour research team and stored frozen prior to start of this study. Ocular melanoma usually presents in culture with a range of different morphologies. The morphology of UM is characterized as; spindle, epithelioid and mixed cells. Spindle cells are long and narrow with large nuclei and nucleoli (McLean et al., 1978), whereas epithelioid cells are larger, with an eosinophilic cytoplasm, and can be poorly cohesive (Figure 3.1).

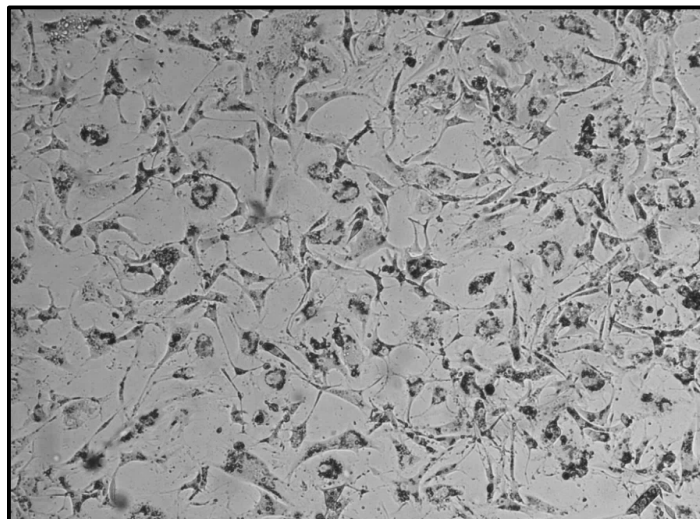


**Figure 3.1: Illustrating a sample of UM (Mel 585) cells in culture at passage 18. Image captured at x40 magnification showing a mixed cell type. Kindly provided by N. Alshammari.**

For the ConM samples, initial outgrowth had proliferating spindle-shaped cells growing outwards from an adherent piece of tissue, as presented in figure 3.2.

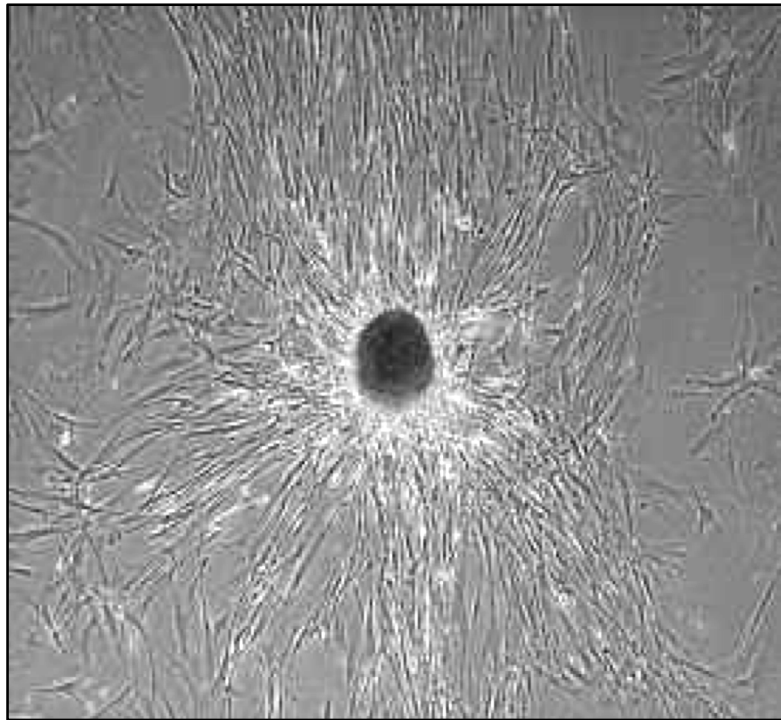


**Figure 3.2:** An example of early culture of primary tumour showing proliferating spindle-shaped cells growing radially outwards from an adherent piece of tissue. kindly provided by Dr. A. Salawu.

Subsequent passages produced cultures in which the cells in ConM were mainly spindle. The spindle cells presented with cytoplasmic processes and some cells showed a marked dendritic shape with nuclei that were round and prominent after spreading. After continued maintenance in culture both Mel 621 and Mel 635 retained and shared the same characteristics, i.e. the spindle shape, (Figures 3.3).

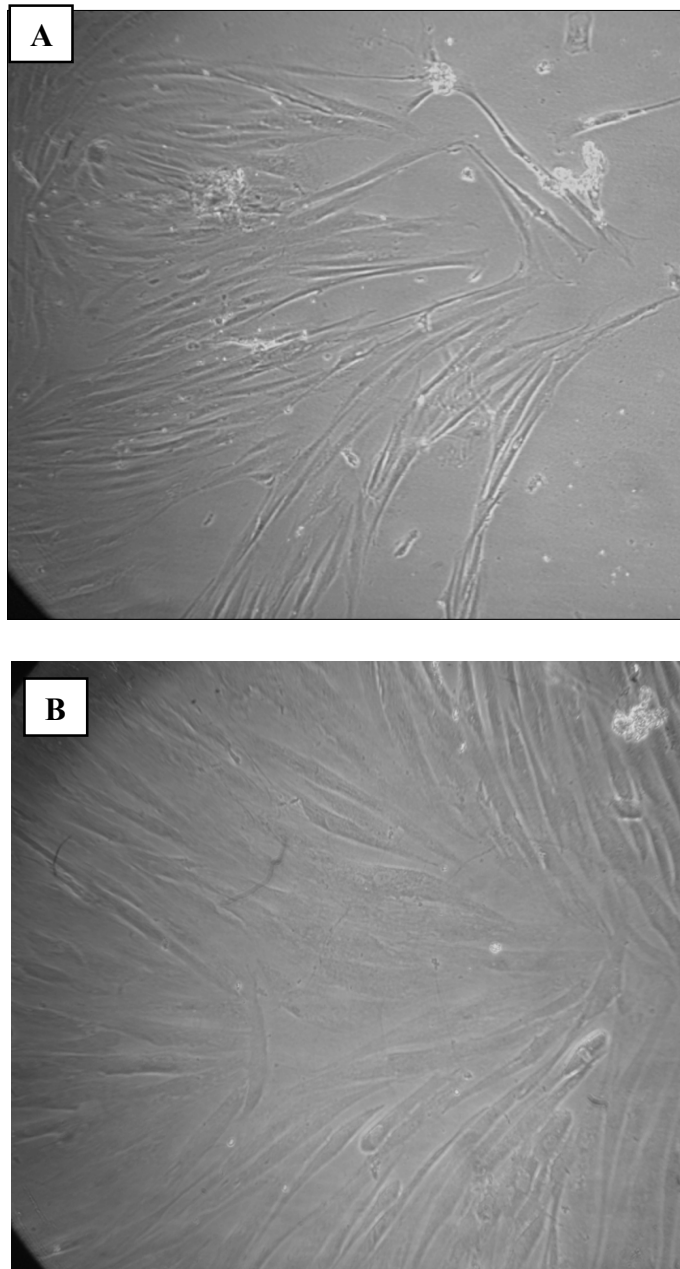


**Figure 3.3: Showing growth of Mel 621 cells in culture at passage11.** A) Image captured at 100X magnification showing the pattern of growth in loose colonies. B) Image captured at 100X magnification showing that most cells are spindle shaped.

The short-term culture of both ConM developed evidence for a lack of contact inhibition and the ability to form multiple layers if left to grow for long enough (Figure 3.4A). These findings were similarly found in some studies that have successfully cultured ocular melanoma cell lines (Hu et al., 2008, Diebold et al., 2009).

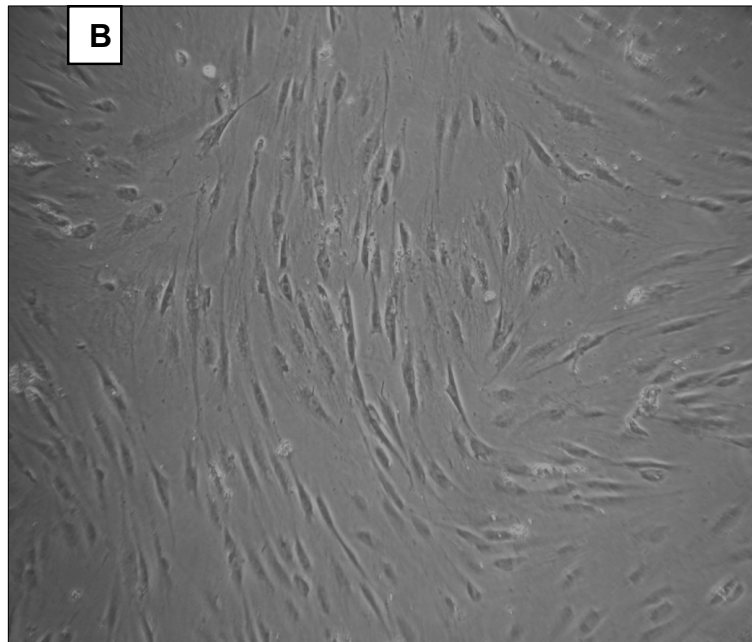
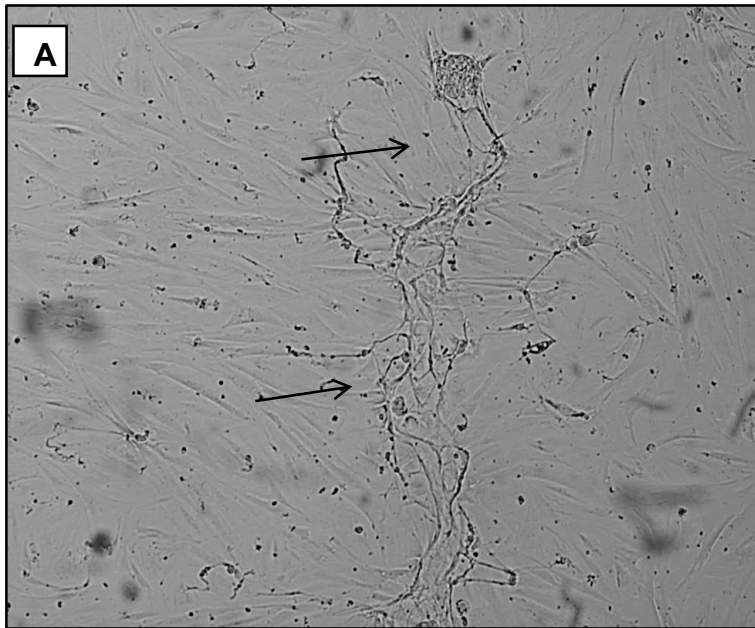


**Figure 3.4:** *Illustrating growth of Mel 635 cells lines at passage 8. A) Image captured at x40 magnification, the arrow shows areas of growth with loss of contact inhibition. B) Image captured at x100 magnification showing that most cells have a spindle-shaped morphology.*

## 3.2.2 Genetic Characterisations

### 3.2.2.1 Karyotyping

While cytogenetic analysis (karyotyping) has always been the starting point for identifying chromosomal abnormalities, it can be a problematic technique. Several attempts were made at harvesting and chromosome banding, and karyotype analysis was done by Dr Karen Sisley. Detailed structural karyotype analysis was not possible, however, even though chromosome enumeration was carried out and gross structural chromosomal abnormalities were observed. Neither of the ConM cell lines used showed evidence of a high level of chromosomal alterations, in comparison to the metaphase spreads of highly abnormal tumour, that have gross structural abnormalities such as double centromeres/constrictions, as shown in figure 3.5.

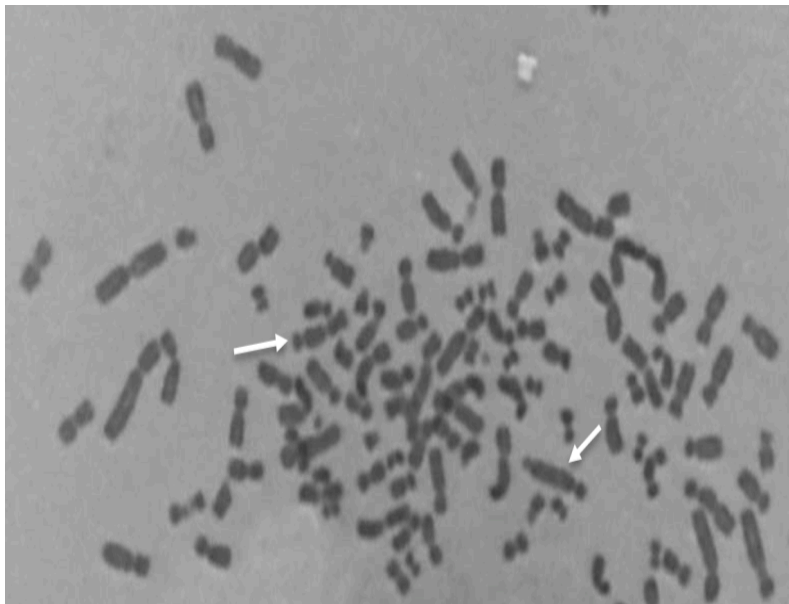


**Figure 3.5:** An example of Metaphase Chromosome Spread adapted from Dr. A. Salawu. The chromosomes and adjacent intact nucleus are stained with Leishmann's stain. The tumour cells are polyploid with the metaphase spread, some of which have gross structural abnormalities such as double centromeres/constrictions (White arrows).

Metaphase chromosomes were obtained from early cultures in only two cases from the primary short-term culture cells Mel 621 and Mel 635, but, none of them showed any level of chromosomal abnormalities (Figure 3.6).

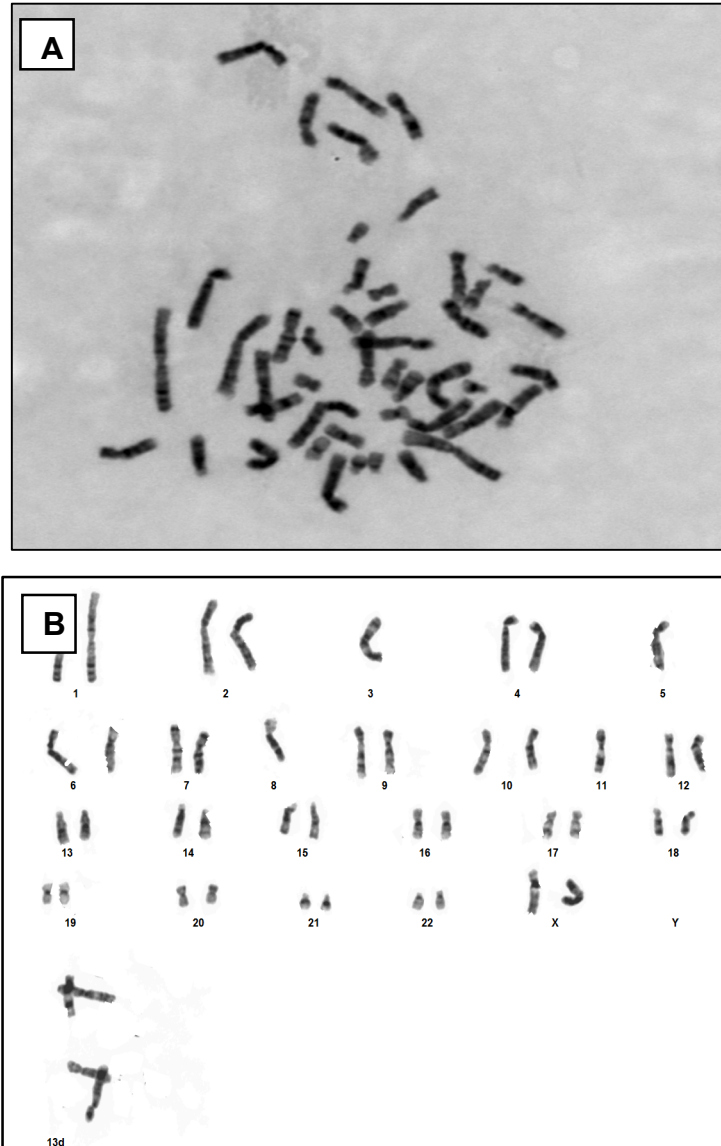


**Figure 3.6: A and B showing an example of Metaphase Chromosome Spread and karyotype from Mel 621. The average chromosome counts obtained from this metaphase spread about 46.**

### 3.2.2.2 Array Comparative Genomic Hybridisation

Array-CGH was carried out to investigate genetic alterations using DNA extracted from the short-term cultures of Mel 621 and Mel 635, and to compare their genomic copy number profiles to their counterparts in UM. Array-CGH profiles of fresh frozen UM tumour tissue (Mel 562), as illustrated in figure 3.7, was used as an example for this comparison.

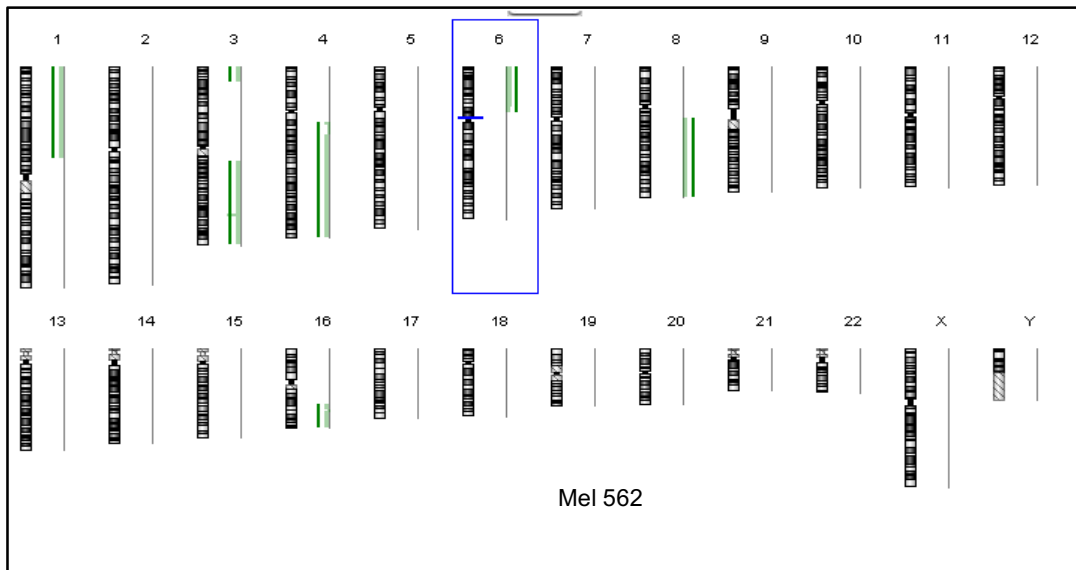


**Figure 3.7: Array-CGH ideograms of chromosomal aberrations in primary fresh frozen UM tissue (Mel 562).** Coloured bars to the right indicate copy number gains. Coloured bars to the left show copy number losses. This genomic view illustrates deletion of 1p, 3q, 4q and 16q, and gain of 6p and 8q. Kindly supplied by N. Alshammari as an example for comparison.

In the present study, however, the two samples of primary ConM (Mel 621 and 635) were only established as a short-term culture. The cultured cells (Mel 621 and 635) had featureless array-CGH profiles, as shown in figures 3.8 and 3.9, and matched the information from the karyotypes were no consistent abnormalities were identified just random gains of chromosomes that would not be detected by array-CGH. Another sample of ConM (Mel 568) was previously run on an array as a primary uncultured tumour from fresh frozen tumour material. This case, Mel 568, showed complex genomic profiles and had multiple abnormalities affecting chromosomes 1, 4, 6, 8, 9, 10, 11, 13, 15, 16, 19, 20, 21 and 22, as illustrated in figure 3.10.

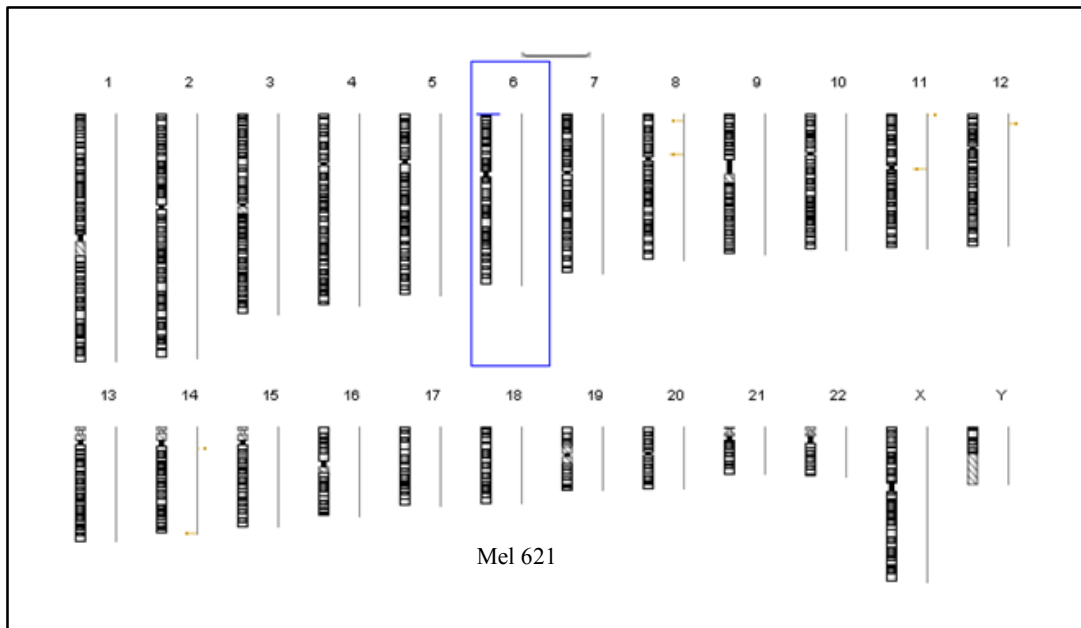


**Figure 3.8:** Array-CGH ideograms of primary short-term cultures of ConM (Mel 621). This genomic view illustrates that no chromosomal aberrations were found.

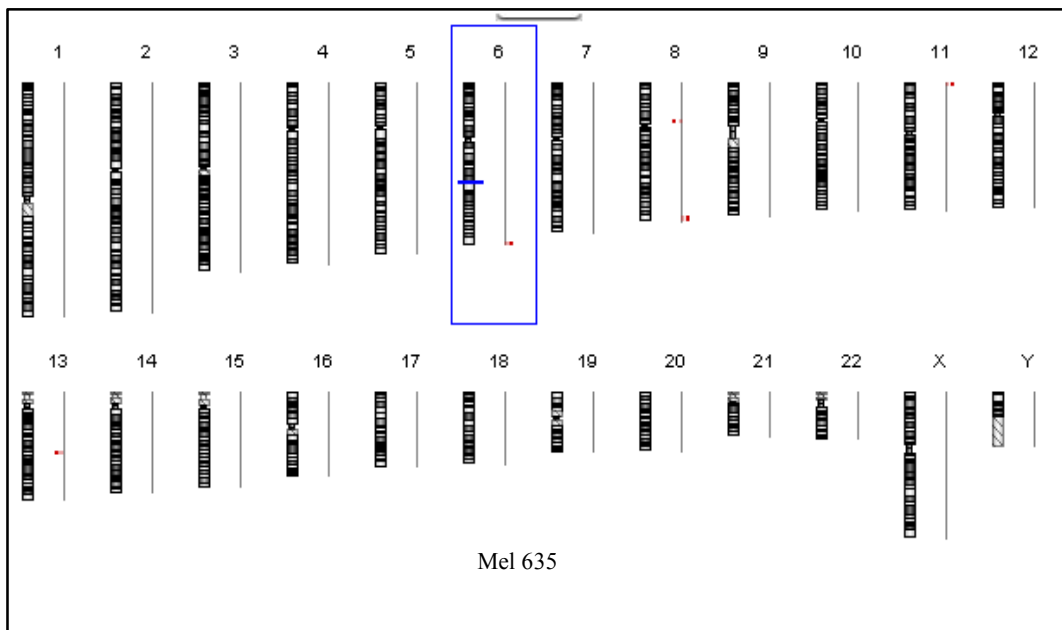


**Figure 3.9:** Array-CGH ideograms of primary short-term cultures cell of ConM (Mel 635). This genomic view also illustrates that no chromosomal aberrations were found.

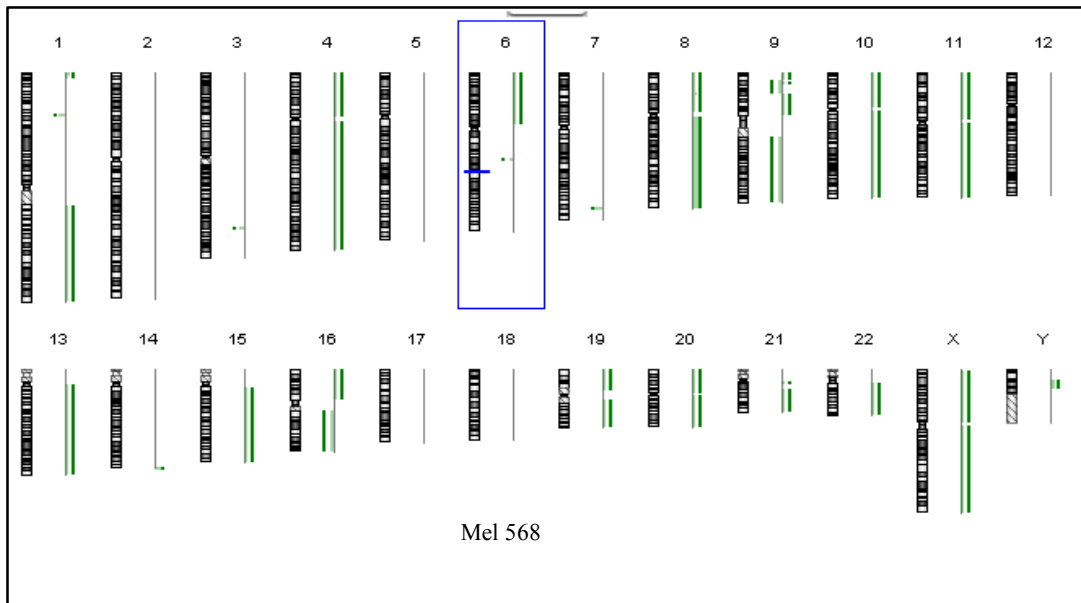


**Figure 3.10: Array-CGH ideograms of a primary uncultured tumour of ConM (Mel 568).** This genomic view case had multiple abnormalities affecting chromosomes 1, 4, 6, 8, 9, 10, 11, 13, 15, 16, 19, 20, 21 and 22.

### 3.2.2.3 Mutational analysis for *BRAF*, *NRAS*, *GNAQ*, *GNA11* and *TERT* genes

The short-term cultures of the MEL 621 and MEL 635 samples were screened to investigate any mutations within *BRAF*, *NRAS*, *GNAQ*, *GNA11* and *TERT* promoter. The purified PCR products were sequenced for mutation hotspot regions of *BRAF*, i.e. both exon 15 and 11, *NRAS*, both exon 1 and 2, and *GNAQ* and *GNA11*, codon 209, and the fragment DNA sizes were compared against a 1Kb DNA ladder as previously described in section (2.1.3). Sequencing of the other genes was achieved successfully, however, and sequencing traces were analysed using FinchTV software (Geospiza, Massachusetts, USA), but no mutations were detected in these short-term cultures, as shown in figure 3.11.

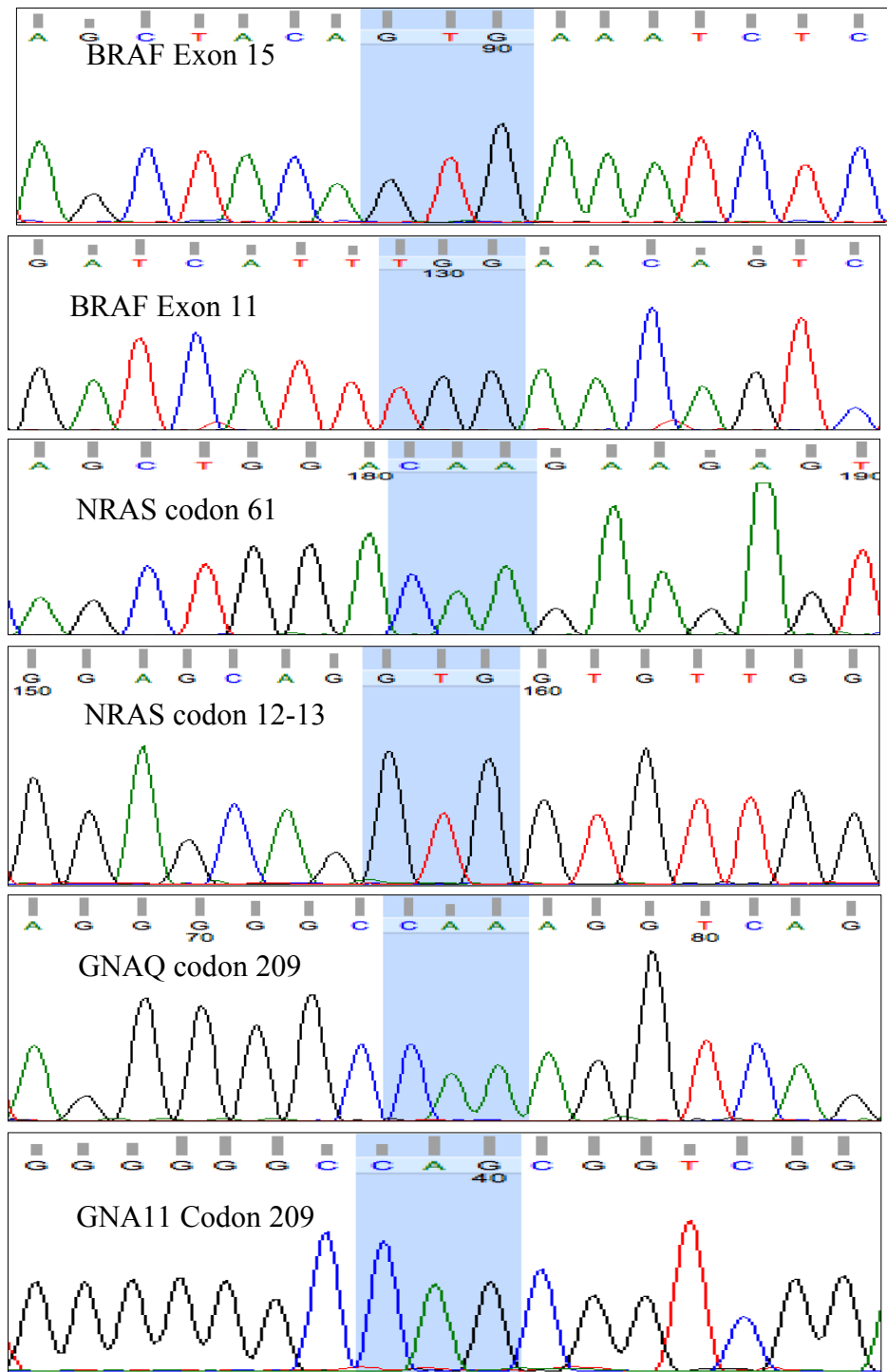


**Figure 3.11: Chromatogram sequencing traces for short-term culture samples showing the wildtype for BRAF, NRAS, GNAQ, GNA11.** An example of a wildtype sequencing chromatogram with BRAF codon 600 at GTG, and also with NRAS codon 61 with normal sequence CCA and GNAQ codon 209 with normal sequence CAA, GNA11 codon 209 with normal sequence at CAG. Traces were visualized using Finch TV software (Geospiza).

#### 3.2.2.4 Fluorescence in situ hybridisation (FISH)

FISH requires DNA probes labelled with fluorochromes to visualize DNA sequences on metaphase chromosomes or interphase nuclei allowing detection of chromosomal re-arrangements, gene amplification and deletion. Many of the probes applied in FISH are now commercially available. The commercial probes used in this study were CEP 3 (Chr 3 centromere 3p11.1-q11.1, spectrum orange) and CEP 8 (Chr 8 centromere 8p11.1-q11.1, spectrum green). In this chapter, samples of ConM, Mel 621 and 635 have been analysed by FISH to detect any imbalance of chromosomes 3 and 8 as shown figure 3.12. But, none of these samples shows any genetic imbalance.

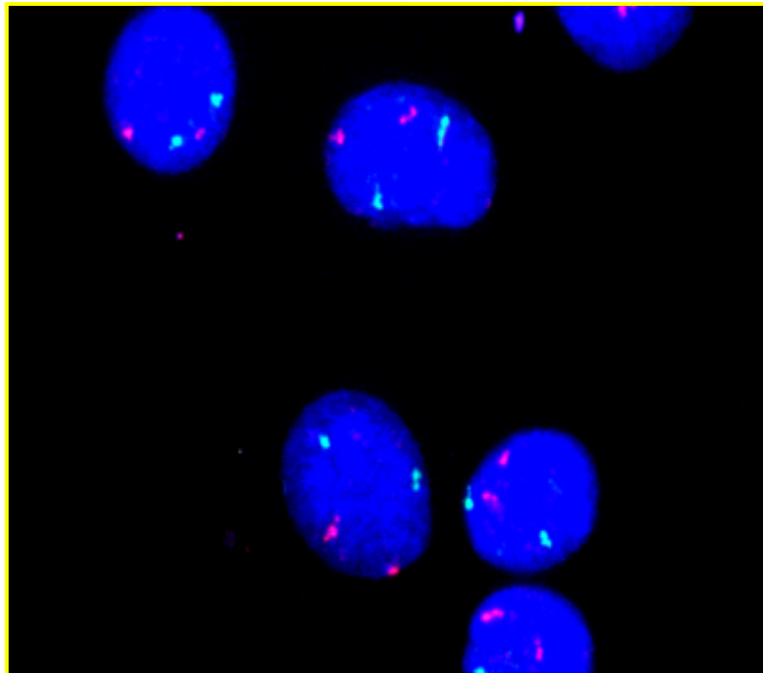


**Figure 3.12: FISH Image illustrating a lack of genetic imbalance (GI) for chromosomes 3 and 8 as found in primary short-term cultures of both ConM 621 and 635 where the two green signals represent (CEP8) and two red signals represent (CEP3) in most nuclei, blue stain (DAPI counterstain).**

### **3.3 Discussion**

#### **3.3.1 Primary tissue culture characteristics**

In the present study, the morphology of both Mel 621 and Mel 635 ConM were similar where most of cells were spindle cells, but distinct to their counterpart UM which have mixed between epithelioid and spindle cells. There is very little literature available on cultured ConM cells. However, some studies have demonstrated that histologically, ConM is composed of malignant melanocytic cells, which can be confirmed by nuclear atypia, and a lack of contact inhibition or prominent nuclei. Furthermore, previous studies reported four different cell types have been detected such as small polyhedral cells, large epithelioid cells, spindle cells and balloon cells (Zembowicz et al., 2010, Oellers and Karp, 2012).

Contact inhibition in confluent cell cultures is well-defined as a reduction of cell mobility and mitotic rate with increasing cell density. It is usually expected that contact inhibition, as the term suggests, is caused by cell contact and is a feature of normal cells growing in culture (Heckman, 2009). Puliafito et al. (2012) also defined contact inhibition in culture as a change from proliferating non-confluent cells to a fully differentiated dense epithelial monolayer (Puliafito et al., 2012). The loss therefore of contact inhibition, is considered to indicate non-normal cell behavior (Zembowicz et al., 2010, Oellers and Karp, 2012). Since both Mel 621 and Mel 635 displayed evidence of lack of contact inhibition with rounding up of cells to form spheroids and overlying to form channels they do not appear to be normal (Figure 3.4a). Certainly, similar observations have been reported previously, with Diebold et al. (2009) reporting on some cases of ConM cell lines and describing them as having variations in morphology matching those observed in this study (Diebold et al., 2009).

### 3.3.2 Genetic Characteristics

In this study, a combination of techniques was used to investigate the genetic alterations of ConM. array-CGH was used to conduct an analysis of the DNA copy number changes associated with ConM. A literature search has revealed no previous data on the array-CGH profile on short-term cultures of ConM cell lines. ConM Mel 568 DNA extracted from a frozen tissue sample was, however, previously run and was revealed to have a complex genomic profile with multiple chromosomal changes (Figure 3.10). The array-CGH profiles generated from the primary short-term cultures of the Mel 621 and 635 cell lines however, gave a negative flat genomic profile array-CGH result. Although a rare melanoma may give an array-CGH negative result; these findings would suggest that the cell lines are from a normal cell population. Alternatively, it could be that the DNA concentration of the cell lines was not good enough, which would distort the ratio of normal to tumour DNA, thus resulting in a flat profile. Therefore, further work is required to establish the reason for this result.

A large percentage of melanomas (but not UM) carry an activating somatic mutation in the *BRAF* and *NRAS* genes (Davies et al., 2002; Pollock et al., 2003), and some reports have found up to 50% of *BRAF* mutation and 18% of *NRAS* mutation in ConM (Lake et al., 2011a, Griewank et al., 2013b, Larsen et al., 2015). No *GNAQ* and *GNA11* mutations have been detected in ConM however, a driver mutation of the *TERT* promoter has recently been detected to be quite frequent in ConM (32%-41% in ConM and 70% in cutaneous melanoma) (Griewank et al., 2013a, Koopmans et al., 2014, Huang et al., 2013b). Here, ConM cell lines Mel 621 and Mel 635 were screened to detect any oncogenic mutation of *BRAF* exon 15 and 11, *NRAS*, *GNAQ*, *GNA11* and *TERT* however, both cell lines were wildtype for all these oncogenes (Figure 3.11).

In this chapter, cytogenetic analysis was also performed to assess the karyotype of ConM samples (Mel 621 and Mel 635) (Figure 3.6). Full G banding was not performed however, by chromosome counting and comparison of gross structural chromosomal abnormalities were observed (Figure 3.5). The findings were in

agreement to some extent with the array-CGH results, finding essentially a pseudo-diploid karyotype with inconsistent aneuploidy, observations that would likely produce a flat array-CGH profile. Conversely, Dahlenfors et al. (1993) found a gain of 4q by using karyotyping on one sample of short-term culture (Dahlenfors et al., 1993). In addition, previous cytogenetic work on ConM was done by Keijser et al. (2007), who reported a very complex karyotype with gains, deletions and changes in nearly all chromosomes being detected in the majority of cultured cells (Keijser et al., 2007). Again, this suggest that our ConM cell lines have arisen from normal cells and are not representative of a ConM tumour.

Several studies have proposed that a fluorescence *in situ* hybridization (FISH) assay for chromosomal aberrations commonly associated with melanoma can identify diagnostically meaningful adjunct information in respect to the distinction of cutaneous melanocytic nevi from melanoma (Curtin et al., 2005, Gerami et al., 2009, Morey et al., 2009). Numerous studies reported that the most common recurrent unbalanced genomic aberrations assessed using the FISH probe set were copy number increases of 6p (*RREB1* at 6p25) and *CCND1* (11q13) and deletion of 6q (*MYB* at 6q23), and the reason of choose theses probes because, the FISH assay consists of a limited number of probes and does not include all of the common unbalanced aberrations in melanoma across the whole genome (Clemente et al., 2009, Gerami et al., 2010, Vergier et al., 2011, Abasolo et al., 2012). A study by Busman et al. (2010) validated the FISH technique as useful in establishing a distinction between conjunctival nevi from melanoma, and reported that gains of *RREB1* and cyclin D1 were found in 100% (6 of 6) and 66% (4 of 6) of cases respectively and loss of *MYB* was detected in all six ConM cases (Busam et al., 2010). Mudhar et al. (2013) also used FISH assays on conjunctival melanocytic lesions and showed that ConM had similar genetic aberrations to CM; unlike UM that has distinct chromosomal changes, principally of chromosomes 3 and 8. In this study neither Mel 621 nor Mel 635 had abnormalities of chromosomes 3 or 8, and other probes have yet to be investigated. The initial findings are not therefore helpful in clarifying the origin of the ConM cell lines, but it is clear that they are distinct from UM.

### 3.3.3 Origin of ConM cell lines Mel 621 and Mel 635.

The most common *de novo* site for ConM is at the limbus with a short horizontal growth followed by a rapid vertical growth (Jakobiec et al., 1989). This type has a higher risk of metastasis and death compared to PAM or naevi (Shields et al., 2011). The limbus is an area found at the corneo-scleral junction that is rich with limbal epithelial stem cells (LESCs) (Varga and Wrana, 2005). Stem cells share some characteristics of cancer cells, such as an ability to proliferate by a process of self-renewal and the potential for pluripotency. The term stem cell refers to the capability for unlimited cell divisions during the life of an organism, giving rise to progeny that enter differentiated pathways with subsequent terminal differentiation (Potten and Loeffler, 1990, Chee et al., 2006). In general, stem cells have certain features that are distinctive from other cells, such as a lack of differentiation, slow cycle, asymmetric division and high proliferative capacity.

LESCs are usually located at the basal layer of the limbal epithelium, while transient amplifying cells (TACs) are found in the basal layer of both the limbal and corneal epithelium (Kruse, 1994, Chee et al., 2006). They share common features with other adult somatic stem cells, such as a small size and a high nuclear-to-cytoplasmic ratio (Barrandon and Green, 1987, Romano et al., 2003, Yoon et al., 2014). They are considered primitive because they are characterized by slow cycling during homeostasis and thus maintain DNA labels for a long time, but in the case of injury they have the capacity to increase their mitotic rate (Lehrer et al., 1998, Lavker and Sun, 2003). In 1971, Davanger and Evensen first proposed that epithelial cells in the limbal location are included in the renewal of the corneal epithelium (Davanger and Evensen, 1971). Moreover, they function as a barrier to conjunctival epithelial cells, preventing them from migrating onto the corneal surface (Ebrahimi et al., 2009). Given the information we currently have available for Mel 621 and Mel 635, it is possible that the cultures derived from these samples have been developed from LESCs that were contaminating the tumours, since they demonstrate atypical behavior in culture but do not have the clear genetic alterations that would suggest they are from ConM.

There are contradictions between several studies about the morphological criteria of LESC, which include the amount of melanin granules present, the prominence of the nuclei and basal membrane invaginations, and there is confusion as to the morphological differentiation between the stem cells and TACs (Cotsarelis et al., 1989, Schlotzer-Schrehardt and Kruse, 2005, Zhao et al., 2009). The expression of the protein markers of the LESC can occur in different cell types of the ocular surface. The well-established marker for LESC is cytokeratin 19, however, which is also expressed in the conjunctival epithelium (Ang et al., 2004, Yoon et al., 2014). So far, the molecular markers for LESC can be classified into two types; stem cell-associated markers such as p63, or differentiation markers, such as K3. Differentiation markers distinguish stem cells from the more lineage committed cells. Although no single marker can reliably identify a LESC, the presence, absence or relative expression of these markers in the corneal epithelium allows the description of a putative stem cell phenotype (Awaya, 2005, Chee et al., 2006).

Finally, it is possible that the cultured Mel 621 and 635 cell lines are derived from a cancer stem cell population rather than a normal stem cell population. Such a population may not demonstrate the high levels of genetic change which would normally be associated with the development and progression of cancer. There is much debate, however, about the role of cancer stem cells and further work is required to explore these points. Overall, to our knowledge, there is little known about the genetic changes that are associated with this malignancy. In this chapter however, a clearly abnormal array-CGH profile has been obtained from a frozen tissue sample of a ConM. However, two ConM cell lines produced abnormal cultural growth but showed no evidence of consistent genetic alterations. Further work is therefore required to clarify these initial findings. In the next step, array-CGH will be used to analyse samples for regions of interest, including samples of fresh and archival tumours. A series of archival samples are available through collaboration with the ocular oncology pathologist Dr Hardeep Mudhar.

# CHAPTER FOUR

Direct sequencing & Array-Comparative  
Genomic Hybridisation of conjunctival melanoma

## 4.1 Introduction

Innovations in biotechnology have allowed cancer research to become ever more clinically appropriate. Several analytical techniques, such as mutational sequencing, cytogenetics and proteomics now allow specific genetic, chromosomal and protein abnormalities to be connected to specific cancers, thereby serving as diagnostic and prognostic biomarkers. Consequently, earlier detection, more accurate clinical diagnoses and more effective and targeted therapies have helped to decrease mortality rates for some cancers (Jemal et al., 2009). A powerful way to improve patient outcomes by these means is to identify the earliest genetic changes that initiate carcinogenesis and thus to discover the genes that play fundamental roles in this process by identifying genomic regions that undergo frequent alterations in human cancers. Over the past period, the field of cancer research has practiced important improvements and developments subsequent to the achievement of the human genome project by the International Human Genome Sequencing (2004). This achievement has led to an improved understanding of the mutational screening of regulatory genes which control the cell cycle and other cellular pathways (Stratton et al., 2009).

In this context, array-CGH is one useful method used to identify tumour suppressors and oncogenes in solid tumours. (van Beers et al., 2006). Array-CGH was established in the late 1990s, bringing with it the benefits of rapid, high-resolution screening of entire genomes that is essential for analysis, with minimal cytogenetic information (Kallioniemi et al., 1992). Array-CGH contains of co-hybridising fragments of test and reference genomic DNA that have been labelled with fluorescent dyes to a set of mapped and marked DNA sequence (probes) on microarray slides. These are then scanned to produce an image of differential signal intensities. It is possible to identify the copy number alterations between tumour and normal DNA by assessing the ratio of fluorescence at each probe at that mapped genomic site. Since its introduction, progress in microarray technologies has led to improvements in various genomic analysis array platforms with even higher resolutions, involving tiling path bacterial artificial chromosome (BAC) arrays of up to B50–100kb resolution (Oostlander et al., 2004) and

oligonucleotide arrays with a theoretical resolution of up to 2kb (Ou et al., 2008). Array-CGH allows the identification of gains and losses within chromosomal regions, providing an essential tool for studying cancer and developmental disorders and for developing diagnostic and therapeutic targets (Shaw-Smith et al., 2004).

In the previous chapter, the primary short-term cultures of Mel 621 and Mel 635 cells were analysed by array-CGH and screened for all known oncogenes that have been reported in ConM however, both tumours were wildtype for all these oncogenes and gave a negative flat genomic profile figure 3.7 and 3.8. These findings suggest that the origin of these cultures may be from a normal cell population. In this chapter, direct sequencing and array-CGH were used on archival and FFPE samples to identify any mutations and genetic alterations that might be correlated with ConM tumours and to detect any recurrent focal SCNA that might be missed by previous report. In addition, the study aimed to corroborate that the genetic alterations in ConM distributed across the genome in a pattern reminiscent of cutaneous melanoma but different markedly from UM as previously reported.

## 4.2 Results

### 4.2.1 Tumour sample

Twenty-One ConM tumour samples that have been reported in this study were collected as fresh specimens and/or archival FFPE blocks. Fresh samples were obtained from patients treated in the Department of Ophthalmology at Hallamshire Hospital (Sheffield, UK) and the archival FFPE samples were usually available from the ocular histopathology department by Dr. Hardeep Mudhar. 17 of the 21 samples were FFPE samples with some of the samples being paired samples. Since fresh frozen tissue is limited, due to the rarity of this tumour, only four such cases were included. Another four CM cell lines were used as a positive control for subtype comparison. The clinical pathological data were also collected based on the information available for each sample as shown in (appendix 2 and 3)

### 4.2.2 Technical issue with DNA purity and quality

While the DNA obtained from fresh frozen tissue produces sufficient good quality DNA for array-CGH, the DNA from archival FFPE tissues is not always suitable for molecular analysis, since it typically has inadequate quality (low yield and highly fragmented) because of the degradative effects of formalin (Srinivasan et al., 2002, van Beers et al., 2006). Besides, several studies have demonstrated that comparing the array-CGH presentation of high and low quality of DNA revealed that fragment sizes less than 200 base pairs might produce noisy and error in the results (van Beers et al., 2006, Mc Sherry et al., 2007). Another reason for the limitations of using DNA from FFPE in high-resolution oligonucleotide array-CGH is the technical difficulty of labelling fragmented DNA. The old enzymatic techniques for labelling DNA, for instance, Nick translation or Random priming, include a fragmentation step with DNase or restriction digestion correspondingly. The more recent non-enzymatic method, referred to as the Universal Linkage System (ULS), however, directly labels the DNA by a chemical reaction that integrates platinum-conjugated fluorophores into the DNA without require for further fragmentation, making it appropriate for low quality fragmented DNA like

that from FFPE tissue (Alers et al., 1999). In terms of quantity, although the DNA yield in most samples, was generally good, (exceeding 10µg in most cases), in some samples, the yield was low. Therefore, Whole-genome amplification used in the low DNA yield samples using Sigma's GenomePlex Single Cell Whole Genome Amplification Kit as described previously (Geigl and Speicher, 2007).

#### 4.2.3 Screening of known oncogenes for *BRAF*, *NRAS*, *GNAQ*, *GNA11* and *TERT* promoters

##### 4.2.3.1 *BRAF* and *NRAS* screening

Since the screening conducted in several studies has indicated that *BRAF* mutation is the most frequent driver mutation in ConM, direct sequencing was conducted to screen this known oncogene in all 21 tumour samples, as well as in the four-positive control CM cell lines. An activating mutation in exon 15 of the *BRAF* gene was found in 24% (5 of 21) ConM tumours at position V600E (T1799A), and the same mutation was found in two of the four positive control CM cell lines. Most of these mutations represented by the valine to glutamic acid substitution at position 600 (V600E), as shown in (Figure 4.1). Mutations within exon 11 of the *BRAF* gene were also screened for, but, no mutations were detected (Figure 4.2).

*NRAS* mutations however, have not been analysed in most genetic studies of ConM. The current study detected *NRAS* mutations at codon 61 (exon 2) in 10% (2 of 21) ConM samples which represents a substitution of a glutamine to arginine Q61R (A182G). On the other hand, *NRAS* mutations at codons 12-13 (exon 1), which result in an amino acid substitution at position 12 from a glycine to an aspartic acid (GGT>GAT), were not detected in this study (Figure 4.3).

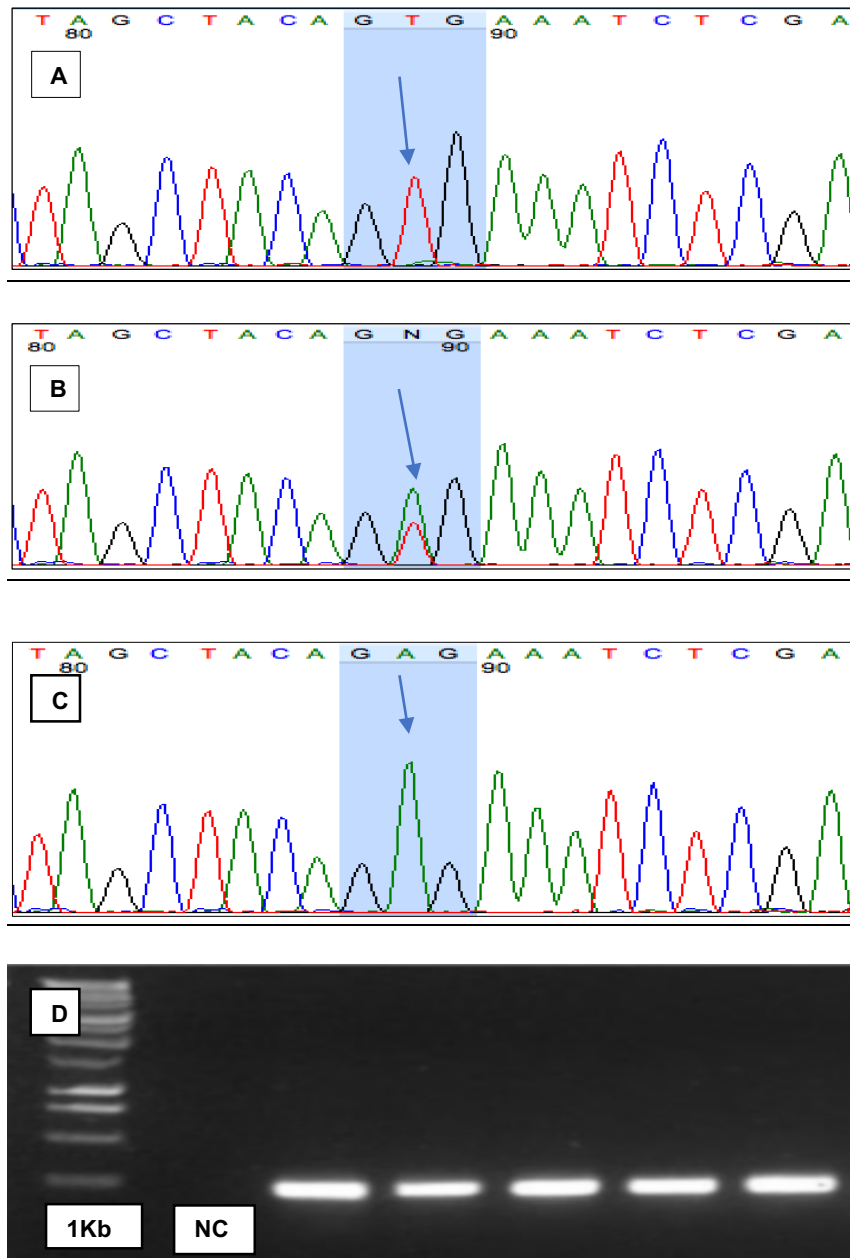


**Figure 4.1: Wild-type and mutant sequence chromatograms of BRAF exon 15.**

**A.** an example of wildtype BRAF, indicated by the blue arrow, with a normal sequence of GTG. **B.** a mutated example of BRAF shows heterogenous thymine to adenine transversion at nucleotide position 1799 (indicated by the blue arrow). **C.** a mutated example of homozygous BRAF at codon 600 in CM indicated by the blue arrow GTG>GAG. **D.** gel electrophoresis with a 1kb marker displaying BRAF amplified PCR product with a 224bp template size. Sequencing traces analysed on Finch TV (Geospiza, USA). 1Kb (1 kilo base marker) NC (Negative control).

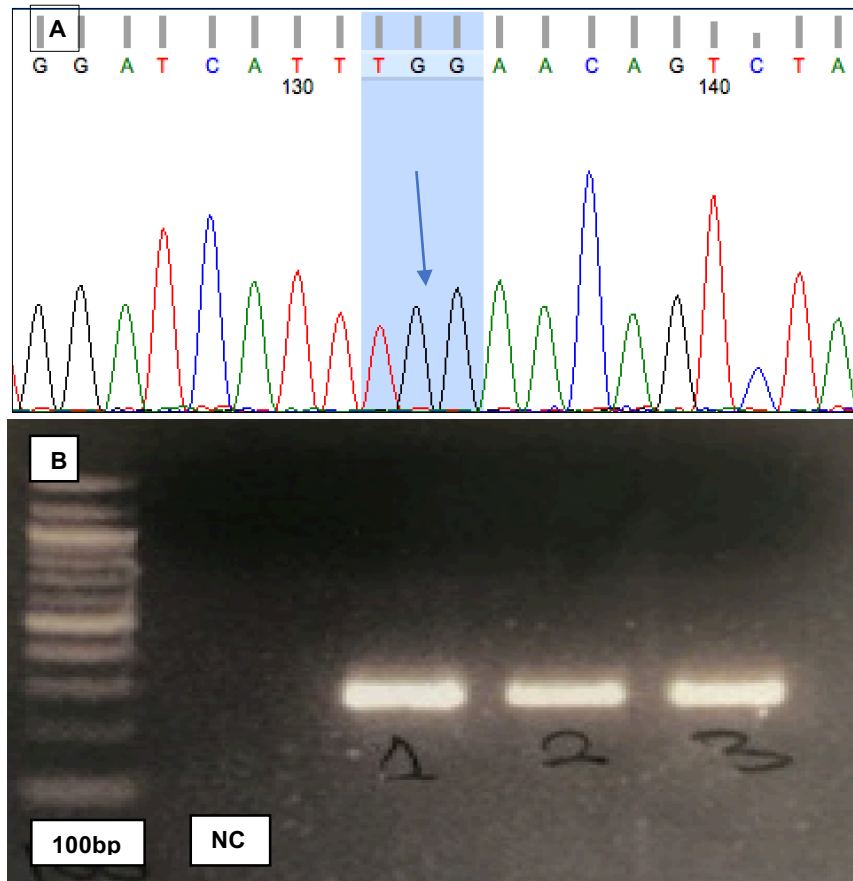


**Figure 4.2: Wild-type sequence chromatograms of BRAF exon 11.**

**A.** an example of wildtype BRAF exon 11, indicated by blue arrow, with a normal sequence of TGG. **B.** Gel electrophoresis with a 100bp marker displaying BRAF exon 11 amplified PCR product with a 295bp template size. Sequencing traces analysed on Finch TV (Geospiza, USA).

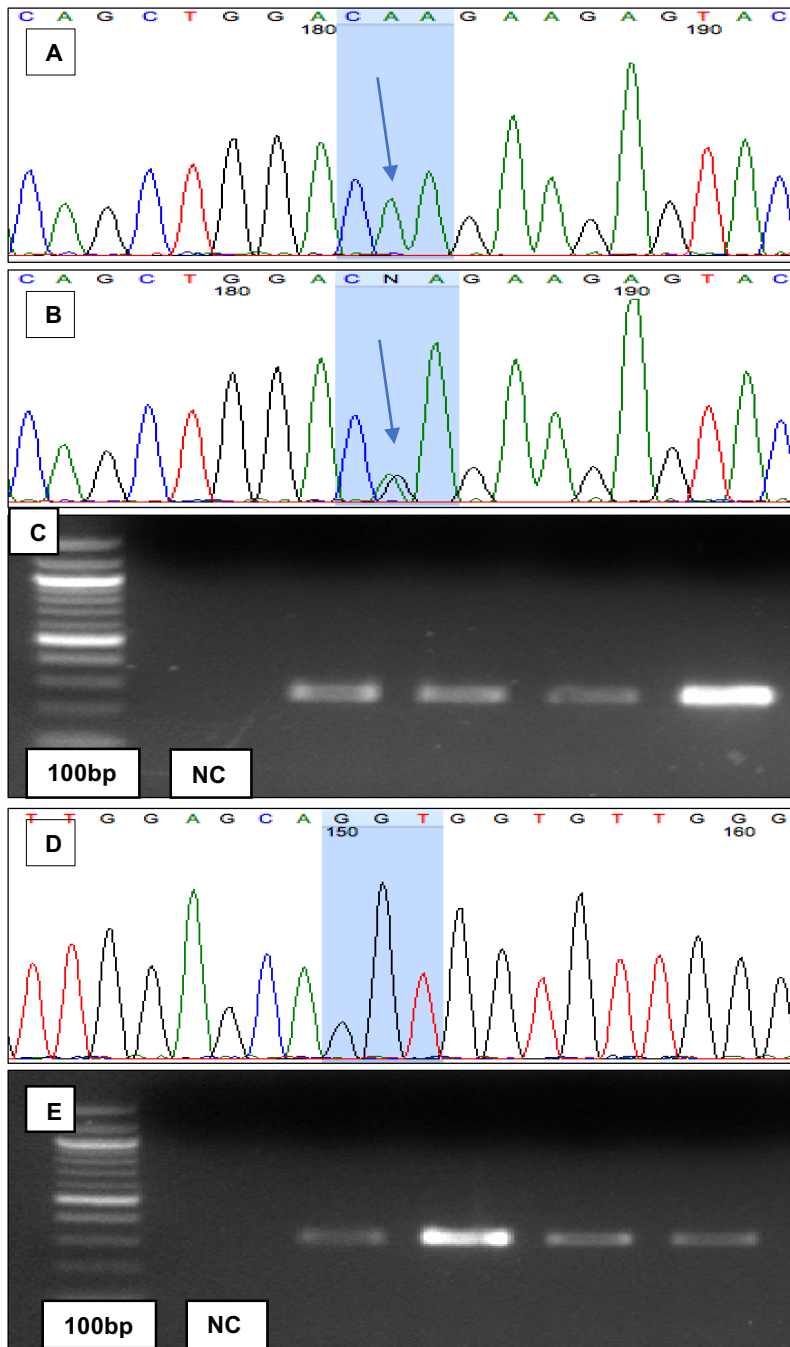


**Figure 4.3: Wild-type and mutant sequence chromatograms of NRAS gene.** **A.** an example of a wildtype NRAS at codon 61 heterozygous indicated by the blue arrow, with a normal sequence of CAA. **B.** a mutated example of NRAS at codon 61 at CAA>CGA (indicated by the blue arrow CGA). **C.** gel electrophoresis with 1kb marker demonstrating the NRAS amplified PCR product with a 262bp template size. **D.** an example of a wildtype NRAS at codon 12-13 exon 2, indicated by the blue arrow with a normal sequence of GGT. **E.** gel electrophoresis with a 100bp marker demonstrating the NRAS codon 12-13 amplified PCR product with a 318bp template size. Sequencing traces analysed on Finch TV (Geospiza, USA).

#### 4.2.3.2 GNAQ and GNA11 exon 5 screening

To investigate the mutations within *GNAQ* and *GNA11* exon 5, all purified PCR products were sequenced directly. This sequencing was successful across all 21 samples. Among the 21 samples screened for *GNAQ* and *GNA11* mutations, the overall mutation frequency was 4% (1/21) and 14% (3/21), respectively. Mutations affecting codon 209 in both *GNAQ* and *GNA11* were c.626A>T(Q209L), resulting in a glutamine to leucine substitution, as shown respectively in figure 4.4 and 4.5.

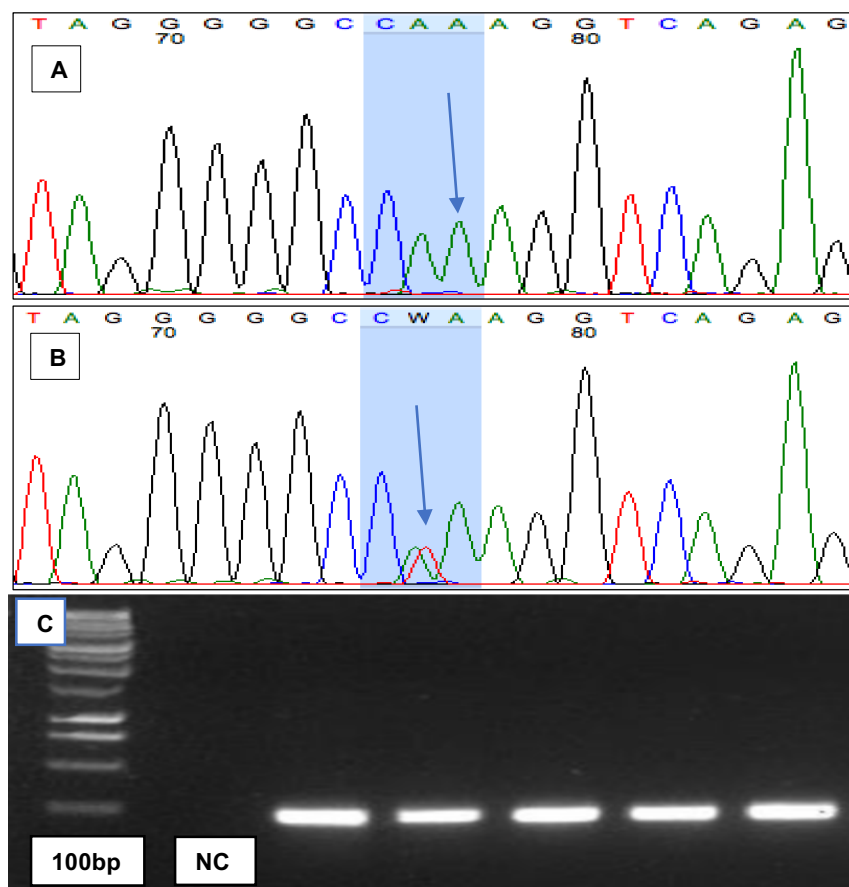


**Figure 4.4: Wild-type and mutant sequence chromatograms of *GNAQ* gene.** **A.** an example of a wildtype *GNAQ* at codon 209, indicating by the blue arrow, showing the normal sequence of *GNAQ*. **B.** clarification of a point mutation at Q209 with an A to T alteration indicated by a blue arrow (CAA>CTA). This mutation predicts substitution by leucine (Q209L). **C.** gel electrophoresis with a 100bp marker demonstrating the *GNAQ* amplified PCR products with a 137bp template size. Sequencing traces analysed on Finch TV (Geospiza, USA).

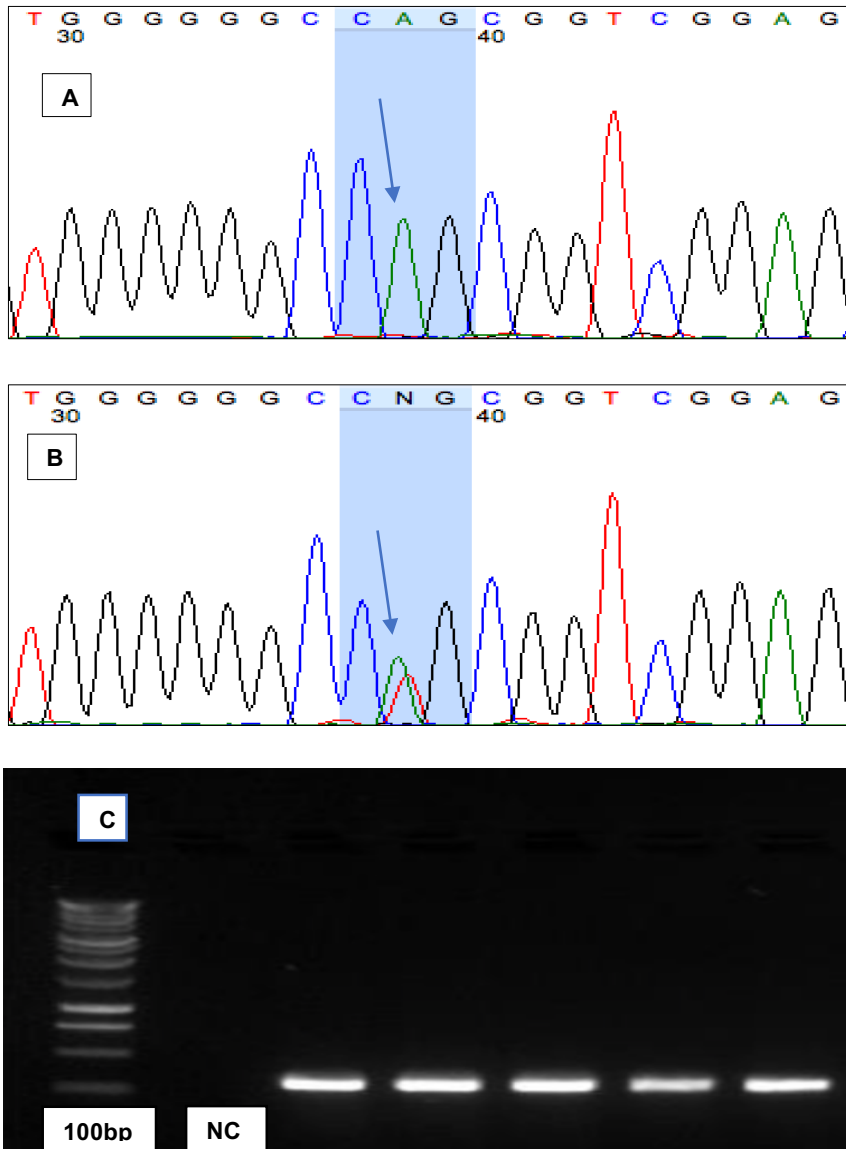
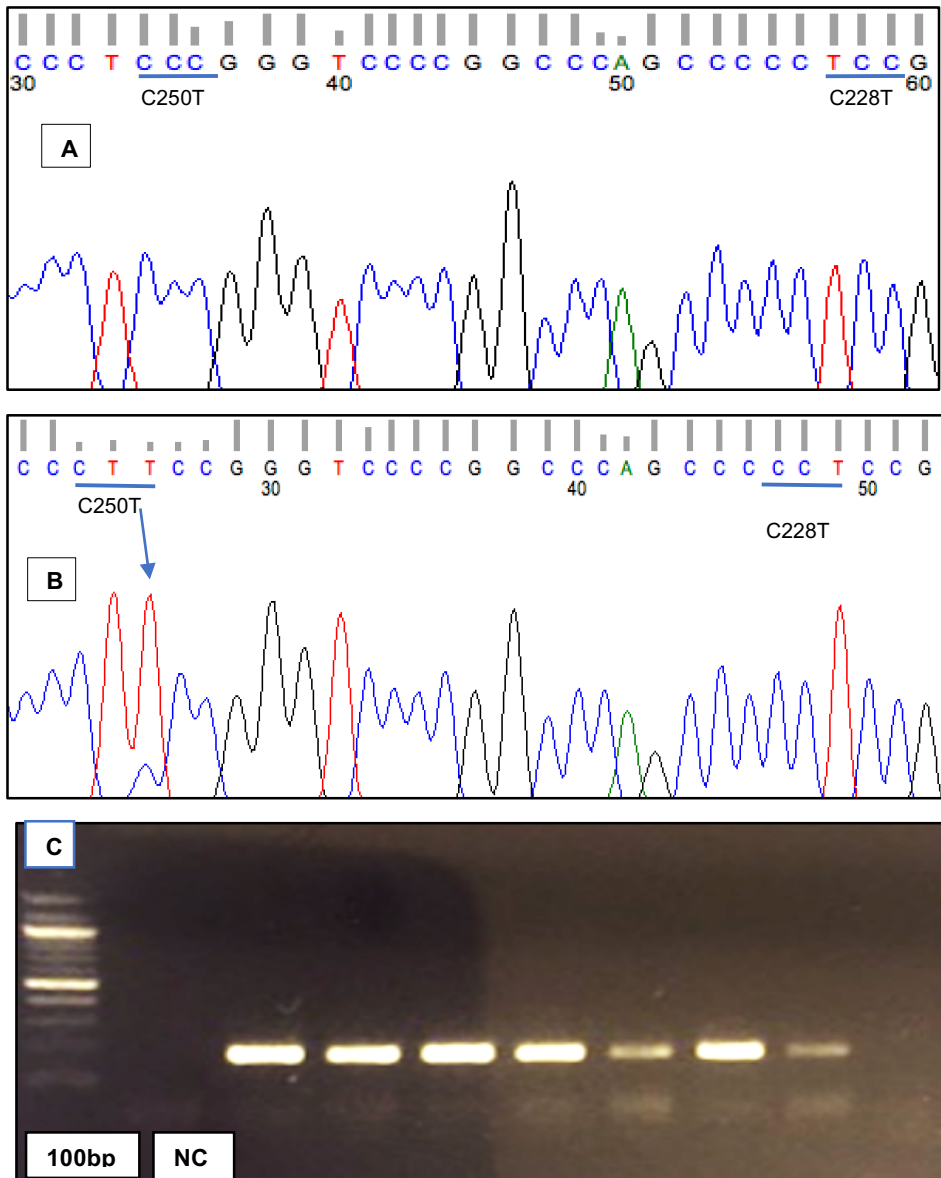


**Figure 4.5: Wild-type and mutant sequence chromatograms of GNA11 gene.**

**A.** an example of a wildtype GNA11 at codon 209, indicating by the blue arrow, showing the normal sequence of GNA11. **B.** clarification of a point mutation at Q209 with an A to T alteration, indicated by a blue arrow (CAG>CTG). This mutation predicts substitution by leucine (Q209L). **C.** gel electrophoresis with a 100bp marker demonstrating the GNA11 amplified PCR products with a 147bp template size. Sequencing traces analysed on Finch TV (Geospiza, USA).

#### 4.2.3.3 *TERT* promoter screening

Recently, several studies have illustrated that up to 71% of CM harbour novel mutations in the promoter region of *TERT*, coding for the catalytic subunit of the telomerase holoenzyme in both familial and sporadic malignant melanoma (Horn et al., 2013, Huang et al., 2013b). It was initially a challenge to optimised the *TERT* promoter. Direct sequencing was conducted to screen all 21 tumour samples, as well as the four-positive control CM cell lines by using a *TERT* primer which was designed similarly to that in Dono et al. (2014). When the sequencing of the *TERT* promoter failed, it was realised that the primers for the *TERT* promoter had a low viability. While unusual for the PCR primers, this may be due to a problem with the life-span of the primer or the quality of the DNA. Another primer designed by Horn et al. (2013), who suggested two different primers for frozen tissue and FFPE samples was then tested, with annealing temperatures 62 °C and 55 °C, respectively, and with the addition of 5% of dimethyl sulfoxide (DMSO) to the master mix. As the primer were still not working different sets of MgCl<sub>2</sub> concentrations and changes in the thermocycler conditions, were also studies, but the sequencing still failed. To overcome this issue a GC rich system kit was used to help support the primer template. Then, direct sequencing was conducted to screen all 21 ConM samples, as well as in the four-positive control CM cell lines. The *TERT* promoter was successfully PCR-amplified and sequenced in 17 of the 21 of ConM samples. Four FFPE samples failed to sequence due to a problem with quality of the DNA. Overall, *TERT* mutations were detected in 47% (8 of 17) of ConM samples. All the identified mutations were located at hotspot region C250T, which displays the nucleotide exchange from cytosine to thymine, as shown in figure 4.6. In the present study, the details of all the known oncogenes mutations that found in ConM tumours are listed in table 4.1 below.



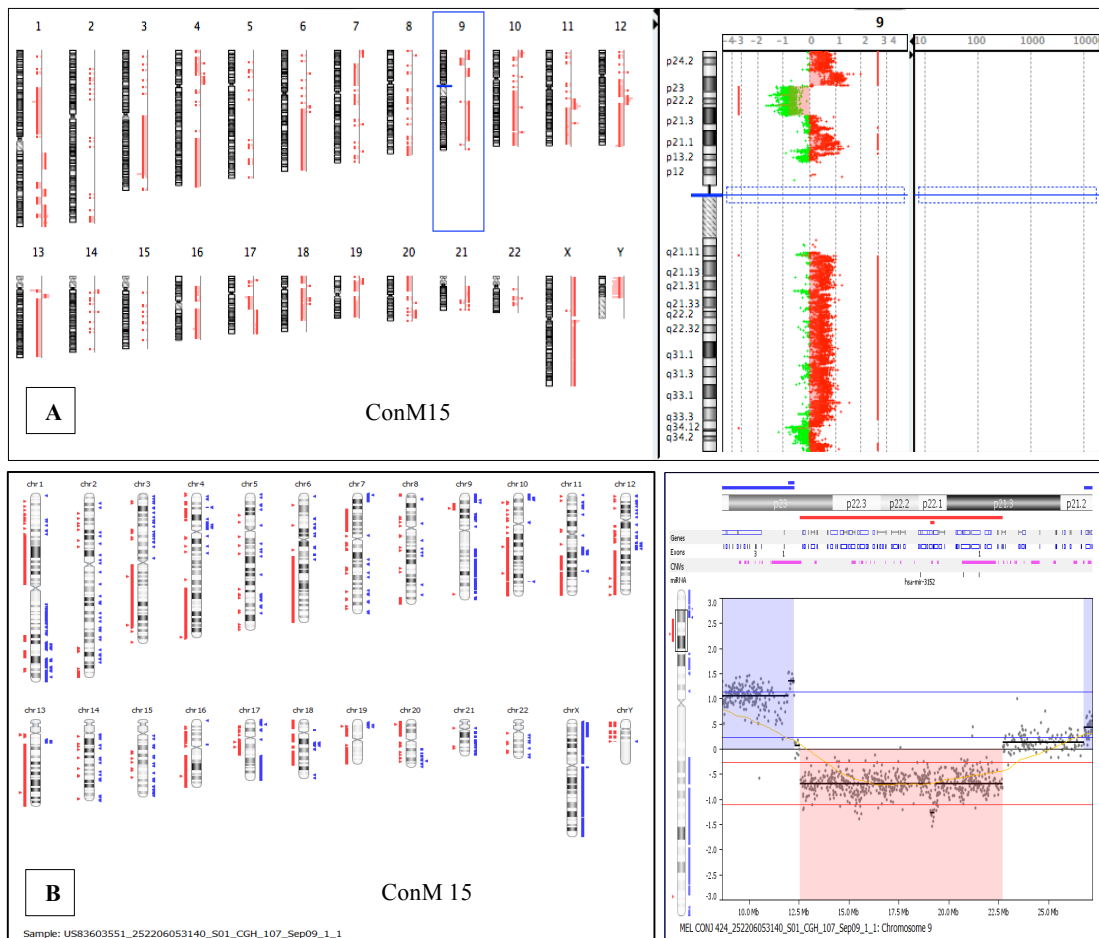
**Figure 4.6: Wild-type and mutant sequence chromatograms of the TERT gene.**  
**A.** an example of a wildtype strand of the TERT promoter represents the hotspot positions at C228T and C250T, indicated by the blue line. **B.** A mutated strand, which displays the nucleotide exchange from cytosine to thymine indicated by a blue arrow (CTC>CTT). **C.** gel electrophoresis with a 100bp marker demonstrating the TERT promoter amplified PCR products with a 187bp template size. Sequencing traces analysed on Finch TV (Geospiza, USA).

Table 4.1 Summary of all the samples sequenced with *BRAF* exon 11 & 15, *NRAS* exon 1 and 2, *GNAQ/GNA11* Q209 exon 5 and *TERT* promoter.

Case Number	<i>BRAF</i> exon 15	<i>BRAF</i> exon 11	<i>GNAQ_Q209</i>	<i>GNA11_Q209</i>	<i>NRAS_61</i>	<i>NRAS</i> 12-13	<i>TERT</i> promoter
ConM 1a	WT	WT	WT	WT	WT	WT	C250T
ConM 1b	WT	WT	WT	WT	WT	WT	C250T
ConM 2a	WT	WT	WT	Q209L	WT	WT	Failed
ConM 2b	WT	WT	WT	Q209L	WT	WT	WT
ConM 3a	T1799A	WT	WT	WT	WT	WT	C250T
ConM 3b	T1799A	WT	WT	WT	WT	WT	C250T
ConM 4	WT	WT	WT	Q209L	WT	WT	Failed
ConM 5	T1799A	WT	WT	WT	WT	WT	C250T
ConM 6	WT	WT	WT	WT	WT	WT	WT
ConM 7	T1799A	WT	WT	WT	WT	WT	WT
ConM 8	WT	WT	WT	WT	WT	WT	Failed
ConM 9	WT	WT	WT	WT	WT	WT	WT
ConM10	WT	WT	WT	WT	WT	WT	WT
ConM11	WT	WT	WT	WT	WT	WT	Failed
ConM12	WT	WT	WT	WT	WT	WT	C250T
ConM13	WT	WT	WT	WT	Q61R(A182G)	WT	C250T
ConM14	T1799A	WT	WT	WT	WT	WT	C250T
ConM15	WT	WT	WT	WT	WT	WT	WT
ConM16	WT	WT	Q209L	WT	WT	WT	WT
ConM17	WT	WT	WT	WT	WT	WT	WT
ConM18	WT	WT	WT	WT	Q61R(A182G)	WT	WT
CM1	WT	WT	WT	WT	WT	WT	WT
CM2	WT	WT	WT	WT	WT	WT	WT
CM3	T1799A	WT	WT	WT	WT	WT	WT
CM4	T1799A	WT	WT	WT	WT	WT	C250T

#### 4.2.4 Copy Number Aberrations (CNAs) in Conjunctival melanoma tumours

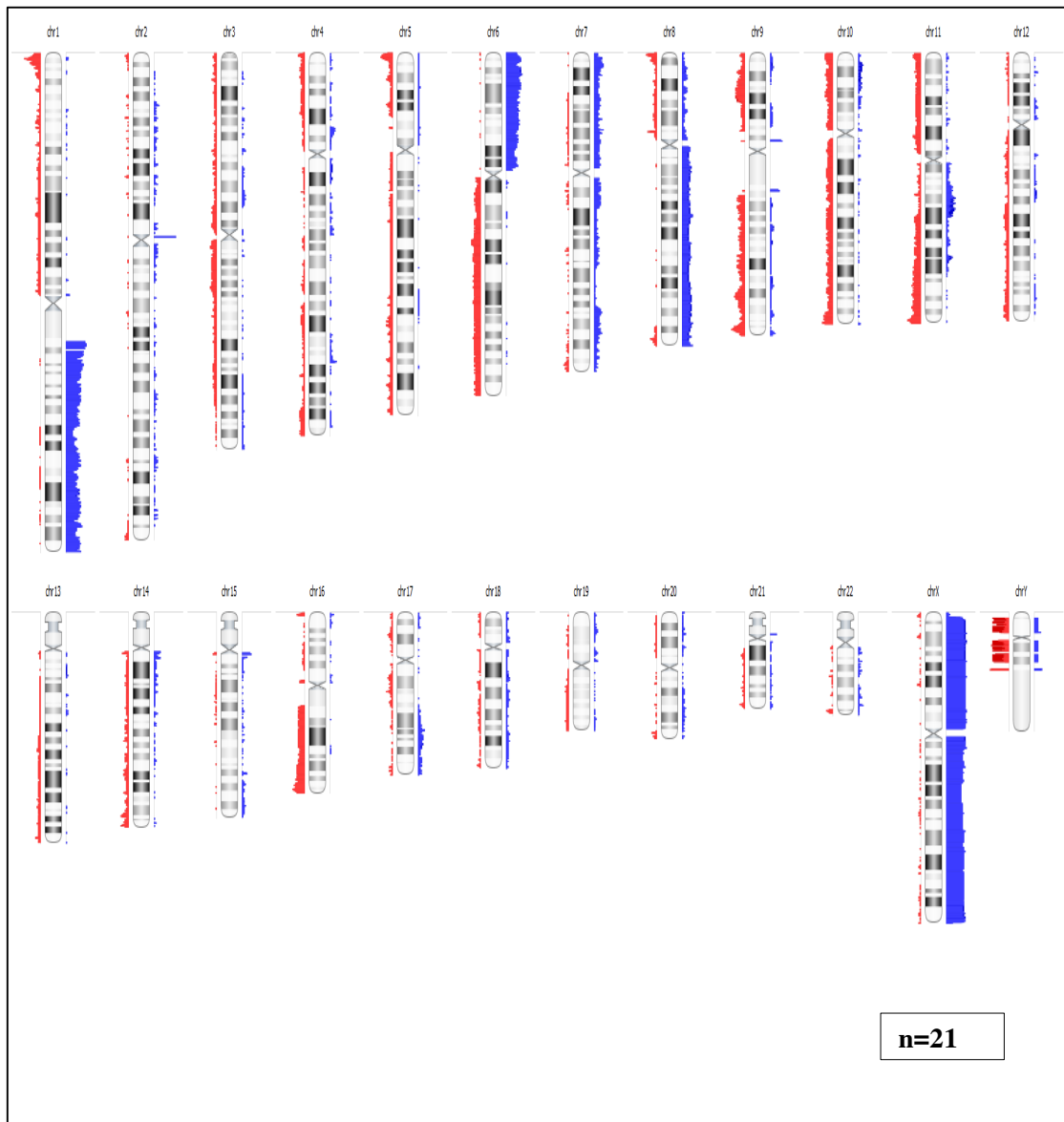
Melanomas are usually characterised by the presence of numerous genomic CNAs. Recurrent unbalanced genomic aberrations known to occur in melanomas are copy number increases of 1q, 6p, 7, 8q, 17q and 20q, and frequent losses of 6q, 8p, 9p, 10q and 21q (Curtin et al., 2009, Blokx et al., 2010). The genomic profile of individual sample, performed by using Agilent software (ADM2 algorithm), showed a range of chromosomal imbalances, and the same CNAs were confirmed by means of a different algorithm, FASST2 (Nexus), as indicated in figure 4.7. Most of the CNAs found in the current study were recurrent gains of 1q (62%), 6p (57%), 7q (29%), 8q (48%), 11q (29%) and 17q (24%) and recurrent losses of 3q (20%), 5p (29%), 6q (24%), 8p (19%), 9p (33%), 10q (29%), 11q (38%), 12q (19%), 13q, 16q (33%), as shown in figures 4.8 and 4.9 respectively. These were consistent with common DNA copy number aberrations that might be associated with ConM. In general, ConM had simple genomic profiles that were described mostly by large whole arm or near whole arm chromosomal aberrations. Most of the large alterations identified were amplifications whereas the focal somatic copy number alterations (SCNA) were mostly losses.



**Figure 4.7: Individual array-CGH ideograms of chromosomal aberrations in primary conjunctival melanoma frozen tissue ConM 15).** **A:** Genomic view from Agilent software elucidating changes in all chromosomes affecting ConM 16 with alterations involving chromosomes 1, 3, 4, 6, 7,8, 9p, 10, 11, 12, 13, 16, 17,18, 19, 20, and chromosome 21. The right panel provides a high-resolution image of chromosome 9, illustrating the areas of amplification (red dots) and the areas of deletion (green dots). **B:** whole genomic view derived from Nexus software, displaying the chromosomal abnormalities that were found in the same case (ConM 15) using a different logarithm, indicated by red triangles to the left (loss) and blue triangles to the right (gain) of the chromosome. In the detailed panel for chromosome 9 on right, the x-axis signifies the whole of chromosome 9 and the y-axis signifies the  $\log_2$  ratio of tumour/reference. The dots represent single probes, the horizontal blue line which above zero shows the detection of copy number gain, with consistent blue shaded area above, and the red line below the zero line shows the detection of copy number losses with consistent red shading below the zero line. Images in **A** were adapted from Agilent Genomic workbench v7.0.4. The ADM2 algorithm was used to detect all the CNAs. Images in **B** were adapted from Biodiscovery's Nexus v8.0, and the FASST2 algorithm was used to detect all the CNA

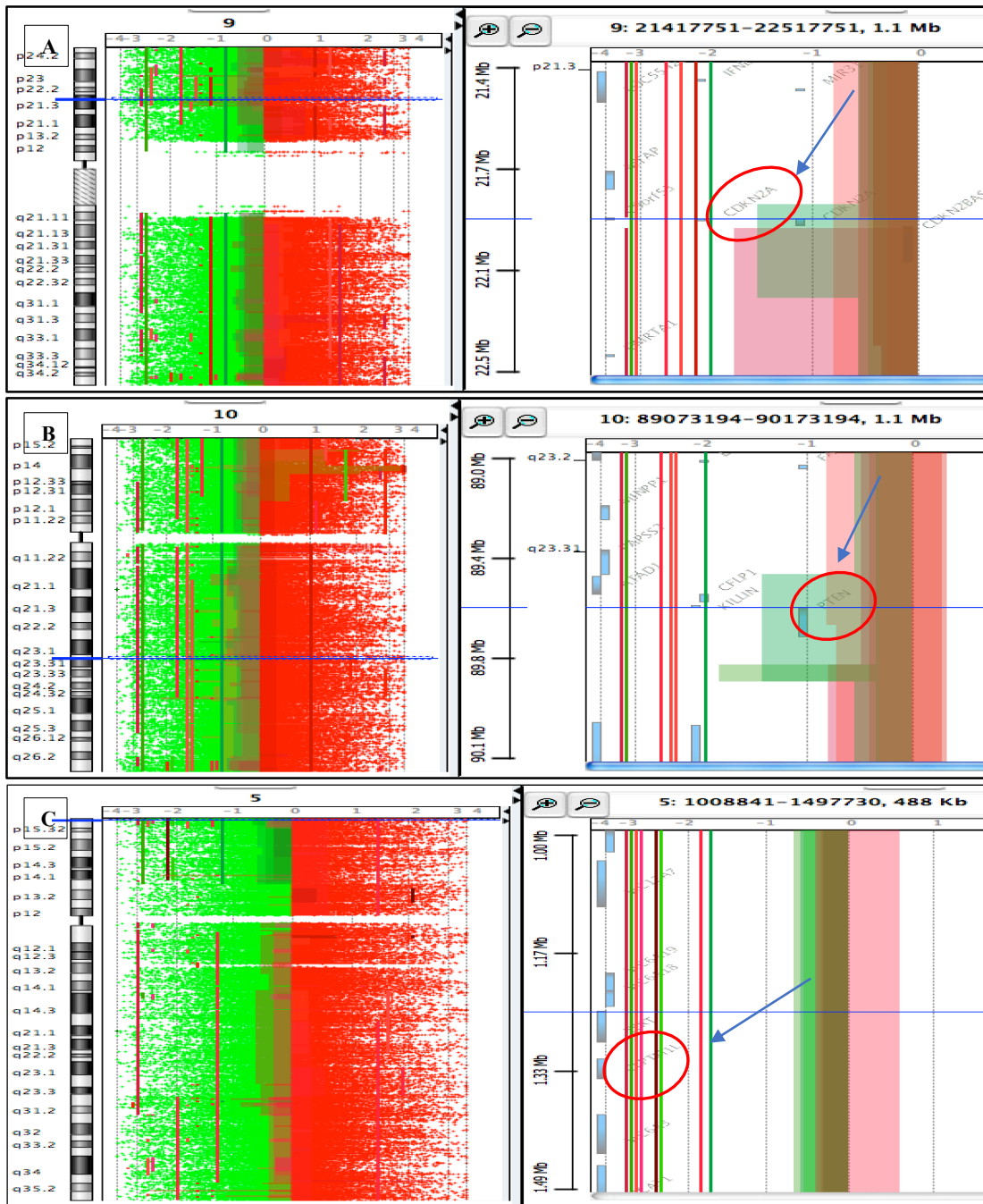


**Figure 4.8: Individual chromosome penetrance plots of 21 conjunctival melanoma tumours.** In this diagram, the most commonly aberrant regions are plotted as a function of their chromosomal position. Red bars to the right of the chromosome represent the frequency of amplifications and green bars to the left of the chromosome represent deletions. Dotted lines on the right and left side of each chromosome ideogram indicate the frequency (0% to 100%) of the identified aberrations, the heights of the bars correspond to the relative frequency of aberrations among the cases. Images were adapted from Agilent Genomic workbench v7.0.4. The ADM2 algorithm was used to detect all the CNAs.



**Figure 4.9: Frequency Plot of Common Genomic Copy Number Aberrations among 21 conjunctival melanoma tumours using Nexus software.** The most common aberrant regions are plotted according to their chromosomal site. Where the red bars to the left of the chromosome identify deletions and blue bars to the right of the chromosome identify the frequency of amplifications. The heights of the bars resemble to the relative frequency of aberrations among the cases. Images were adapted from Biodiscovery's Nexus v8.0. All SCNAs are detected using the FASST2 algorithm.

In the present study, several focal amplifications of oncogenes and homozygous deletions of tumour suppressor genes were revealed by array-CGH using Agilent software (ADM2 algorithm). The most common recurrent DNA copy number changes that were observed was the homozygous deletion of the *CDKN2A* gene on 9p21 in 33% (7 of 21) of the ConM tumours, and the *PTEN* gene on chromosome 10q23 was detected in 29% (6 of 21) tumours. An example of these loci is illustrated in figure 4.10. In addition, loss of telomerase reverse transcriptase *TERT* promoter genes at loci 5p15 was also observed in 29% (6 of 21) of the tumours. Other focal amplifications and deletion of oncogene loci that have been reported previously in ConM studies, either by array-CGH or FISH, were also observed in the current study, such as receptor tyrosine kinase (*KIT*), cyclin D1 (*CCND1*), ras-responsive element-binding protein 1 (*RREB1*) and MYB (myeloblastosis) genes (Busam et al., 2010, Mudhar et al., 2013, Griewank et al., 2013b). In the present study, a gain at the *KIT* locus on chromosome 4q was noticed in 14% (3 of 21) of tumours. A gain of *CCND1* on 11q was found in 24% (5 of 21) of cases, whereas the gain of *RREB1* (6p25) and the loss of *MYB* (6q23) were detected in 57% (12 of 21) and 24% (5 of 21) of ConM tumours, respectively, as summarised in (table 4. 2).



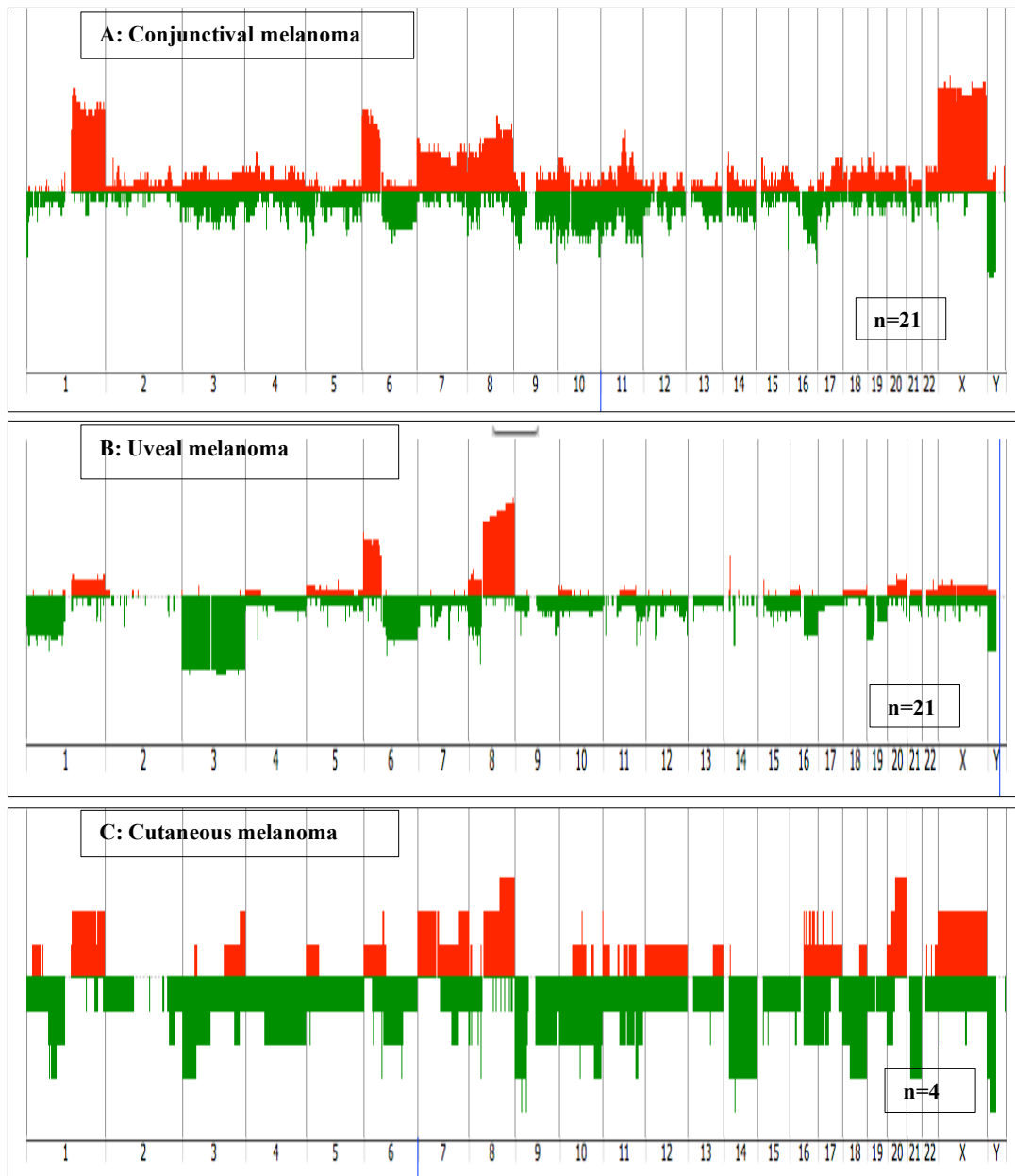
**Figure 4.10: A high-resolution image of chromosomes illustrating focal amplifications of oncogenes and homozygous deletions of tumour suppressor genes revealed by array-CGH.** A: focal losses at the loci of CDKN2A. A view of the whole of chromosome 9 is presented in the left image, while the right side is a magnified image depicting individual CGH probes and the affected genes. The exact location of the genes on 9p21 is marked by the arrowheads. B: focal loss of PTEN. A view of the whole of chromosome 10 is presented in the left image, while the specifically affected gene is shown on the right side, showing the exact location of the gene 10q23. C: focal loss of TERT. A view of the whole of chromosome 5 is presented in the left image, while the specifically affected gene is shown on the right side, showing the exact location of the gene at 5p15. Images were output from Agilent Genomic workbench v7.0.4. The ADM2 algorithm was used to detect all the CNAs.

Table 4.2: Summary of all the most frequent focal CNAs among the conjunctival melanoma tumours in this study as derived from Agilent software.

<b>Gene</b>	<b>Loci Amp/Deletion</b>	<b>Start</b>	<b>End</b>	<b>Size</b>	<b>Percentage %</b>	<b>case code</b>
<b><i>KIT</i></b>	4q12 Amplification	54,657,918 bp	54,740,715bp	82.798 bases	14% (3/21)	ConM 6 ConM 3 ConM 19
<b><i>TERT</i></b>	5p15.33 Deletion	1,253, 147 bp	1,295,069 bp	41,923 bases	29% (6/21)	ConM 12 ConM 4 ConM 14 ConM 9 ConM 13 ConM 5
<b><i>RREB1</i></b>	6p25 Amplification	7,107,597 bp	7,251,980 bp	144,389 bases	57% (12/21)	ConM15 ConM1a ConM14 ConM 5 ConM13 ConM1b ConM 3 ConM 5 ConM11 ConM19 ConM18 ConM17
<b><i>MYB</i></b>	6q23 Deletion	135,180,981 bp	135,219,173 bp	38,193 bases	24% (5/21)	ConM 6 ConM 2b ConM 5 ConM 17 ConM 16
<b><i>CDKN2A</i></b>	9p21.3 Deletion	21,967,752 bp	21,995,301 bp	27,550 bases	33% (7/21)	ConM19 ConM 6 ConM 4 ConM12 ConM16 ConM14 ConM2b
<b><i>PTEN</i></b>	10q23.31 Deletion	87,863,113 bp	87,971,930 bp	108,818 bases	29% (6/21)	ConM6 ConM4 ConM12 ConM16 ConM2b ConM5
<b><i>CCND1</i></b>	11q13.3 Amplification	69,641,087 bp	69,654,474 bp	13,388 bases	24% (5/21)	ConM6 ConM1a ConM2b ConM19 ConM10

#### 4.2.5 Common aberrations in different melanoma subtypes

To our knowledge, ConM have not been well characterised at the genetic level. Previous studies, however, have demonstrated that the most common alterations found in ConM are similar to those in cutaneous and mucosal melanomas, but different from UM. In order to assess the common aberration in different subtypes of melanoma, array-CGH profiles of a similar number of uveal melanomas obtained from one of the researchers in oncology team (Mohammed Alfawaz) were analysed and compared to both ConM samples, and the four profiles of cutaneous melanoma samples that being used as a positive control. These comparisons showed that the most copy alterations in ConM, for instance, gain of 1p, 6p, 7, 8 and 9 and loss of 1, 3, 4, 6, 8, 9, 10, 11, 12, 13 and 16 which were analogous to the copy number variations found in the cutaneous melanoma subtype but different from those in uveal melanomas, which often have losses of 1p, 3, and 6q, and gains of 6p and 8q, as shown in figures 4.11 and 4.12. The changes seen in UM at chromosomes 6 and 8, as well as the losses of 1p, are also frequent in CM, but losses at any point in chromosome 3 are rare in cutaneous tumours (van den Bosch et al., 2010).



**Figure 4.11: DNA copy number profiles of different melanoma subtypes. A and B** show grouped CNAs results for 21 conjunctival and uveal melanoma samples, respectively. **C:** Copy number alterations of a group of four cutaneous melanomas. All groups were analysed identically with Agilent software. Alterations are presented as penetrance plots; with gains in red and losses in green. Images were output from Agilent Genomic workbench v7.0.4. The ADM2 algorithm was used to detect all the CNAs.

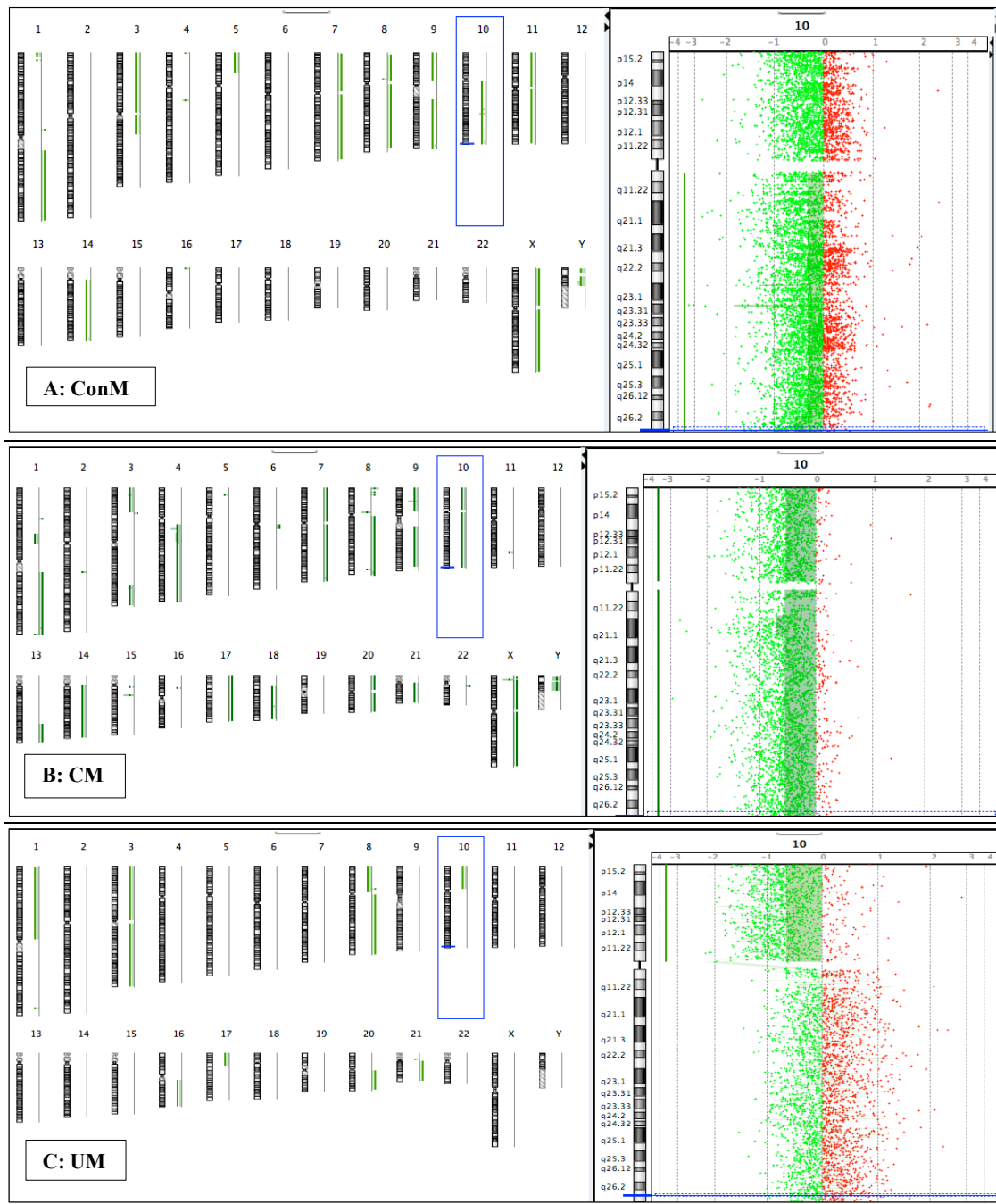


**Figure 4.12: Individual Array-based CGH ideograms for different melanoma subtypes. (A):** genomic profiles illustrating the chromosomal abnormalities of conjunctival melanoma in comparison with chromosomal alterations found in **(B)** cutaneous melanoma, and **(C)** uveal melanoma. The latter can be seen to be completely distinct from the other melanoma subtypes. All groups were analysed identically with Agilent software. Gain are presented in red, losses in green. Images were adapted from Agilent Genomic workbench v7.0.4. The ADM2 algorithm was used to detect all the CNAs.

#### 4.2.6 Copy number aberrations among BRAF and NRAS mutations

The copy number profiles of 21 ConM tumour samples were also grouped according to the presence of the activating oncogene mutation. These groups consisted of five *BRAF*-mutant tumours, two *NRAS*-mutant tumours, and fourteen tumours having neither *NRAS* nor *BRAF* mutations. Generally, wild-type tumours have higher numbers of chromosomal alterations, a finding that was also seen in *BRAF-NRAS* wildtype in CM (Gast et al., 2010). In this current study, the genomic profile of the two *NRAS* mutation group showed losses of 9p and 16q and gains of 1q, 6p and 8q. However, the most common copy number alterations correlated with the five *BRAF* mutations were gains of 1q, 6p, 7 and 8, and losses of 3p, 5p, 10q and 14. The losses of 10q, including the *PTEN* locus 10q23, were particularly prominent in *BRAF* mutations tumours, which were comparable to those reported in *BRAF*-mutant CM (Gast et al., 2010, Lazar et al., 2012) (Figure 4.13).

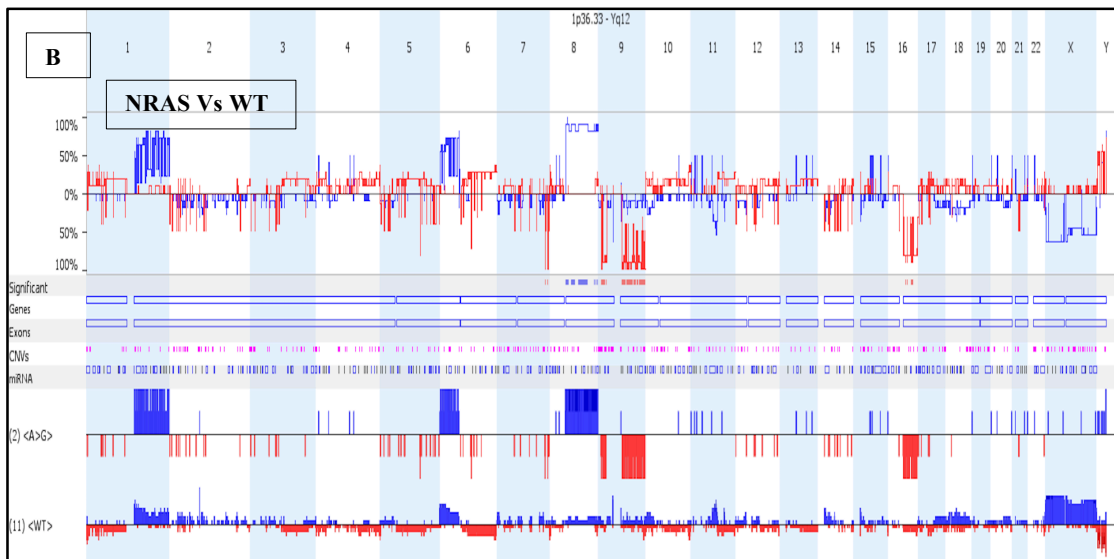
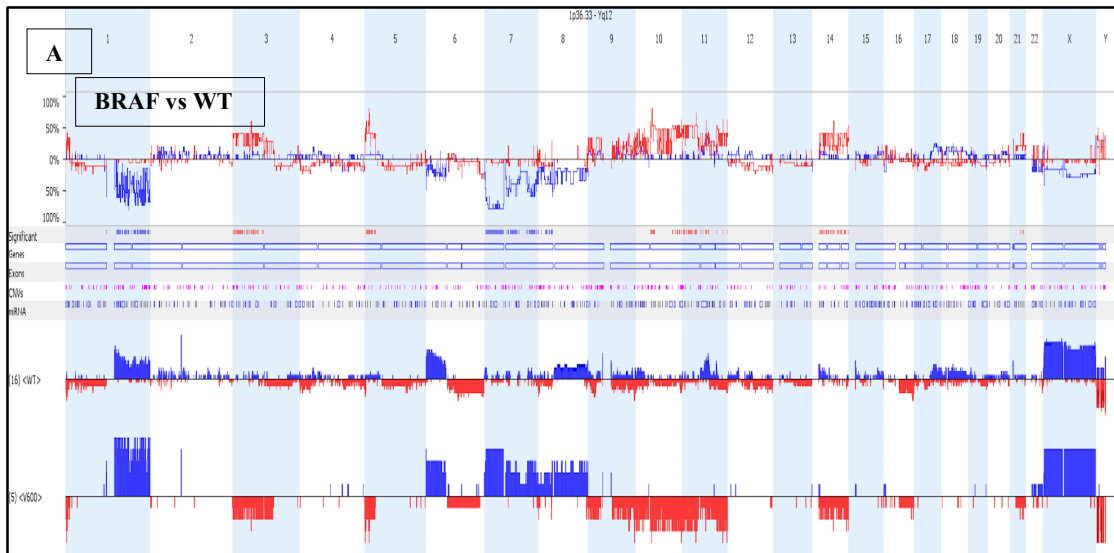


**Figure 4.13: Frequency plot of the genomic view comparing BRAF mutations with wildtype and NRAS with wildtype.** The magnitude of the amplifications or deletions were indicated as short or long bars, where the amplifications presented in blue above the zero baseline and, the deletions were presented in red below the zero baseline. The bigger bars indicate larger magnitude, and the opposite for the smaller bars. **A.** BRAF mutations tumours showed more association with gain of 1q, 6p, 7 and 8, and with loss of 3p, 5p, 10q, 11 and 14 compared to wildtype groups, which shows a higher range of copy number changes. **B.** NRAS mutations tumours showed more correlated with gain of 1q, 6p and 8q and loss 9p and 16q than the wildtype. All aberrations in each sample were identified using the FASST2 Algorithm.

#### 4.2.7 Copy number aberrations among cases with *TERT* mutation and without mutations

The ConM tumour samples were also grouped according to the presence of *TERT* mutation. These groups consisted of eight *TERT*-mutant tumours and nine tumours were *TERT* wild-type. Generally, wild-type tumours have higher numbers of chromosomal alterations, a finding shows more genome instability associated with this group. However, *TERT* mutations cases showed more association with gain of 1q, 6p, 7 and 8, and with loss of 3p, 5p, 9p, 10q, 11 and 16 and this indicates that this group had less genome instability.

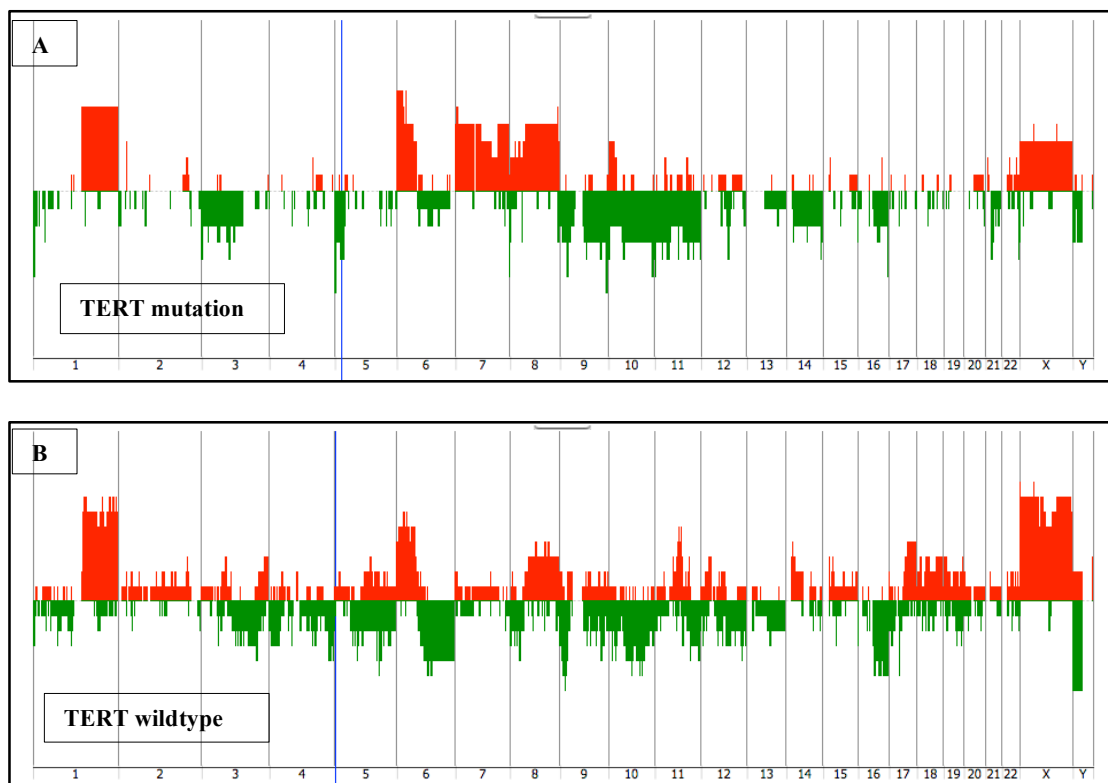


**Figure 4.14: Penetrance plots of DNA copy number profiles among conjunctival melanomas comparing the samples that have *TERT* mutations and wild type. A:** This diagram shows the most common CNAs found in conjunctival melanomas, where *TERT* mutations tumours showed more association with gain of 1q, 6p, 7 and 8, and with loss of 3p, 5p, 10q, 11 and 16 compared to wildtype groups, which shows a higher range of copy number changes. Where the areas of amplification are represented by the red bars and the areas of deletion are represented by the green bars. The heights of the bars correspond to the relative frequency of aberrations among the cases. Images were output from Agilent Genomic workbench v7.0.4. All the CNAs was detected by using the ADM2 algorithm.

#### 4.2.8 Common aberrations among primary and metastatic conjunctival melanoma

Based on reviewing the clinical information of the research patients obtained by ocular histopathologist Dr. Hardeep. Of 21 cases included in this study between female and male, their aged range from 37-85 years old. The majority of the samples for the series were chosen without previous knowledge of the genetic changes or outcome. The data from Array-CGH shows that approximately 62% of all ConM samples were originally from primary ConM and 38% were metastasized. The most frequent CNAs among 13 samples in the primary conjunctival group associated with recurrent gains of 1q, 4q, 6p, 7q, 8q, 11q, 17q, 19p and recurrent loss of 3q, 5p, 6q, 9p, 10q, 11q, 12q and 16q. Losses of chromosome 6q and 9p and gains of 1q, 6p and 8q were prominent in primary ConM, meaning that these changes may play important roles in ConM development.

The most CNAs observed in the eight metastatic ConM samples, were recurrent gains of 1q, 6p and 7q, 11q, and losses of 3q, 5p, 6q, 9p, 10, 11q, 12q and 16q (Table 4.3) and (Figure 4.15). The genetic alterations associated with primary ConM shows more instability compared to metastasis group that had less genome instability where a lot of focal CNAs, including losses of 5p, 9p, 11q and 16q, were more frequent, suggesting that these alterations may have a later role in ConM tumorigenesis and disease progression.

Table 4.3: Summary of the most frequent CNAs among Primary and Metastatic Conjunctival melanomas tumours in this study.

<b>Region</b>	<b>Primary n=13</b>	<b>Metastasis n=8</b>	<b>All Samples n=21</b>
<b>1q gain</b>	69% (9/13)	50% (4/8)	62% (13/21)
<b>3q loss</b>	23% (3/13)	13% (1/8)	19% (4/21)
<b>4q gain</b>	23% (3/13)	None	14% (3/21)
<b>5p loss</b>	23% (3/13)	38% (3/8)	29% (6/21)
<b>6p gain</b>	62% (8/13)	50% (4/8)	57% (12/21)
<b>6q loss</b>	31% (4/13)	13% (1/8)	24% (5/21)
<b>7q gain</b>	23% (3/13)	50% (4/8)	33% (7/21)
<b>8q gain</b>	69% (9/13)	25% (2/8)	52% (11/21)
<b>9p loss</b>	31% (4/13)	38% (3/8)	33% (7/21)
<b>10q loss</b>	31% (4/13)	25% (2/8)	29% (6/21)
<b>11q loss</b>	31% (4/13)	50% (4/8)	38% (8/21)
<b>11q gain</b>	23% (3/13)	25%(2/8)	24% (5/21)
<b>12q loss</b>	8% (1/13)	13% (1/8)	10% (2/21)
<b>16q loss</b>	23% (3/13)	50% (4/8)	33% (7/21)
<b>17q gain</b>	31% (4/13)	13% (1/8)	24% (5/21)

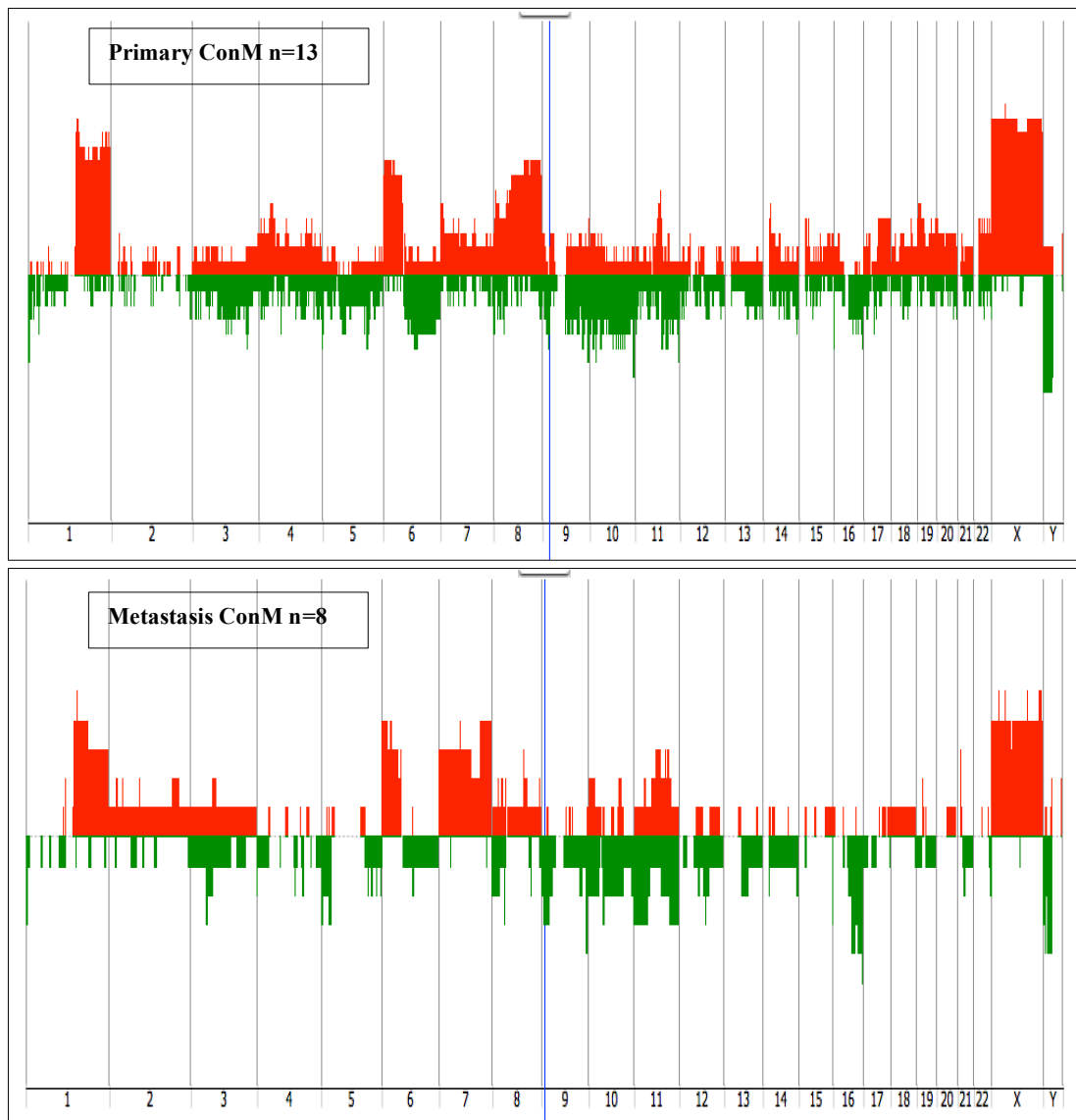


**Figure 4.15: Penetrance plots of DNA copy number profiles of 21 cases of conjunctival melanomas according to the original clinical data. A:** This diagram shows the most common CNAs found in primary conjunctival melanomas, with gains of 1q, 6p, 8,11q, 17p,19 and 20, and losses of 5, 6q, 9, 10, 11 and 16q. **B:** CNAs found in metastasis conjunctival melanoma cases, illustrating gains of 1q, 6p, 7, 11q, and losses of 5p, 9p, 10, 11 and 16q, where the areas of amplification are represented by the red bars and the areas of deletion are represented by the green bars. The heights of the bars correspond to the relative frequency of aberrations among the cases. Images were output from Agilent Genomic workbench v7.0.4. All the CNAs was detected by using the ADM2 algorithm.

### 4.3 Discussion

Array-CGH can play a crucial role in identifying oncogenes in solid tumours, in identifying tumour suppressors, and in the classification of tumours. In addition, it allows the identification of chromosomal regions of gains and losses, providing an essential tool for studying cancer and developmental disorders and for developing diagnostic and therapeutic targets (Shaw-Smith et al., 2004, Awaya, 2005, van Beers et al., 2006). Array-CGH is commonly used in genomic research for identifying DNA copy number aberrations, and are gradually being applied as a choice in diagnostic evaluation for congenital and acquired genomic aberrations (cancers) (Wang et al., 2013).

#### 4.3.1 Known oncogene mutations in conjunctival melanoma

The most relevant mutations in CM are the activating mutations of *BRAF* and *NRAS*, since these oncogenes activate the MAPK pathway by stimulating the mitogen-activated protein kinase1 (MEK1) (Akslen et al., 2005). Likewise, in ConM *BRAF* mutations are reported in 14% to 50% of ConM and by *NRAS* mutations in up to 18% of tumours (Gear et al., 2004a, Spendlove et al., 2004, Lake et al., 2011a, Griewank et al., 2013b, Griewank et al., 2013a, Larsen et al., 2015). The *BRAF* mutations found in ConM like those of CM and have been detected mainly in two different small regions of the kinase domain of the *BRAF* molecule (Gear et al., 2004a), most commonly in exon 15, with a single T-A substitution whereas the other mutations were also detected in a region of exon 11, as previously described (Brose et al., 2002). In the current study, the most common oncogene mutations found were *BRAF* V600E at exon 15, which were detected in 24% (5 of 21) of the samples as well as in the positive control, (2 of 4) of the cutaneous melanoma cell lines. The mutation was in the form of a single nucleotide mutation, resulting in substitution of glutamic acid for valine (*BRAF*V600E: nucleotide 1799 T>A; codon GTG>GAG), which is related to what has been reported in previous studies (Long et al., 2011, Griewank et al., 2013b, Wilson et al., 2014). The five cases of *BRAF* mutations found in the present study at exon 15 were comparable to those previously described in the literature. The mutation however, appeared to be

heterozygous, whereas in the two cases in the CM positive control, it was homozygous (Figure 4.1). The *BRAF* mutation at exon 11 was also screened, but no mutations were detected (Figure 4.2). Mutations in *BRAF* exon 11 have previously been observed, although only rarely. One study reported a G1402A point mutation of exon 11 which encodes a G468R substitution, and found it to be associated with *NRAS* mutation. It is likely, therefore, that the *BRAF* exon 11 mutation does not provide sufficient stimulus to the MAPK pathway and that the addition of RAS activity is required for adequate activation (Gorden et al., 2003). In contrast to ConM, several studies have failed to confirm the presence of the *BRAF* mutation in UM, including primary and metastatic choroidal and ciliary body melanomas (Cohen et al., 2003, Cruz et al., 2003, Edmunds et al., 2003). The recent study done by Griewank et al. (2013) was the first study to identify frequent *NRAS* mutations as a relevant oncogene in ConM. The identified frequency of 18% (14 of 78) is comparable to that found in CM (Ko and Fisher, 2011, Griewank et al., 2013b). Nevertheless, in the current study, only two of the 21 tumours 10% were found to harbour a point mutation affecting codon Q61R (A182G) within exon 2 of *NRAS* (Figure 4.3). Mutations in the other two RAS family members, *HRAS* and *KRAS*, are extremely rare in melanoma (Jakob et al., 2012). However, a novel *KRAS* p.k117Y mutation in exon 4 was detected for the first time in the case of a 48-year-old patient with metastatic ConM which may indicate the role of this mutation in disease progression (Del Carpio Huerta et al., 2017). Conversely, this was not detected in any of our samples. Several studies have verified the absence of any *GNA11* or *GNAQ* mutations in ConM, which suggests that these mutations are probably very rare in this tumour type (Van Raamsdonk et al., 2009, Dratviman-Storobinsky et al., 2010, Van Raamsdonk et al., 2010). A previous study however, has reported that the only ConM tumour harbouring a *GNA11* Q209L mutation was a metastasis from UM (Griewank et al., 2013b). Nevertheless, *GNAQ* mutations at codon Q209 have been found in 45% of primary UM, 22% of UM metastases, and 55% of blue nevi (Van Raamsdonk et al., 2010). Mutations in *GNA11* at codon Q209, meanwhile, have been found in 32% of primary UM, 57% of the UM metastases, and 7% of blue nevi (Van Raamsdonk et al., 2010). In the present study, one of the frozen tissue cases was found to have a *GNAQ* mutation (ConM16) and their profile clearly show that the CNAs was comparable to UM with clear alterations in chromosome 3, 6 and 8 (Appendix 5).

This mean that this case might be metastasize from UM. Another three samples had *GNA11* Q209L mutations, two of them was one pair and found to be ConM metastasis and their profile was not clear enough therefore more clinical information about their origin are required.

Recently, a high frequency of *TERT* promoter mutations was discovered in CM (Horn et al., 2013, Huang et al., 2013b) and these have also been identified with different frequencies in various other types of human cancer, such as glioblastoma and bladder cancer, suggesting that these mutations have a wide ranging role in human tumorigenesis (Huang et al., 2013b, Killela et al., 2013b, Vinagre et al., 2013, Liu et al., 2013, Hosler et al., 2015). The identified hotspot mutations, which cause a cytidine-to-thymidine (C>T) di-pyrimidine transition at chromosome 5 were identified in two regions and are thus named C228T and C250T, respectively. Mutations of the *TERT* promoter have not been identified in UM, but have been detected in 32%-41% of ConM, and are identical to those found in CM (Griewank et al., 2013a, Koopmans et al., 2014). Mutations of the *TERT* promoter have not been identified in conjunctival nevi or PAM without atypia, but have been detected in 8% (2 of 25) of PAM with atypia (Koopmans et al., 2014). After optimising the *TERT* promoter by using a GC-rich PCR system the primers were able to work but were still found to be highly labile and not suitable for continual usage and hence new aliquots were required. The GC-rich system is designed to amplify DNA/cDNA templated up to 5Kb in length including GC-rich targets and repetitive sequences. It is composed of an enzyme blend of thermostable Taq DNA polymerase and Tgo DNA polymerase, a thermostable enzyme with proofreading (3'-5' exonuclease) activity. All the ConM tumours samples were run on the thermocycler using TD-PCR (Table 2.13) and their PCR products were amplified at 187bp. The *TERT* promoter was successfully PCR-amplified and sequenced in (17 of 21) of ConM cases, although four FFPE samples still failed to sequence due to a problem with the quality of the DNA. Generally, *TERT* mutations were detected in 47% (8 of 17) of ConM tumours. All identified mutations were located at hotspot region C250T which displays the nucleotide exchange from cytosine to thymine (Figure 4.6). These findings are comparable to the previous study done by Griewank et al. (2013a) who found *TERT* mutations in 32% (12 of 38) of ConM tumours. Similar findings were also reported by Koopmans et al. (2014) who detected that 41% (16

of 39) of ConM tumours had mutations of the *TERT* promoter, which were located at different hotspot positions, between C250T and C228T. The high prevalence of C228T and C250T suggests that these *TERT* promoter mutations may comprise early genetic events in the genesis of melanoma and other cancer types (Huang et al., 2013b).

Previous studies have revealed that tumours with *BRAF* or *NRAS* mutations were found to harbour *TERT* promoter mutations significantly more often than tumours lacking *BRAF* or *NRAS* mutations (Griewank et al., 2013a, Koopmans et al., 2014). These results are in accordance with the present study where four out of five *BRAF*-mutant samples and one in two *NRAS*-mutants had a concomitant *TERT* promoter mutations. The two hotspots C228T and C250T, created binding sites for ETS transcription factors which are targets of the MAPK signaling pathway (Whitmarsh et al., 1995). *BRAF* and *TERT* promoter mutation therefore forms a distinctive mechanism in which the *BRAF* activated MAPK pathway which supports the up regulation of the *TERT* gene by creating and enhancing the interaction of ETS factors with the *TERT* promoter (Vinagre et al., 2013, Liu et al., 2014). To date, no information is available on the association of *TERT* promoter mutations with prognosis, not even for CM, as this has not been addressed by the original studies (Horn et al, 2013; Huang et al, 2013). However, in terms of grouped the ConM according to cases with and without *TERT* mutation, wild-type tumours have higher numbers of chromosomal alterations, where clearly shows more genome instability clearly associated with this group compared to *TERT* mutations cases that showed more association with gain of 1q, 6p, 7 and 8, and with loss of 3p, 5p, 9p,10q, 11 and 16 and this indicates that this group had less genome instability that might have had a role in the tumour development.

#### 4.3.2 Genetic alterations of conjunctival melanoma

The changes seen in UM at chromosomes 6 and 8, as well as the losses of 1p, are also frequent in CM, but losses at any point in chromosome 3 are rare in CM (van den Bosch et al., 2010). In the present study, 21 ConM tumours were analysed using high resolution array-CGH and their copy number profiles confirmed by two different algorithms; the ADM2 and FASST2 algorithms both showed the same range of complex CNAs. The most CNAs found in this study

figure 4.8 and 4.9 respectively were in agreed to some extent with the study done by Griewank et al. (2013) who also conducted a large genetic analysis of 30 ConM samples by using array-CGH. They showed that the genetic alterations in ConM were similar to what has been found in cutaneous and mucosal melanomas, with gains of 1q, 3p, 7, 17q and losses of 9p, 10, 11, and 12q (Griewank et al., 2013b). In addition, Vajdic et al. (2003) reported multiple chromosomal changes by using array-CGH on two ConM samples, with the most notable changes being the losses of 10q and 16q, which are also found in CM (Vajdic et al., 2003a). The aggregated array-CGH findings of Wang et al. (2013) revealed several recurrent unbalanced genomic aberrations in CM involving gains of 1q, 6p, 7p and 8q and losses of 9p, 6q, and 10, which are consistent with common CNAs known to be associated with melanomas (Wang et al., 2013). They also identified some non-random focal amplifications or deletions in loci known to harbour critical cancer genes, such as Cyclin-dependent kinase inhibitor 2A (*CDKN2A*) and phosphate and tensin homologue (*PTEN*) loci, which were the major targets of hemizygous or homozygous deletions in melanoma (Stark and Hayward, 2007, Gast et al., 2010, Wang et al., 2013).

In the current study, several focal amplifications of oncogenes and homozygous deletions of tumour suppressor genes were also detected by array-CGH. One of the most common recurrent CNAs that was observed in this study was the homozygous deletion of the *CDKN2A* gene on chromosome 9p21, which was detected in 33% (7 of 21) of ConM tumours (Figure 4.10). This is consistent with Stark and Hayward. (2007) who reported that the most common homozygous deletion identified in melanomas targeted the *CDKN2A* gene at chromosome 9p21 (Stark and Hayward, 2007). These revelations of *CDKN2A* deletion and homozygous deletion could help with the classification of a given sample. In addition, *CDKN2A* mutations are the most frequent genetic events underlying familial melanoma susceptibility, and have been reported in the germline of 8% to 57% of familial melanoma cases (Newton Bishop and Gruis, 2007). *CDKN2A* is also the most frequently affected tumour suppressor gene, occurring in 50% to 80% of sporadic melanomas (Curtin et al., 2005, Bennett, 2008, Gast et al., 2010, Aoude et al., 2015). In the present study, loss of 10q was also most frequent in 29% (6 of 21) of ConM tumours, and this includes the loss of the *PTEN* gene on

chromosome 10q23. Vajdic et al. (2003) also reported loss of 10q in 100% (2 of 2) of ConM, and this finding has also been reported in CM (Vajdic et al., 2003a). The tumour suppressor gene *PTEN* deleted on chromosome 10 is one of the common recurrent aberrations identified in malignant melanomas (Curtin et al., 2005, Stark and Hayward, 2007, Gast et al., 2010). Several studies have reported the loss of *PTEN* in 63% to 70% of melanomas (Curtin et al., 2005, Gast et al., 2010). Any mutation and deletion of *PTEN* could contribute to the development and progression of malignant melanoma (Birck et al., 2000). *PTEN* functions as a tumour suppressor by inhibiting PI3K signalling. *PTEN*'s lipid phosphatase dephosphorylates PI3K 3-phosphoinositide products, leading to inhibition of different signalling pathways. *PTEN* is a negative regulator of this pathway, and loss of this gene leads to an increase in, and constitutive activation of, the PI3K-AKT pathway (Hodis et al., 2012). Furthermore, loss of 5p including telomerase reverse transcriptase *TERT* promoter genes on loci 5p15, which has recently been found as driver mutation in melanomas, was also observed in 29% (6 of 21) of ConM samples in the present study (Table 4.2). This gene encodes the catalytic reverse transcriptase subunit of telomerase, which is part of the ribonucleoprotein complex of telomeric DNA responsible for maintaining the telomere length at the chromosome ends (Dwyer et al., 2007). Other focal amplifications and deletion oncogenes loci reported previously in ConM, either by array-CGH or FISH, were also observed in the current study (Table 4.3).

#### [4.3.3 Do \*KIT\*, \*CCND1\*, \*CDK4\*, \*RREB1\*, \*MYB\* and \*NF1\* genes correlate to the genetic alterations in conjunctival melanoma?](#)

In the current study, gains of *KIT* (receptor tyrosine kinase) locus on 4q12 were identified in 14% (3 of 21) of ConM tumours, but we did not screen for this known oncogene mutation due to the time constraints of this study. Previous work done by Beadling et al., however, has reported that mutation of the *KIT* gene was found in 7.7% (1 of 13) of ConM and 1.7% (1 of 58) of CM but not in any of 60 UM samples, and increased *KIT* copy number changes were less common among ConM 7.1% (1 of 14) and CM 6.7% (3 of 45) (Beadling et al., 2008). In addition, Griewank et al. (2013) found that gains of the *KIT* locus on chromosome 4 were detected in 17% (5 of 30) tumours by array-CGH, but no known activating

mutations in *KIT* were detected. *KIT* mutations therefore appear to occur very rarely in ConM (Beadling et al. 2008; Griewank et al. 2013a). A recent study of 53 Chinese ConM patients, however, determined *KIT* mutations in 11% (6 of 47) of ConM, suggesting that there may be different pathways of tumour development in different ethnic groups (Sheng et al., 2015). Further studies are therefore required to investigate the oncogenic role of *KIT* in ConM.

In the present study, gains of *CCND1* at 11q were found in 5 of 21 cases (24%), whereas gains of *RREB1* (6p25) and loss of *MYB* (6q23) were detected in 57% (12 of 21) and 24% (5 of 21) of ConM samples respectively. *CCND1*, *RREB1* and *MYB* are among the most common genetic alteration loci that have been detected previously by FISH. A study by Busam et al. (2010) validated the FISH technique as useful in establishing a distinction between conjunctival nevi from ConM and reported that gains of *RREB1* and cyclin D1 were found in 100% (6 of 6) and 66% (4 of 6) of samples, respectively, while loss of *MYB* was detected in all six conjunctival melanoma cases (Busam et al., 2010). Mudhar et al. (2013) also used FISH assays on conjunctival melanocytic lesions and showed that ConM had similar genetic aberrations to CM. Due to the time frame of this study further investigation need to study these genes in more depth on large series to find out their role in development of ConMs.

Recently, Scholz et al. (2018) analysed a large cohort of ConM tumours with a targeted next-generation sequencing covering genes which are frequently mutated in CM and UM. Their study was the first one to document *NF1* as mutated oncogene in 33% (21 of 63) in ConM samples (Scholz et al., 2018). *NF1* is a tumor suppressor gene that encodes the protein neurofibromin, which interacts with RAS and negatively regulates its function by inducing hydrolysis of RAS-bound GTP to GDP (Martin et al., 1990). *NF1* has also recently been detected as the third most frequently mutated gene in CM, after *BRAF* and *NRAS*, which also activate the MAPK pathway (Wiesner et al., 2015). These mutations were also found to be associated with harbouring activating *NRAS* or *BRAF* mutations, this is comparable to the finding in CM where *NF1* with *BRAF*, *NRAS* and other mutations are well known (Krauthammer et al., 2015, Cosgarea et al., 2017). *NF1* mutations are mostly recurrent in melanoma subtypes that are associated with high sun

exposure, such as CM. Sun exposure is also a known pathogenic factor in ConM and this might clarify the high number of *NF1* mutations detected (Nissan et al., 2014). In the present study, there was no evidence for CNAs of *NF1*.

*BRAF* mutations were detected in 24% (5 of 21) of ConM cases. The most frequent genetic changes associated with *BRAF* mutations cases were gains of 1q, 6p, 7 and 8q and loss of 3p, 6q, 5p, 9p 10q,11q and 14. Losses of chromosome 10, including the *PTEN* locus 10q23, were particularly prominent in *BRAF*-mutant tumours (Figure 4.13). This is also demonstrated by Curtin et al. (2005), who reported a positive correlation between the loss of *PTEN* and mutations in *BRAF*, in support of the PI3K pathway as an independent somatic target that is frequently activated in primary melanoma. In addition, Griewank et al. (2013) reported that *BRAF*-mutant tumours more frequently had losses of chromosome 10q at the *PTEN* locus, and this supporting the concept that *BRAF* mutant tumours require an additional genetic event leading to the activation of the AKT pathway. This event is not as relevant in *NRAS*-mutant tumours, however, where the mutation directly leads to downstream AKT activation. Furthermore, it seems from this study that *BRAF* and *NRAS* mutations may define a subset of ConM that have more focal genetic changes, since as seen in figure 4.13 where wildtype tumours appear to have more generalized CAs across the genome.

#### [4.3.4 Genetic alterations associated with primary and metastatic conjunctival melanoma groups](#)

Among 21 cases included in this study 50%, 64% were male and female respectively, however, the clinical data of two patients were not available. The age of the patients which range from 37-85 years old was in pattern similar to previous studies (Shields et al., 2000, Jovanovic et al., 2013). Tumours location were also identified in this study and most of ConM tumour arising from bulbar and tarsal, inferior or superior fornix, nasal or temporal conjunctiva. It is notable that most of the samples presented with in-situ and invasive melanoma and the others diagnosed as in-transit metastasis with depth vary between 0.2-6mm. Our findings show that 14 samples (62%) of ConM tumour were initially derived from primary ConM and 7 samples (38%) were metastasised, either from the lymph-nodes or

metastasis in different part of the eye (Table 4.3). The most frequent CNAs among 13 samples in the primary conjunctival group showed clear less genome instability. The most common oncogenic mutations among the primary samples were 60% (3/5) *BRAF*, 50% (1/2) *NRAS* and 38% (3/8) *TERT* mutations.

However, the highest frequency of CNAs observed among the eight metastatic ConM samples, shows clear genome instability which include recurrent gains of 1q, 6p and 7q, 11q, and losses of 3q, 5p, 6q, 9p, 10, 11q, 12q and 16q, (Figure 4.15). The most relevant mutations correlated with metastasis cases were 40% (2/5) *BRAF* and 50% (1/2) *NRAS* and 63% (5/8) *TERT* mutations. The statistical analysis was not practicable due to the small size of metastatic ConM samples and some of these samples were paired. The common aberrations detected among the metastatic ConM tumours therefore, require further corroboration in a larger cohort of ConMs with more comprehensive clinical and follow-up information. Such a study would establish whether the genetic changes identified here are important factors in the pathology of ConMs and thus whether they could be used to identify ConM patients at high risk of metastatic spread.

# CHAPTER FIVE

Confirmation of the significance of candidate genes by Nexus-Software and further exploration using Immunohistochemistry

## 5.1 Introduction

Among cancers in general, amplification of oncogenes and/or deletion of tumour suppressor genes are common aberrations linked to tumour progression. Some of these have been shown to be recurrent and accumulating, and might cause cancer phenotypes, resulting in the formation of recurrent somatic copy number aberrations (SCNA) (Hanahan and Weinberg, 2011). Investigation of recurrent SCNAs can help in identification of genes with roles in tumour development and even recommended novel therapeutic lines in different type of cancers, such as lung cancer (Chitale et al., 2009), ovarian cancer (Eder et al., 2005), and glioblastoma (Wiedemeyer et al., 2008). Across the whole genome, in virtually all cancer types, the most recurrent SCNAs (losses or gains) either affect the whole chromosome arm (Arm-level) or very short genomic regions (focal) (Beroukhim et al., 2010). Most of the cancer genome around 10% is caused by focal SCNAs, and they are also far more possible to occur with high amplitude (homozygous amplification deletion), in contrast to the whole arm events (Beroukhim et al., 2010).

Focal SCNAs, therefore, would be statistically more likely to target specific genes and, from a research viewpoint the smaller and clearer the region, the easier it is to realize the identification of target genes (Beroukhim et al., 2010). Due to the genetic instability seen in majority of cancers, there are likely to be large number of focal usually SCNAs, with the majority of these being random so-called passenger aberrations that have no functional role. It is therefore important to distinguish these from the driver SCNAs which are important because they contribute to the cancer phenotype (Beroukhim et al., 2010). This chapter therefore reports the design of a high-resolution oligonucleotide array-CGH technique to resolve the difficulty of identifying recurrent focal SCNAs, especially for those that are small and that therefore might have been missed by previous studies when using lower resolution techniques such as chromosomal CGH, spectral karyotyping, or even BAC arrays.

Analysing array-CGH data in combination with the Nexus software tool provides a validated shortlist of candidate genes on different chromosomes, through a combination of approaches to survey the measurable probability that SCNA were non-random events. Therefore, genes influenced eventually by these non-random SCNA represented a shortlist of candidate 'driver' genes, that can be examined further for potential relevance on the basis of their biological significance. The overview for the identification of candidate genes is summarised in Figure 5.1, and in the subsequent sections the methodology is explained in more depth. The basis of array-CGH aberration calling algorithms has been previously discussed in chapter 2 (section 2.3.6). Evidence that amplification or deletion of possible candidate genes might contribute to the acquisition of any of the hallmarks of cancer was assessed by Hanahan et al. (2011) and this was used to compile a final list of candidate genes (Hanahan and Weinberg, 2011). This allowed us to pay special attention to gains or losses of individual genes and pathways that might have a significant role in DNA damage responses and the conservation of genomic integrity, and this could provide perceptions into the mechanisms for genomic instability in ConM.

In the previous chapter, array-CGH was used in combination with the Nexus software tool to analyse the genetic alterations of ConM melanoma, and their genomic profile was compiled using Agilent software (ADM2 algorithm) and then confirmed by means of a different algorithm, FASST2 (Nexus). As a result, potential candidate genes are areas of interest were identified. In this chapter, FASST2 Nexus software was used to further explore and confirm candidate genes that had already been detected by Agilent software across the set of ConM, as potentially acting as drivers and influencing patient outcomes, selecting the most common candidate genes and confirming their protein expression by using immunohistochemistry (IHC).

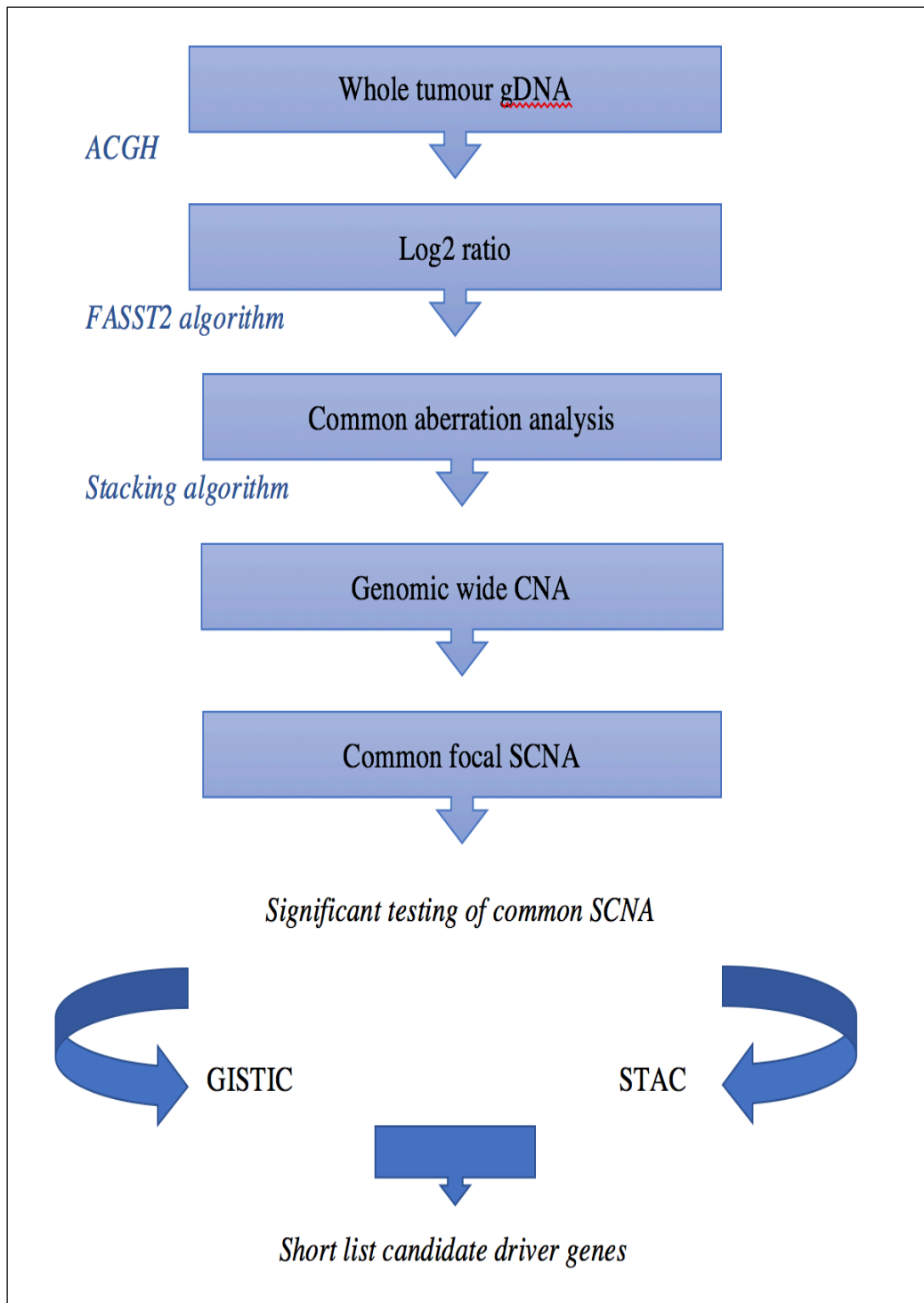


**Figure 5.1: Summary of work-flow chart for array-CGH data analysis and short list of candidate gene identification.**

## 5.2 Results

### 5.2.1 Identification of common focal SCNA

A similar approach to Beroukhim et al. (2010) was adopted, whereby larger size SCNA of 5Mb or more (including whole arm events) were considered generally as gains or losses. Consequently, these larger SCNA events were differentiated from focal SCNA with a median length (1.8 Mb) which were introduced as amplifications and deletions (Beroukhim et al., 2010). By using a stacking algorithm, all SCNA recognised within genomic regions in an appropriate set of ConM cases were stacked over each other to create a frequency plot, as illustrated in figure 5.2. The common focal SCNAs can be identified as the minimal common region (MCR) of overlap to be recognized among the SCNA covering that locus. This region is most likely to be statistically significant in term of having targeted genes, where the threshold frequency of focal SCNA was reduce to 20% to increase the sensitivity of the data analysis (Beroukhim et al., 2010).

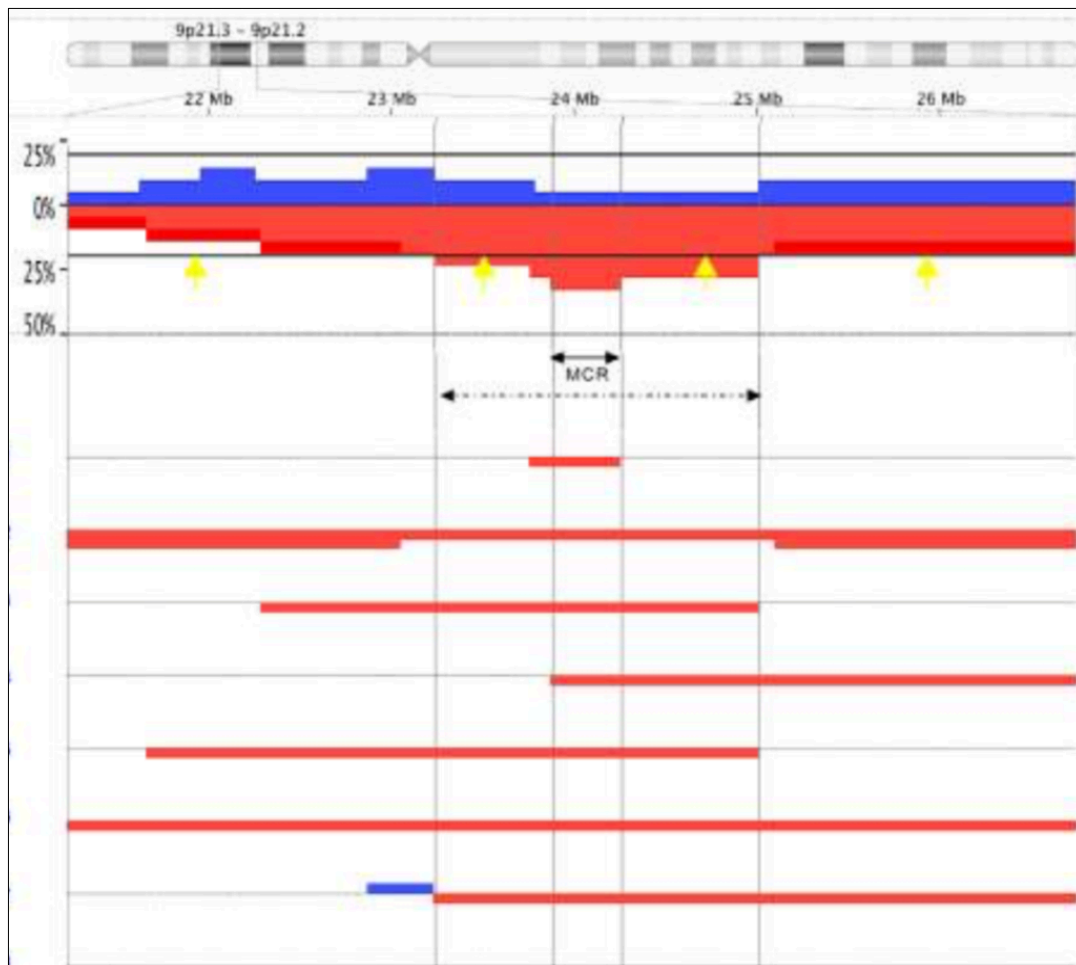


**Figure 5.2: Frequency Plot and Stacked SCNA from Individual ConM Cases.** Illustrated example of a Minimal Common Region (MCR) where the upper panel displays the chromosomal region (9p21) and its approximate size and the middle panel displays the frequency plot of alterations plotted as percentages alongside the y-axis. Blue shading above the zero line represents amplification frequency and red shading under the zero line represents deletion frequency, while the horizontal lines in the bottom panel indicate individual samples. The MCR is the minimum region that is occurs in all the affected samples (represented by the small arrow). The whole region of common aberration (indicated by the double spotted arrow) usually occurs with a higher frequency than the threshold of 20% (represented by the yellow arrows). All SCNAs are modified using the FASST2 algorithm.

## 5.2.2 Significance Testing of Common recurrent CNAs regions

### 5.2.2.1 Common Aberration Analyses

Both GISTIC and STAC algorithm tools were used to evaluate the most common focal copy number alterations among a set of ConM cases where the high frequency of aberrant regions in the genome was detected to be statistically significant. These methods are built into the Nexus Software (Biodiscovery®) to detect the potential driver alterations depending on their frequency of appearance, using the SCNAs which had already been detected by means of the FASST2 algorithm. Both tools operate different statistical approaches as summarized in table 5.1, making the overall strategy for the data analysis more robust (Rueda et al., 2013).

#### 5.2.2.1.1 Genomic Identification of Significant Targets in Cancer (GISTIC)

GISTIC is a very useful method developed at the Broad Institute by Beroukhim et al. (2007) to identify regions that are significantly gained or lost across a set of samples. GISTIC detects significant aberrations by two main steps. Firstly, it determines a statistical region using the 'G score', which includes both the frequency of occurrence and the amplitude of the aberration. Secondly, it assesses the statistical significance of each aberration by comparing the observed statistic to the results that would occur by chance, using a permutation test that is based on the overall pattern of aberrations observed across the genome. The method accounts for multiple sample testing using the false discovery rate (FDR) correction and assigns a  $q$  value for that region. For each significant region, the method defines a peak region with the greatest frequency and amplitude of aberration. GISTIC results are highly sensitive in term of identifying lower frequency significant regions (Beroukhim et al., 2007).

#### 5.2.2.1.2 Significance Testing for Aberrant Copy Number (STAC)

The STAC algorithm was developed by Diskin et al. (2006) and is used to detect the statistical significance of aberrations amongst a set of tumour samples that

are stacked on top of each other, such that the aberration would not appear randomly across multiple array experiments. The algorithm uses the permutations of SCNAs in each chromosomal arm, to define how likely it is for each SCNA to appear at any given location with a certain frequency, using a p-value with a cut-off of 0.05. This highlights the common aberrant regions that have a higher frequency than that of aberrations occurring by chance (Diskin et al., 2006).

Table 5.1: Illustrates the comparison between the STAC and GISTIC algorithms kindly supplied by Dr. A. Salawu.

	<b>STAC</b>	<b>GISTIC</b>
<b>Criteria region selection</b>	<i>Frequency of aberrations only</i>	<i>Both frequency and amplitude of aberration</i>
<b>Null mode (statistical significant)</b>	<i>Permutation of regions within a chromosome arm</i>	<i>Permutation of props over the entire genome</i>
<b>Correction for multiple sample testing</b>	<i>Does not require correction</i>	<i>Require correction FDR</i>
<b>Peak region identification</b>	No	Yes

The GISTIC and STAC statistical methods created a validated shortlist of candidate genes, which were then assessed individually for biological function and their association with cancer by using the Atlas of Genetics and Cytogenetics in Oncology and Hematology (<http://AtlasGeneticsOncology.org>).

The functional evaluation of the detected genes was based on the potential functional implication in numerous cancer types and their role in the acquisition of cancer hallmarks.

In the previous chapter, the study has demonstrated patterns of chromosomal amplifications and deletions, some of which are common to both ConM and CM, but, different from their counterpart UM. Agilent software was used to identify some non-random focal amplifications and deletions in loci known to harbour critical cancer genes, including homozygous deletions in 33% of *CDKN2A* and 29% of *PTEN* and *TERT* promoter (Table 4.2). In this chapter, FASST2 Nexus software was used to identify the most statistically significant candidate genes across the set of ConM tumour samples with aim of confirming the results seen with the Agilent software. Due to the small number of samples which may have influenced our findings, the STAC algorithm only called the significant peaks which does not include longer extended regions. Since these regions may include some of the driver candidate genes that we are interested in, the list of candidate genes was generated after applying the GISTIC algorithm only. This algorithm can indicate peak and extended regions and is very sensitive at capturing lower frequency significant regions. The threshold was therefore reduced to 0.25 to best capture the results, as shown in figure 5.3.

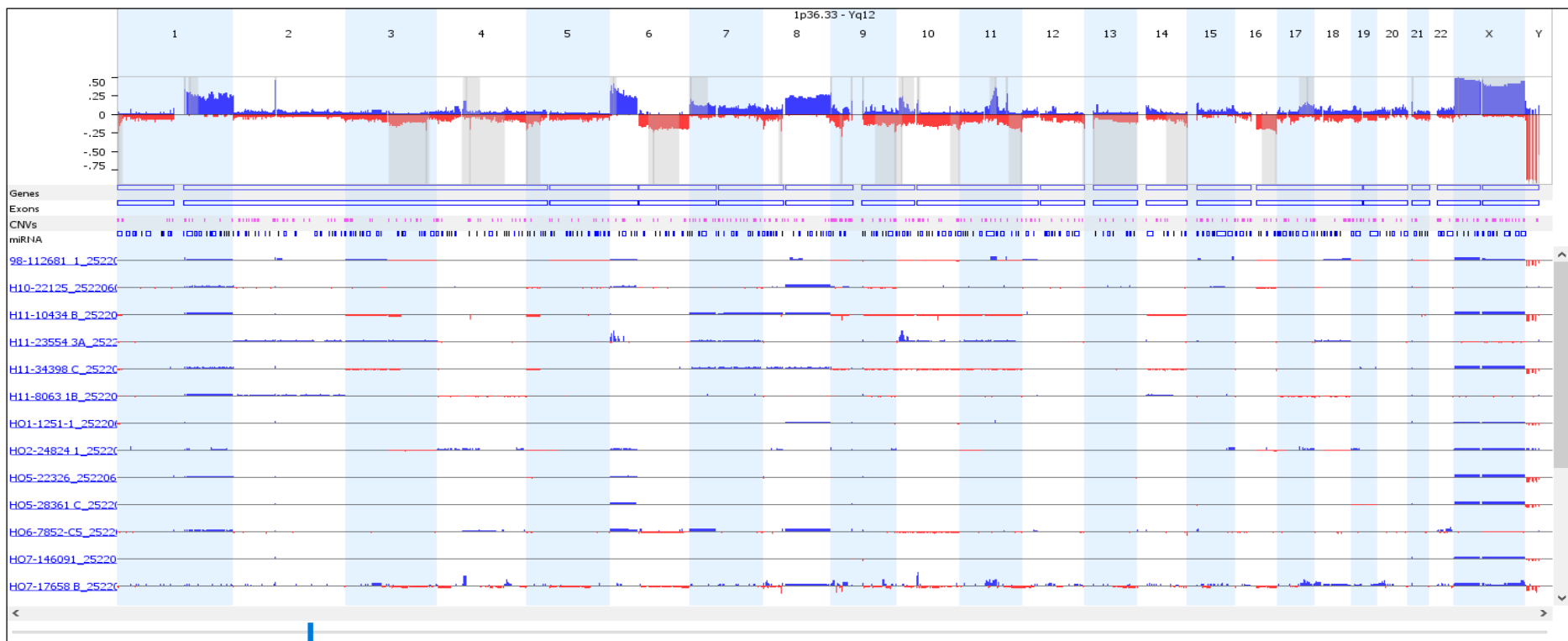


**Figure 5.3: Statistically significant common genomic CNAs amongst ConM cases detected by using the GISTIC algorithm.** Commonly aberrant regions are plotted along the x-axis as a function of their chromosomal position and their q-values are plotted on the y-axis where the highest bars represent most significant genomic regions. Blue bars represent commonly amplified regions and red bars represent commonly deleted regions. Genomic regions with G-score > 10 and q-values > 0.05 are considered significant and are represented by the shaded grey area. These regions contain the important candidate genes. The FASST2 algorithm was used to call alterations in individual samples.

## 5.2.3 The most statistically significant focal SCNAs

### 5.2.3.1 *CDKN2A* gene

The commonly deleted region of 9p among ConM cases extends from 9p21–9p23, and the most relevant focal SCNA was located on chromosome 9p21.3 locus. It is in this region that the Cyclin-dependent kinase inhibitor 2A (*CDKN2A*) is located, the first gene to be associated with melanoma susceptibility (Cannon-Albright et al., 1992). *CDKN2A* is commonly expressed in many tissues and cell types and is involved in regulating the cell cycle (Hussussian et al., 1994, Kamb et al., 1994). The gene encodes two tumor suppressor proteins, including p16INK4A and p14ARF. In the current study, 33% (7 of 21) of *CDKN2A* copy number loss were identified as the most significant focal deletions among ConM cases (Figure 5.4).



**Figure 5.4: Frequency plot of SCNAs affecting the CDKN2A gene locus.** The array-CGH data was analysed by applying the GISTIC algorithm to identify regions of copy number alterations that might have candidate genes. Where the most common alterations regions are plotted along the x-axis against their chromosomal locations, and the q values are plotted on the y-axis, where the most significant commonly deleted genomic regions among ConM cases are indicated by the highest red bars. Statistically significant genomic regions with a maximal G-score and minimal q-value (10 and 0.25 respectively) are identified in grey and that cover the most important genes in this region, where the red circle shows the CDKN2A gene located at 9p21.3. The FASSTS algorithm was used to call alterations in individual samples.

### 5.2.3.2 *TERT* gene

Another clearly significant aberration region among ConM samples was the deleted region of 5p, where the most relevant focal SCNAs were located on chromosome 5p15.33 locus. It is in this region that the *TERT* gene is located. This gene encodes the catalytic reverse transcriptase subunit of telomerase, which is part of the ribonucleoprotein complex (Dwyer et al., 2007). In the present study, the *TERT* gene was found to be the most statistically significant region in 42% (9 of 21) of ConM samples according to the GISTIC algorithm, as figure 5.5 elucidates.



### 5.2.3.3 Other significant candidate genes

For most ConM cases where amplifications of 6p were found the whole arm was affected. The most relevant focal SCNA was located on chromosome 6p25 locus and, in this region, there were a number of candidate genes identified (Table 5.2). *RREB1* (*Ras* responsive element binding protein 1) gene was also found by GISTIC. This gene has been previously reported in ConM using the FISH technique (Busam et al., 2010, Mudhar et al., 2013). The protein encoded by this gene is a zinc finger transcription factor that binds to RAS-responsive elements (RREs) of gene promoters. It has been shown that the calcitonin gene promoter contains an RRE and that the encoded protein binds there and increases expression of calcitonin, which may be involved in Ras/Raf-mediated cell differentiation. Although, multiple transcript variants encoding several different isoforms have been found for this gene (Thiagalingam et al., 1996), little is known about the expression of RREB1 isoforms in cell lines or in human tumours, or indeed about the clinical relevance of the altered gene expression of RREB1 (Nitz et al., 2011). Another significant aberration region among the ConM samples was clear amplifications of 1q, with the most relevant focal SCNA in this region being located on chromosome 1q22 locus. The candidate genes found in this region are listed in table 5.2. The current findings propose that although the focal amplifications affecting chromosome 1q and 6p target a large and gene dense region, several tumour suppressor genes are statistically relevant. Further studies are required to clarify the role of these genes in ConM since they may support the tumorigenesis and thus may assist in qualifying prognosis of patients.

Table 5.2: List of significant candidate genes located on 6p25.

<b>Gene symbol</b>	<b>start</b>	<b>End</b>	<b>Biological process</b>	<b>Molecular function</b>
<b>RREB1 (ras responsive element binding protein 1)</b>	7107829	7252213	Ras protein signal transduction, multicellular organism development, negative regulation of lamellilodium morphogenesis, positive regulation of mammary gland epithelial cell proliferation, positive regulation of wound healing, regulation of transcription.	RNA polymerase II core promoter sequence-specific DNA binding, metal ion binding, transcription factor activity; sequence-specific DNA binding
<b>Y_RNA</b>	7187814	7187919	IRE1-mediated unfolded protein response, cotranslational protein targeting to membrane, positive regulation of cell proliferation	
<b>RIOK1 (RIO kinase 1)</b>	7390061	7418270	protein phosphorylation, rRNA processing	ATP binding, metal ion binding, protein serine/threonine kinase activity
<b>SSR1 (signal sequence receptor subunit 1)</b>	7281375	7313547		

Table 5.3: List of significant candidate genes located on 1q22.

Gene symbol and name	start	End	Length	Biological process	Molecular function
<b>RXFP4</b> (relaxin/insulin like family peptide receptor 4)	155911479	155912625	1147	Adenylate cyclase-modulating G-protein coupled receptor signaling pathway, neuropeptide signaling pathway, phospholipase C-activating G-protein coupled receptor signaling pathway, positive regulation of feeding behavior	Galanin receptor activity, protein binding
<b>ARHGEF2</b> (Rho/Rac guanine nucleotide exchange factor 2)	155916629	155959864	43236	Actin filament organization, cell division, cell morphogenesis, cellular hyperosmotic response, cellular response to muramyl dipeptide, cellular response to tumor necrosis factor, establishment of mitotic spindle orientation, innate immune response,	Rac/Rho GTPase binding, Rac/Rho guanyl-nucleotide exchange factor. Rho guanyl-nucleotide exchange factor activity, guanyl-nucleotide exchange factor activity, microtubule binding, protein binding, transcription factor binding, zinc ion binding
<b>SSR2</b> (signal sequence receptor subunit 2)	155978838	155990758	11921	Cotranslational protein targeting to membrane	ATP binding, metal ion binding, protein serine/threonine kinase activity
<b>UBQLN4</b> (Ubiquilin 4)	156005084	156023616	18533	Autophagy, negative regulation of autophagosome maturation, regulation of proteasomal ubiquitin-dependent protein catabolic process	identical protein binding, polyubiquitin binding, protein binding
<b>RAB25</b> (A member of RAS oncogene family)	156030939	156040305	9367	Epithelial cell morphogenesis, positive regulation of cell proliferation, positive regulation of epithelial cell migration, protein transport, pseudopodium organization, regulation of vesicle-mediated transport	GTP binding, GTPase activity, myosin V binding, protein binding

#### 5.2.4 Assessment of protein expression by Immunohistochemistry

IHC is a relatively cheap and easy to achieve technique that could be adaptable to the classification of ConM tumours. In this study, cases were chosen based on the ConM tissues provided for IHC by Dr. Hardeep. Due to lack of time and resource, however, it was not possible to increase the sample numbers. IHC analysis therefore, was achieved to evaluate the protein expression on 14 sections of ConM, some of which were known from previous array-CGH analysis to have deletions in *CDKN2A* and *TERT*. 5µm-thick tissue sections that carried out in this IHC were pre-treated firstly with potassium permanganate/oxalic acid melanin bleaching to remove the melanin before incubating them with primary antibody. Mouse monoclonal antibody was created against specific 1-156 amino acid fragments for *CDKN2A* and rabbit polyclonal antibody was created against 1120-1132 amino acid fragments for *TERT*.

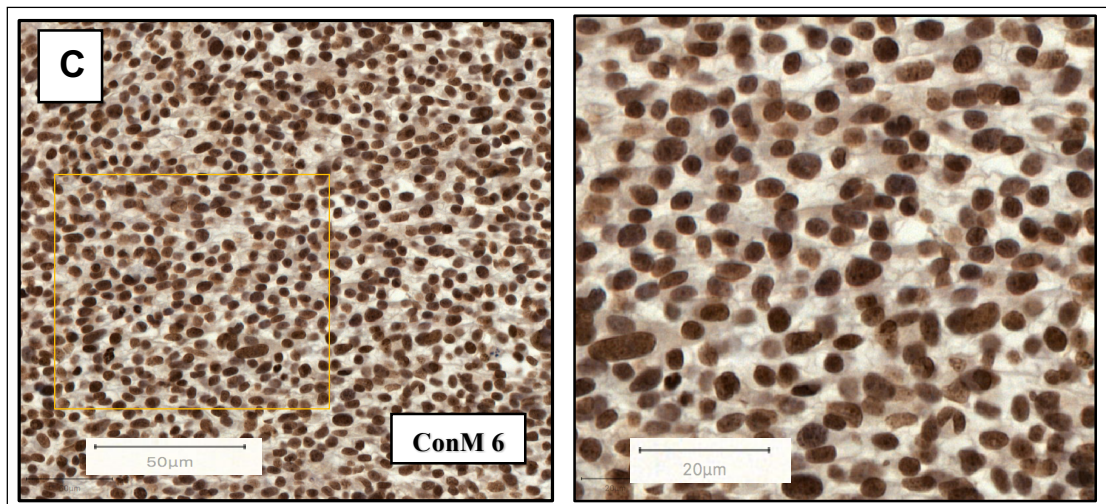
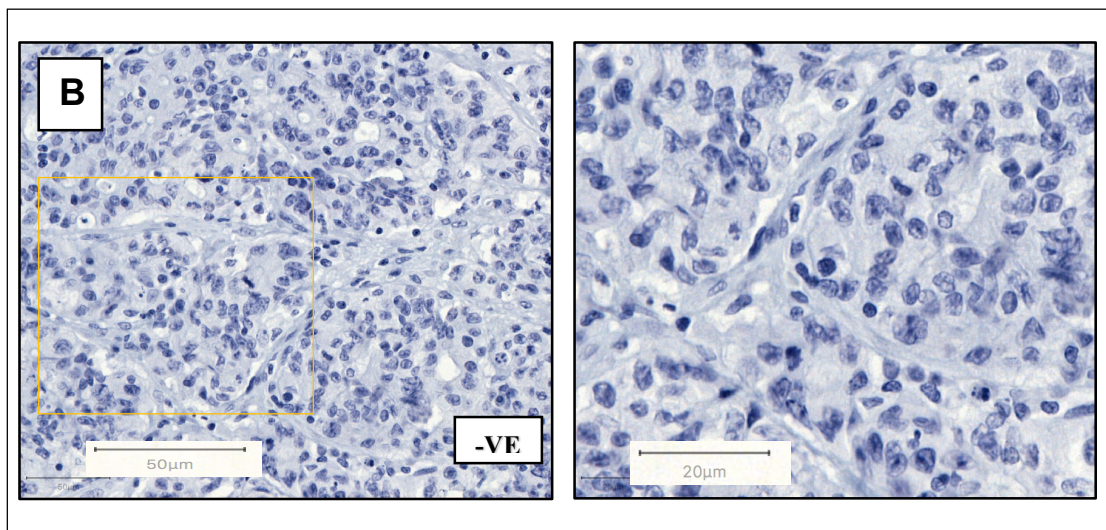
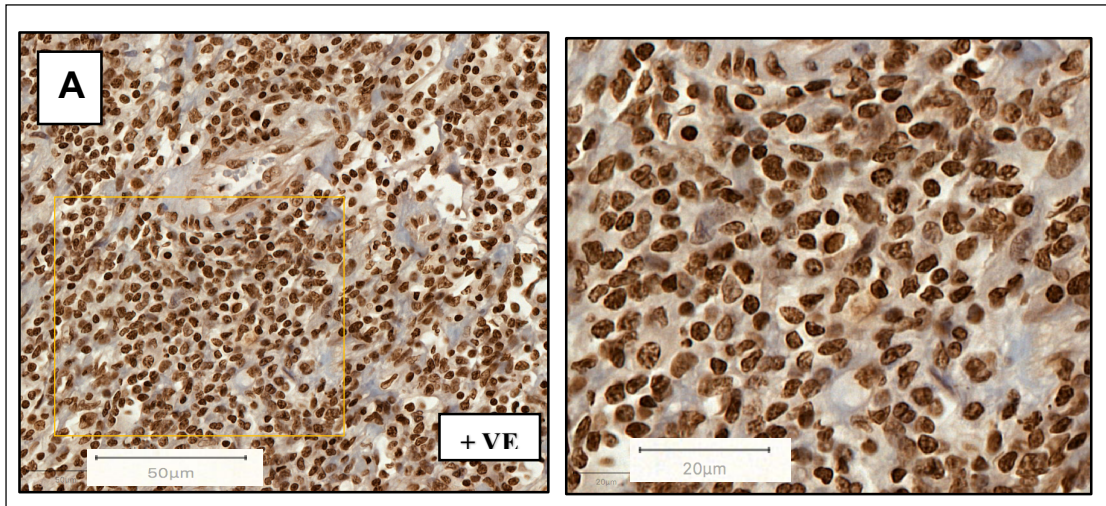
##### 5.2.4.1 Evaluation of staining

The experiment was visualised using the DAB colorimetric system to identify the positive protein expression (brown staining) with haematoxylin as a counter stain (blue staining). The immuno-stained sections were assessed at 200X magnification, and the results categorized as positive or negative for *CDKN2A* and *TERT* expression based on cytoplasmic or nuclear staining in tumour cells. The positives were recorded as either weak, moderate or strong based on the intensity of the stain shown in the tumour. All the immune-staining sections were evaluated using Allred et al.'s (1998) scoring system. This scoring system gives a statistical significance to both the overall stain intensity and the staining pattern, with the two values are simply added together to produce the final Allred score (Allred et al., 1998, Harvey et al., 1999).

The proportion score (PS) was assessed from 0-5 based on distribution of the stained cells whereas the intensity score (IS) was measured based on a four-point system: 0, 1, 2 and 3 representing none, light, medium, or dark, respectively. Then, the sum between PS and IS would act to give the total Allred score which can vary between 0 and 8. The details of all ConM sections that used in the present study were scored as coded samples so that there was no information on the genetic changes for each section. The results were assessed by three an independent observer Dr. Hardeep, Mohammed Alfawaz and Shamsa Ihmed. The results of the IHC for all ConM sections are summarised in Table 5.1. Due to time constraints, the IHC experiment in this study was conducted simply to assess the preliminary protein expression of *CDKN2A* and *TERT* only.

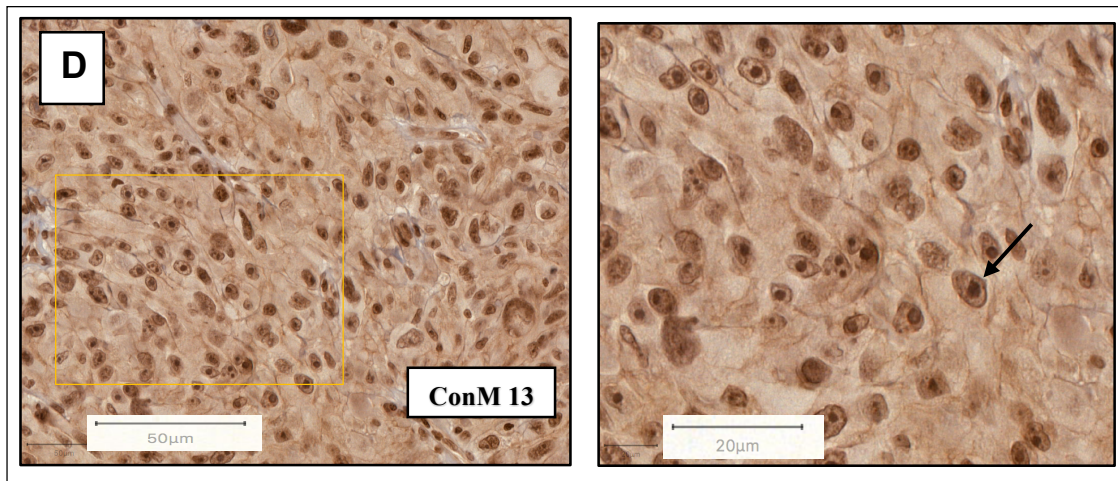
#### 5.2.4.2 *CDKN2A* protein expression

Normal colon tissue obtained from the histopathology laboratory was used as a positive control as it has physiological *CDKN2A* expression with cells showing moderate to strong positive nuclear and cytoplasmic staining (Figure 5.6A). Negative controls of the same normal colon tissue with the antibody omitted were established with every stained section. These only displayed blue haematoxylin counter-stain (Figure 5.6B). In the ConM sections, the stain was mainly noticed in cytoplasmic areas in positive tumour cells (Figure 5.6C). Some cases showed weak to mild cytoplasmic and nuclear stains (Figure 5.6D). The *CDKN2A* protein was clearly expressed in most of the FFPE ConM sections and this comparable to what was seen in the positive controls, but in some sections *CDKN2A* antibody was still expressed in the tissue with a weak to mild cytoplasmic stain (Table 5.4). The finding indicated that some cases of ConM that were shown to have deletions of *CDKN2A* by Nexus software correlate often with IHC results showing some weak to mild *CDKN2A* protein expression.



200X Magnification

400X Magnification



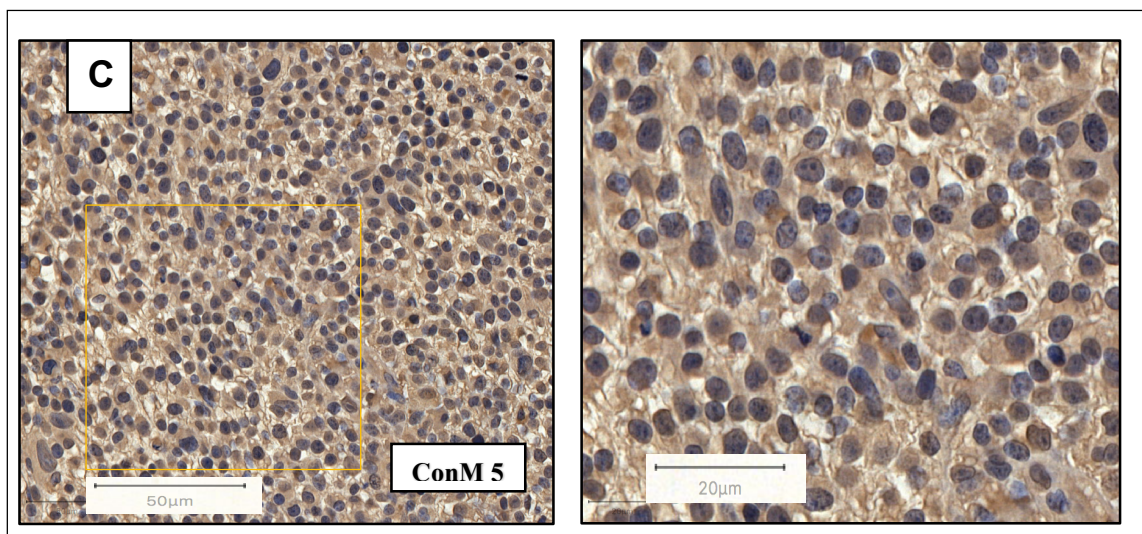
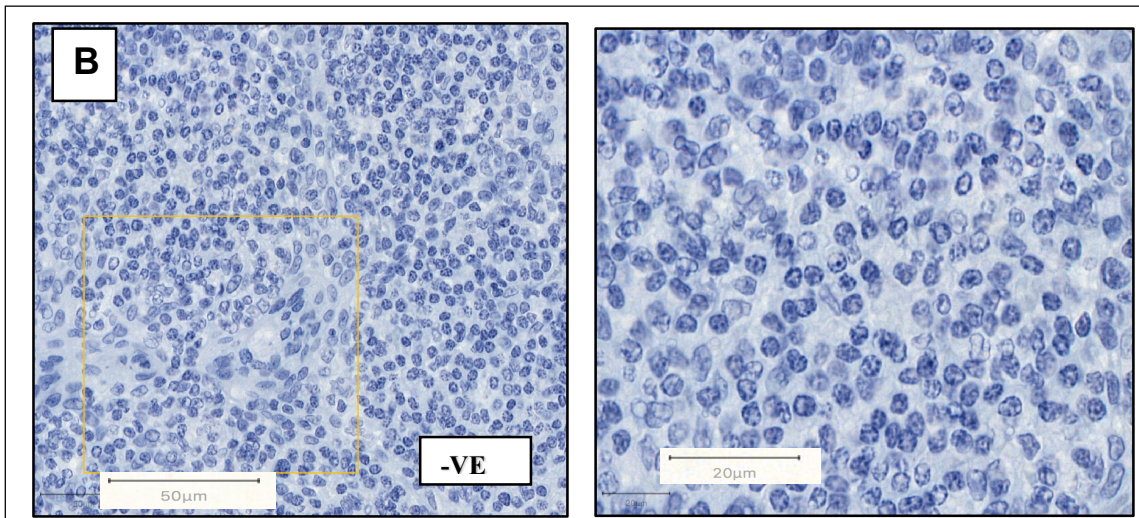
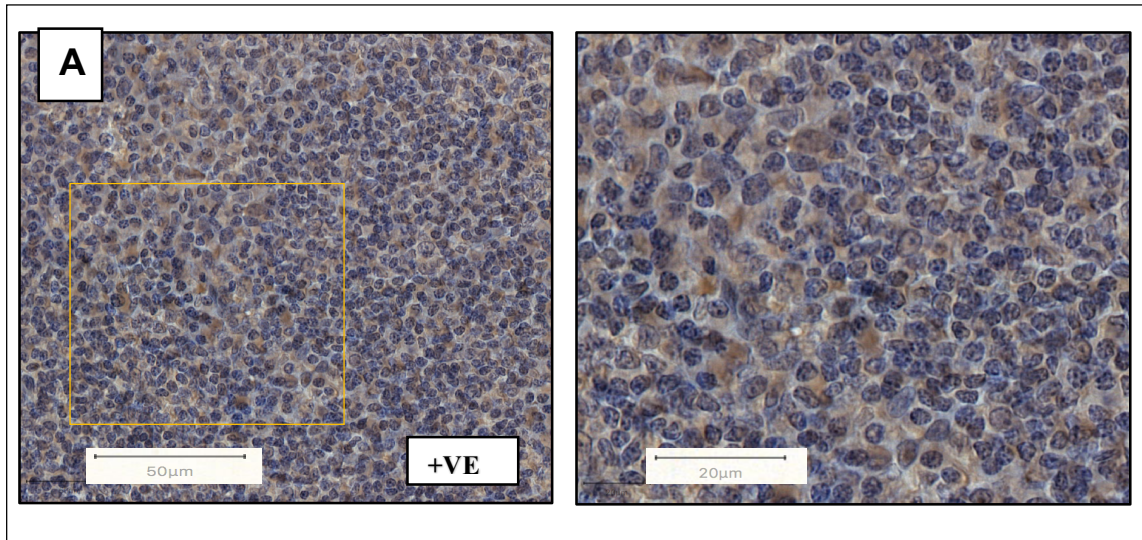
200X Magnification

400X Magnification

**Figure 5.6: Evaluation of CDKN2A protein expression in ConM samples using IHC.** **A)** a colon FFPE section obtained from a Histopathology laboratory used as positive control and immune-stained with CDKN2A antibody showing a moderate to strong cytoplasmic and nuclear stain (brown) with blue haematoxylin as counter stain, where the left images were capture at 200X magnification and the right images were captured at 400X from the original orange square. **B)** Negative control of the same normal colon tissue with omitted antibody showing only haematoxylin counter stain. **C)** Representative FFPE section of ConM stained with CDKN2A antibody (brown) and classified as a moderate cytoplasmic and nuclear stain. **D)** Mild intensity positive nuclear staining highlighted by the black arrow. Images for A, B, C, D were captured from a Qupath viewer after scanning them from a panoramic digital slide scanner (3D HISTECH, Ltd, UK).

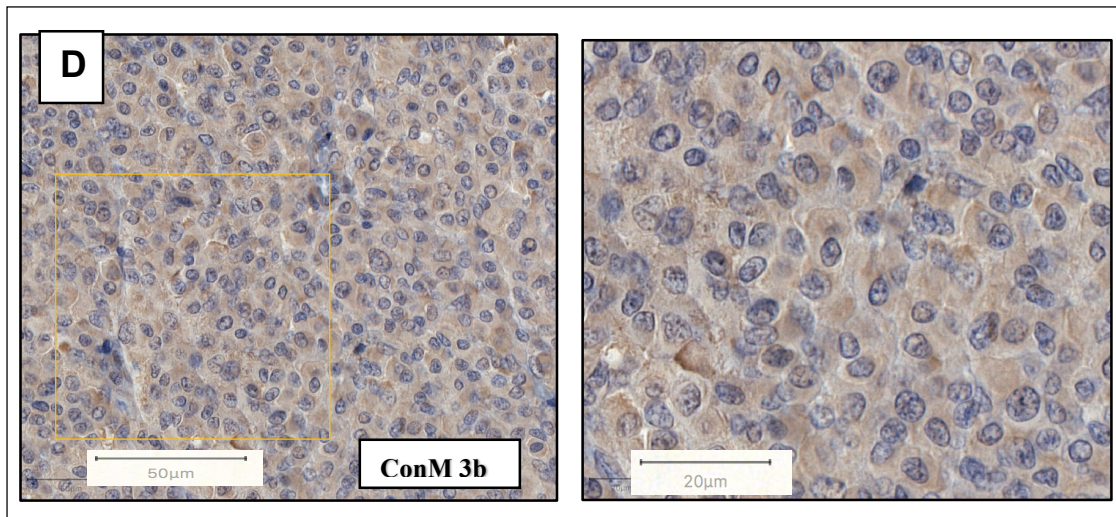
#### 5.2.4.3 TERT protein expression

IHC analysis for the *TERT* protein was achieved to evaluate its expression in ConM tissues. Normal FFPE tonsil tissue was used as a positive control with physiological *TERT* expression obtained from the histopathology laboratory. The cells in the positive control section displayed mild to moderate positive cytoplasmic staining (Figure 5.7A). The observed IHC staining patterns for the ConM tissues are seen in Figure 5.7C, showing that *TERT* was mainly expressed in the cytoplasm of positive ConM cases. Although a specific stain was detected in the cytoplasm of the positive control in the normal tonsil tissues, the ConM tissue was often expressed as a mild to moderate cytoplasmic stain in the ConM cases. The IHC finding showed that *TERT* expression was weak in some of the cases (Figure 5.7D). The previous result from Nexus software shows that 42% (9 of 21) had a loss of 5p15 where the *TERT* gene was located and seven of these cases had mutations in the promoter region of *TERT*. Some of these cases with mutations were found to showed weak to moderate *TERT* expression by IHC (Table 5.4). It was challenging to assess the expression of *TERT* protein due to the high concentration recommended, Therefore, if time had allowed, the run would have been repeated to find the best result.



X200 Magnification

X400 Magnification



X200 Magnification

X400 Magnification

**Figure 5.7: Evaluation of TERT protein expression in ConM samples using IHC.**

**A)** Tonsil FFPE section obtained from Histopathology laboratory used as positive control and immune-stained with TERT antibody, showing a mild to moderate cytoplasmic stain (brown). The left images were captured at X200 magnification and the right images were capture at X400 from the original orange square. **B)** Negative control of the same normal tonsil tissue with the antibody omitted, showing only cytoplasmic staining with haematoxylin counter stain. **C)** Representative FFPE section of ConM stained with TERT antibody (brown) and classified as a mild to moderate cytoplasmic stain. **D)** Low expression of TERT in ConM tissue represented a negative IHC reaction as an internal control. Images for A, B, C, D were captured from a Qupath viewer after scanning them from a panoramic digital slide scanner (3D HISTECH, Ltd, UK).

Table 5.4: Allred scoring system for *CDKN2A* and *TERT* antibodies.

Case code	<i>Anti-CDKN2A</i>			<i>Anti-TERT</i>		
	<i>IS</i> <i>Cyto/N</i>	<i>PS</i> <i>Cyto/N</i>	<i>ATS</i>	<i>IS</i> <i>Cyto/N</i>	<i>PS</i> <i>Cyto/N</i>	<i>ATS</i>
Positive control	3/2	5/5	8/7	2/1	4/3	7/4
Negative control	0	0	0	0	0	0
ConM 1a	1/2	2/4	3/6	1/0	2/1	3/1
ConM 1b	2/2	4/4	6/6	2/2	3/2	5/4
ConM 2a	1/3	5/5	6/8	1/2	4/2	5/4
ConM 3a	2/2	4/4	6/6	2/1	3/4	5/5
ConM 3b	1/2	3/5	4/7	1/0	2/0	3/0
ConM 5	1/3	5/5	6/8	2/1	4/1	6/2
ConM 6	3/2	5/5	8/7	2/2	5/2	7/4
ConM 7	1/4	2/4	3/8	2/2	5/3	7/5
ConM 9	3/2	4/4	7/7	2/1	3/1	5/2
ConM 10	1/3	3/5	4/8	2/1	4/1	6/2
ConM 11	1/2	2/4	3/6	2/1	3/2	5/3
ConM 12	2/3	3/5	5/8	2/2	5/4	7/6
ConM 13	1/2	5/5	6/7	1/0	4/0	5/0
ConM 14	1/2	1/2	5/5	1/0	5/0	6/0

Cy= Cytoplasmic

N= Nuclear stain

Allred Scored System:

IS= Intensity Score (0-4)

0= Negative stain      1= Weak      2= Mild      3= Moderate      4= Strong

PS = Proportion Score (0-5)

0= No stain      1= 1/100 cells stained      2 = 1/10 cells stained

3= 1/3 cells stained      4= 2/3 cells stained      5= All cells stained

ATS= Allred Total Score, Sum of (PI+SI).

The number on the left signifies the cytoplasmic stained and the number on right signifies the nuclear stained cells.

## 5.3 Discussion

### 5.3.1 Most statistically significant candidate genes

All the SCNAs recognised within genomic regions were stacked over each other to create a frequency plot (Figure 5.2). The common focal SCNAs were identified as the minimal common region (MCR) of overlap to be identified amongst the SCNA covering that locus. This region was found to have statistically significant targeted genes. The small number of the samples caused a problem when we analysed the samples by STAC; specifically, that the list of driver candidate genes did not include the genes that we were interested in. This was because the STAC algorithm only indicates the significant peaks and did not call the longer extended regions that might include genes of interest in ConM tumours. The GISTIC algorithm was therefore applied on its own to indicate the peak and extended region. The threshold was reduced to 0.25 in order to capture the results better, since this algorithm is very sensitive at capturing lower frequency significant regions. Two genes were represented in this study, with the functional analysis showing that deletion of *CDKN2A* and *TERT* could possibly be related to the tumour progression.

In the current study, the GISTIC algorithm revealed that the *CDKN2A* gene was found to be the most relevant focal SCNA in 33% of ConM samples (Figure 5.4). This verifies the result seen when Agilent software was used (Chapter 4). These findings are in agreement with previous studies showing that loss of *CDKN2A* occurs in approximately 50% of melanoma cases (Curtin et al., 2005). Loss of function of *CDKN2A* due to either a deletion or mutation and/or promoter methylation, leads to uncontrolled cell proliferation that may cause neoplastic transformation (Shima et al., 2011). The gene is well-known as a tumour suppressor gene because it is often mutated and deleted in different types of cancer. Moreover, this mutation is the most frequent genetic event underlying familial melanoma susceptibility and has been documented in the germline of 8%-57% of familial melanoma cases (Eliason et al., 2006, Bishop et al., 2007). It is also found to be a frequently affected tumour suppressor gene in 50-80% of sporadic melanoma (Bastian et al., 1998, Curtin et al., 2005, Gast et al., 2010).

Although, carrying a germline mutation in the *CDKN2A* gene is the strongest known inherited risk factor for CM (Helgadottir and Höiom, 2016), these germline mutations are very rare in UM (Buecher et al., 2010, Harbour, 2012).

The next significant aberration region among ConM samples was the deleted region of 5p, where the most relevant focal SCNA was located on chromosome 5p15.33 locus, which is where the *TERT* gene was located. This gene was first discovered at a high frequency in CM (Horn et al., 2013, Huang et al., 2013b) and later has been recognised at various frequencies in a number of other types of human cancer (Huang et al., 2013b, Killela et al., 2013b, Vinagre et al., 2013, Hosler et al., 2015). In the present study, the GISTIC algorithm, revealed that *TERT* gene was the most statistically significant region in 42% of cases (Figure 5.5). This finding correlated with most of the cases that have *TERT* mutations (Table 4.1). The other focal SCNAs that have been found previously by Agilent such as *PTEN*, *KIT* and *CCND1* were not detected by the GISTIC algorithm. While the reason for this is not entirely clear, it might be due to the small size of ConM samples. The *RREB1* gene was also one of the most statistically significant genes found by GISTIC (Table 5.2). This gene has been previously reported in ConM by using FISH (Busam et al., 2010, Mudhar et al., 2013). Little is known about the expression of RREB1 isoforms in cell lines or human tumours, however, or about the clinical relevance of the latter (Nitz et al., 2011). Another significant aberration region among ConM cases was amplifications of 1q. In this case, the most relevant focal SCNA was located on chromosome 1q22 locus (Table 5.3). These findings recommend that although the focal amplifications affecting chromosome 1q and 6p target a large and gene dense region, numerous tumour suppressor genes are statistically relevant. Therefore, further investigations are needed to clarify the function of these genes in ConM and to determine if they could support the tumorigenesis of this condition.

### 5.3.2 Assessment of protein expression by IHC

The 17 FFPE ConM samples that have been analysed previously by array-CGH were selected for IHC in order to study the expression of the selected genes and to correlate them to the array/Nexus data. Two target genes were identified in this study, and the IHC shows that *CDKN2A* and *TERT* protein expression may be involved in the tumour progression. IHC was carried out as a useful way to assess ConM tissue and to detect the expression of these genes, and it is an excellent procedure to show the location of protein inside the examined tissue.

The *CDKN2A* gene was one of the candidate genes whose protein expression studied in ConM tissue. The gene encodes two tumour suppressor proteins including p16INK4A and p14ARF. Both proteins have anti-proliferative biological activity that is involved in the retinoblastoma protein (Rb) and p53 pathways. These proteins and their interactions play an important role in understanding the crucial points of tumor suppression (Serrano, 1997, Weber et al., 2000, Pei and Xiong, 2005). The p16INK4A controls the cell cycle by negatively regulated the cyclin-dependent kinases (CDK 4 and 6) by blocking phosphorylation of the Rb (Ortega et al., 2002). Phosphorylation of Rb leads to release of the E2F transcription factor, permitting the cell cycle to carry on from G1 to S stage (Eliason et al., 2006). The other protein, however, p14ARF however, has negative regulatory control on growth as it acts to stabilise p53. Once p53 is activated, it interacts with various downstream targets that can arrest cyclin-dependent kinases at the G1 and G2 checkpoints and also initiates apoptosis (Robertson and Jones, 1999, McWilliams et al., 2011). The *CDKN2A* protein has also been involved in many biological processes, such as cell invasion, apoptosis and angiogenesis, and these activities could be correlated to its overexpression in cancer. Their expression is well-organised in cellular senescence, and increases markedly with aging in some human tissues (Collado et al., 2007, Shima et al., 2011). The expression of *CDKN2A* has been assessed in various types of cancer with different results, ranging from clear overexpression to its loss (Schneider-Stock et al., 2005, Angiero et al., 2008, Buajeeb et al., 2009, Ayhan et al., 2010). *CDKN2A* overexpression has been detected at the invasive front of endometrial, colorectal and basal cell carcinoma (Jung et al., 2001, Svensson et al., 2003, Horree et al., 2007).

Furthermore, *CDKN2A* expression was mainly cytoplasmic and has been correlated with tumour progression and prognosis in some types of cancer. For instance, in breast cancer, the overexpression of *CDKN2A* was preferentially limited to the nucleus in fibro-adenoma and mainly to the cytoplasm in carcinoma and has been significantly correlated with poor prognostic factors, such as high grade and damaging oestrogen receptor status (Milde-Langosch et al., 2001). In addition, overexpression of *CDKN2A* in colorectal cancer has been linked with strong nuclear/cytoplasmic positivity in adenomas and primary or metastatic adenocarcinomas and this correlated with clinical features of poor prognosis such as sex, distal location and tumour stage (Dai et al., 2000, Zhao et al., 2006, Lam et al., 2008).

*CDKN2A* antibody has been recommended as a prognostic marker in cutaneous melanocytic lesions (Gould Rothberg et al., 2009). Karim and colleagues have reported that CM, but not benign melanocytic lesions, display reduced nuclear p16 expression compared to nevi, which showed a higher expression of p16 (Karim et al., 2009). Similarly, Zoroquiain et al. (2012) also reported that p16 seems to be a promising marker to distinguish between conjunctival nevi and PAM with atypia arising from ConM (Zoroquiain et al., 2012). They found that p16 expression is similar in ConM and CM, but different in other conjunctival melanocytic lesions in that cases of melanoma showed weaker p16 expression than all the other melanocytic lesions of the conjunctiva (Zoroquiain et al., 2012).

In this study, the IHC results reveal that *CDKN2A* antibody was mainly expressed in the cytoplasm, and to some extent in the nucleus of ConM cells as illustrated in (figure 5.6 C and D). The results of *CDKN2A* protein expression in ConM tumors are in concordance with previously reported studies that some cases showed weak to moderate *CDKN2A* expression. Although the sample size was limited, this study serves as proof of concept that results were generally in line with what would be expected from the deletions of the relevant genes detected by Nexus Software. Additional studies with a large set of samples are therefore required to verify these findings.

The *TERT* gene was the next candidate gene that studied for its protein expression among ConM cases. Telomerase is a ribonucleoprotein polymerase which supports telomere ends by addition of the telomere repeat TTAGGG. The enzyme contains of a protein element with reverse transcriptase activity, encoded by this gene. *TERT* expression is strongly regulated and developed during early embryonic growth but remains suppressed in most adult human somatic cells. Conversely, *TERT* is actively expressed in self-renewing cells such as stem cells (Blasco, 2005). *TERT* overexpression and telomere dysfunction has been identified in various human cancers, including thyroid cancer, bladder cancer, and brain tumours (Xing et al., 2014, Li et al., 2015, Yang et al., 2016). This *TERT* overexpression has been noticed in up to 90% of cancer cells, in contrast to <20% of normal cells (Kim et al., 1994). Li et al. (2015) reported in their study of bladder cancer that patients with high expression of *TERT* had significantly worse prognosis than patients with weak expression (Li et al., 2015). The protein expression of *TERT* in CM is still not well described, however, Zygouris et al. (2007) found that *TERT* protein expression was associated with tumour thickness and ulceration, whereas Populo et al. (2014) reported that *TERT* expression was cytoplasmic and nuclear in 98% of CM but found no difference in *TERT* expression levels between tumours with and without *TERT* promoter mutations (Populo et al., 2014). In addition, a recent study done by Hugdahl et al. (2018) on a large series of primary and metastasis CM shows that *TERT* expression was mainly cytoplasmic and usually homogenous, and that variations in staining intensity between tumour areas were hard to distinguish. They reported that *TERT* expression was positive in 44% of primary melanomas and 16% of metastatic melanomas, but found that there was no correlation between increased *TERT* protein expression and *TERT* mutations (Hugdahl et al., 2018).

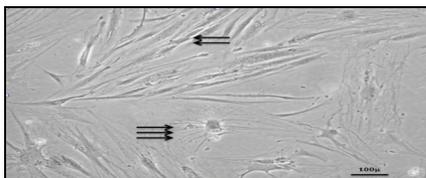
No previous studies have documented the *TERT* expression on conjunctival melanocytic lesion and their correlation with pathological finding or *TERT* mutations. In the current study, *TERT* protein was mainly expressed in the cytoplasm of positive ConM tissues and the cells displayed mild to moderate cell stain (Figure 5.7C) whereas *TERT* expression was weak in some of the other samples. The sample that shows weak *TERT* expression (Figure 5.7D) is quite similar to the negative *TERT* expression sample that created by Hugdahl et al.

(2018) in their study of primary CM (Hugdahl et al., 2018). The IHC results regarding *TERT* expression were in line with what would be expected of SCNA analysis conducted by Nexus software. The samples that revealed a loss of 5p and had mutations in the *TERT* promoter were in agreement with some samples that showed weak to mild *TERT* protein expression. Overall, the observations from this array CGH with IHC need further investigation on large sample, since the copy number, alterations are often correlated with gene expression.

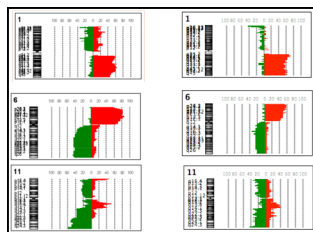
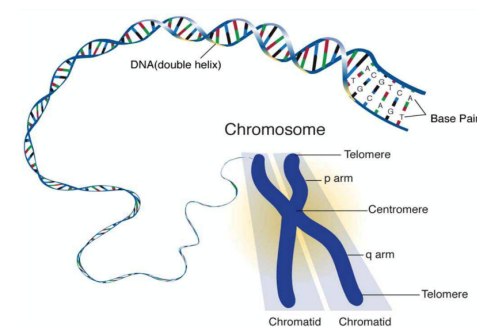
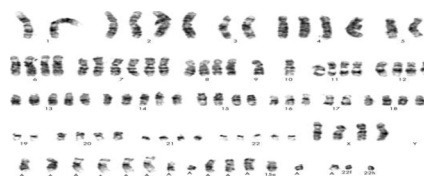
# CHAPTER SIX

## General Discussion

Figure 6.1: Outline of the approach used in this PhD study and the major finding in each section.

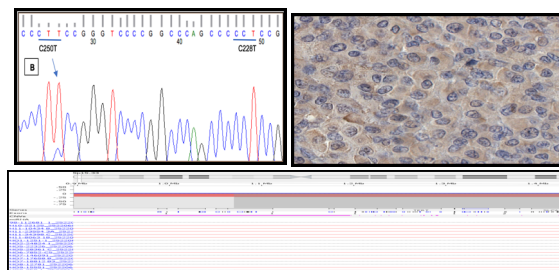


**CHAPTER THREE:** the aim of this chapter to perform tests on two short-term cultures and characterize them morphologically and to study their molecular and genetic profiles. However, the results showed that the cultures cells might be derived from normal stem cells population as the cells started to slow down to grow when reached passage 20.



Gene	Mutation type	Tumors harboring
BRAF	V600E (T1799A)	(2/6) (5 of 21)
NRAS	Q61R (A182G)	(9%) (2 of 21)
GNAI1	A626T (Q209L)	(1/6) (3 of 21)
GNAQ	A626T (Q209L)	(4%) (1 of 21)
TERT	C250T /C228T	47% (8 of 17)

**CHAPTER FOUR:** The Array-CGH and standard PCR identified the most relevant genetic changes that associated with conjunctival melanoma and the finding were in agreement with several previous studies that shows the similarity to genetic alterations of CM but, distinctive from UM.



**CHAPTER FIVE:** The most statically significant candidate genes that identified by Nexus Software were CDKN2A and TERT. The protein expression finding from IHC were linked to genes mutations and copy losses that identified previously in chapter 4. The result was often comparable in some cases to weak expressions, mutations and copy losses.

## 6.1 Final discussion

### 6.1.1 Objective of this PhD study

Ocular melanoma is the most common primary intraocular cancer of adults but although many studies have investigated the changes in UM, but there is insufficient information available to make similar comparisons for ConM. This biologic information is essential not only for understanding the pathophysiology of the disease progression, but also on account of its implications for therapy and for the enrolment of patients in clinical trials of new treatments. By using the early investigations, a clear association would possibly be made between certain chromosomal changes in ConM and the disease progression. Therefore, the main objective of this PhD study was to address two major issues. Firstly, to identify chromosomal changes that leading to amplifications and deletions among a series of ConM tumours and compared the finding with the other melanoma subtype such UM and CM. Secondly, to see if potential driver genes can be identified by array-CGH and correlate with the other finding from different approach such as standard PCR and/or IHC, which may lead to both an improved understanding of ConM metastasis and how to treat it. A summary of the approach to molecular pathway identification used in this PhD study is outlined in Figure 6.1 above.

### 6.1.2 Are there any early changes in Conjunctival melanoma?

The past studies had little information about ConM cells *in vitro* (Aubert et al., 1993, Nareyeck et al., 2005, Keijser et al., 2007). This is because the tumour is so rare and hard to culture. However, if these cell lines had been developed and verified as being ConM then they would be useful models for looking at the impact of the driver genes, and for investigation of therapeutic options. The present study investigated the two short-term cultures in chapter 3, but the absence of multiple genetics changes (Figure 3. 8 and 3.9) and the lack of mutations (Figure 3.11), altogether the finding suggest that the culture had been developed from normal stem cell population that were contaminating the tumours, especially as the cultures ultimately started to senesce at around passage 20. The other possibility would be that as a cancer stem cell population they may yet have acquired

additional abnormalities such as those commonly reported to be associated with the ConM and found in this study. There were some primary ConM samples that had none or very little changes by array-CGH such as those had 6p and 10q (Appendix 1), these samples may be originated from cancer stem cells or early progenitor cancer stem cells that had not acquired the other necessary genetic changes to take it further and may also indicate that these changes are the early drivers for ConM.

### 6.1.3 Does the data from the array-CGH coexist with the finding of mutations and how does that related to IHC and clinical data?

To find more strong investigation, all the clinical and genetic information available among ConM patients were reviewed involving those for which no clinical information was available (Appendix 1, 2 and 3). Initial 62% of ConM patients were identified as originally presenting with primary ConM. All these cases shared a genetic alteration of recurrent gains of 1q, 4q, 6p, 7q, 8q, 11q, 17q, 19p and recurrent loss of 3q, 5p, 6q, 9p, 10q, 11q, 12q and 16q. However, the most CNAs observed in the eight 38% of metastatic ConM samples, were recurrent gains of 1q, 6p and 7q, 11q, and losses of 3q, 5p, 6q, 9p, 10, 11q, 12q and 16q (Table 4.3, Figure 4.15). In term of clinical information or genetic alterations, there was no significant difference between the samples that metastases from either lymph node or metastases in different area within the eye. The age of the patients was range from 37-85 years old and that was in pattern similar to previous studies (Shields et al., 2000, Jovanovic et al., 2013, Kalirai et al., 2017). Among ConM samples, there were 50% male and 64% female however, based on clinical information both genders usually presented with in-situ and invasive melanoma. Most of the CNAS identified between the both gender was gain of 1q, 6p, 7, 8, 11q and loss of 5p, 9p, 16q. In addition, it is essential to correlate genomic copy number aberrations to valid gene expression. This is because gene expression is highly complex and controlled by numerous genetic and epigenetic factors in addition to genomic copy number. Interestingly, detection of tumour suppressors genes such as *CDKN2A* and *TERT* among ConM and correlates the finding from the array-CGH and other approach such as PCR/IHC might help understand their role in the pathogenesis of ConM

Loss of 5p was detected by nexus software in 9 cases, where the region of *TERT* genes was found at 5p15 loci, seven of these cases carry oncogenic mutation of *TERT* promoter and from the clinical data most of these samples represented as in-transit metastasis and equal in both sex. Some of these cases had tumours thickness with more than 0.8mm which also indications of poor prognosis (Appendix 4). The protein expression of *TERT* genes clearly shows that some samples that have 5p deletion and mutation shows clear weak expression especially metastasis samples (Table 5.1). The data also shows that cases with *TERT* mutations had less genomic instability which considered to be more aggressive and might associated with poor prognosis compared to the cases that had wildtype which clearly shows more genomic instability (Figure 4.14).

Losses of 9p including focal deletions of *CDKN2A* were also detected in seven cases most of them female and presented more with invasive melanoma. While the IHC finding were well-matched with common alterations that found by Nexus software, where the most statistically significant candidate driver gene was detected, further investigation is required to reveal the role of these genes in prognosis and metastasis. Overall, the study was limited in number but as a verification of concept study indicated that results were generally in agreement with the expected expression which correlated with the predicted finding by deletions of the relevant genes in some cases detected by Nexus Software. Therefore, it is very early to draw conclusions on the role of these genes and additional studies on larger series are required to verify these findings.

#### 6.1.4 Technical issue during this study

There were limited number of fresh tissue available for use in this study. Therefore, the main limitation was the use of FFPE tumours, the DNA was not always suitable for analysis since it typically had inadequate quality (low yield and highly fragmented) because of the degradative effects of formalin (Srinivasan et al., 2002, van Beers et al., 2006). As this affected the type of methods which can be used for studying genetic or molecular changes such as high-resolution analysis of genomic copy number by array CGH (Wang et al., 2013). Therefore, to overcome this issue, whole-genomic amplification was conducted on some cases that had

low DNA yield by using Sigma's GenomePlex Single Cell. Because of the challenging nature of the yield of DNA from FFPE for some cases repeated extractions were also required, in addition, the *TERT* primers proved particularly difficult to work with, and the working up of the *TERT* sequencing data proved particularly challenging and consequently restricted the time available to expand the analysis of the chosen genes by IHC. Finally, there were a number of reasons that limited the choice of what targets to take forward. As time was limited it was decided that IHC would be the best approach to explore the findings. Antibodies were readily available for some targets and not others, which did restrict the additional studies. *CDKN2A* was chosen as a good comparison to both previous studies on ConM and also CM. As there is very little information on *TERT* in ConM, and tumours from this study had both deletions and mutations, *TERT* was therefore chosen as the first target. Had time permitted the amplification of *RREB1* would also have been confirmed in additional tumours using FISH.

#### 6.1.5 Future Work

It is important to correlate genomic copy number abnormalities to actual gene expression, more so in the context of molecular pathway abnormalities. This is because gene expression is highly complex and regulated by various genetic and epigenetic factors in addition to genomic copy number. Whole transcriptome analysis carried out on the same tumours would be ideal for correlation analysis. In addition, the explanations of this array-CGH with IHC need further investigation, since the copy number, alterations are often but not always correlated with gene expression. However, in spite of recent technological developments such analysis on old FFPE samples remains technically challenging. In addition, the common aberrations detected among the primary and metastatic ConM tumours also require further corroboration in a larger cohort of ConMs with more comprehensive clinical and follow-up information. Such a study would establish whether the genetic changes identified here are important factors in the pathology of ConMs and thus whether they could be used to identify ConM patients at high risk of metastatic spread. Further steps to target even stronger pathogenic candidate's genes which help overcome the limitation of sample size and add statistical power could be done by using technique such as next-generation exome or whole genome sequencing.

# References

- AALTO, Y., ERIKSSON, L., SEREGARD, S., LARSSON, O. & KNUUTILA, S. 2001. Concomitant loss of chromosome 3 and whole arm losses and gains of chromosome 1, 6, or 8 in metastasizing primary uveal melanoma. *Invest Ophthalmol Vis Sci*, 42, 313-7.
- ABASOLO, A., VARGAS, M. T., RIOS-MARTIN, J. J., TRIGO, I., ARJONA, A. & GONZALEZ-CAMPORA, R. 2012. Application of fluorescence in situ hybridization as a diagnostic tool in melanocytic lesions, using paraffin wax-embedded tissues and imprint-cytology specimens. *Clin Exp Dermatol*, 37, 838-43.
- ABRAHAM, L. M., SELVA, D., CASSON, R. & LEIBOVITCH, I. 2006. Mitomycin: clinical applications in ophthalmic practice. *Drugs*, 66, 321-40.
- ADAMI, H. O., KUPER, H., ANDERSSON, S. O., BERGSTROM, R. & DILLNER, J. 2003. Prostate cancer risk and serologic evidence of human papilloma virus infection: a population-based case-control study. *Cancer Epidemiol Biomarkers Prev*, 12, 872-5.
- AKSLEN, L. A., ANGELINI, S., STRAUME, O., BACHMANN, I. M., MOLVEN, A., HEMMINKI, K. & KUMAR, R. 2005. BRAF and NRAS mutations are frequent in nodular melanoma but are not associated with tumor cell proliferation or patient survival. *J Invest Dermatol*. United States.
- ALBERTSON, D. G., COLLINS, C., MCCORMICK, F. & GRAY, J. W. 2003. Chromosome aberrations in solid tumors. *Nat Genet*, 34, 369-76.
- ALBREIKI, D. H., GILBERG, S. M. & FARMER, J. P. 2012. Conjunctival malignant melanoma: A rare variant and review of important diagnostic and therapeutic considerations. *Saudi Journal of Ophthalmology*, 26, 151-156.
- ALERS, J. C., ROCHAT, J., KRIJTENBURG, P. J., VAN DEKKEN, H., RAAP, A. K. & ROSENBERG, C. 1999. Universal linkage system: an improved method for labeling archival DNA for comparative genomic hybridization. *Genes Chromosomes Cancer*, 25, 301-5.
- ALLRED, D. C., HARVEY, J. M., BERARDO, M. & CLARK, G. M. 1998. Prognostic and predictive factors in breast cancer by immunohistochemical analysis. *Mod Pathol*, 11, 155-68.
- AMARO, A., MIRISOLA, V., ANGELINI, G., MUSSO, A., TOSETTI, F., ESPOSITO, A. I., PERRI, P., LANZA, F., NASCIUTI, F., MOSCI, C., PUZONE, R., SALVI, S., TRUINI, M., POGGI, A. & PFEFFER, U. 2013. Evidence of epidermal growth factor receptor expression in uveal melanoma: inhibition of epidermal growth factor-mediated signalling by Gefitinib and Cetuximab triggered antibody-dependent cellular cytotoxicity. *Eur J Cancer*, 49, 3353-65.
- ANAND, P., KUNNUMAKARA, A. B., SUNDARAM, C., HARIKUMAR, K. B., THARAKAN, S. T., LAI, O. S., SUNG, B. & AGGARWAL, B. B. 2008. Cancer is a Preventable Disease that Requires Major Lifestyle Changes. *Pharm Res*, 25, 2097-116.
- ANASTASSIOU, G., HEILIGENHAUS, A., BECHRAKIS, N., BADER, E., BORNFELD, N. & STEUHL, K. P. 2002. Prognostic value of clinical and histopathological parameters in conjunctival melanomas: a retrospective study. *Br J Ophthalmol*, 86, 163-7.
- ANG, L. P., TAN, D. T., PHAN, T. T., LI, J., BEUERMAN, R. & LAVKER, R. M. 2004. The in vitro and in vivo proliferative capacity of serum-free cultivated human conjunctival epithelial cells. *Curr Eye Res*, 28, 307-17.
- ANGI, M., VERSLUIS, M. & KALIRAI, H. 2015. Culturing Uveal Melanoma Cells. *Ocul Oncol Pathol*.

- ANGIERO, F., BERENZI, A., BENETTI, A., ROSSI, E., DEL SORDO, R., SIDONI, A., STEFANI, M. & DESSY, E. 2008. Expression of p16, p53 and Ki-67 proteins in the progression of epithelial dysplasia of the oral cavity. *Anticancer Res*, 28, 2535-9.
- AOUDE, L. G., WADT, K. A., PRITCHARD, A. L. & HAYWARD, N. K. 2015. Genetics of familial melanoma: 20 years after CDKN2A. *Pigment Cell Melanoma Res*, 28, 148-60.
- ARNDT, C. A. & CRIST, W. M. 1999. Common musculoskeletal tumors of childhood and adolescence. *N Engl J Med*, 341, 342-52.
- ARONOW, M. E. & SINGH, A. D. 2013. Radiation therapy: conjunctival and eyelid tumors. *Dev Ophthalmol*, 52, 85-93.
- AUBERT, C., ROUGE, F., REILLAUDOU, M. & METGE, P. 1993. Establishment and characterization of human ocular melanoma cell lines. *Int J Cancer*, 54, 784-92.
- AWAYA, T. 2005. Common ethical issues in regenerative medicine. *J Int Bioethique*, 16, 69-75, 192-3.
- AYHAN, S., ISISAG, A., SARUC, M., NESE, N., DEMIR, M. A. & KUCUKMETIN, N. T. 2010. The role of pRB, p16 and cyclin D1 in colonic carcinogenesis. *Hepatogastroenterology*, 57, 251-6.
- BARRANDON, Y. & GREEN, H. 1987. Three clonal types of keratinocyte with different capacities for multiplication. *Proc Natl Acad Sci U S A*, 84, 2302-6.
- BASTIAN, B. C., LEBIT, P. E., HAMM, H., BROCKER, E. B. & PINKEL, D. 1998. Chromosomal gains and losses in primary cutaneous melanomas detected by comparative genomic hybridization. *Cancer Res*, 58, 2170-5.
- BAUER, J., CURTIN, J. A., PINKEL, D. & BASTIAN, B. C. 2007. Congenital melanocytic nevi frequently harbor NRAS mutations but no BRAF mutations. *J Invest Dermatol*, 127, 179-82.
- BEADLING, C., JACOBSON-DUNLOP, E., HODI, F. S., LE, C., WARRICK, A., PATTERSON, J., TOWN, A., HARLOW, A., CRUZ, F., 3RD, AZAR, S., RUBIN, B. P., MULLER, S., WEST, R., HEINRICH, M. C. & CORLESS, C. L. 2008. KIT gene mutations and copy number in melanoma subtypes. *Clin Cancer Res*, 14, 6821-8.
- BENNETT, D. C. 2008. How to make a melanoma: what do we know of the primary clonal events? *Pigment Cell Melanoma Res*, 21, 27-38.
- BEROUKHIM, R., GETZ, G., NGHIEMPHU, L., BARRETINA, J., HSUEH, T., LINHART, D., VIVANCO, I., LEE, J. C., HUANG, J. H., ALEXANDER, S., DU, J., KAU, T., THOMAS, R. K., SHAH, K., SOTO, H., PERNER, S., PRENSNER, J., DEBIASI, R. M., DEMICHELIS, F., HATTON, C., RUBIN, M. A., GARRAWAY, L. A., NELSON, S. F., LIAU, L., MISCHER, P. S., CLOUGHESY, T. F., MEYERSON, M., GOLUB, T. A., LANDER, E. S., MELLINGHOFF, I. K. & SELLERS, W. R. 2007. Assessing the significance of chromosomal aberrations in cancer: Methodology and application to glioma.
- BEROUKHIM, R., MERMEL, C. H., PORTER, D., WEI, G., RAYCHAUDHURI, S., DONOVAN, J., BARRETINA, J., BOEHM, J. S., DOBSON, J., URASHIMA, M., MC HENRY, K. T., PINCHBACK, R. M., LIGON, A. H., CHO, Y. J., HAERY, L., GREULICH, H., REICH, M., WINCKLER, W., LAWRENCE, M. S., WEIR, B. A., TANAKA, K. E., CHIANG, D. Y., BASS, A. J., LOO, A., HOFFMAN, C., PRENSNER, J., LIEFELD, T., GAO, Q., YECIES, D., SIGNORETTI, S., MAHER, E., KAYE, F. J., SASAKI, H., TEPPER, J. E., FLETCHER, J. A., TABERNERO, J., BASELGA, J., TSAO, M. S., DEMICHELIS, F., RUBIN, M. A., JANNE, P. A., DALY, M. J., NUCERA, C., LEVINE, R. L., EBERT, B. L., GABRIEL, S., RUSTGI,

- A. K., ANTONESCU, C. R., LADANYI, M., LETAI, A., GARRAWAY, L. A., LODA, M., BEER, D. G., TRUE, L. D., OKAMOTO, A., POMEROY, S. L., SINGER, S., GOLUB, T. R., LANDER, E. S., GETZ, G., SELLERS, W. R. & MEYERSON, M. 2010. The landscape of somatic copy-number alteration across human cancers. *Nature*, 463, 899-905.
- BERTA-ANTALICS, A. I., KRUSE, F. E. & HOLBACH, L. 2015. [Pathology and prognostic factors of conjunctival melanoma]. *Ophthalmologie*, 112, 892, 894-8.
- BIRCK, A., AHRENKIEL, V., ZEUTHEN, J., HOU-JENSEN, K. & GULDBERG, P. 2000. Mutation and allelic loss of the PTEN/MMAC1 gene in primary and metastatic melanoma biopsies. *J Invest Dermatol*, 114, 277-80.
- BISHOP, J. A. N., J.NEWTON-BISHOP@CANCER.ORG.UK, SECTION OF EPIDEMIOLOGY AND BIostatISTICS, L. I. O. M. M., ST JAMES'S HOSPITAL, LEEDS, UNITED KINGDOM., GRUIS, N. A. & SKIN RESEARCH LABORATORY, L. U. M. C., LEIDEN, THE NETHERLANDS. 2007. Genetics: What Advice for Patients Who Present With a Family History of Melanoma? *Seminars in Oncology*, 34, 452-459.
- BLASCO, M. A. 2005. Telomeres and human disease: ageing, cancer and beyond. *Nat Rev Genet*, 6, 611-22.
- BLOKX, W. A., VAN DIJK, M. C. & RUITER, D. J. 2010. Molecular cytogenetics of cutaneous melanocytic lesions - diagnostic, prognostic and therapeutic aspects. *Histopathology*, 56, 121-32.
- BONNIOL, M., AUTIER, P., BOYLE, P. & GANDINI, S. 2012. Cutaneous melanoma attributable to sunbed use : systematic review and meta-analysis.
- BOVERI, T. 1902. Über mehrpolige Mitosen als Mittel zur Analyse des Zellkerns.
- BROSE, M. S., VOLPE, P., FELDMAN, M., KUMAR, M., RISHI, I., GERRERO, R., EINHORN, E., HERLYN, M., MINNA, J., NICHOLSON, A., ROTH, J. A., ALBELDA, S. M., DAVIES, H., COX, C., BRIGNELL, G., STEPHENS, P., FUTREAL, P. A., WOOSTER, R., STRATTON, M. R. & WEBER, B. L. 2002. BRAF and RAS mutations in human lung cancer and melanoma. *Cancer Res*, 62, 6997-7000.
- BROUWER, N. J., MARINKOVIC, M., DUINEN, S. G. V., BLEEKER, J. C., JAGER, M. J. & LUYTEN, G. P. M. 2017. Treatment of conjunctival melanoma in a Dutch referral centre.
- BROWNSTEIN, S., FARAJI, H., JACKSON, W. B. & FONT, R. L. 2006. Conjunctival Melanoma in Children: A Clinicopathologic Study of 2 Cases. *Archives of Ophthalmology*, 124, 1190-1193.
- BUAJEED, W., POOMSAWAT, S., PUNYASINGH, J. & SANGUANSIN, S. 2009. Expression of p16 in oral cancer and premalignant lesions. *J Oral Pathol Med*, 38, 104-8.
- BUECHER, B., GAUTHIER-VILLARS, M., DESJARDINS, L., LUMBROSO-LE ROUIC, L., LEVY, C., DE PAUW, A., BOMBLED, J., TIRAPO, C., HOUDAYER, C., BRESSAC-DE PAILLERETS, B. & STOPPA-LYONNET, D. 2010. Contribution of CDKN2A/P16 ( INK4A ), P14 (ARF), CDK4 and BRCA1/2 germline mutations in individuals with suspected genetic predisposition to uveal melanoma. *Fam Cancer*, 9, 663-7.
- BUSAM, K. J., FANG, Y., JHANWAR, S. C., PULITZER, M. P., MARR, B. & ABRAMSON, D. H. 2010. Distinction of conjunctival melanocytic nevi from melanomas by fluorescence in situ hybridization. *J Cutan Pathol*, 37, 196-203.
- CANNON-ALBRIGHT, L. A., GOLDGAR, D. E., MEYER, L. J., LEWIS, C. M., ANDERSON, D. E., FOUNTAIN, J. W., HEGI, M. E., WISEMAN, R. W., PETTY,

- E. M., BALE, A. E. & ET AL. 1992. Assignment of a locus for familial melanoma, MLM, to chromosome 9p13-p22. *Science*, 258, 1148-52.
- CHEE, K. Y., KICIC, A. & WIFFEN, S. J. 2006. Limbal stem cells: the search for a marker. *Clin Experiment Ophthalmol*. Australia.
- CHITALE, D., GONG, Y., TAYLOR, B. S., BRODERICK, S., BRENNAN, C., SOMWAR, R., GOLAS, B., WANG, L., MOTOI, N., SZOKE, J., REINERSMAN, J. M., MAJOR, J., SANDER, C., SESHAN, V. E., ZAKOWSKI, M. F., RUSCH, V., PAO, W., GERALD, W. & LADANYI, M. 2009. An integrated genomic analysis of lung cancer reveals loss of DUSP4 in EGFR-mutant tumors. *Oncogene*, 28, 2773-83.
- CHUNG, H. Y., LEE, E. K., CHOI, Y. J., KIM, J. M., KIM, D. H., ZOU, Y., KIM, C. H., LEE, J., KIM, H. S., KIM, N. D., JUNG, J. H. & YU, B. P. 2011. Molecular inflammation as an underlying mechanism of the aging process and age-related diseases. *J Dent Res*, 90, 830-40.
- CLEMENTE, C., BETTIO, D., VENCI, A., SCOPSI, L., RAO, S., FERRARI, A., PIRIS, A. & MIHM, M. C., JR. 2009. A fluorescence in situ hybridization (FISH) procedure to assist in differentiating benign from malignant melanocytic lesions. *Pathologica*, 101, 169-74.
- COHEN, Y., GOLDENBERG-COHEN, N., PARRELLA, P., CHOWERS, I., MERBS, S. L., PE'ER, J. & SIDRANSKY, D. 2003. Lack of BRAF mutation in primary uveal melanoma. *Invest Ophthalmol Vis Sci*, 44, 2876-8.
- COLLADO, M., BLASCO, M. A. & SERRANO, M. 2007. Cellular senescence in cancer and aging. *Cell*, 130, 223-33.
- COOK, B. E., JR., LUCARELLI, M. J., LEMKE, B. N., DORTZBACH, R. K., KAUFMAN, P. L., FORREST, L., GREENE, E. & GABELT, B. T. 2002. Eyelid lymphatics II: a search for drainage patterns in the monkey and correlations with human lymphatics. *Ophthal Plast Reconstr Surg*, 18, 99-106.
- COSGAREA, I., UGUREL, S., SUCKER, A., LIVINGSTONE, E., ZIMMER, L., ZIEMER, M., UTIKAL, J., MOHR, P., PFEIFFER, C., PFOHLER, C., HILLEN, U., HORN, S., SCHADENDORF, D., GRIEWANK, K. G. & ROESCH, A. 2017. Targeted next generation sequencing of mucosal melanomas identifies frequent NF1 and RAS mutations. *Oncotarget*, 8, 40683-40692.
- CRAWFORD, J. B. 1980. Conjunctival melanomas: prognostic factors a review and an analysis of a series. *Trans Am Ophthalmol Soc*, 78, 467-502.
- CRUZ, F., 3RD, RUBIN, B. P., WILSON, D., TOWN, A., SCHROEDER, A., HALEY, A., BAINBRIDGE, T., HEINRICH, M. C. & CORLESS, C. L. 2003. Absence of BRAF and NRAS mutations in uveal melanoma. *Cancer Res*, 63, 5761-6.
- CURTIN, J. A., FRIDLAND, J., KAGESHITA, T., PATEL, H. N., BUSAM, K. J., KUTZNER, H., CHO, K. H., AIBA, S., BROCKER, E. B., LEBOIT, P. E., PINKEL, D. & BASTIAN, B. C. 2005. Distinct sets of genetic alterations in melanoma. *N Engl J Med*. United States: 2005 Massachusetts Medical Society.
- DAI, C. Y., FURTH, E. E., MICK, R., KOH, J., TAKAYAMA, T., NIITSU, Y. & ENDERS, G. H. 2000. p16(INK4a) expression begins early in human colon neoplasia and correlates inversely with markers of cell proliferation. *Gastroenterology*, 119, 929-42.
- DAMATO, B. & COUPLAND, S. E. 2008. Conjunctival melanoma and melanosis: a reappraisal of terminology, classification and staging. *Clin Experiment Ophthalmol*, 36, 786-95.
- DAMATO, B. & COUPLAND, S. E. 2009. Management of conjunctival melanoma. *Expert Rev Anticancer Ther*, 9, 1227-39.

- DAMATO, B. E. & COUPLAND, S. E. 2012. Ocular melanoma. *Saudi Journal of Ophthalmology*, 26, 137-144.
- DAVANGER, M. & EVENSEN, A. 1971. Role of the pericorneal papillary structure in renewal of corneal epithelium. *Nature*, 229, 560-1.
- DAVIES, H., BIGNELL, G. R., COX, C., STEPHENS, P., EDKINS, S., CLEGG, S., TEAGUE, J., WOFFENDIN, H., GARNETT, M. J., BOTTOMLEY, W., DAVIS, N., DICKS, E., EWING, R., FLOYD, Y., GRAY, K., HALL, S., HAWES, R., HUGHES, J., KOSMIDOU, V., MENZIES, A., MOULD, C., PARKER, A., STEVENS, C., WATT, S., HOOPER, S., WILSON, R., JAYATILAKE, H., GUSTERSON, B. A., COOPER, C., SHIPLEY, J., HARGRAVE, D., PRITCHARD-JONES, K., MAITLAND, N., CHENEVIX-TRENCH, G., RIGGINS, G. J., BIGNER, D. D., PALMIERI, G., COSSU, A., FLANAGAN, A., NICHOLSON, A., HO, J. W., LEUNG, S. Y., YUEN, S. T., WEBER, B. L., SEIGLER, H. F., DARROW, T. L., PATERSON, H., MARAIS, R., MARSHALL, C. J., WOOSTER, R., STRATTON, M. R. & FUTREAL, P. A. 2002. Mutations of the BRAF gene in human cancer. *Nature*, 417, 949-54.
- DE POTTER, P., SHIELDS, C. L., SHIELDS, J. A. & MENDUKE, H. 1993. Clinical predictive factors for development of recurrence and metastasis in conjunctival melanoma: a review of 68 cases. *Br J Ophthalmol*, 77, 624-30.
- DE WOLFF-ROUENDAAL, D. & OOSTERHUIS, J. A. 1983. Conjunctival melanomas in The Netherlands: a follow-up study. *Doc Ophthalmol*, 56, 49-54.
- DEL CARPIO HUERTA, L. P., MAS CASTELLS, M., ANGUERA PALACIOS, G., SULLIVAN, I., GONZALEZ VIDAL, A. & MAJEM TARRUELLA, M. 2017. A novel KRAS mutation in metastatic conjunctival melanoma: a case report and literature review. *Melanoma Res*.
- DING, S. Z., MINOHARA, Y., FAN, X. J., WANG, J., REYES, V. E., PATEL, J., DIRDEN-KRAMER, B., BOLDOGH, I., ERNST, P. B. & CROWE, S. E. 2007. Helicobacter pylori infection induces oxidative stress and programmed cell death in human gastric epithelial cells. *Infect Immun*, 75, 4030-9.
- DITTA, L. C., SHILDKROT, Y. & WILSON, M. W. 2011. Outcomes in 15 patients with conjunctival melanoma treated with adjuvant topical mitomycin C: complications and recurrences. *Ophthalmology*, 118, 1754-9.
- DONO, M., ANGELINI, G., CECCONI, M., AMARO, A., ESPOSITO, A. I., MIRISOLA, V., MARIC, I., LANZA, F., NASCIUTI, F., VIAGGI, S., GUALCO, M., BANDELLONI, R., TRUINI, M., COVIELLO, D. A., ZUPO, S., MOSCI, C. & PFEFFER, U. 2014. Mutation frequencies of GNAQ, GNA11, BAP1, SF3B1, EIF1AX and TERT in uveal melanoma: detection of an activating mutation in the TERT gene promoter in a single case of uveal melanoma. *Br J Cancer*.
- DRATVIMAN-STOROBINSKY, O., COHEN, Y., FRENKEL, S., PE'ER, J. & GOLDENBERG-COHEN, N. 2010. Lack of oncogenic GNAQ mutations in melanocytic lesions of the conjunctiva as compared to uveal melanoma. *Invest Ophthalmol Vis Sci*, 51, 6180-2.
- DUMAZ, N. 2011. Mechanism of RAF isoform switching induced by oncogenic RAS in melanoma. *Small GTPases*, 2, 289-292.
- DWYER, J., LI, H., XU, D. & LIU, J. P. 2007. Transcriptional regulation of telomerase activity: roles of the the Ets transcription factor family. *Ann N Y Acad Sci*, 1114, 36-47.
- EDER, A. M., SUI, X., ROSEN, D. G., NOLDEN, L. K., CHENG, K. W., LAHAD, J. P., KANGO-SINGH, M., LU, K. H., WARNEKE, C. L., ATKINSON, E. N., BEDROSIAN, I., KEYOMARSI, K., KUO, W., GRAY, J. W., YIN, J. C. P., LIU, J.,

- HALDER, G. & MILLS, G. B. 2005. Atypical PKC $\alpha$  contributes to poor prognosis through loss of apical-basal polarity and Cyclin E overexpression in ovarian cancer. *Proc Natl Acad Sci U S A*.
- EDMUNDS, S. C., CREE, I. A., DI NICOLANTONIO, F., HUNGERFORD, J. L., HURREN, J. S. & KELSELL, D. P. 2003. Absence of BRAF gene mutations in uveal melanomas in contrast to cutaneous melanomas. *Br J Cancer*, 88, 1403-5.
- EGAN, K. M., SEDDON, J. M., GLYNN, R. J., GRAGOUDAS, E. S. & ALBERT, D. M. 1988. Epidemiologic aspects of uveal melanoma. *Surv Ophthalmol*, 32, 239-51.
- ELIASON, M. J., LARSON, A. A., FLORELL, S. R., ZONE, J. J., CANNON-ALBRIGHT, L. A., SAMLOWSKI, W. E. & LEACHMAN, S. A. 2006. Population-based prevalence of CDKN2A mutations in Utah melanoma families. *J Invest Dermatol*, 126, 660-6.
- ESMAELI, B., WANG, X., YOUSSEF, A. & GERSHENWALD, J. E. 2001. Patterns of regional and distant metastasis in patients with conjunctival melanoma: experience at a cancer center over four decades. *Ophthalmology*, 108, 2101-5.
- FERLAY, J., SHIN, H. R., BRAY, F., FORMAN, D., MATHERS, C. & PARKIN, D. M. 2010. Estimates of worldwide burden of cancer in 2008: GLOBOCAN 2008. *Int J Cancer*, 127, 2893-917.
- FIALA, E. S., SOHN, O. S., WANG, C. X., SEIBERT, E., TSURUTANI, J., DENNIS, P. A., EL-BAYOUMY, K., SODUM, R. S., DESAI, D., REINHARDT, J. & ALIAGA, C. 2005. Induction of preneoplastic lung lesions in guinea pigs by cigarette smoke inhalation and their exacerbation by high dietary levels of vitamins C and E. *Carcinogenesis*, 26, 605-12.
- FINGER, P., CZECHONSKA, G. & LIARIKOS, S. 1998. Topical mitomycin C chemotherapy for conjunctival melanoma and PAM with atypia. *Br J Ophthalmol*, 82, 476-9.
- FOLBERG, R., MCLEAN, I. W. & ZIMMERMAN, L. E. 1985. Malignant melanoma of the conjunctiva. *Hum Pathol*, 16, 136-43.
- FUCHS, U., KIVEL, A. T., LIESTO, K. & TARKKANEN, A. 1989. Prognosis of conjunctival melanomas in relation to histopathological features. *Br J Cancer*, 59, 261-7.
- GAST, A., SCHERER, D., CHEN, B., BLOETHNER, S., MELCHERT, S., SUCKER, A., HEMMINKI, K., SCHADENDORF, D. & KUMAR, R. 2010. Somatic alterations in the melanoma genome: a high-resolution array-based comparative genomic hybridization study. *Genes Chromosomes Cancer*, 49, 733-45.
- GEAR, H., WILLIAMS, H., KEMP, E. G. & ROBERTS, F. 2004a. BRAF mutations in conjunctival melanoma. *Invest Ophthalmol Vis Sci*, 45, 2484-8.
- GEIGL, J. B. & SPEICHER, M. R. 2007. Single-cell isolation from cell suspensions and whole genome amplification from single cells to provide templates for CGH analysis. *Nat Protoc*, 2, 3173-84.
- GERAMI, P., JEWELL, S. S., MORRISON, L. E., BLONDIN, B., SCHULZ, J., RUFFALO, T., MATUSHEK, P. T., LEGATOR, M., JACOBSON, K., DALTON, S. R., CHARZAN, S., KOLAITIS, N. A., GUITART, J., LERTSBARAPA, T., BOONE, S., LEBOIT, P. E. & BASTIAN, B. C. 2009. Fluorescence in situ hybridization (FISH) as an ancillary diagnostic tool in the diagnosis of melanoma. *Am J Surg Pathol*, 33, 1146-56.
- GERAMI, P., MAFEE, M., LURTSBARAPA, T., GUITART, J., HAGHIGHAT, Z. & NEWMAN, M. 2010. Sensitivity of fluorescence in situ hybridization for melanoma diagnosis using RREB1, MYB, Cep6, and 11q13 probes in melanoma subtypes. *Arch Dermatol*, 146, 273-8.

- GOLDENBERG-COHEN, N., COHEN, Y., ROSENBAUM, E., HERSCOVICI, Z., CHOWERS, I., WEINBERGER, D., PE'ER, J. & SIDRANSKY, D. 2005. T1799A BRAF mutations in conjunctival melanocytic lesions. *Invest Ophthalmol Vis Sci*, 46, 3027-30.
- GOULD ROTHBERG, B. E., BERGER, A. J., MOLINARO, A. M., SUBTIL, A., KRAUTHAMMER, M. O., CAMP, R. L., BRADLEY, W. R., ARIYAN, S., KLUGER, H. M. & RIMM, D. L. 2009. Melanoma prognostic model using tissue microarrays and genetic algorithms. *J Clin Oncol*, 27, 5772-80.
- GREENE, V. R., JOHNSON, M. M., GRIMM, E. A. & ELLERHORST, J. A. 2009. Frequencies of NRAS and BRAF mutations increase from the radial to the vertical growth phase in cutaneous melanoma. *J Invest Dermatol*, 129, 1483-8.
- GRIEWANK, K. G., MURALI, R., SCHILLING, B., SCHOLZ, S., SUCKER, A., SONG, M., SÜSSKIND, D., GRABELLUS, F., ZIMMER, L., HILLEN, U., STEUHL, K. P., SCHADENDORF, D., WESTEKEMPER, H. & ZESCHNIGK, M. 2013a. TERT promoter mutations in ocular melanoma distinguish between conjunctival and uveal tumours. *Br J Cancer*.
- GRIEWANK, K. G., WESTEKEMPER, H., MURALI, R., MACH, M., SCHILLING, B., WIESNER, T., SCHIMMING, T., LIVINGSTONE, E., SUCKER, A., GRABELLUS, F., METZ, C., SÜSSKIND, D., HILLEN, U., SPEICHER, M. R., WOODMAN, S. E., STEUHL, K. P. & SCHADENDORF, D. 2013b. Conjunctival melanomas harbor BRAF and NRAS mutations and copy number changes similar to cutaneous and mucosal melanomas. *Clinical Cancer Research*, 19, 3143-3152.
- GRIFFIN, C. A., LONG, P. P. & SCHACHAT, A. P. 1988. Trisomy 6p in an ocular melanoma. *Cancer Genet Cytogenet*, 32, 129-32.
- HABER, M. & STEWART, B. W. 1985. Oncogenes. A possible role for cancer genes in human malignant disease. *Med J Aust*, 142, 402-6.
- HAHN, W. C. & WEINBERG, R. A. 2002. Modelling the molecular circuitry of cancer. *Nat Rev Cancer*, 2, 331-41.
- HALL, J. & ANGELE, S. 1999. Radiation, DNA damage and cancer. *Mol Med Today*, 5, 157-64.
- HANAHAN, D. & WEINBERG, R. A. 2000. The hallmarks of cancer. *Cell*, 100, 57-70.
- HANAHAN, D. & WEINBERG, R. A. 2011. Hallmarks of cancer: the next generation. *Cell*, 144, 646-74.
- HARBOUR, J. W. 2012. The genetics of uveal melanoma: an emerging framework for targeted therapy. *Pigment Cell Melanoma Res*, 25, 171-81.
- HAROONI, H., SCHOENFIELD, L. R. & SINGH, A. D. 2011. Current appraisal of conjunctival melanocytic tumors: classification and treatment. *Future Oncol*, 7, 435-46.
- HARVEY, J. M., CLARK, G. M., OSBORNE, C. K. & ALLRED, D. C. 1999. Estrogen receptor status by immunohistochemistry is superior to the ligand-binding assay for predicting response to adjuvant endocrine therapy in breast cancer. *J Clin Oncol*, 17, 1474-81.
- HECKMAN, C. A. 2009. Contact inhibition revisited. *J Cell Physiol*, 220, 574-5.
- HEINDL, L. M., HOFMANN-RUMMELT, C., ADLER, W., BOSCH, J. J., HOLBACH, L. M., NAUMANN, G. O., KRUSE, F. E. & CURSIEFEN, C. 2011. Prognostic significance of tumor-associated lymphangiogenesis in malignant melanomas of the conjunctiva. *Ophthalmology*, 118, 2351-60.
- HEINDL, L. M., KOCH, K. R., SCHLAAK, M., MAUCH, C. & CURSIEFEN, C. 2015. [Adjuvant therapy and interdisciplinary follow-up care of conjunctival melanoma]. *Ophthalmologe*, 112, 907-11.

- HELGDOTTIR, H. & HÖIOM, V. 2016. The genetics of uveal melanoma: current insights. *Appl Clin Genet*.
- HODIS, E., WATSON, I. R., KRYUKOV, G. V., AROLD, S. T., IMIELINSKI, M., THEURILLAT, J. P., NICKERSON, E., AUCLAIR, D., LI, L., PLACE, C., DICARA, D., RAMOS, A. H., LAWRENCE, M. S., CIBULSKIS, K., SIVACHENKO, A., VOET, D., SAKSENA, G., STRANSKY, N., ONOFRIO, R. C., WINCKLER, W., ARDLIE, K., WAGLE, N., WARGO, J., CHONG, K., MORTON, D. L., STEMKEHALE, K., CHEN, G., NOBLE, M., MEYERSON, M., LADBURY, J. E., DAVIES, M. A., GERSHENWALD, J. E., WAGNER, S. N., HOON, D. S., SCHADENDORF, D., LANDER, E. S., GABRIEL, S. B., GETZ, G., GARRAWAY, L. A. & CHIN, L. 2012. A Landscape of Driver Mutations in Melanoma. *Cell*, 150, 251-63.
- HORN, S., FIGL, A., RACHAKONDA, P. S., FISCHER, C., SUCKER, A., GAST, A., KADEL, S., MOLL, I., NAGORE, E., HEMMINKI, K., SCHADENDORF, D. & KUMAR, R. 2013. TERT promoter mutations in familial and sporadic melanoma. *Science*, 339, 959-61.
- HORREE, N., VAN DIEST, P. J., SIE-GO, D. M. & HEINTZ, A. P. 2007. The invasive front in endometrial carcinoma: higher proliferation and associated derailment of cell cycle regulators. *Hum Pathol*, 38, 1232-8.
- HOSLER, G. A., DAVOLI, T., MENDER, I., LITZNER, B., CHOI, J., KAPUR, P., SHAY, J. W. & WANG, R. C. 2015. A Primary Melanoma and its Asynchronous Metastasis Highlight the Role of BRAF, CDKN2A, and TERT. *J Cutan Pathol*, 42, 108-17.
- HOUBEN, R., BECKER, J. C., KAPPEL, A., TERHEYDEN, P., BROCKER, E. B., GOETZ, R. & RAPP, U. R. 2004. Constitutive activation of the Ras-Raf signaling pathway in metastatic melanoma is associated with poor prognosis. *J Carcinog*, 3, 6.
- HU, D.-N., YU, G., MCCORMICK, S. A. & FINGER, P. T. 2008. Population-Based Incidence of Conjunctival Melanoma in Various Races and Ethnic Groups and Comparison With Other Melanomas. *American Journal of Ophthalmology*, 145, 418-423.e1.
- HUANG, F. W., HODIS, E., XU, M. J., KRYUKOV, G. V., CHIN, L. & GARRAWAY, L. A. 2013a. Highly Recurrent TERT Promoter Mutations in Human Melanoma.
- HUGDAHL, E., KALVENES, M. B., MANNELQVIST, M., LADSTEIN, R. G. & AKSLEN, L. A. 2018. Prognostic impact and concordance of TERT promoter mutation and protein expression in matched primary and metastatic cutaneous melanoma. *Br J Cancer*, 118, 98-105.
- HUSSAIN, S. P., SCHWANK, J., STAIB, F., WANG, X. W. & HARRIS, C. C. 2007. TP53 mutations and hepatocellular carcinoma: insights into the etiology and pathogenesis of liver cancer. *Oncogene*, 26, 2166-2176.
- HUSSUSSIAN, C. J., STRUEWING, J. P., GOLDSTEIN, A. M., HIGGINS, P. A., ALLY, D. S., SHEAHAN, M. D., CLARK, W. H., JR., TUCKER, M. A. & DRACOPOLI, N. C. 1994. Germline p16 mutations in familial melanoma. *Nat Genet*, 8, 15-21.
- IANNACONE, M. R., YOULDEN, D. R., BAADE, P. D., AITKEN, J. F. & GREEN, A. C. 2015. Melanoma incidence trends and survival in adolescents and young adults in Queensland, Australia. *Int J Cancer*, 136, 603-9.
- INSKIP, P. D., DEVESA, S. S. & FRAUMENI JR, J. F. 2003. Trends in the incidence of ocular melanoma in the United States, 1974-1998. *Cancer Causes and Control*, 14, 251-257.

- IRAC 1994. Schistosomes, liver flukes and Helicobacter pylori. IARC Working Group on the Evaluation of Carcinogenic Risks to Humans. Lyon, 7-14 June 1994. *IARC Monogr Eval Carcinog Risks Hum*, 61, 1-241.
- IRVINE, F., KUMARASAMY, M., KEMP, E. & ROBERTS, F. 2012. Progression of primary acquired melanosis with atypia during pregnancy. *Arch Ophthalmol. United States*.
- ISAGER, P., ENGHOLM, G., OVERGAARD, J. & STORM, H. 2006. Uveal and conjunctival malignant melanoma in denmark 1943-97: observed and relative survival of patients followed through 2002. *Ophthalmic Epidemiol*, 13, 85-96.
- JACKSON, A. L. & LOEB, L. A. 1998. On the origin of multiple mutations in human cancers. *Semin Cancer Biol*, 8, 421-9.
- JAKOB, J. A., BASSETT, R. L., NG, C. S., CURRY, J. L., JOSEPH, R. W., ALVARADO, G. C., ROHLFS, M. L., RICHARD, J., GERSHENWALD, J. E., HWU, P., KIM, K. B., LAZAR, A. J. & DAVIES, M. A. 2012. NRAS Mutation Status is an Independent Prognostic Factor in Metastatic Melanoma. *Cancer*, 118, 4014-23.
- JAKOBIEC, F. A., BROWNSTEIN, S., ALBERT, W., SCHWARZ, F. & ANDERSON, R. 1982. The Role of Cryotherapy in the Management of Conjunctival Melanoma. *Ophthalmology*, 89, 502-515.
- JAKOBIEC, F. A., FOLBERG, R. & IWAMOTO, T. 1989. Clinicopathologic characteristics of premalignant and malignant melanocytic lesions of the conjunctiva. *Ophthalmology*, 96, 147-66.
- JAKOBIEC, F. A., RINI, F. J., FRAUNFELDER, F. T. & BROWNSTEIN, S. 1988. Cryotherapy for conjunctival primary acquired melanosis and malignant melanoma. Experience with 62 cases. *Ophthalmology*, 95, 1058-70.
- JAY, B. 1965. NAEVI AND MELANOMATA OF THE CONJUNCTIVA\*†. *Br J Ophthalmol*, 49, 169-204.
- JEMAL, A., SIEGEL, R., WARD, E., HAO, Y., XU, J., MURRAY, T. & THUN, M. J. 2008. Cancer statistics, 2008. *CA Cancer J Clin*, 58, 71-96.
- JEMAL, A., SIEGEL, R., WARD, E., HAO, Y., XU, J. & THUN, M. J. 2009. Cancer statistics, 2009. *CA Cancer J Clin*, 59, 225-49.
- JOVANOVIĆ, P., MIHAJLOVIĆ, M., DJORDJEVIĆ-JOVIĆ, J., VLAJKOVIĆ, S., CEKIĆ, S. & STEFANOVIĆ, V. 2013. Ocular melanoma: an overview of the current status. *Int J Clin Exp Pathol*, 6, 1230-44.
- JUNG, A., SCHRAUDER, M., OSWALD, U., KNOLL, C., SELLBERG, P., PALMQVIST, R., NIEDOBITEK, G., BRABLETZ, T. & KIRCHNER, T. 2001. The invasion front of human colorectal adenocarcinomas shows co-localization of nuclear beta-catenin, cyclin D1, and p16INK4A and is a region of low proliferation. *Am J Pathol*, 159, 1613-7.
- JURDY, L., MERKS, J. H., PIETERS, B. R., MOURITS, M. P., KLOOS, R. J., STRACKEE, S. D. & SAEED, P. 2013. Orbital rhabdomyosarcomas: A review. *Saudi J Ophthalmol*.
- KALIKI, S., SHIELDS, C. L. & SHIELDS, J. A. 2015. Uveal melanoma: estimating prognosis. *Indian J Ophthalmol*, 63, 93-102.
- KALIRAI, H., MULLER, P. L., JAEHNE, D. & COUPLAND, S. E. 2017. [Ocular melanomas : An update]. *Pathologe*, 38, 491-499.
- KALLIONIEMI, A., KALLIONIEMI, O. P., SUDAR, D., RUTOVITZ, D., GRAY, J. W., WALDMAN, F. & PINKEL, D. 1992. Comparative genomic hybridization for molecular cytogenetic analysis of solid tumors. *Science*, 258, 818-21.
- KAMB, A., GRUIS, N. A., WEAVER-FELDHaus, J., LIU, Q., HARSHMAN, K., TAVTIGIAN, S. V., STOCKERT, E., DAY, R. S., 3RD, JOHNSON, B. E. &

- SKOLNICK, M. H. 1994. A cell cycle regulator potentially involved in genesis of many tumor types. *Science*, 264, 436-40.
- KARIM, R. Z., LI, W., SANKI, A., COLMAN, M. H., YANG, Y. H., THOMPSON, J. F. & SCOLYER, R. A. 2009. Reduced p16 and increased cyclin D1 and pRb expression are correlated with progression in cutaneous melanocytic tumors. *Int J Surg Pathol*, 17, 361-7.
- KEIJSER, S., MAAT, W., MISSOTTEN, G. S. & DE KEIZER, R. J. W. 2007. A new cell line from a recurrent conjunctival melanoma. *Br J Ophthalmol*, 91, 1566-7.
- KILLELA, P. J., REITMAN, Z. J., JIAO, Y., BETTEGOWDA, C., AGRAWAL, N., LUIS A. DIAZ, J., FRIEDMAN, A. H., FRIEDMAN, H., GALLIA, G. L., GIOVANELLA, B. C., GROLLMAN, A. P., HE, T.-C., HE, Y., HRUBAN, R. H., JALLO, G. I., MANDAHN, N., MEEKER, A. K., MERTENS, F., NETTO, G. J., RASHEED, B. A., RIGGINS, G. J., ROSENQUIST, T. A., SCHIFFMAN, M., SHIH, I.-M., THEODORESCU, D., TORBENSON, M. S., VELCULESCU, V. E., WANG, T.-L., WENTZENSEN, N., WOOD, L. D., ZHANG, M., MCLENDON, R. E., BIGNER, D. D., KINZLER, K. W., VOGELSTEIN, B., PAPADOPOULOS, N. & YAN, H. 2013b. TERT promoter mutations occur frequently in gliomas and a subset of tumors derived from cells with low rates of self-renewal.
- KIM, N. W., PIATYSZEK, M. A., PROWSE, K. R., HARLEY, C. B., WEST, M. D., HO, P. L., COVIELLO, G. M., WRIGHT, W. E., WEINRICH, S. L. & SHAY, J. W. 1994. Specific association of human telomerase activity with immortal cells and cancer. *Science*, 266, 2011-5.
- KIRKWOOD, B. J. & KIRKWOOD, R. A. 2010. Pigmented conjunctival lesions. *Insight*, 35, 18-21.
- KIRSCH-VOLDERS, M., VANHAUWAERT, A., DE BOECK, M. & DECORDER, I. 2002. Importance of detecting numerical versus structural chromosome aberrations. *Mutat Res*, 504, 137-48.
- KLEUSS, C., RAW, A. S., LEE, E., SPRANG, S. R. & GILMAN, A. G. 1994. Mechanism of GTP hydrolysis by G-protein alpha subunits. *Proc Natl Acad Sci U S A*, 91, 9828-31.
- KO, J. M. & FISHER, D. E. 2011. A new era: melanoma genetics and therapeutics. *J Pathol*, 223, 241-50.
- KOELSCH, C., RENNER, M., HARTMANN, W., BRANDT, R., LEHNER, B., WALDBURGER, N., ALLDINGER, I., SCHMITT, T., EGERER, G., PENZEL, R., WARDELMANN, E., SCHIRMACHER, P., VON DEIMLING, A. & MECHTERSHEIMER, G. 2014. TERT promoter hotspot mutations are recurrent in myxoid liposarcomas but rare in other soft tissue sarcoma entities. *J Exp Clin Cancer Res*, 33, 33.
- KOOPMANS, A. E., OBER, K., DUBBINK, H. J., PARIDAENS, D., NAUS, N. C., BELUNEK, S., KRIST, B., POST, E., ZWARTHOF, E. C., DE KLEIN, A. & VERDIJK, R. M. 2014. Prevalence and implications of TERT promoter mutation in uveal and conjunctival melanoma and in benign and premalignant conjunctival melanocytic lesions. *Invest Ophthalmol Vis Sci*, 55, 6024-30.
- KRAUTHAMMER, M., KONG, Y., BACCHIOCCHI, A., EVANS, P., PORNPUTTAPONG, N., WU, C., MCCUSKER, J. P., MA, S., CHENG, E., STRAUB, R., SERIN, M., BOSENBERG, M., ARIYAN, S., NARAYAN, D., SZNOL, M., KLUGER, H. M., MANE, S., SCHLESSINGER, J., LIFTON, R. P. & HALABAN, R. 2015. Exome sequencing identifies recurrent mutations in NF1 and RASopathy genes in sun-exposed melanomas. *Nat Genet*, 47, 996-1002.

- KRUSE, F. E. 1994. Stem cells and corneal epithelial regeneration. *Eye (Lond)*, 8 ( Pt 2), 170-83.
- KUSTERS-VANDEVELDE, H. V., KLAASEN, A., KUSTERS, B., GROENEN, P. J., VAN ENGEN-VAN GRUNSVEN, I. A., VAN DIJK, M. R., REIFENBERGER, G., WESSELING, P. & BLOKX, W. A. 2010. Activating mutations of the GNAQ gene: a frequent event in primary melanocytic neoplasms of the central nervous system. *Acta Neuropathol*, 119, 317-23.
- LAKE, S. L., JMOR, F., DOPIERALA, J., TAKTAK, A. F., COUPLAND, S. E. & DAMATO, B. E. 2011a. Multiplex ligation-dependent probe amplification of conjunctival melanoma reveals common BRAF V600E gene mutation and gene copy number changes. *Invest Ophthalmol Vis Sci*, 52, 5598-604.
- LAM, A. K., ONG, K., GIV, M. J. & HO, Y. H. 2008. p16 expression in colorectal adenocarcinoma: marker of aggressiveness and morphological types. *Pathology*, 40, 580-5.
- LANGER, S., KRAUS, J., JENTSCH, I. & SPEICHER, M. R. 2004. Multicolor chromosome painting in diagnostic and research applications. *Chromosome Res*, 12, 15-23.
- LANGER-SAFER, P. R., LEVINE, M. & WARD, D. C. 1982. Immunological method for mapping genes on Drosophila polytene chromosomes. *Proc Natl Acad Sci U S A*, 79, 4381-5.
- LARSEN, A. C., DAHMCKE, C. M., DAHL, C., SIERSMA, V. D., TOFT, P. B., COUPLAND, S. E., PRAUSE, J. U., GULDBERG, P. & HEEGAARD, S. 2015. A Retrospective Review of Conjunctival Melanoma Presentation, Treatment, and Outcome and an Investigation of Features Associated With BRAF Mutations. *JAMA Ophthalmol*, 133, 1295-303.
- LAVKER, R. M. & SUN, T. T. 2003. Epithelial stem cells: the eye provides a vision. *Eye (Lond)*. England.
- LAYTON, C. & GLASSON, W. 2002. Clinical aspects of conjunctival melanoma. *Clin Experiment Ophthalmol*. Australia.
- LAZAR, V., ECSEDI, S., VIZKELETI, L., RAKOSY, Z., BOROSS, G., SZAPPANOS, B., BEGANY, A., EMRI, G., ADANY, R. & BALAZS, M. 2012. Marked genetic differences between BRAF and NRAS mutated primary melanomas as revealed by array comparative genomic hybridization. *Melanoma Res*, 22, 202-14.
- LEHRER, M. S., SUN, T. T. & LAVKER, R. M. 1998. Strategies of epithelial repair: modulation of stem cell and transit amplifying cell proliferation. *J Cell Sci*, 111 ( Pt 19), 2867-75.
- LI, C., WU, S., WANG, H., BI, X., YANG, Z., DU, Y., HE, L., CAI, Z., WANG, J. & FAN, Z. 2015. The C228T mutation of TERT promoter frequently occurs in bladder cancer stem cells and contributes to tumorigenesis of bladder cancer. *Oncotarget*, 6, 19542-51.
- LIESEGANG, T. J. & CAMPBELL, R. J. 1980. Mayo Clinic experience with conjunctival melanomas. *Arch Ophthalmol*, 98, 1385-9.
- LIN, S. M. & FERRUCCI, S. 2006. Primary acquired melanosis of the conjunctiva. *Optometry-Journal of the American Optometric Association*, 77, 223-228.
- LIU, X., QU, S., LIU, R., SHENG, C., SHI, X., ZHU, G., MURUGAN, A. K., GUAN, H., YU, H., WANG, Y., SUN, H., SHAN, Z., TENG, W. & XING, M. 2014. TERT promoter mutations and their association with BRAF V600E mutation and aggressive clinicopathological characteristics of thyroid cancer. *J Clin Endocrinol Metab*, 99, E1130-6.

- LOEB, K. R. & LOEB, L. A. 2000. Significance of multiple mutations in cancer. *Carcinogenesis*, 21, 379-85.
- LOMMATZSCH, P. K., LOMMATZSCH, R. E., KIRSCH, I. & FUHRMANN, P. 1990b. Therapeutic outcome of patients suffering from malignant melanomas of the conjunctiva. *Br J Ophthalmology*, 74, 615-9.
- LONG, G. V., MENZIES, A. M., NAGRAL, A. M., HAYDU, L. E., HAMILTON, A. L., MANN, G. J., HUGHES, T. M., THOMPSON, J. F., SCOLYER, R. A. & KEFFORD, R. F. 2011. Prognostic and clinicopathologic associations of oncogenic BRAF in metastatic melanoma. *J Clin Oncol*, 29, 1239-46.
- LOPEZ-OTIN, C., BLASCO, M. A., PARTRIDGE, L., SERRANO, M. & KROEMER, G. 2013. The hallmarks of aging. *Cell*, 153, 1194-217.
- LUKE, J. J. & HODI, F. S. 2012. Vemurafenib and BRAF inhibition: a new class of treatment for metastatic melanoma. *Clin Cancer Res*, 18, 9-14.
- MACCARTHY, A., BIRCH, J. M., DRAPER, G. J., HUNGERFORD, J. L., KINGSTON, J. E., KROLL, M. E., ONADIM, Z., STILLER, C. A., VINCENT, T. J. & MURPHY, M. F. 2009. Retinoblastoma in Great Britain 1963-2002. *Br J Ophthalmol*, 93, 33-7.
- MARTIN, G. A., VISKOCHIL, D., BOLLAG, G., MCCABE, P. C., CROSIER, W. J., HAUBRUCK, H., CONROY, L., CLARK, R., O'CONNELL, P., CAWTHON, R. M. & ET AL. 1990. The GAP-related domain of the neurofibromatosis type 1 gene product interacts with ras p21. *Cell*, 63, 843-9.
- MC SHERRY, E. A., MC GOLDRICK, A., KAY, E. W., HOPKINS, A. M., GALLAGHER, W. M. & DERVAN, P. A. 2007. Formalin-fixed paraffin-embedded clinical tissues show spurious copy number changes in array-CGH profiles. *Clin Genet*, 72, 441-7.
- MCGUIRE, S. 2016. World Cancer Report 2014. Geneva, Switzerland: World Health Organization, International Agency for Research on Cancer, WHO Press, 2015. *Adv Nutr*, 7, 418-9.
- MCLAUGHLIN, C. C., WU, X. C., JEMAL, A., MARTIN, H. J., ROCHE, L. M. & CHEN, V. W. 2005. Incidence of noncutaneous melanomas in the U.S. *Cancer*, 103, 1000-7.
- MCLEAN, I. W., ZIMMERMAN, L. E. & EVANS, R. M. 1978. Reappraisal of Callender's spindle a type of malignant melanoma of choroid and ciliary body. *Am J Ophthalmol*, 86, 557-64.
- MCNAMARA, M., FELIX, C., DAVISON, E. V., FENTON, M. & KENNEDY, S. M. 1997. Assessment of chromosome 3 copy number in ocular melanoma using fluorescence in situ hybridization. *Cancer Genet Cytogenet*, 98, 4-8.
- MCWILLIAMS, R. R., WIEBEN, E. D., RABE, K. G., PEDERSEN, K. S., WU, Y., SICOTTE, H. & PETERSEN, G. M. 2011. Prevalence of CDKN2A mutations in pancreatic cancer patients: implications for genetic counseling. *Eur J Hum Genet*.
- MENG, X. R. & LU, P. 2012. [Relationship between heat shock protein 70 expression and radiotherapeutic effect in esophageal squamous cell carcinoma]. *Zhonghua Yi Xue Za Zhi*, 92, 3367-70.
- MEYERSON, M., GABRIEL, S. & GETZ, G. 2010. Advances in understanding cancer genomes through second-generation sequencing. *Nat Rev Genet*, 11, 685-96.
- MICHOR, F., IWASA, Y., VOGELSTEIN, B., LENGAUER, C. & NOWAK, M. A. 2005. Can chromosomal instability initiate tumorigenesis? *Semin Cancer Biol*, 15, 43-9.
- MILDE-LANGOSCH, K., BAMBERGER, A. M., RIECK, G., KELP, B. & LONING, T. 2001. Overexpression of the p16 cell cycle inhibitor in breast cancer is

- associated with a more malignant phenotype. *Breast Cancer Res Treat*, 67, 61-70.
- MISSOTTEN, G. S., KEIJSER, S., DE KEIZER, R. J. & DE WOLFF-ROUENDAAL, D. 2005a. Conjunctival melanoma in the Netherlands: a nationwide study. *Invest Ophthalmol Vis Sci*, 46, 75-82.
- MISSOTTEN, G. S., KEIJSER, S., KEIZER, R. J. W. D. & WOLFF-ROUENDAAL, D. D. 2005b. Conjunctival Melanoma in The Netherlands: A Nationwide Study.
- MITELMAN, F., MERTENS, F. & JOHANSSON, B. 1997. A breakpoint map of recurrent chromosomal rearrangements in human neoplasia. *Nature Genetics*, 15, 417.
- MOREY, A. L., MURALI, R., MCCARTHY, S. W., MANN, G. J. & SCOLYER, R. A. 2009. Diagnosis of cutaneous melanocytic tumours by four-colour fluorescence in situ hybridisation. *Pathology*, 41, 383-7.
- MUDHAR, H. S., SMITH, K., TALLEY, P., WHITWORTH, A., ATKEY, N. & RENNIE, I. G. 2013. Fluorescence in situ hybridisation (FISH) in histologically challenging conjunctival melanocytic lesions. *Br J Ophthalmol*, 97, 40-6.
- MULTANI, A. S., OZEN, M., NARAYAN, S., KUMAR, V., CHANDRA, J., MCCONKEY, D. J., NEWMAN, R. A. & PATHAK, S. 2000. Caspase-dependent apoptosis induced by telomere cleavage and TRF2 loss. *Neoplasia*, 2, 339-45.
- NAREYECK, G., WUESTEMEYER, H., VON DER HAAR, D. & ANASTASSIOU, G. 2005. Establishment of two cell lines derived from conjunctival melanomas. *Experimental Eye Research*, 81, 361-362.
- NASSER, Q. J. & ESMAELI, B. 2011. Conjunctival Melanoma. *Ophthalmology*, 118, 2307-2308.
- NEWTON BISHOP, J. A. & GRUIS, N. A. 2007. Genetics: what advice for patients who present with a family history of melanoma? *Semin Oncol*, 34, 452-9.
- NISSAN, M. H., PRATILAS, C. A., JONES, A. M., RAMIREZ, R., WON, H., LIU, C., TIWARI, S., KONG, L., HANRAHAN, A. J., YAO, Z., MERGHOU, T., RIBAS, A., CHAPMAN, P. B., YAEGER, R., TAYLOR, B. S., SCHULTZ, N., BERGER, M. F., ROSEN, N. & SOLIT, D. B. 2014. Loss of NF1 in Cutaneous Melanoma Is Associated with RAS Activation and MEK Dependence.
- NITZ, M. D., HARDING, M. A., SMITH, S. C., THOMAS, S. & THEODORESCU, D. 2011. RREB1 Transcription Factor Splice Variants in Urologic Cancer. *Am J Pathol*.
- NORDLING, C. O. 1953. A new theory on cancer-inducing mechanism. *Br J Cancer*, 7, 68-72.
- OELLERS, P. & KARP, C. L. 2012. Management of pigmented conjunctival lesions. *Ocul Surf*, 10, 251-63.
- OMHOLT, K., PLATZ, A., KANTER, L., RINGBORG, U. & HANSSON, J. 2003. NRAS and BRAF mutations arise early during melanoma pathogenesis and are preserved throughout tumor progression. *Clin Cancer Res*, 9, 6483-8.
- OOSTLANDER, A. E., MEIJER, G. A. & YLSTRA, B. 2004. Microarray-based comparative genomic hybridization and its applications in human genetics. *Clin Genet*, 66, 488-95.
- ORTEGA, S., MALUMBRES, M. & BARBACID, M. 2002. Cyclin D-dependent kinases, INK4 inhibitors and cancer. *Biochim Biophys Acta*, 1602, 73-87.
- OU, Z., KANG, S. H. L., SHAW, C. A., CARMACK, C. E., WHITE, L. D., PATEL, A., BEAUDET, A. L., CHEUNG, S. W. & CHINAULT, A. C. 2008. Bacterial artificial chromosome-emulation oligonucleotide arrays for targeted clinical array-comparative genomic hybridization analyses. *Genet Med*, 10, 278-89.

- PARIDAENS, A. D., MCCARTNEY, A. C., MINASSIAN, D. C. & HUNGERFORD, J. L. 1994. Orbital exenteration in 95 cases of primary conjunctival malignant melanoma. *Br J Ophthalmol*, 78, 520-8.
- PATEL, M., SMYTH, E., CHAPMAN, P. B., WOLCHOK, J. D., SCHWARTZ, G. K., ABRAMSON, D. H. & CARVAJAL, R. D. 2011. Therapeutic implications of the emerging molecular biology of uveal melanoma. *Clin Cancer Res*, 17, 2087-100.
- PEI, X. H. & XIONG, Y. 2005. Biochemical and cellular mechanisms of mammalian CDK inhibitors: a few unresolved issues. *Oncogene*, 24, 2787-95.
- PFÄFFENBACH, D. D., GREEN, W. R. & MAUMENEE, A. E. 1972. Balloon cell nevus of the conjunctiva. *Arch Ophthalmol*, 87, 192-5.
- POPULO, H., BOAVENTURA, P., VINAGRE, J., BATISTA, R., MENDES, A., CALDAS, R., PARDAL, J., AZEVEDO, F., HONAVAR, M., GUIMARAES, I., MANUEL LOPES, J., SOBRINHO-SIMÕES, M. & SOARES, P. 2014. TERT promoter mutations in skin cancer: the effects of sun exposure and X-irradiation. *J Invest Dermatol*, 134, 2251-2257.
- POTTEN, C. S. & LOEFFLER, M. 1990. Stem cells: attributes, cycles, spirals, pitfalls and uncertainties. Lessons for and from the crypt. *Development*, 110, 1001-20.
- PRESCHER, G., BORNFELD, N. & BECHER, R. 1990. Nonrandom chromosomal abnormalities in primary uveal melanoma. *J Natl Cancer Inst*, 82, 1765-9.
- RAAMSDONK, C. D. V., FITCH, K. R., FUCHS, H., ANGELIS, M. H. D. & BARSH, G. S. 2004. Effects of G-protein mutations on skin color. *Nature Genetics*, 36, 961.
- RAMOS, J., VILLA, J., RUIZ, A., ARMSTRONG, R. & MATTA, J. 2004. UV dose determines key characteristics of nonmelanoma skin cancer. *Cancer Epidemiol Biomarkers Prev*, 13, 2006-11.
- REESE 1938. Precancerous melanosis and diffuse malignant melanoma of the conjunctiva. *Arch Ophthalmol*, 19, 354-365.
- RIELY, G. J., KRIS, M. G., ROSENBAUM, D., MARKS, J., LI, A., CHITALE, D. A., NAFA, K., RIEDEL, E. R., HSU, M., PAO, W., MILLER, V. A. & LADANYI, M. 2008. Frequency and distinctive spectrum of KRAS mutations in never smokers with lung adenocarcinoma. *Clin Cancer Res*, 14, 5731-4.
- ROBERTSON, K. D. & JONES, P. A. 1999. Tissue-specific alternative splicing in the human INK4a/ARF cell cycle regulatory locus. *Oncogene*, 18, 3810-20.
- ROMANO, A. C., ESPANA, E. M., YOO, S. H., BUDAK, M. T., WOLOSIN, J. M. & TSENG, S. C. 2003. Different cell sizes in human limbal and central corneal basal epithelia measured by confocal microscopy and flow cytometry. *Invest Ophthalmol Vis Sci*, 44, 5125-9.
- ROYLANCE, R. 2002. Methods of molecular analysis: assessing losses and gains in tumours. *Mol Pathol*, 55, 25-8.
- RUEDA, O. M., DIAZ-URIARTE, R. & CALDAS, C. 2013. Finding common regions of alteration in copy number data. *Methods Mol Biol*, 973, 339-53.
- SALAZAR MENDEZ, R., BAAMONDE ARBAIZA, B., DE LA ROZ MARTIN, P. & PARRA RODRIGUEZ, T. 2014. [Treatment of conjunctival melanoma]. *Arch Soc Esp Oftalmol*, 89, 82-4.
- SAVAR, A., ESMAELI, B., HO, H., LIU, S. & PRIETO, V. G. 2011. Conjunctival melanoma: local-regional control rates, and impact of high-risk histopathologic features. *J Cutan Pathol*, 38, 18-24.
- SAVAR, A., ROSS, M. I., PRIETO, V. G., IVAN, D., KIM, S. & ESMAELI, B. 2009. Sentinel lymph node biopsy for ocular adnexal melanoma: experience in 30 patients. *Ophthalmology*, 116, 2217-23.

- SCHLOTZER-SCHREHARDT, U. & KRUSE, F. E. 2005. Identification and characterization of limbal stem cells. *Exp Eye Res*. England.
- SCHOLZ, S. L., COSGAREA, I., SUSSKIND, D., MURALI, R., MOLLER, I., REIS, H., LEONARDELLI, S., SCHILLING, B., SCHIMMING, T., HADASCHIK, E., FRANKLIN, C., PASCHEN, A., SUCKER, A., STEUHL, K. P., SCHADENDORF, D., WESTEKEMPER, H. & GRIEWANK, K. G. 2018. NF1 mutations in conjunctival melanoma. *Br J Cancer*.
- SCOTTO, J., FRAUMENI, J. F., JR. & LEE, J. A. 1976. Melanomas of the eye and other noncutaneous sites: epidemiologic aspects. *J Natl Cancer Inst*, 56, 489-91.
- SEREGARD, S. 1998a. Conjunctival Melanoma. *Survey of Ophthalmology*, 42, 321-350.
- SEREGARD, S. & KOCK, E. 1992. Conjunctival malignant melanoma in Sweden 1969-91. *Acta Ophthalmol (Copenh)*, 70, 289-96.
- SERRANO, M. 1997. The tumor suppressor protein p16INK4a. *Exp Cell Res*, 237, 7-13.
- SHAW-SMITH, C., REDON, R., RICKMAN, L., RIO, M., WILLATT, L., FIEGLER, H., FIRTH, H., SANLAVILLE, D., WINTER, R., COLLEAUX, L., BOBROW, M. & CARTER, N. 2004. Microarray based comparative genomic hybridisation (array-CGH) detects submicroscopic chromosomal deletions and duplications in patients with learning disability/mental retardation and dysmorphic features. *J Med Genet*, 41, 241-8.
- SHIELDS, C. L. 2002. Conjunctival melanoma. *Br J Ophthalmol*, 86, 127.
- SHIELDS, C. L., CHIEN, J. L., SURAKIATCHANUKUL, T., SIOUFI, K., LALLY, S. E. & SHIELDS, J. A. 2017. Conjunctival Tumors: Review of Clinical Features, Risks, Biomarkers, and Outcomes--The 2017 J. Donald M. Gass Lecture. *Asia Pac J Ophthalmol (Phila)*. China: Copyright 2017 Asia-Pacific Academy of Ophthalmology.
- SHIELDS, C. L., DEMIRCI, H., KARATZA, E. & SHIELDS, J. A. 2004a. Clinical survey of 1643 melanocytic and nonmelanocytic conjunctival tumors. *Ophthalmology*, 111, 1747-54.
- SHIELDS, C. L., FASIUDDIN, A. F., MASHAYEKHI, A. & SHIELDS, J. A. 2004b. Conjunctival nevi: clinical features and natural course in 410 consecutive patients. *Arch Ophthalmol*, 122, 167-75.
- SHIELDS, C. L., MARKOWITZ, J. S., BELINSKY, I., SCHWARTZSTEIN, H., GEORGE, N. S., LALLY, S. E., MASHAYEKHI, A. & SHIELDS, J. A. 2011. Conjunctival Melanoma: Outcomes Based on Tumor Origin in 382 Consecutive Cases. *Ophthalmology*, 118, 389-395.e2.
- SHIELDS, C. L., SHIELDS, J. A., GÜNDÜZ, K., CATER, J., MERCADO, G. V., GROSS, N. & LALLY, B. 2000. Conjunctival melanoma: Risk factors for recurrence, exenteration, metastasis, and death in 150 consecutive patients. *Archives of Ophthalmology*, 118, 1497-1507.
- SHIELDS, J. A. & SHIELDS, C. L. 2003. Rhabdomyosarcoma: review for the ophthalmologist. *Surv Ophthalmol*, 48, 39-57.
- SHIELDS, J. A., SHIELDS, C. L. & DE POTTER, P. 1997. Surgical management of conjunctival tumors. The 1994 Lynn B. McMahan Lecture. *Arch Ophthalmol*, 115, 808-15.
- SHIELDS, J. A., SHIELDS, C. L. & DE POTTER, P. 1998. Surgical management of circumscribed conjunctival melanomas. *Ophthal Plast Reconstr Surg*, 14, 208-15.
- SHIELDS, J. A., SHIELDS, C. L., MASHAYEKHI, A., MARR, B. P., BENAVIDES, R., THANGAPPAN, A., PHAN, L. & EAGLE JR, R. C. 2008a. Primary Acquired

- Melanosis of the Conjunctiva: Risks for Progression to Melanoma in 311 Eyes: The 2006 Lorenz E. Zimmerman Lecture. *Ophthalmology*, 115, 511-519.e2.
- SHIELDS, J. A., SHIELDS, C. L., MASHAYEKHI, A., MARR, B. P., BENAVIDES, R., THANGAPPAN, A., PHAN, L. & EAGLE, R. C. 2007. PRIMARY ACQUIRED MELANOSIS OF THE CONJUNCTIVA: EXPERIENCE WITH 311 EYES. *Trans Am Ophthalmol Soc*, 105, 61-72.
- SHIELDS, J. A., SHIELDS, C. L., MASHAYEKHI, A., MARR, B. P., BENAVIDES, R., THANGAPPAN, A., PHAN, L. & EAGLE, R. C., JR. 2008b. Primary acquired melanosis of the conjunctiva: risks for progression to melanoma in 311 eyes. The 2006 Lorenz E. Zimmerman lecture. *Ophthalmology*. United States.
- SHIMA, K., NOSHO, K., BABA, Y., CANTOR, M., MEYERHARDT, J. A., GIOVANNUCCI, E. L., FUCHS, C. S. & OGINO, S. 2011. Prognostic Significance of CDKN2A (p16) Promoter Methylation and Loss of Expression in 902 Colorectal Cancers: Cohort Study and Literature Review. *Int J Cancer*, 128, 1080-94.
- SHOUSHTARI, A. N. & CARVAJAL, R. D. 2016. Treatment of Uveal Melanoma. *Cancer Treat Res*, 167, 281-93.
- SIEGEL, R., NAISHADHAM, D. & JEMAL, A. 2013. Cancer statistics, 2013. *CA Cancer J Clin*, 63, 11-30.
- SISLEY, K., RENNIE, I. G., COTTAM, D. W., POTTER, A. M., POTTER, C. W. & REES, R. C. 1990. Cytogenetic findings in six posterior uveal melanomas: involvement of chromosomes 3, 6, and 8. *Genes Chromosomes Cancer*, 2, 205-9.
- SLOMINSKI, A., TOBIN, D. J., SHIBAHARA, S. & WORTSMAN, J. 2004. Melanin pigmentation in mammalian skin and its hormonal regulation. *Physiol Rev*, 84, 1155-228.
- SPENCER 1985. *Ophthalmic Pathology: an atlas and textbook*, The American academy of ophthalmology and the armed forces institute of pathology.
- SPENDLOVE, H. E., DAMATO, B. E., HUMPHREYS, J., BARKER, K. T., HISCOTT, P. S. & HOULSTON, R. S. 2004. BRAF mutations are detectable in conjunctival but not uveal melanomas. *Melanoma Res*, 14, 449-52.
- SRINIVASAN, M., SEDMAK, D. & JEWELL, S. 2002. Effect of fixatives and tissue processing on the content and integrity of nucleic acids. *Am J Pathol*, 161, 1961-71.
- STANNARD, C. E., SEALY, G. R., HERING, E. R., PEREIRA, S. B., KNOWLES, R. & HILL, J. C. 2000. Malignant melanoma of the eyelid and palpebral conjunctiva treated with iodine-125 brachytherapy. *Ophthalmology*, 107, 951-8.
- STARK, M. & HAYWARD, N. 2007. Genome-wide loss of heterozygosity and copy number analysis in melanoma using high-density single-nucleotide polymorphism arrays. *Cancer Res*, 67, 2632-42.
- STEILING, K., RYAN, J., BRODY, J. S. & SPIRA, A. 2008. The Field of Tissue Injury in the Lung and Airway. *Cancer Prev Res (Phila)*, 1, 396-403.
- STRATTON, M. R., CAMPBELL, P. J. & FUTREAL, P. A. 2009. The cancer genome. *Nature*, 458, 719-24.
- STREMPEL, I. & KROLL, P. 1999. Conjunctival malignant melanoma in children. *Ophthalmologica*, 213, 129-32.
- SVENSSON, S., NILSSON, K., RINGBERG, A. & LANDBERG, G. 2003. Invade or proliferate? Two contrasting events in malignant behavior governed by p16(INK4a) and an intact Rb pathway illustrated by a model system of basal cell carcinoma. *Cancer Res*, 63, 1737-42.

- THIAGALINGAM, A., DE BUSTROS, A., BORGES, M., JASTI, R., COMPTON, D., DIAMOND, L., MABRY, M., BALL, D. W., BAYLIN, S. B. & NELKIN, B. D. 1996. RREB-1, a novel zinc finger protein, is involved in the differentiation response to Ras in human medullary thyroid carcinomas. *Mol Cell Biol*, 16, 5335-45.
- THIAGALINGAM, S., JOHNSON, M. M., COLBY, K. A. & ZEMBOWICZ, A. 2008. Juvenile conjunctival nevus: clinicopathologic analysis of 33 cases. *Am J Surg Pathol*, 32, 399-406.
- TRIAY, E., BERGMAN, L., NILSSON, B., ALL-ERICSSON, C. & SEREGARD, S. 2009. Time trends in the incidence of conjunctival melanoma in Sweden. *British Journal of Ophthalmology*, 93, 1524-1528.
- TRIOZZI, P. L., ENG, C. & SINGH, A. D. 2008. Targeted therapy for uveal melanoma. *Cancer Treat Rev*, 34, 247-58.
- TUCKER, M. A., SHIELDS, J. A., HARTGE, P., AUGSBURGER, J., HOOVER, R. N. & FRAUMENI, J. F., JR. 1985. Sunlight exposure as risk factor for intraocular malignant melanoma. *N Engl J Med*, 313, 789-92.
- TUOMAALA, S. & KIVELA, T. 2004. Metastatic pattern and survival in disseminated conjunctival melanoma: implications for sentinel lymph node biopsy. *Ophthalmology*, 111, 816-21.
- VAJDIC, C. M., HUTCHINS, A. M., KRICKER, A., AITKEN, J. F., ARMSTRONG, B. K., HAYWARD, N. K. & ARMES, J. E. 2003a. Chromosomal gains and losses in ocular melanoma detected by comparative genomic hybridization in an Australian population-based study. *Cancer Genet Cytogenet*, 144, 12-7.
- VAJDIC, C. M., KRICKER, A., GIBLIN, M., MCKENZIE, J., AITKEN, J., GILES, G. G. & ARMSTRONG, B. K. 2003b. Incidence of ocular melanoma in Australia from 1990 to 1998. *Int J Cancer*, 105, 117-22.
- VAN BEERS, E. H., JOOSSE, S. A., LIGTENBERG, M. J., FLES, R., HOGERVORST, F. B., VERHOEF, S. & NEDERLOF, P. M. 2006. A multiplex PCR predictor for aCGH success of FFPE samples. *Br J Cancer*, 94, 333-7.
- VAN DEN BOSCH, T., KILIC, E., PARIDAENS, D. & DE KLEIN, A. 2010. Genetics of Uveal Melanoma and Cutaneous Melanoma: Two of a Kind? *Dermatol Res Pract*, 2010.
- VAN RAAMSDONK, C. D., BEZROOKOVE, V., GREEN, G., BAUER, J., GAUGLER, L., O'BRIEN, J. M., SIMPSON, E. M., BARSH, G. S. & BASTIAN, B. C. 2009. Frequent somatic mutations of GNAQ in uveal melanoma and blue naevi. *Nature*, 457, 599-602.
- VAN RAAMSDONK, C. D., GRIEWANK, K. G., CROSBY, M. B., GARRIDO, M. C., VEMULA, S., WIESNER, T., OBENAUF, A. C., WACKERNAGEL, W., GREEN, G., BOUVIER, N., SOZEN, M. M., BAIMUKANOVA, G., ROY, R., HEGUY, A., DOLGALEV, I., KHANIN, R., BUSAM, K., SPEICHER, M. R., O'BRIEN, J. & BASTIAN, B. C. 2010. Mutations in GNA11 in uveal melanoma. *N Engl J Med*, 363, 2191-9.
- VARGA, A. C. & WRANA, J. L. 2005. The disparate role of BMP in stem cell biology. *Oncogene*. England.
- VERGIER, B., PROCHAZKOVA-CARLOTTI, M., DE LA FOUCHARDIERE, A., CERRONI, L., MASSI, D., DE GIORGI, V., BAILLY, C., WESSELMANN, U., KARLSELADZE, A., AVRIL, M. F., JOUARY, T. & MERLIO, J. P. 2011. Fluorescence in situ hybridization, a diagnostic aid in ambiguous melanocytic tumors: European study of 113 cases. *Mod Pathol*, 24, 613-23.
- VILLEGAS, V. M., HESS, D. J., WILDNER, A., GOLD, A. S. & MURRAY, T. G. 2013. Retinoblastoma. *Curr Opin Ophthalmol*, 24, 581-8.

- VINAGRE, J., ALMEIDA, A., POPULO, H., BATISTA, R., LYRA, J., PINTO, V., COELHO, R., CELESTINO, R., PRAZERES, H., LIMA, L., MELO, M., DA ROCHA, A. G., PRETO, A., CASTRO, P., CASTRO, L., PARDAL, F., LOPES, J. M., SANTOS, L. L., REIS, R. M., CAMESELLE-TEIJEIRO, J., SOBRINHO-SIMÕES, M., LIMA, J., MAXIMO, V. & SOARES, P. 2013. Frequency of TERT promoter mutations in human cancers. *Nat Commun*, 4, 2185.
- VORA, G. K., DEMIRCI, H., MARR, B. & MRUTHYUNJAYA, P. 2017. Advances in the management of conjunctival melanoma. *Surv Ophthalmol*, 62, 26-42.
- WAN, P. T., GARNETT, M. J., ROE, S. M., LEE, S., NICULESCU-DUVAZ, D., GOOD, V. M., JONES, C. M., MARSHALL, C. J., SPRINGER, C. J., BARFORD, D. & MARAIS, R. 2004. Mechanism of activation of the RAF-ERK signaling pathway by oncogenic mutations of B-RAF. *Cell*, 116, 855-67.
- WANG, L., RAO, M., FANG, Y., HAMEED, M., VIALE, A., BUSAM, K. & JHANWAR, S. C. 2013. A genome-wide high-resolution array-CGH analysis of cutaneous melanoma and comparison of array-CGH to FISH in diagnostic evaluation. *J Mol Diagn*, 15, 581-91.
- WANG, N. 2002. Methodologies in cancer cytogenetics and molecular cytogenetics. *Am J Med Genet*, 115, 118-24.
- WESTEKEMPER, H., KARIMI, S., SUSSKIND, D., ANASTASSIOU, G., FREISTUHLER, M., STEUHL, K. P., BORNFIELD, N., SCHMID, K. W. & GRABELLUS, F. 2011. Expression of HSP 90, PTEN and Bcl-2 in conjunctival melanoma. *Br J Ophthalmol*, 95, 853-8.
- WHITMARSH, A. J., SHORE, P., SHARROCKS, A. D. & DAVIS, R. J. 1995. Integration of MAP kinase signal transduction pathways at the serum response element. *Science*, 269, 403-7.
- WIEDEMEYER, R., BRENNAN, C., HEFFERNAN, T. P., XIAO, Y., MAHONEY, J., PROTOPOPOV, A., ZHENG, H., BIGNELL, G., FURNARI, F., CAVENEE, W. K., HAHN, W. C., ICHIMURA, K., COLLINS, V. P., CHU, G. C., STRATTON, M. R., LIGON, K. L., FUTREAL, P. A. & CHIN, L. 2008. Feedback Circuit among INK4 Tumor Suppressors Constrains Human Glioblastoma Development. *Cancer Cell*, 13, 355-364.
- WIESNER, T., KIURU, M., SCOTT, S. N., ARCILA, M., HALPERN, A. C., HOLLMANN, T., BERGER, M. F. & BUSAM, K. J. 2015. NF1 Mutations Are Common in Desmoplastic Melanoma. *Am J Surg Pathol*, 39, 1357-62.
- WIESNER, T., MURALI, R., FRIED, I., CERRONI, L., BUSAM, K., KUTZNER, H. & BASTIAN, B. C. 2012. A distinct subset of atypical Spitz tumors is characterized by BRAF mutation and loss of BAP1 expression. *Am J Surg Pathol*, 36, 818-30.
- WILSON, M. A., MORRISSETTE, J. J., MCGETTIGAN, S., ROTH, D., ELDER, D., SCHUCHTER, L. M. & DABER, R. D. 2014. What you are missing could matter: a rare, complex BRAF mutation affecting codons 599, 600, and 601 uncovered by next generation sequencing. *Cancer Genet*, 207, 272-5.
- WONG, C. W., FAN, Y. S., CHAN, T. L., CHAN, A. S., HO, L. C., MA, T. K., YUEN, S. T. & LEUNG, S. Y. 2005. BRAF and NRAS mutations are uncommon in melanomas arising in diverse internal organs. *J Clin Pathol*, 58, 640-4.
- WONG, J. R., NANJI, A. A., GALOR, A. & KARP, C. L. 2014. Management of conjunctival malignant melanoma: a review and update. *Expert Rev Ophthalmol*, 9, 185-204.
- XING, M., LIU, R., LIU, X., MURUGAN, A. K., ZHU, G., ZEIGER, M. A., PAI, S. & BISHOP, J. 2014. BRAF V600E and TERT promoter mutations cooperatively

- identify the most aggressive papillary thyroid cancer with highest recurrence. *J Clin Oncol*, 32, 2718-26.
- YANG, P., CAI, J., YAN, W., ZHANG, W., WANG, Y., CHEN, B., LI, G., LI, S., WU, C., YAO, K., LI, W., PENG, X., YOU, Y., CHEN, L., JIANG, C., QIU, X. & JIANG, T. 2016. Classification based on mutations of TERT promoter and IDH characterizes subtypes in grade II/III gliomas. *Neuro Oncol*, 18, 1099-108.
- YEH, I. & BASTIAN, B. C. 2009. Genome-Wide Associations Studies for Melanoma and Nevi. *Pigment Cell Melanoma Res*, 22, 527-8.
- YOON, J. J., ISMAIL, S. & SHERWIN, T. 2014. Limbal stem cells: Central concepts of corneal epithelial homeostasis. *World J Stem Cells*, 6, 391-403.
- ZEMBOWICZ, A., MANDAL, R. V. & CHOOPONG, P. 2010. Melanocytic lesions of the conjunctiva. *Arch Pathol Lab Med*. United States.
- ZHAO, J., MO, V. & NAGASAKI, T. 2009. Distribution of label-retaining cells in the limbal epithelium of a mouse eye. *J Histochem Cytochem*. United States.
- ZHAO, P., MAO, X. & TALBOT, I. C. 2006. Aberrant cytological localization of p16 and CDK4 in colorectal epithelia in the normal adenoma carcinoma sequence. *World J Gastroenterol*, 12, 6391-6.
- ZHOU, Y., MA, B. G. & ZHANG, H. Y. 2007. Human oncogene tissue-specific expression level significantly correlates with sequence compositional features. *FEBS Lett*, 581, 4361-5.

# Appendices

## Appendix 1

Table 1A: Summary of most copy number variations among conjunctival melanoma tumours used in this study.

Sample ID	Sample type	Orgine of tumors	Gains	Loses
ConM 1a	FFPE	Primary ConM	6p and 10p	-----
ConM 1b	FFPE	Lymphnode metastasis	2, 3, 6p, 7, 10, 11 and 18.	-----
ConM 2a	FFPE	Metastasis in the eye	-----	-----
ConM 2b	FFPE	lymphnode metastasis	5q, 11q and 17q.	4p, 5q, 6q, 8p, 9p, 10p, 11, 12q, 16q and 19q.
ConM 3a	FFPE	primary ConM	1q, 7 and 8	3p, 5p, 9, 10, 11 and 14q
ConM 3b	FFPE	lymphnode metastasis	1q, 7, and 8p	3p, 5p, 9, 10,11 and 14q
ConM 4	FFPE	primary ConM	1q, 4, 6, 8, 9q, 15q, 17q and 19p.	-----
ConM 5	FFPE	primary ConM	1q, 6p, 7p and 8q.	5p, 6q and 10.
ConM 6	FFPE	Primary ConM	3p, 4q, 8q, 9, 11q, 12q, 16p, 17q 18, 19 and 20p	3q, 4, 5q, 6q, 8p, 9p, 9q, 10, 11q, 12p and 16q.
ConM 7	FFPE	primary ConM	1q and 6p.	-----
ConM 8	FFPE	primary ConM	-----	-----
ConM 9	FFPE	lymphnode metastasis	1q and 17p.	5p
ConM 10	FFPE	primary ConM	1q, 2q, 8q, 11q, 12p and 18q.	5q, 11q.
ConM 11	FFPE	primary ConM	6p	-----
ConM 12	FFPE	metastasis in the eye	1q, 2q, 6p, 7q, 10p, 12q, 15q and 20q.	5p, 8p, 11q, 12q , 13q and 16q.
ConM 13	FFPE	metastasis in the eye	1q, 6p and 8q.	5p, 9p and 16q
ConM 14	FFPE	metastasis in the eye	1q,6p,7, 17q	7p, 11,16q and 21q
ConM 15	FF	primary ConM	1q, 9p, 12p, 14q, 17q, 20q, 21q.	1p, 3q, 4q, 6q, 7p, 9p, 10q, 11q, 12q, 13q, 16, 17p, 18, 19, 20
ConM 16	FF	primary ConM	3q, 6p, 8q and 14q	6q.
ConM 17	FF	primary ConM	1q, 3, 4p, 5, 6p, 7, 8, 14q, 16p, 17q, 18p, 19, 20, 22q	10p
ConM 18	FF	primary ConM	1q, 4, 6p, 8, 9p, 10, 11, 13, 15q, 16p,1 9, 20, 21q, 22q	9p and 16q.

## Appendix 2

Table 2A: Summary of clinical information among FFPE conjunctival melanoma samples used in this study.

Sample ID	Age	Sex	Site	Diagnosed	Depth	Excision	Treatment
ConM 1a	66 Y	Male	Right Bulbar conjunctiva	in-situ and ivasive melanoam	0.8mm	Incomplete	Proton beam therapy
ConM 1b	66 Y	Male	Right side facial lymph nodes	.....	...	...	.....
ConM 2a	57Y	Female	Left inferior fornix	in-transit metastasis	1.8mm	Incomplete	Cryotherapy and Topical Mitomycine C
ConM 2b	57Y	Female	Left submandibular lymph node	.....	....	....	.....
ConM 3a	65Y	Female	Left limbal conjunctiva	In-situe and ivasive melanoma	2.2mm	Incomplete	Cryotherapy and Topical Mitomycine C
ConM 3b	65Y	Female	Left parotid lymph node	in-transit metastasis	...	....	Surgery to left parotid gland
ConM 4	.....	.....	.....	.....	.....	.....	.....
ConM 5	37Y	Female	Right inferior conjunctiva	In-situe and ivasive melanoma	1.5mm	Incomplete	Cryotherapy and Mitomycine therapy
ConM 6	80Y	Female	Right superior fornix conjunctiva	In-situe and ivasive melanoma	6mm	Incomplete	3 Cycles of Mitomycine C
ConM 7	73Y	Female	Left limbal conjunctiva	In-situe and ivasive melanoma	1.5mm	Incomplete	....
ConM 8	.....	.....	.....	.....	.....	.....	.....
ConM 9	77Y	Male	Left temporal conjunctiva	in-transit metastasis	2mm	Incomplete	.....
ConM 10	50Y	Female	Right tarasal conjunctiva	In-situe and ivasive melanoma	2mm	Incomplete	Cryotherapy and Topical Mitomycine C
ConM 11	74Y	Female	Left nasal conjunctiva	In-situ melanoma	1mm	Incomplete	Mitomycine C
ConM 12	43Y	Male	Right inferior conjunctiva	in-situ melanoam	0.2mm		Mitomycine therapy
ConM 13	66 Y	Male	Right inferior fornix limbal	in-transit metastasis	0.6mm	Complete	.....
ConM 14	85Y	Female	Left lower lid	in-transit metastasis	5.5mm		.....

### Appendix 3

Table 3A: Summary of clinical information among Frozen tissue conjunctival melanoma samples used in this study.

Sample ID	Age	Sex	Site	Cell type	Metastatic disease Yes/No	Treatment	Survival time/ date of death	Prognosis F=Fish/ C=Cyto
ConM 15	55Y	Meal	Conjunctiva	Epitheloid	Yes	Excision only	Died liver Metastasis 39 months	F=Poor
ConM 16	85Y	Meal	Conjunctiva	Spindle	No	Excision only	Alive 72 months	F=Good
ConM 17	81Y	Female	Conjunctiva	Unknown	No	Exteneration	Died Cause not 74 months	F=Good
ConM 18	74Y	Meal	Conjunctiva	Unknown	...	Exteneration and cryotherapy	Alive 31months	....

## Appendix 4

Table 4A: Relevance of TERT deletion, mutation and protein expression to conjunctival melanoma

Case Number	TERT Mutations	5 p deletion	IHC	Sex	Site	Diagnosed	Depth
ConM 1a	C250T	yes	Weak	Male	Right side facial lymph nodes	.....	...
ConM 1b	C250T	No	Mild/Mild	Male	Right Bulbar conjunctiva	<i>in-situ and ivasive melanoam</i>	0.8mm
ConM 2a	Failed	No	Weak/mild	Female	Left inferior fornix	<i>in-transit metastasis</i>	1.8mm
ConM 2b	WT	No	.....	Female	Left submandibular lymph node	.....	...
ConM 3a	C250T	yes	Mild/Weak	Female	Left limbal conjunctiva	<i>In-situe and ivasive melanoma</i>	2.2mm
ConM 3b	C250T	yes	Weak	Female	Left parotid lymph node	<i>in-transit metastasis</i>	...
ConM 4	Failed	No	.....	.....	.....	.....	.....
ConM 5	C250T	yes	Mild/Weak	Female	Right inferior conjunctiva	<i>In-situe and ivasive melanoma</i>	1.5mm
ConM 6	WT	yes	Mild	Female	Right superior fornix conjunctiva	<i>In-situe and ivasive melanoma</i>	6mm
ConM 7	WT	No	Mild	Female	Left limbal conjunctiva	<i>In-situe and ivasive melanoma</i>	1.5mm
ConM 8	Failed	No	.....	.....	.....	.....	.....
ConM 9	WT	yes	Mild/Weak	Male	Left temporal conjunctiva	<i>in-transit metastasis</i>	2mm
ConM10	WT	No	Mild/Weak	Female	Right tarasal conjunctiva	<i>In-situe and ivasive melanoma</i>	2mm
ConM11	Failed	No	Mild/Weak	Female	Left nasal conjunctiva	<i>In-situ melanoma</i>	1mm
ConM12	C250T	yes	Mild	Male	Right inferior conjunctiva	<i>in-situ melanoam</i>	0.2mm
ConM13	C250T	yes	Weak	Male	Right inferior fornix limbal	<i>in-transit metastasis</i>	0.6mm
ConM14	C250T	yes	Weak	Female	Left lower lid	<i>in-transit metastasis</i>	5.5mm

## Appendix 5

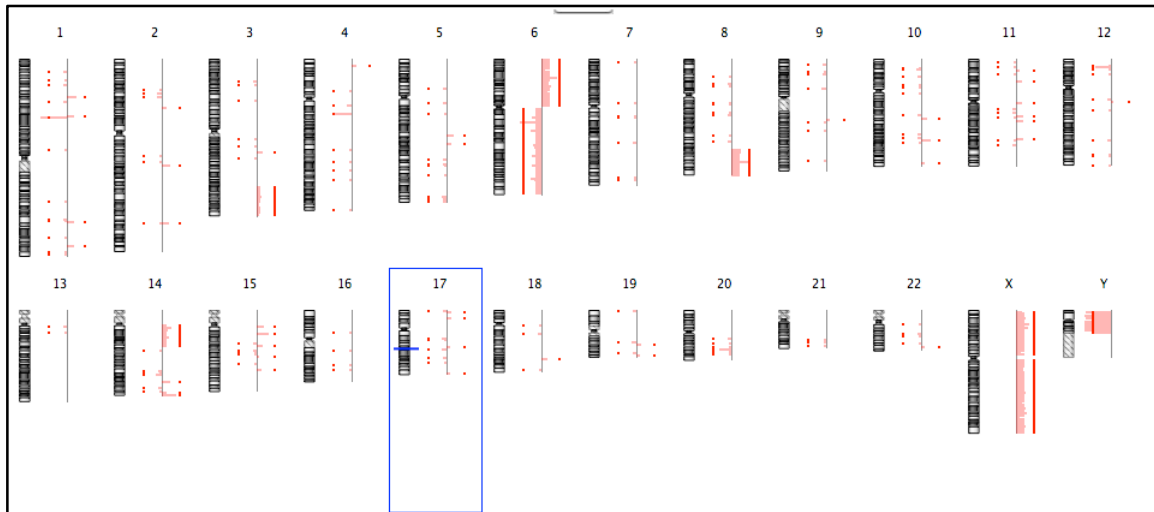


**Figure 1A: Array-CGH ideograms of frozen tissue tumour of ConM (ConM 16) which have *GNAQ* mutation. This genomic view had some abnormalities affecting chromosomes 3, 6 and 8 which is comparable to the genetic changes in UM.**

